DOCTORAL THESIS

Optical Spectrum Services in Open Disaggregated Transport Networks

Kaida Kaeval

Optical Spectrum Services in Open Disaggregated Transport Networks

KAIDA KAEVAL

TALLINN UNIVERSITY OF TECHNOLOGY
School of Information Technologies
Department of Computer Systems
This dissertation was accepted for the defence of the degree of Doctor of Philosophy in Information and Communication Technology on 03/05/2023

Supervisor:

Prof. Gert Jervan
Department of Computer Systems
Tallinn University of Technology
Tallinn, Estonia

Co-supervisors:

Dr.-Ing. Helmut Grieβer
Advanced Technology
ADVA Optical Networking
Munich, Germany

Dr.-Ing. Klaus Grobe
Global Sustainability
ADVA Optical Networking
Munich, Germany

Opponents:

Prof. Nicola Sambo
TeCIP Institute
Sant'Anna School of Advanced Studies
Pisa, Italy

Dr. Fatima Cristina Garcia Gunning
Tyndall National Institute
University College Cork
Cork, Ireland

Defence of the thesis: 23/05/2023, Tallinn

Declaration:
Hereby I declare that this doctoral thesis, my original investigation and achievement, submitted for the doctoral degree at Tallinn University of Technology has not been submitted for doctoral or equivalent academic degree elsewhere.

Kaida Kaeval

----
signature

Optilise spektri teenused avatud lainepikkustihendus võrkudes

KAIDA KAEVAL

Contents

LIST OF PUBLICATIONS

List of publications included in the thesis

The list of author's publications, based on which the thesis has been prepared:

I   Kaeval, K., Jansen, S.L., Fehenberger, T., Spinty, F., Grobe, K., Grieβer, H., Tikas, M., and Jervan, G., "Characterization of the Optical Spectrum as a Service", *Journal of Optical Communications and Networking*, Vol. 14 No. 5, (2022).

II   Kaeval, K., Rafique, D., Blawat, K., Grobe, K., Grieβer, H., Elbers, J.P., Rydlichowski, P., Binczewski, A. and Tikas, M., 2020, March. "Exploring channel probing to determine coherent optical transponder configurations in a long-haul network", *Optical Fibre Communication Conference 2020*, pp. 1–3.

III Kaeval, K., Grieβer, H., K. Grobe, J. -P. Elbers, M. Tikas and G. Jervan, "Channel Performance Estimations with Extended Channel Probing," *ITG-PN 2020*, pp. 1–5.

IV Kaeval, K., Elbers, J.P., Grobe, K., Tikas, M., Fehenberger, T., Grieβer, H., Jervan, G., "Black-Box Assessment of Optical Spectrum Services," *Optical Fibre Communication Conference 2021*, pp. 1–3.

V   Kaeval, K., Fehenberger, T., Zou, J., Jansen, S.L., Grobe, K., Grieβer, H., Elbers, J.P., Tikas, M., and Jervan, G., "QoT assessment of the optical spectrum as a service in disaggregated network scenarios", *Journal of Optical Communications and Networking*, 13, E1–E12 (2021).

VI Kaeval, K., Myyry, J., Grobe, K., Grieβer, H. and Jervan, G., 2021, October. "Concatenated GSNR Profiles for End-to-End Performance Estimations in Disaggregated Networks", *Optical Fibre Communication Conference 2022*, pp. 1–3.

VII Kaeval, K., Slyne, F., Troia, S., Kenny, E., Pedreño-Manresa, J., Patri, S., Grobe, K., Kilper, D.C., Ruffini, M., Jervan, G., "Exploring Service Margins for Optical Spectrum Services", *European Conference on Optical Communication* 2022.

VIII Kaeval, K., Patri, S.K., Pedreno-Manresa, J., Grobe, K., Elbers, J.P., Grieβer, H., Tikas, M., Jervan, G., "Service Margins for Wide-Band Optical Spectrum Services Implemented in Long-Haul Raman-Enabled Networks", *Optical Fibre Communication Conference 2023,* pp. W3H-6.

IX Kaeval, K., Slyne, F., Troia, S., Kenny, E., Grobe, K., Griesβer, H., Kilper, D.C., Ruffini, M., Pedreño-Manresa, J., Patri, S.K., and Jervan, G., "Employing Channel Probing to Derive End-of-Life Service Margins for Optical Spectrum Services", *Journal of Optical Communications and Networking*, 15, C63-C73 (2023).

Related publications

The list of other relevant publications, where the author has contributed and that are relevant to the thesis:

X   Müller, J., Fehenberger, T., Patri, S. K., Kaeval, K., Grieβer, H., Tikas, M., and Elbers, J.P., "Estimating Quality of Transmission in a Live Production Network using Machine Learning," in *Optical Fiber Communication Conference (OFC) 2021*, paper Tu1G.2.

XI   Müller, J., Slyne, F., Kaeval, K., Troia, S., Fehenberger, T., Elbers, J.P., Kilper, D.C., Ruffini, M., Mas-Machuca, C., "Experimental Demonstration of ML-Based DWDM System Margin Estimation," presented at *Optical Fibre Communication Conference 2023*.

XII Patri, S.K., Dick, I., Kaeval, K., Müller, J., Pedreno-Manresa, J.J., Autenrieth, A., Elbers, J.P., Tikas, M., Mas-Machuca, C., "Machine Learning Enabled Fault-Detection Algorithms for Optical Spectrum-As-a-Service Users", presented at *International Conference on Optical Network Design and Modelling 2023.*

Patents

The list of author's patents, based on which the thesis has been prepared:

XIII K. Kaeval, K. Grobe, J.P. Elbers, "Method and apparatus for providing end-to-end optical spectrum services over multiple transparent optical network domains", Europe Patent Application 22166038.4, priority date: 1st of April 2022.

Author's contribution to the publications

For the relevant publications, the contribution as a first author included the formation of the article idea, first hypotheses and test set-up required to collect the data to verify the hypothesis. The test setups in the lab and live networks were assembled by colleagues or co-authors according to author's directions. Author was responsible for testing out the different scenarios and analyzing the data. Finally, the full body of the initial manuscript was written for all the papers. Co-authors provided help in discussing the initial flow of the papers, finetuning the explanations and details presented in the papers, and finally, proofreading the work.

For related publications, the author contributed with proposing the test scenario. For X and XII, the author was also responsible for the system testing, data collection and collected data verification.

For patent application, the contribution as a first author included formulating the idea of the independent Network Domain Interface Device and transparent overlay network concept, as well preparing the materials for the Patent attorney, as well as working with the patent documentation to be filed along with the patent attorney.

Abbreviations

Explanations of abbreviations used in the thesis – the table.

3R	Reamplify, Reshape, Regenerate
ASE	Amplified Spontaneous Emission
AWG	Arrayed Waveguide Grating
AWGN	Additive White Gaussian Noise
B2B	Back-to-back
B2B-1	Inverse Back-to-Back method
BER	Bit Error Ratio
BL	Bit rate to Length product
BL	Bandwidth-to-Length product
BOL	Beginning-of-Life
CAPEX	Capital investments
CO2	Carbon dioxide
CSV	Comma-Separated Values
CuT	Channel under Test
DCF	Dispersion Compensation Fibres
DCG	Dispersion Compensation Grating
DP	Dual Polarization
DSP	Digital Signal Processor
DWDM	Dense Wavelength Division Multiplexing
EDFA	Erbium Doped Fiber Amplifier
EOL	End-of-Life
FEC	Forward Error Correction
GN	Gaussian Noise
GOSNR	Generalized Optical Signal to Noise Ratio
GSNR	Generalized Signal to Noise Ratio
I/F	Interface
ICT	Information and Communication technology
IF	Interworking Functions
IMDD	Intensity Modulated Direct-Detection
IP	Internet Protocol
IRU	Indefeasible Right of Use
ITU	International Telecommunications Union
LCoS	Liquid Crystal on Silicon
MC	Media Channel
MEMS	Microelectron-Mechanical Systems
ML	Machine Learning
MTBF	Mean Time Between Failure
MTTR	Mean Time to Repair

NeDID	Network Domain Interface Device
NLI	Nonlinear impairments
NMC	Network Media Channel
NMS	Network Management Server
NREN	Research and Education Network
OADM	Optical Add Drop Multiplexer
Och	Optical Channel
OLS	Open Line System
OOK	On Off Keying
OPEX	Operational costs
OSA	Optical Spectrum Analyzer
OSaaS	Optical Spectrum as a Service
OSNR	Optical Signal to Noise Ratio
OTDR	Optical Time-Domain Reflectometer
OTSi	Optical Tributary Signal
OXC	Optical Cross Connect
PLT	Probing Light Transceiver
PMD	Polarization Mode Dispersion
PSD	Power Spectral Density
QAM	Quadrature Amplitude Modulation
QoT	Quality of Transmission
QPSK	Quadrature Phase Shift Keying
ROADM	Reconfigurable Optical Add Drop Multiplexer
RRC	Root Raised Cosine
Rx	Receive
S-BVT	Sliceable Bandwidth Variable Transceiver
SDM	Spatial Division Multiplexing
SDN	Software Defined Networking
SHB	Spectral Hole Burning
SLA	Service Level Agreement
SNR	Signal to Noise Ratio
SPM	Self Phase Modulation
TTL	To The Line
Tx	Transmit
VOA	Variable Optical Attenuator
WDM	Wavelength Division Multiplexing
WSS	Wavelength Selective Switch

1 INTRODUCTION

With the growing digitalization trend, broadband connectivity is often referred to as a human right. While access technologies like 5G and upcoming 6G are in the forefront in creating the seamless user experience, optical Dense Wavelength Division Multiplexing (DWDM) networks form the backbone of our digital environments. These networks provide Tbits/s of capacity per connectivity and are required to interconnect datacenters, reach cloud applications, stream high-quality video, etc. The most commonly deployed service type in Dense Wavelength Division Multiplexing (DWDM) networks is based on the leased line service model, where the operator provides the agreed amount of capacity, using standardized customer interfaces at the service endpoints. This does not satisfy the capacity-hungry end-customers, as the service type lacks the flexibility to optimize reach-to-capacity product and, with it, the cost per bit and efficiency achievable in these modern optical networks. Furthermore, the continuous chase for higher capacities requires frequent transceiver upgrades that are financially costly and environmentally exhausting in multi-domain, multi-operator environments, impacting the price of the end-to-end connectivity.

Over the last decade, two big trends have emerged in the industry:

1) the advent of sliceable bandwidth variable transceivers (S-BVT) [1-3], providing flexibility in modulation format and symbol rate combinations to adapt closely to exact performance of the optical line system, consisting of Reconfigurable Optical Add/Drop Multiplexers (ROADMs) and optical amplifiers, and

2) the disaggregation trend [4-6], empowering operators with vendor neutrality that boosts the adoption of the best-of-breed technology in the networks, IP over DWDM operations, and protection against supply chain interruptions. In its simplest form, disaggregation enables third-party transceiver operation over any optical line system by providing the solutions for control and management systems.

Combined, these trends empower the rise of a new cost-efficient service model in the DWDM networks, called Optical Spectrum as a Service (OSaaS) [7]. In this service model, the optical line system is disaggregated from the transceiver equipment in order to efficiently share spectral resources in the network and the end user is granted a direct access to the dedicated spectral resources in the Open Line System (OLS) utilizing an available free ROADM port. This is where the disaggregation happens, as with the direct access, the end-customer can select, operate, and upgrade the S-BVT transceiver equipment in the end points of the OLS, or just route the light signals generated in the previous domain closer to it's final destination. The primary benefit of such service model is that if the spectral resources are available and the performance of the individual OLS segments is good, optical carriers within OSaaS can be operated over thousands of kilometers regardless of the number of domains and operators involved. This reduces the costs associated to equip and operate the border-crossing regeneration sites required in the leased-line service model, reducing the environmental footprint from unnecessary regeneration equipment production, transportation, operation, maintenance, and finally utilization. However, better control over incoming light parameters should be

gained before operators can commit to wide-scale deployments of the OSaaS service model in existing brownfield production network environments.

This thesis investigates the aspects of the Optical Spectrum as a Service in Disaggregated Transport Networks. It provides a structured overview of the possible configurations and related operational aspects of the OSaaS deployed in the brownfield terrestrial DWDM networks. The work explains how experimental channel probing method, used in the submarine communication space [8, 9] can be extended to terrestrial OSaaS use-cases and proposes a Generalized Signal-to-Noise Ratio (GSNR) based performance characterization to enable precise end-to-end capacity estimations without revealing operator's infrastructure-related business-sensitive information. In addition to the characterization, required service margins and general probing accuracy are investigated. To cover fast and slow performance fluctuations, long-term telemetry data is analyzed, and standard deviation-based approach is proposed. For the accommodation of direct neighboring channels and end-of-life (EOL) channel loads, experimental data from a systematic lab study in Open Ireland CONNECT lab is used. Finally, the work proposes a new underlying infrastructure independent Network Domain Interface Device (NeDID) which would enable creation of the transparent optical overlay networks, that allows safe and controlled end-to-end cross-border connectivity to be operated in multi-domain, multi-operator environments.

1.1 Motivation

Considering the relentless efforts to improve efficiency and experience in sending messages over long distances, modern telecommunication networks have come a long way. Whereas the carrier for these messages has changed from smoke, and pigeons to guided electricity and light, the impellent force for these inventions has always been the higher availability and increased system capacity. Through this journey, the end-user of these systems rarely had a chance to sabotage the service delivery due to discrete demarcation points these telecommunication systems provided – be it a human being in the case of telegraph or a modern-day standardized optical client interface in DWDM systems. However, such a service model with clear customer-service provider demarcation is being challenged by the advent of a new optical service called Optical Spectrum as a Service (OSaaS).

Over the years, establishing connectivity between two endpoints in the optical networks has been possible through different service models [10]. Fig. 1 shows the different models for a service provider to provide connectivity to a customer. From the
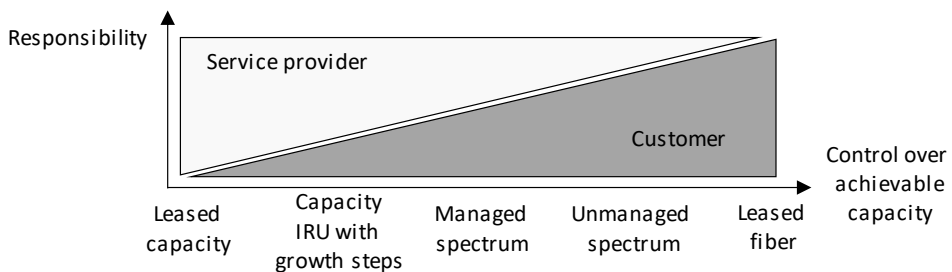

Fig. 1. Service models in optical networks

customer perspective, the simplest model is the leased capacity, where the investments, operational aspects and service performance assurance are the responsibility of the service provider. At the other end of the responsibility scale lays the dark fiber lease, where the service provider only provides rack space and guaranteed power along the fiber route. The customer is responsible for the whole network lifecycle from the OLS system planning, commissioning, and operation to upgrade or possible decommissioning. However, while the leased capacity model may not be cost effective, when high capacity is required, dark fiber lease may not be available for purchase. With the emerging disaggregation trend, supported by the flexible grid defined in ITU-T recommendation ITU-T G.694.1 (10/2020) [11] and S-BVT transceivers, Optical Spectrum as a Service (OSaaS) positions as an attractive service model to fill the gap on the responsibility scale. Motivated by the potential to lower the investment and operational cost, OLS operators are ready to open their networks for a wide range of service models including capacity indefeasible rights of use (IRU), managed and unmanaged OSaaS [12-19].

OSaaS utilizes the generic functional architecture of the ITU-T G.807's generic architecture of the optical media network [20], and the ITU-T G. 698.2's black-link approach [21-23]. This means, that the service can be operated in any optical system, that can provide a section from its spectrum to be used by the third-party transceivers. Through the usage of the concepts of elastic optical networking [24, 25], sliceable transceivers [2, 3, 26] and network disaggregation [27-30], OSaaS end customers can gain exceptional flexibility over the performance of their end-to-end services. This may mean different optimization aspects for different end customers. Very often optimizing a capacity-to-reach product is the target. Other end customers may target to increase the availability or decrease the latency. In all cases, OSaaS enables different approaches to achieve these targets, either through minimizing service margins, implementing GSNR-based signal pre-emphasis, or optimizing signal regeneration points.

The new OSaaS service model is particularly interesting in multi-domain, multi-operator environments. Example of such can be illustrated based on the national networks in Europe, that are operated by different operators, but interconnected at the country borders. In conventional service models, the optical signal is re-amplified, re-timed, and re-generated (3R) at every border crossing. This is quickly soaring the cost of multi-domain international connectivity and deteriorates the availability and latency, which are directly impacted by the number of transceiver equipment involved in the end-to-end connectivity. Furthermore, as the transponders age faster than the OLS equipment, it requires high capital investments (CAPEX) every three to five years to avoid operations in an end-of-life regime. The burden from 3R can be significantly reduced if the spectral slot allocated for OSaaS is available in multiple consecutive operator domains. In this case, only one set of transceivers is required to implement end-to-end connectivity, which in addition to increased availability and decreased latency creates economic and environmental benefits like:

- CAPEX reduction from the transponder or demarcation equipment,
- reduction of energy consumption,
- reduction of CO_2 production,
- reduction of required human resources and
- reduction of waste products.

While the reduction in the CAPEX savings is expected, OLS operators also benefit from remarkably reduced operational costs (OPEX) due to the reduced amount of equipment. As the transceivers are the primary energy consumers in all-optical communication networks, OSaaS service model enables to discard the 3R at the domain borders, resulting in lower electricity, space, and cooling requirements, and thus the power consumption when compared to traditional service models for providing end-to-end connectivity. Over the years of operation, this can significantly reduce the CO_2 footprint, especially when human resources, indirect costs for equipment maintenance and utilization costs after transceiver end-of-life are considered. Fig. 2 compares the total investment required to implement a 100-Gbit/s DP-QPSK service through the Nordic and Baltic region, reaching from Helsinki to Frankfurt and traversing six OLS segments and 3000 km in end-to-end service distance. The presented example is based on calculations and not on financial figures or measured data from operators. With an example transceiver CAPEX cost of 25 000 EUR and a yearly energy consumption cost accounting for the operation and cooling based on the average NordPool market price per region (150 EUR/MWh) [31], the cost reduction from conventional to OSaaS-based end-to-end service is almost linear with the number of OLS segments traversed. While the CAPEX investments in both scenarios are creating the primary chunk of the costs, the reduction in OPEX costs should not be underestimated. In a world with increasing energy prices and a shortage of qualified workforce available for service commissioning, maintenance, operation and decommissioning activities, reduction in active network components is generally welcomed.

Another major benefit of the OSaaS service model is the increased availability of the end-to-end service. Based on the Helsinki-Frankfurt service example above, the OSaaS model is likely to reduce the service downtime by at least 14 hours and 23 minutes per year solely from the transceiver failures, which were previously required for the signal regeneration purposes at the border crossing sites, and can be dismissed in the new OSaaS operation model. This value is calculated based on a 200 000 h mean time between failure (MTBF) value for a single transceiver and a 4-hour repair time, which may highly differ between the operators considering the maintenance crew availability and driving distance to the remote border-crossing facilities. As the number of failures increases linearly with the number of services on the same route, the operational
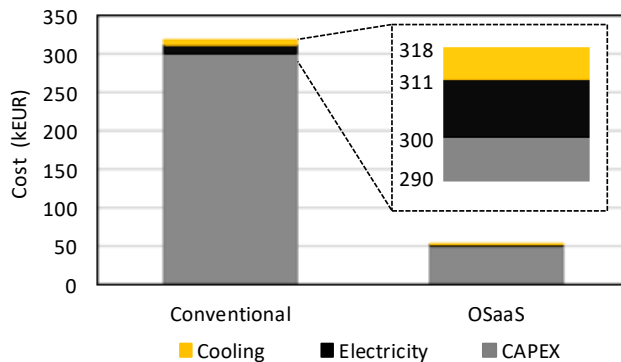

Fig. 2. Cost components over a 3-year service life-cycle

benefits that may seem negligible for a single 100-Gbit/s service scenario would sum up to a considerable win when the traffic requirements grow into hundreds of Terabits per second between the worlds distributed data centers.

Finally, OSaaS service model contributes to reduced emissions in multiple direct and indirect ways. The direct impact on the end-to-end service emissions introduced by OSaaS is considered as Greening-of-ICT (Information and Communication Technology). This shows through avoided production costs of the transceivers, reductions in operation costs (electricity consumption of the transceivers and avoided maintenance activities like driving to the site to swap or repair the broken device), and utilization costs. These costs are considered in the Net Zero strategy by European Commission, with the intention to minimize the CO_2 footprint by 2050 to net 0 [32].

In addition, sustainable systems lead to greening-by-ICT effect, which is caused by indirect emission reduction, achieved through working from home and hence reducing the emissions from commute, optimizations from smart home devices benefitting from Internet of Things, reduced private waste when using cloud computing, etc.

1.2 Challenges and research questions

Although the OSaaS concept has been around for a decade and the service model is common in submarine systems [33-35], there are four major problems, that require investigation, before the service model can be deployed in terrestrial brownfield production networks. These form the primary research questions for this thesis:

a) The generic functional architecture of the optical media network and the black-link approach do not define the possible implementation configurations for the Optical Spectrum as a Service. Therefore, no structured overview exists on how and in which production networks the service model can be implemented.

b) The service end customer sees the OSaaS as a "black box". Due to technology and component variations in production DWDM networks, it is complicated to estimate the exact service performance based on the proprietary or open Quality of Transmission (QoT) estimation tools. Solving the "black box" problem requires a development of a commonly accepted method to reliably capture the performance of the spectral slot.

c) The distinguishing service parameters for OSaaS have not been presented in a systematic manner. Previous works suggests using Optical Signal to Noise Ratio (OSNR) and Generalized Signal to Noise Ratio (GSNR), but in cases of OSaaS, these metrics alone may not characterize the OSaaS sufficiently in terrestrial brown-field systems. A more precise parameter set and method for OSaaS characterization should be developed that captures the possible wavelength-dependent variations, filtering penalty and operation regime.

d) There is no method and apparatus to provide demarcation functions and signal policing for the bundled signals operated within the OSaaS. This poses a threat to the OLS integrity, as the same customer light that enables the end-to-end service within the OSaaS can impact the performance of the whole OLS. Furthermore, the blurred operation model without clear service demarcation boundaries prevents the reliable service availability calculations.

1.3 Contributions of the thesis

This thesis approaches the four primary concerns raised in 1.2 and proposes solutions that are applicable for terrestrial brownfield optical networks. The primary contributions of the thesis are the following:

a) For the first time, a structured overview of the possible OSaaS implementation configurations is given, considering the terrestrial brownfield systems. This is complemented with the discussions on operational aspects related to each of the implementations, providing the end customers and service providers a clear picture of the benefits and concerns when deciding to implement a certain OSaaS configuration.

b) A comprehensive performance estimation toolkit for terrestrial brownfield DWDM systems proposed. Furthermore, a detailed overview of the error sources related to the performance estimation method is given to achieve the highest performance estimation accuracy.

c) A clear OSaaS characterization method is presented alongside with the required service margins to accommodate fast- and slow performance fluctuations in the networks, enabling neighboring channels, and end-of-life channel loads.

d) Finally, a Network Domain Interface Device alongside with a transparent Optical Overlay Networks concept is introduced. The device provides a set of interworking functions, among which are the service policing, telemetry data collection, and service level agreement compatibility calculations. The overlay networks concept proposes a market-changing new service model for open optical networks, enabling higher flexibility and transparency in future optical networks.

Due to the experimental nature of the derived concepts and verifications in live production networks, the contributions of the thesis enable the operators to take weighted decisions and measurable steps in implementing OSaaS in their production networks. As a result, higher network efficiency can be achieved, be it as easy as confidently allowing IP-over-DWDM traffic into the networks or interconnecting multiple network and operator domains to implement an end-to-end connectivity between geographically diverse datacenter sites with reduced environmental impact.

Table 1 maps the research questions to corresponding thesis chapters, publications, and contributions.

Table 1: Mapping of research questions to corresponding thesis chapters, publications, and contributions.

Research Questions	Chapters	Publications	Contributions
a	3	I	a
b	5	II-V	b
c	6	VI-IX	c
d	7	XIII	d

1.4 Thesis organization

This section introduces the layout of this thesis.

The second chapter of the thesis provides the background information about the optical communication networks and the service concept of the OSaaS. It provides insights to the available literature and standards covering the topic and provides an overview to taxonomy used in the research to describe the service.

The third chapter introduces the operator feedback gathered from 25 participants, operating telecommunication network worldwide. The chapter defines the OSaaS, as used in this work and discusses the management aspects of the service. It then presents the OSaaS implementation configurations and explains the operational aspects behind each of the configuration.

The fourth chapter introduces the OSaaS implementations built in the lab and commissioned in the live production networks that were required to address the research questions raised in section 1.2.

The fifth chapter introduces the experimental method used for the OSaaS performance estimations. The chapter covers various aspects impacting the accuracy of the method and explores the required changes to the method, applicable for OSaaS use-cases in brownfield terrestrial networks.

Sixth chapter analyzes the requirements for OSaaS characterization and required service margins to compensate for the possible future degradations. It introduces GSNR profile to capture the necessary characteristics of the service, like wavelength-dependent performance variations or filtering penalty at the service edges. In this chapter, also service margins to cover for fast and slow performance fluctuations, neighboring channel impact and end-of-life channel loads are derived, utilizing telemetry data collected from the live networks and systematic lab study in Open Ireland CONNECT lab. This chapter also demonstrates how GSNR profiles from individual network segments can be concatenated in procurement phase of the services to estimate the final achievable capacity of the end-to-end link.

The seventh chapter proposes the Network Domain Interface Device (NeDID) and transparent optical overlay network concept to safely implement any domain-to-domain transition for the bundled optical signals. The chapter explains the functions provided by the device and how these help to provide clear demarcation boundaries, monitor and police the signals entering the device and the next domain. In addition, the optimization perspective of such overlay optical networks is discussed using the channel probing technique.

Finally, the last chapter concludes the work included in this thesis and provides some insights to the future work.

2 BACKGROUND

2.1 Fiber-optic transport basics

Early optical communication systems (semaphores) implementing smoke, mirrors, or fire beacons to send messages over long distances date back to ancient civilizations. The primary limitation of such systems was the limited pre-agreed content of the transmitted messages. Such messages were used in a broadcast mode to announce winning a battle or foreseeing a threat. Attempts to enhance the content of the messages and therefore increase the amount of transmitted information have been made throughout history. In 1792, an optical telegraph was invented by Claude Chappe. His invention presented a device with a set of predefined messages, that enabled transmitting mechanically coded messages over intermediate relay stations, located 10-15 km apart. Although the effective bit rate of such systems was less than 1 bit/s, it enabled sending a new, not pre-agreed content to the endpoint. The optical telegraph system was replaced by the electrical telegraph in the 1830s. The new electrical communication system enabled bit rates of a few bits/s by using a Morse code, employing two electrical pulses of different durations (dots and dashes). With the use of intermediate relay stations, the first successful transatlantic telegraph cable went into operation in 1866, interconnecting two continents.

There is a strong interplay between the technology and society – the way we interact with them, the way they phase in and out of use, the way they dictate our actions [36]. To set a scene for the customer expectations at the time, the world had entered an "age of invention," extensively presenting the latest achievements of industrial civilization at the World Expos events held in London (1851), New York (1983), Paris (1855), etc. Only a decade later, in 1876, the invention of the telephone brought a major change inasmuch as electric signals were transmitted in an analogue form through a continuously varying electric current. The electrical era in telecommunication, which lasted a century, ended in 1970s, when mutual effort to reduce fiber loss made it possible to use it for a long-haul communication (10 km at a time). With the improvements of lasers and introductions of erbium doped fiber amplifier in 1987, optical communication has become the primary form to transport voice and data.

The primary principles developed in 1970s are still valid for optical communication even today: modulated light signals are used to transport data in a guided medium formed from a narrow silica glass cylinder, referred to as optical fiber. Today, common for a long-haul network interconnecting cities, countries and continents, the signal is optically amplified every 60 to 100 km and multiple signal carriers with slightly different wavelengths are transported together in one fiber pair using wavelength division multiplexing. Depending on the system design and components, these light signals can travel thousands of kilometers without the need for signal regeneration.

While the first optical communication systems were mostly carrying voice, the introduction of World Wide Web and the Internet in 1995 started to increase the share of the data traffic used on the links. In parallel to growing online gaming and video streaming mostly used for entertainment, first video conferencing platforms became available in early 2000s. The growing social media trend increased the interest to express themselves and stay connected through platforms like Orkut, Twitter,

Instagram, and Facebook, while Internet of Things is paving the way for continuously connected devices – be it a video surveillance camera, an electricity metering device or a robotic lawnmower. In addition to this, a huge amount of the information transported on long-haul links today is used by datacenter operators to sync the data between datacenters and enable fast and reliable cloud computing experience for humans and devices. Furthermore, as the conventional broadcasters also move to Internet in order to stay competitive with the video-on-demand providers like Netflix, YouTube, and others, the amount of traffic transported in optical networks grows exponentially.

Based on Govind Agrawal's book "Optical Communication: Its History and Recent Progress" [37], there are six generations, when it comes to optical communications. The first generation was available starting from 1975 and used GaAs semiconductor lasers operating at a wavelength near 850 nm, and the optical bit stream was transmitted through graded-index multimode fibers. The second generation was available from early 1980s and was operated near 1300 nm using InGaAsP semiconductor lasers. The second distinguishing factor was the swap of the graded-index multimode fibers to single-mode fibers to better control the modal dispersion. The third-generation optical communication systems became available commercially in 1990. The initial bit rate 2.5 Gbit/s was soon extended to 10 Gbit/s, as the performance was continuously optimized by using dispersion-shifted fibers and lasers oscillating in a single longitudinal mode around 1550 nm. The fourth generation of optical communication systems made use of optical amplifiers for increasing the repeater spacing, in combination with the Wavelength Division Multiplexing (WDM) technique for increasing the system capacity. The focus of fifth-generation systems was on making the WDM systems more efficient spectrally. This was accomplished by reviving the coherent detection scheme that was studied in the late 1980s but abandoned soon after fiber-based optical amplifiers became available. Coherent receivers capable of detecting both the amplitude and phase of an optical signal through a heterodyne scheme were adopted soon after the year 2000. Even within this generation, sub-generations can be distinguished – from the first coherent transceivers to flexible modulation, to fully flexible sliceable transceivers, capable of varying both modulation, and symbol rate. To overcome the intrinsic capacity limit of the single-mode fiber, Spatial Division Multiplexing (SDM) schemes became under interest. Similarly to the WDM technology, the implementation of SDM requires not only new types of fibers but also many other active and passive optical components such as mode multiplexers/demultiplexers and fiber amplifiers that can amplify signals in all modes/cores simultaneously. Fig. 3 introduces the increase in the Bit rate-to-length
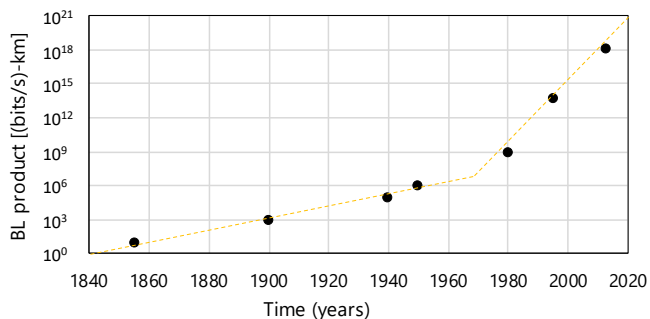

Fig. 3. Bit rate-to-Length (BL) product as per Agrawal [37]

or capacity-to-reach product during the period 1840–2015. The emergence of new technologies is marked by markers. Dashed line shows the trend as an aid for the eye with a change in slope around 1977 when optical fibers were first used for optical communications. A comprehensive overview of the history of optical communications over the past two decades and insights to the next decades to come are outlined in [38].

With the passing of time, the technologies used to provide connectivity mature and the networks are continuously built out to cover higher percentage of populations to provide affordable wireless and broadband access. Together with the digitalization and continuous developments in other Information and communication technology (ICT) sectors, the availability of ICT infrastructure and network access has an increasing impact on the success of businesses, individual human beings and – our economy in general [39-41]. This leads the end-customers to demand for specific characteristics to be applied to the end-to-end connectivity, starting with higher throughputs and spectral efficiencies, to highest achievable availability, highest security, and lowest latency. Very often, these demands are carried over the same optical infrastructure, and over the same DWDM system. These different demands can be met by employing different end-transceivers, manufactured and finetuned for specific requirements. For example, optical transceivers with lowest MTBF can be used to reduce unavailability of the connection and cryptography can be added to the optical transceivers commissioned to provide secure connectivity. The latency can be targeted by avoiding any obsolete active processing equipment and keeping the signal routing in all-optical domain using transceivers with minimum latency as the simplest solution. However, achieving higher capacities in a predetermined spectral slot may require a more complex solution. As the fiber-optical medium is nonlinear by nature, the power of the signal cannot be infinitely increased in order to maximize the capacity. Instead, following three methods can be used to increase the efficiency of the system: Increase the number of carriers (WDM), increase the symbol rate or increase the constellation, as pictured on Fig. 4. The beauty of the WDM systems is, that in each part of the spectrum, same three methods can be used and therefore, the achievable capacity-to-reach product can be optimized for different use cases.

Short-haul Fibre Channel and InfiniBand connectivity used in connecting datacenter mainframes, can use the highest constellation, symbol rate and number of carriers applicable for the link OSNR, while some of the long-haul connectivity would be optimized for maximum capacity-to-reach product, and others for minimum transmission delay.
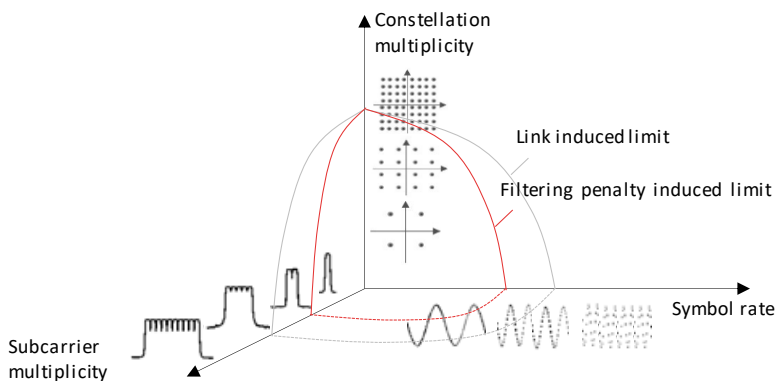

Fig. 4. *Methods to increase efficiency per polarization mode in WDM systems*

2.2 Disaggregation trend and OSaaS

Conventionally, services in telecommunication networks are provided end-to-end by the service operator. Distinguished by the provided capacity, transmission protocol, expected service availability, and sometimes delay, the service parameters are fixed during service hand-over and keeping the services operational as per agreement is the sole responsibility of the operator. However, the advancements in the transceiver technology have been fast in the last decade, providing the possibilities to meet the unique demands of the end-customers. This has triggered a will to use third-party transceivers over the available optical communication system infrastructure, that was conventionally optimized for a specific transceiver type, manufactured or at least, approved, by the system vendor. As the line system components in the WDM systems are transparent to any light, many of the customers negotiated the service providers to just provide the spectral slot in the systems, using a so-called alien wavelength concept. In alien wavelength service model, a spectral slot with 50-GHz or 100-GHz nominal channel bandwidth in the network is sold to the end-customer with the right to deploy one third-party terminal per alien wavelength service. The service is usually characterized with an optical signal to noise ratio (OSNR) and a fixed Transmit (Tx) power To-The-Line (TTL). Mostly, also the allowed third party transceiver configurations are pre-agreed. This kicked off the disaggregated era within the optical communication systems. The more such services became an integral part of an operator's service portfolio, the more end-customers were encouraged to seek the flexibility, that a wider block of spectrum would allow in terms of spectral efficiency. This led the optical spectrum as a service (OSaaS) to gain traction.

In OSaaS, the spectral slot to be allocated for the customer is only partially dependent on the nominal channel bandwidth of the network. Differentiated from an alien wavelength service, which can be viewed as the bandwidth restricted form of an OSaaS, the OSaaS is capable of transporting multiple carriers over a wider, continuous spectrum slot. This allows the spectral resources within OSaaS to be operated by the end-user as desired, either prioritizing spectral efficiency, availability, security, or latency. If the desired spectrum is continuously available in all included network segments, similarly to alien wavelength, OSaaS can be operated over thousands of kilometers without signal regeneration at the domain end nodes. Avoiding unnecessary regeneration can provide multiple benefits compared to traditional network architecture: reduced capital investments into the expensive transponder and demarcation equipment, reduced energy consumption, reduced requirements for human resources to maintain the service, and reduced electronic waste products and utilization costs at the end of the equipment lifetime. As the OSaaS service model allows end-user to use the spectrum as desired, and the provider does not have to carry the expensive transceiver-related costs to implement end-to-end connectivity, the service model became quickly attractive.

2.3 State-of-the-art

The first work in literature addressing the operation of third-party equipment over an OLS dates back to the early 2000s. Enabled by the so-called "black-link" approach, introduced in ITU-T recommendations G.695, G.698.1 and G.698.2 [21-23], various demonstrations were reported: optical fiber infrastructure sharing to enable triple-play services [42,43], IP-over-WDM [44-47] and alien wavelength services [48,49]. Reference [50] proposed a parameter set for an alien wavelength service and [51,52] discussed the motivation and operational challenges for implementing alien wavelengths over an open Dense Wavelength Division Multiplexing (DWDM) system. Different switching modes for alien wavelengths with wavelength and waveband granularity were discussed in [53]. With the advent of flex-grid systems in the early 2010s, more effort was put into understanding the spectral transfer function [54], spectrum resource allocation [55,56], regeneration requirements due to spectral allocation [57], the wavelength-dependent performance variations in the network [24, 58] and security aspects [59] of alien wavelength services. To stress that the service model fits for various applications, alien wavelength services were also called photonic services [60-63]. In time, more focus was put on standardization efforts of the "black-link" [64-68], which represents the physical medium, or the media channel as per ITU-T recommendation G.872, introduced in October 2012 [69].

With the clear vision for disaggregated networking and motivated by the need to operate real-time applications over DWDM networks, the national research and education network (NREN) community has been continuously at the forefront of the developments of alien wavelength and alien spectrum services. Reference [70] lists many trials and experiments that investigate various aspects of alien services, from spectrum sharing between different NRENs to the development of advanced photonic services. Many transponder upgrade installations and achievable capacity demonstrations using new sliceable transceivers are actually alien wavelength configurations, as the transceivers were managed separately from the OLS system components [71-76]. With the increasing motivation to use alien wavelengths in production networks, disaggregated networking gains further traction. Various papers discuss the control and management questions over elastic, multi-vendor, multi-domain environments [77-81]. The dominant trend from fixed-grid networks towards elastic flex-grid networks triggers investigations in the spectrum assignment and routing domain [82-88]. Simultaneously, QoT estimations in a black-link scenario are investigated [89-97]. Several works also cover the architecture, topological use-cases, and requirements for such alien services [98-104], including the ITU-T recommendation G.807 [20] that defines the generic functional architecture of the optical media network. References [105-109] report multiple benefits and increased efficiency in using third party transponders over an existing OLS. Many papers discuss the implementations in terrestrial and submarine networks [110-112], including ITU-T recommendation G.977.1 [113], providing guidelines for physical layer specifications for DWDM applications on dispersion-unmanaged repeated optical fiber submarine cable systems. However, the author is not aware of any publications that provided answers for the research questions raised in 2.1. This could be explained with the vague definition of the OSaaS in general, as no systematic overview on the possible OLS configurations to formulate the lightpath for

OSaaS existed, nor the exact understanding what data to include in the characterization of this new service type. Furthermore, the lack of clear demarcation point for the OSaaS handover at the service add/drops or domain borders was not addressed, creating further confusion with service characterization.

2.4 Relevant standards and terminology

In order to make connections between different terms, used to explain the same phenomenon in the literature, the taxonomy used on physical, system and lightpath level can be presented as following, starting from the physical infrastructure level. For any optical system to be built, dark fiber is required. The dark fiber term is uniformly understood, referring to an un-lit optical fiber pair within the optical cable, installed between two end locations. These end locations, often called co-location sites, when equipment installation space, electricity and cooling is provided, mark the possible endpoints in the possible network link.

When this dark fiber is equipped with fiber amplifiers, dispersion compensation modules and reconfigurable add/drop multiplexers (ROADMs), an optical link between two endpoints is established with the unique geographical locations marking the route. If the Wavelength Selective Switches (WSSs) within the ROADM modules are flexible, or flex-grid, this link is part of an elastic optical network. If the link operator is open to host third-party transceivers, or sliceable bandwidth variable transceivers (S-BVT), operated by the end-customer, the link is a part of an Open Optical Network or Elastic Optical Network and is often referred to as Open Line System (OLS). On top of this OLS, lightpaths can be created. These may have many terms in the literature. If the parameters of such link are not known to the end user, a black link term can be used. Otherwise, also Elastic Link, Optical Channel (OCh), optical cross-connect (OXC), when opened in all consecutive ROADMs on the link, lightpath, light-trail, media channel (ITU-T), media channel group, alien wavelength, alien spectrum, virtual dark fiber, spectrum connectivity service (by GEANTT). From the service provider and connectivity perspective, these lightpaths can be either provided as Alien Wavelengths, Optical Spectrum-as-a-Service (also Optical Spectrum Services), Network-as-a-Service or Infrastructure-as-a-Service. These services can be opened in one or more segments in the OLS, and continued in one or more operator domains, if the spectrum slot allocated for the service is sequentially available in the next domains. Finally, each of these services can carry one or multiple modulated light signals that carry end-user traffic. These are referred as Optical Tributary Signals (OTSis), carriers, or "bearers". At the service termination site, a demarcation location must be specified. This can be based on signal/lightpath/domain demarcation and are currently just a selected location in the infrastructure, not necessarily related to the OLS. A commonly used demarcation point for alien wavelengths today is a connector at a colocation site providers optical distribution unit, where the signals from third-party transceivers are interconnected to the dedicated port in the service provider OLS system.

To dig once more into the properties of the black link, which refers to a networking approach, where the details of the optical link design are proprietary to the end-to-end link designer and not available for the link end user. Therefore, this kind of black link can consist of any passive elements (e.g. fibers, optical multiplexers, optical demultiplexers, etc.) or active elements like various types of optical amplifiers, reconfigurable add/drop

multiplexers utilizing wavelength selective switches (WSS), etc.). Sometimes, also adjective "elastic" is added to the general "black link" to refer to flexibility in configurations for the spectral region in the optical network covered by the service. This specification method has currently been used in multi-channel transmission specified in Recommendations ITU-T G.695 [21], ITU-T G.698.1 [22] and ITU-T G.698.2 [23], describing the Coarse Wavelength Division Multiplexing, passive Dense Wavelength Division Multiplexing and active Dense Wavelength Division Multiplexing, respectively.

The terminology to describe the media channel, as the building block for OSaaS services is explained in ITU-T Rec. G.807 [20]. It's Appendix 1 [114] gives deeper insights to the relationship and terminology between the Media Channel (MC) and third-party transceiver pair, emitting an alien wavelength called Optical Tributary Signal (OTSi), controlled and operated by the end-user of the OSaaS.

As already mentioned before, a new ITU-T recommendation is targeting the taxonomy of the parameters used to define the service performance from commissioning to end-of-life, which are applicable also for brownfield terrestrial systems [113]. The closest to regulate the usage of the OSaaS, are the recommendations provided in ITU-T Y.3512: Cloud computing – Functional requirements of Network as a Service [115].

3 OSAAS IN DISAGGREGATED NETWORKS

This chapter introduces how OSaaS is defined in this work. The chapter also presents the survey results from 25 participants, operating telecommunication networks around the world, highlighting their desires and concerns about the OSaaS service model. A systemized overview of the OLS configurations based on the Media Channel building blocks is presented, focusing on OSaaS implementations in terrestrial, brown-field network scenarios. Finally, the management and operational aspects of the OSaaS are discussed.

3.1 OSaaS definition used in this work

In this work, Optical Spectrum as a Service is defined as a transparent lightpath connecting two endpoints in a single or multi-domain optical network. Differentiated from an alien wavelength service, the OSaaS is capable of transporting multiple Optical Tributary Signals (OTSi) over a predetermined spectrum slot. If the desired spectrum is continuously available in all included network segments, OSaaS can be operated over thousands of kilometers without signal regeneration at the domain end nodes. Based on [20], the lightpath used for OSaaS is built from a combination of Media Channels. To achieve maximum flexibility of the terminal S-BVTs, this work uses the [20] option to not map individual OTSi into individual Network Media Channels. This reduces the required configurations in the OLS and makes OSaaS service model available also in brown-field systems. The general OSaaS service concept, illustrated for a single domain and multiple domain scenarios, made available by different operators, is illustrated on Fig. 5.

   The OSaaS customer transceivers are inserted into the network using a colorless access. In case of multiple different end customers, each of the end-customers has their own access structures and is connected to a dedicated port in the Reconfigurable Optical Add/Drop Module (ROADM). Alternatively, to provide filtering function for possibly colliding customer signals, a single ROADM customer port equipped with fixed-grid filters can be used.
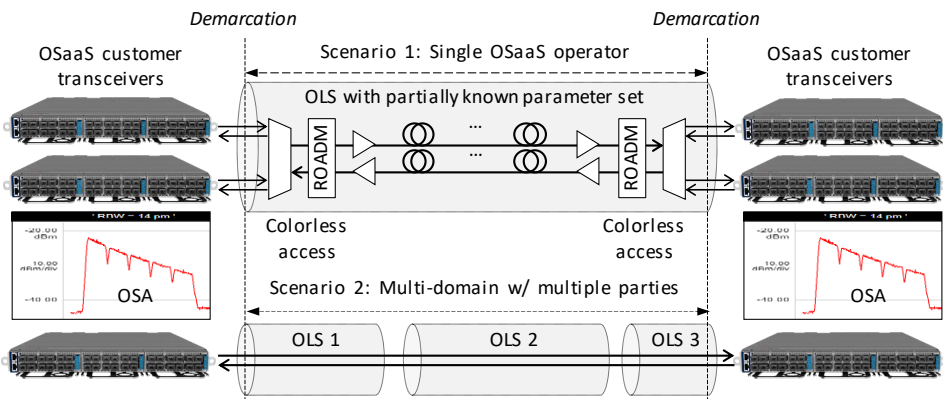

Fig. 5. *OSaaS concept and terminology used in this work*

As the responsibilities in this service model are shared, the operator is only configuring the OLS, while the end-customer is required to provide full signal load as per power spectral density for the OLS equalization. After this activity, the transmitted power levels should be fixed both in the transceivers and in the OLS. Furthermore, the customer is entitled to maintain the power spectral density of the signals in case of transceiver reconfigurations.

3.2 Conclusions from operator survey

Although the concept of the Optical Spectrum as a Service is not new, the mass implementations of OSaaS are not yet common due to various concerns about the configurations, achievable performance, service level agreement uncertainties and technical concerns. Most operators providing the service today provide their spectrum in a form of alien wavelengths to maintain better control over power levels entering the OLS. In order to capture the operators views on Optical Spectrum Services and providing this as a service, a customer survey consisting of 15 questions was compiled by the author. The questionnaire was then shared with operators and the answers were collected between 1st of June and 31st of January 2023 through one-on-one interviews with the author or anonymously filling in the survey questionnaire. During that timeframe, 25 participants operating telecommunication networks in different countries and fields provided the feedback about their current opinions about OSaaS. The top part of the Fig. 6 displays the information about the participants home countries, primary field of operation, and information about their operated networks. The bottom part of the Fig. 6 presents the participant's readiness to provide OSaaS to end customers and to sell it to a wholesale's operator.

According to the answers, 48% of the companies had up to 1 000 employees and 40% of the companies had more than 1 000 employees. Only 12% of participants declared their company size to be less than 100 employees. 40% of the companies were operating in only one country and 28% were operating in up to 10 countries. 32% of the participants company operated in more than 10 countries. By field, the answers divided between National Education and Research companies (NRENs), Wholesale providers and Mobile operators with 20, 20 and 12% from the answers. 24% of the participants operate mission-critical networks, providing services primarily to electricity, gas, water, or other utilities and 24% operate business-critical networks, providing services to banking, media distribution, datacenters, etc).

40% of the systems operated today are 3 to 8 years old and 24% of the systems are nearing end-of-life in age, being more than 8 years old. However, 25 OLS systems out of 33, operated by the survey participants, still have at least 40 to 80% free spectrum available in the OLSs for new services. However, most of the systems are operated with a distributed channel plan, where the native channels are equally or randomly distributed over the C-band. This is good for power balancing but not ideal for providing OSaaS. From the technology perspective, most of the participants operated OLS systems with various technologies. 16 out of 25 participants declared to still operate a 10-Gbit/s optimized dispersion compensated direct detect systems. This was closely followed by standard fixed-grid coherent 100-Gbit/s optimized systems, operated by 13 survey participants and flex-grid coherent 100-Gbit/s systems, also operated by 13 survey participants, both
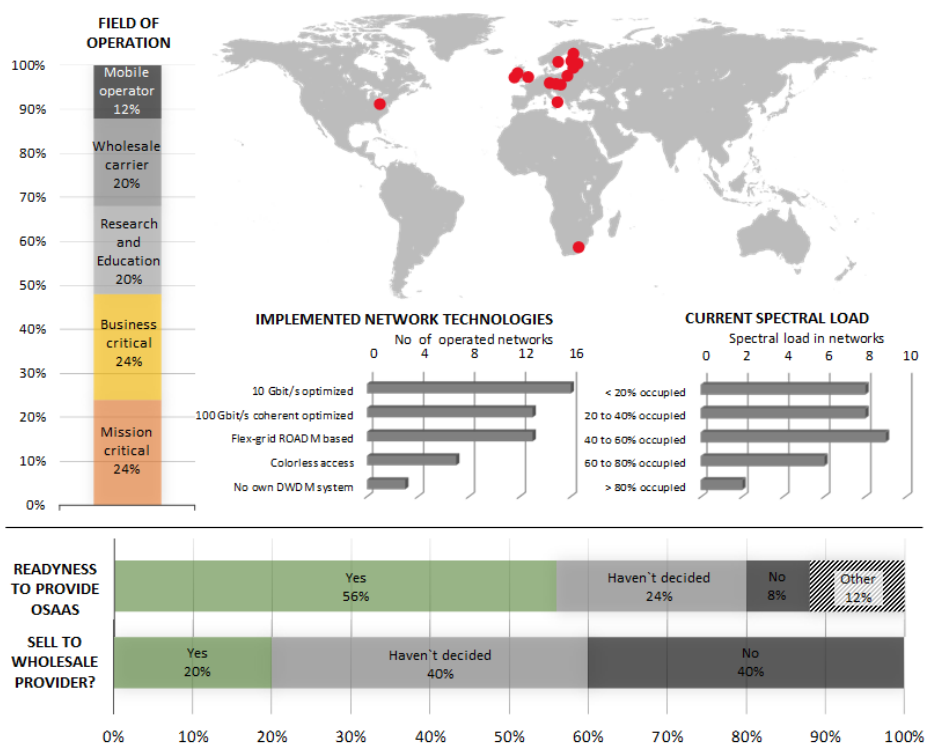
Fig. 6. *Findings form the operator survey*

still using fixed-grid filters in the add/drop structures. Only 7 participants had deployed colorless access for their coherent optimized OLSs.

The primary driver for providing the OSaaS services with nine answers from the participants is the customers requesting the services. This was followed by a free available spectrum that could be monetized, prioritized by six participants. However, for many participants, the main driver for implementing OSaaS was the possibility to avoid 3R and usage of 3rd party transceivers over the OLS infrastructure, either for capacity upgrade or implementing IP-over-DWDM. Some operators also pointed out the reduced cost perspective of the OSaaS implementations.

Today, the operators are well aware of the technical deficiencies in implementing the OSaaS service model. 60% of the participants are most concerned about the power leveling, be it a total power per service or securing power spectral density within the service. While 56% of the participants stress the importance of mutual responsibility in keeping the OSaaS service within the desired performance range, 20% of the participants are eagerly looking for options to keep the performance within the agreed thresholds themselves. Some operators are also cautious of any rough signals that may enter the system (for example On-Off Keying (OOK) signals in coherent-optimized systems). In general, 56% of the participants are ready to provide the service when gaining control over technical concerns and 24% have not yet decided. Only 8% of the participants have a clear decision not to implement OSaaS in their networks. 48% of the participants ready to provide the service would prefer to provide OSaaS only to other carriers or end

customers, who also operate the DWDM systems, as they are familiar with the delicate power balancing aspects of the signals. The other half of the survey participants have a bit more conservative plans, using the new service model primarily for themselves (24%), or providing it only within partnership projects (24%). Out of all the participants, 20% are ready to sell the OSaaS also for a wholesale provider, and 40% have not made up their minds about it. However, 40% of the operators today are not considering this, as an option. Answers in this group were mainly collected from participants operating mission- or business-critical networks.

To charge for the service, 74% of the survey participants plan to tie the cost of the spectral services either to a dark fiber or leased capacity rental costs, finetuning the offer by the amount of spectrum used in the system. Yet, the pricing structure is not yet 100% fixed by the operators, and the discussions to determine the best pricing model are still to be carried out. 26% of the participants plan to swap spectrum to a similar amount of spectrum in a partnership project, or in case of an internal use of OSaaS, not have any cost plan attached to the service.

As a conclusion, operators are aware of the OSaaS service model but are still in a waiting position for the technical deficiencies to be solved by DWDM system vendors before committing to mass deployments of the OSaaS.

3.3 OSaaS configurations

This sub-chapter aims to systemize the possible OLS configurations to implement the OSaaS lightpath between two end points in the network. To implement a lightpath, guidelines from ITU-T Recommendation G.807 [20] describing the generic functional architecture of the optical media network are used. According to this, the primary building block to allocate the spectrum in the OLS is the Media Channel (MC). A desired spectral width can be allocated by using only one MC or combined from multiple MCs. The MC width may be dependent on the technology of the underlying DWDM system, but it does not necessarily have to follow to width of the Optical Tributary Signal(s) (OTSi) that will be implemented by the end customer of the OSaaS. As discussed in 3.1, each OTSi can be directly operated inside the MC, or alternatively, a dedicated Network Media Channel (NMC) per OTSi can be configured. In this work, no NMC configuration for the OSaaS lightpath is not required.

Although the OSaaS can be provided and operated in any DWDM system, regardless of the system technology, the technology may limit the feasible configurations for OSaaS. These depend on the add/drop structures and ROADM technology used. In general, four OSaaS configurations exist. The overview of the four primary configuration options for the transport of five 69-GBd OTSi is illustrated in Fig. 7.

The only configuration option available in networks utilizing fixed-grid filters in the signal add/drop path, channelized dispersion compensation gratings (DCG) for chromatic dispersion compensation, or older ROADM technologies (not liquid crystal on silicon) is a narrow-band OSaaS configuration (a). Although this configuration has been successfully used for alien wavelength services in the past, the configuration is not optimum for modern, variable symbol-rate transceivers. Modern transceivers, typically operated with symbol rates of 60 GBd or higher, may experience a narrowband filtering performance penalty when operated in a fixed-grid networks [94, 95]. The benefits of high baud-rate
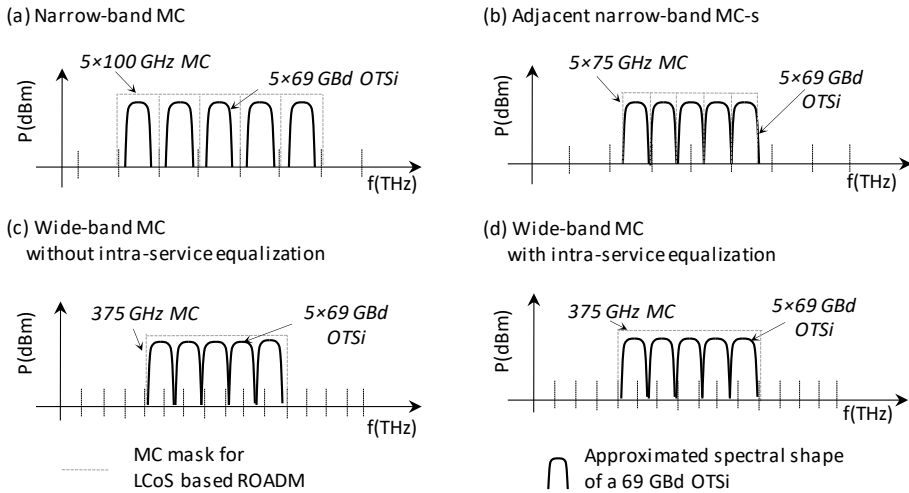
(a) Narrow-band MC

(b) Adjacent narrow-band MC-s

(c) Wide-band MC
   without intra-service equalization

(d) Wide-band MC
   with intra-service equalization

- - - - - MC mask for
         LCoS based ROADM

∩ Approximated spectral shape
   of a 69 GBd OTSi

Fig. 7. *Four configuration options for OSaaS*

transceivers are better utilized when colorless add/drop structures and dispersion-compensation-free OLS are used. Without any channelized component in the OLS, continuous spectrum as per OSaaS configurations (b), (c) and (d) can be provided to the end customer. In fixed-grid ROADMs, 50 GHz or 100 GHz channel spacing from ITU-T Recommendation G.694.1 [11] can be used to combine multiple adjacent MCs into a wide-band OSaaS configuration (b). Flex-grid ROADMs can use any multiples of the 12.5 GHz increments to configure wide-band OSaaS (b) or allocate a single wide-band MC covering the full OSaaS bandwidth. Depending on the capabilities of the ROADM, a wide-band MC can be equalized as per total signal power (configuration (c)) or power spectral density (PSD) (configuration (d)). However, the latter is used only in the newest OLS implementations.

3.4 Challenges in OSaaS management

After the lightpath for the OSaaS is configured by the OLS operator, the end-customer can install the transceivers at the end-locations. As the MCs in the ROADM configuration are enabled, the customer signals from the dedicated C-port of the ROADM are routed to the network port of the ROADM. This typically includes a signal equalization activity, so that the design-based signal power per MC could be met. Furthermore, when different customer transceivers are configured to transmit with different modulation format and symbol rate configurations, it may impact the power spectral density within the OSaaS. If configuration (d) from Fig. 7 is not available, maintaining the PSD in the OSaaS is a complicated task in brownfield terrestrial systems and requires good co-operation between the end customer and service provider. The simplest method to equalize OSaaS spectrum to the design-based PSD of the OLS is to use the OTSi configurations utilizing the widest spectral with, like 200-Gbit/s 69-GBd DP-QPSK and configure the full OSaaS spectrum with OTSis using this configuration only. The signals leaving the ROADM network port can be then equalized using the maximum allowed PSD and total power of the OLS. After this, the customer can change the OTSi configurations as desired, assuring

that each of the reconfigured OTSi is maintaining the PSD of the OLS. This can be achieved by manually adjusting the Tx power levels of individual OTSi. Alternatively, OSaaS configuration option (b) with the smallest available MC width, 12.5 GHz can be used for the signal equalization in the first ROADM. However, this may introduce excessive amount of filtering, even, when such MC width is used only in the first ROADM node on the link. Further discussions on the importance of equalization and why noise loading cannot be used for the task are discussed in [133].

Maintaining the performance of the OLS is the responsibility of the OSaaS service provider. This includes maintaining the ROADMs, amplifiers, and recovering from any possible interruption, that may be caused by the human error, failing device or environmental impact. This means, that fiber repairs, that may increase the attenuation of the impacted span, must be compensated by further amplification power. In addition, daily and yearly performance fluctuations in the network should be addressed through power adjustments of the OLS.

These responsibilities between the end customer and OSaaS provider are unfortunately only agreed on paper, and many unexpected scenarios my impact the parties' capabilities to comply with the committed responsibilities. In case of the OLS performance, one of the common problems is the capability to quickly suppress the power transients, that are caused by a sudden loss of a big chunk of carriers in the OLS. This can be caused by the power outage in the customer premises or a failure in the previous OLS system, in case of a multi-operator, multi-domain OSaaS operation. Such power transients are often not treated in terrestrial brownfield systems, as ROADMs equalization function is not designed to track these sudden changes. Another common problem related to the power levels is the power spectral density distribution within the OSaaS, or generally higher power levels per whole OSaaS, which can introduce spectral hole burning (SHB). The exact mechanism causing the SHB is explained in [116], while references [117] and [118] explain the impact of the SHB in transparent optical networks and it's dependency from channel load conditions. In OSaaS use cases, when the spectrum is lightly populated, but the channel load in OSaaS compared to the total number of channels is high, the changes in the power distributions within OSaaS can be caused by customers changing the configurations of one or more of the OTSi within the OSaaS and not immediately changing the total power of the OTSi to meet the required PSD. With the symbol rates available in the commercially available S-BVTs, which are between 28 to 72 GBd, the difference can be up to 3.5 dBm per carrier. However, as the industry is moving towards higher symbol rates, with 105, and 128 introduced in the research literature [119, 120], this change in the power spectral density can be up to 6 dB between the lowest and highest symbol rate configurations (which equals a 4-fold difference in the linear scale).

The ability to impact the OLS performance with as little as reconfiguring the OTSi creates friction in defining the service level agreement, as the responsibilities and demarcation, although defined, cannot be controlled in the timely manner. Furthermore, as the OLS information is often handled as business-critical information, the end user does not have a visibility to monitoring data collected from OLS components. Similarly, the OLS operator does not have the access to customer equipment. The control and management of the devices in the OSaaS use case is illustrated on Fig. 8. However, as discussed earlier, the agreement-based parameter settings do not provide a good
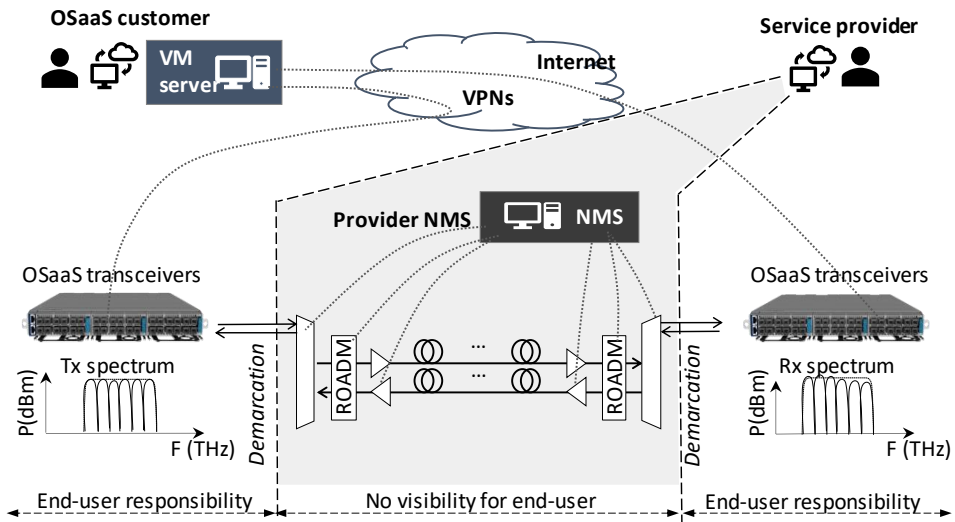
Fig. 8. *OSaaS management*

demarcation point that can be mutually accessed for monitoring and service level agreement connectivity assessments from both ends. Therefore, the length of the system with traversed optical components, number of OTSi operated by the end customer and configuration of the OSaaS has a big role in defining the operational complexity of the OSaaS today.

3.5 Operational complexity

As total signal power from alien carriers increases the vulnerability of the OLS system, it is important for the OSaaS providers to have the maximum control over the individual OTSi used within the OSaaS services. OsaaS configurations with adjacent narrow-band MCs have a smaller power per MC and are therefore simpler to operate by the OsaaS provider, as the MCs can be controlled by the simple, per-MC power adjustments during ROADM equalization. Wide-band MCs without intra-MC PSD-based equalization may lead to scenarios, where total dedicated power per MC is used on a single OTSi within the MC. This can even happen during equalization, when only one customer OTSi is enabled, and the wide spectral slot is equalized per total available power per slot. As discussed in previous subchapter, such introduced power variations in the network may cause spectral hole burning (SHB) or other effects that may impact the performance of the neighboring spectral parts. However, with careful operations, wide-band configurations enable the implementation of various networking techniques, like GSNR-based signal pre-emphasis explained in [8], low-margin networking [121], or flexible spectral allocation within the OSaaS service. As a downside, wide-band OSaaS configurations are more prone to wavelength-dependent performance variations. A single wide-band MC may incorporate a pronounced ripple or tilt effect from the EDFA and Raman gain spectrum, reaching up to 1 dB peak-to-peak ripple per span [116, 122, 123]. This is especially evident on longer transparent links, where the OLS spectrum is not adjusted after each span [124]. The effect can lead to a large power ripple and tilt

within the OSaaS bandwidth, resulting in wavelength-dependent performance variations. This will complicate the achievable capacity calculations within the OSaaS, as the GSNR required for that exercise is not constant over the service bandwidth. While a single MC with an intra-MC PSD-based equalization scheme and multiple adjacent narrow-band MCs in a flex-grid system would significantly suppress the ripple and tilt effect from the transmission medium, they may not be able to entirely compensate for the underlying infrastructure.

3.6 Conclusions

Although Optical Spectrum as a Service is a service type that operators are willing to employ, the implementations in the production networks are delayed due to many technical deficiencies. This chapter provided a definition of the OSaaS and a systematic overview of the possible lightpath configuration options suitable for the terrestrial OLS systems. Based on the available configurations, the OSaaS can be implemented in any DWDM network. However, due to the missing PSD-based equalization functions and dedicated demarcation equipment in the brownfield terrestrial networks, the OSaaS service model can introduce multiple operational problems. These problems have a potential to disrupt the optimal operation of the OLS and cannot be addressed in a timely manner.

4 TEST SETUPS AND IMPLEMENTATIONS USED IN THIS WORK

As explained in Chapter 3, OSaaS has four configuration options, which ultimately determine the achievable capacity within the spectrum slot. However, because of the open and disaggregated environments, it may be complicated to estimate the exact performance, achievable capacity, and required service margins of the OSaaS using proprietary or open planning tools [125-127]. This is especially typical in use-cases where the service provider regards detailed information about OLS as business-critical information. As a result, the end-user perceives the OLS as a black box / black link. However, an experimental approach can be taken to evaluate a specific OSaaS implementation's performance, achievable capacity, and margins. To reliably capture the OSaaS performance-related aspects and verify the experimental concepts proposed in this work, both lab and live environments must be tested. The primary goal of the lab environment is to avoid random fluctuations caused by changing environmental conditions and any interference with live signals. On the other hand, the environmental impact of hundreds of kilometers of live fibers installed in harsh environments exposed to temperature changes, direct sun, freezing, water, and lightning can contribute to time-dependent performance variations. These can only be captured in real-time production environments. Capturing the magnitude of the time-dependent performance variations enables to derive margin estimations methods usable in future OSaaS implementations in live environments.

This chapter introduces the coherent transceivers and experimental setups used in this work to detect OSaaS performance without any knowledge about the OLS's specifics by analyzing the light parameters of the end terminals. In general, the test setups can be divided into three categories:

- PLT transceiver characterization,
- Lab set-up with added broad or channelized amplified spontaneous emission (ASE) noise for variable OSNR and channel load testing, load-dependent margin derivation, and
- Live network environments for concept verification and time-dependent margin estimations.

4.1 Terminal S-BVT transceivers

Various fields of science use probing activity to gather knowledge about something that appears as a black box (or link, in the case of OSaaS). A probing activity is when a tool is inserted into an unknown environment to gather data about its parameters. Various parameters can be collected depending on the probe. In the case of an OSaaS, a characterized light can be inserted into the OSaaS spectrum. This requires the use of a characterized light source, which allows for to compare the sent and received light signals and, as a result, estimate the performance of the OSaaS. In this work, we call this probing activity "channel probing" and use commercially available coherent S-BVT TeraFlex™ transceivers from ADVA [128] to perform the task. This fully reconfigurable S-BVT transceiver enables to reconfigure the signal wavelength, power, roll-off, Forward Error Correction (FEC) algorithm, modulation format and as well symbol rate. If some of

the transceiver's configurations are characterized with Q value-over-OSNR curves, the transceiver equipment under characterization can be transformed into a precise measurement tool, providing the end-user with a powerful tool to fully optimize the spectral usage, regardless of the OLS constraints.

For this work, 14 modulation format and symbol rate combinations were characterized with Q-over-OSNR curves, as suggested in [8]. These configurations are presented in Table 2.

4.2 Transceiver characterization

For the transceiver characterization activity, a dataset consisting of Q value-over-OSNR must be captured in the linear domain as per [8]. If the Q value is not provided by the transceiver, also pre-Forward Error Correction (FEC) Bit Error Ratio (BER) or in short, pre-FEC BER-over-OSNR curves can be collected, as the pre-FEC BER enables to derive Q through calculations [129]. Although the accuracy of the calculation can be approved when adjusted to soft-FEC used in modern S-BVT-s transceivers [130], the method requires additional function storing in soft pre-FEC decoder. This is not a quick fix usable in everyday field operations, but should be considered once these changes become available in new transceiver generations. In case of TeraFlex^{TM}, the Q-value was automatically provided by the transceiver.

Fig. 9 presents a simple lab setup to characterize the S-BVT in the linear domain for channel probing activity. Single network port is enabled in the S-BVT, and the signal is merged with the added noise in 8:1 splitter/combiner module (but any other splitter/combiner type providing the necessary amount of ports can be used, too). The noise power levels are controlled by the variable optical attenuator (VOA) and the whole spectrum of the 8:1 splitter/combiner network transmit (N Tx) port is amplified in the EDFA to compensate for the insertion losses in the module. The signal is then looped back to the Receive (Rx) port of the 8:1 splitter/combiner module and split between the S-BVT Rx port and Optical Spectrum Analyzer (OSA).

For each of the VOA settings, a Q value reading is collected in the Transceiver unit. Simultaneously, Optical Signal to Noise Ratio (OSNR) is calculated for the VOA setting. For this, on/off method is used, meaning power samples at the transceiver central frequency are collected both for signal on and signal off scenario. The measurement with
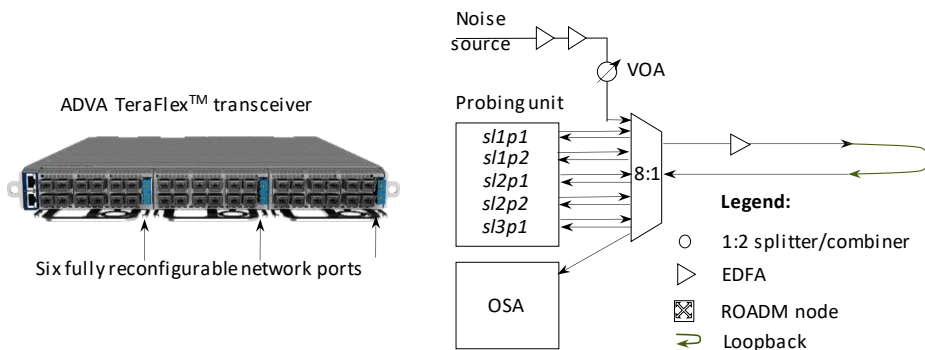

Fig. 9. TeraFlex^{TM} terminal and setup for transceiver characterization

***Table 2**: PLT configurations*

Line rate	Modulation	Symbol rate	Line rate	Modulation	Symbol rate
100 Gbit/s	DP-QPSK	31.5 GBd	400 Gbit/s	DP-32QAM	55.6 GBd
200 Gbit/s	DP-16QAM	34.7 GBd	500 Gbit/s	DP-64QAM	57.9 GBd
300 Gbit/s	DP-64QAM	34.7 GBd	200 Gbit/s	DP-QPSK	69.4 GBd
300 Gbit/s	DP-32QAM	41.7 GBd	300 Gbit/s	DP-P-16QAM	69.4 GBd
200 Gbit/s	DP-P-16QAM	46.3 GBd	400 Gbit/s	DP-16QAM	69.4 GBd
400 Gbit/s	DP-64QAM	46.3 GBd	500 Gbit/s	DP-32QAM	69.4 GBd
300 Gbit/s	DP-16QAM	52.1 GBd	600 Gbit/s	DP-32QAM/64QAM	71.9 GBd

signal on is integrated over the whole signal bandwidth (P_{TOT}) and includes both, ASE power from the noise-loading (P_{ASE}) and signal power (P_{signal}), which cannot be separated. This is followed by disabling the transceiver under characterization and measuring the signal off, or ASE noise power ($N_{0.1nm}$), collected with a 0.1 nm resolution at the central frequency of the signal spectrum. The OSNR resulting from the specific VOA setting is then calculated as per equation (1), where the BW is the signal bandwidth at chosen modulation format and symbol rate configuration and is expressed in dB for reference bandwidth 0.1nm:

$$OSNR_{ASE} = \frac{P_{TOT} - \frac{BW}{12.5} * N_{0.1nm}}{N_{0.1nm}} \qquad (1).$$

The set of a Q value and OSNR value, collected and calculated at the same VOA settings forms a datapoint in the Q-over-OSNR characterization curve. In order to achieve a good dataset for characterization, no more than a 1.0 dB change in VOA settings is recommended, when collecting consecutive datapoints. These datapoints should be then fitted into a second order polynomial, to get a continuous Q-over-OSNR characterization curve for the particular S-BVT port at hand. In this work, the characterized transceiver is referred to as Probing Light Transceiver (PLT).

4.3 Probing method

The experimental measurements presented in this work are based on the channel probing method described in [8], proposed by SubOptic Open Cable working group [131] and further explained in [132]. However, as the terrestrial networks are often more prone to dynamic changes caused by changes in traffic load and exposure to temperature changes compared to submarine systems, the test scenarios from [8] and [132] are modified according to [95] to be used in brown-field terrestrial systems. The specifics of the procedure are explained in chapter 5. All individual performance estimations obtained from the OLS links in lab or live networks compare the received Q value to the Q-over-OSNR polynomial fitting from the characterization exercise. The result from comparison gives us a Generalized Optical Signal to Noise Ratio (GOSNR), that includes all the impairments from the transmission medium and as well transceivers. The GOSNR

is then normalized to the PLT symbol rate, to obtain Generalized Signal to Noise Ratio (GSNR).

All probing signal formats characterized in this work had a root raised cosine (RRC) spectral shape with a roll-off factor r = 0.19. The DP-P-16QAM modulation format in Table 2 DP-P-16QAM stands for a proprietary partial-16QAM modulation format, used to transmit 3 bits per symbol (as 8QAM). To obtain comparable results, constant power spectral density is always maintained for all PLT configurations and for all probing activities in this work. This is possible when the DWDM line systems and their amplifiers operate in constant gain mode. The only exception, when constant PSD regime is switched to constant signal power regime is for the operation regime detection, where both PSD-based and signal power-based probing are used.

In the process of data collection for the OSaaS performance analyses, PLT frequency, PLT configuration, symbol rate, optical receive (Rx) power, Q-value, Pre-FEC BER, PLT estimated Optical Signal to Noise Ratio (OSNR) and PLT estimated Generalized Signal to Noise Ratio (GSNR) were collected. Based on this data, Power Spectral Density (PSD) was derived for the PLT unit.

For the detection of the optimal S-BVT configuration to be used on a specific OSaaS link, a single PLT configuration was used in [93]. To capture the filtering penalty in fixed-grid legacy networks, a symbol rate variable probing was introduced in [94], using all characterized PLT configurations to detect the filtering penalty. Symbol-rate variable probing was also used in [95] to verify the feasibility of the channel probing method in dispersion compensated networks.

In order to record the GSNR profile [95, 96, 133] of the OSaaS, the central frequency of the PLT module was systematically altered and swept over the OSaaS spectrum slot. The sweep procedure implemented various frequency steps between 12.5 and 25 GHz in the central part of the OSaaS spectrum, whereas a 6.25-GHz step was employed at the service edges for increased accuracy. Sweep procedure was also used to verify the concatenated GSNR profile approach in [134]. For [133], also multiple-probe approach was used, in which probing light from multiple PLT ports was simultaneously inserted into the OLS spectrum through 8:1 splitter/combiner module and performance data was read from all the respective modules. Finally, a single and multiple-probe method was used for OSaaS margin estimations [135-137].

In some of the works, the used S-BVTs did not have a transceiver-specific characterization curves available for the task. In these cases, non-transceiver-specific characterization curves from the same S-BVT type have been used. This was true for [134], [135] and partially for [137]. The probing activities in this work, including configuration changes, have been all performed manually.

4.4 Lab setup

Although adding a single PLT signal to the network usually does not cause any problems, if the network's power spectral density is maintained, multiple side effects from environmental conditions and neighboring channels may complicate the interpretation of probing results. Implementation in the lab provides a stable measurement environment, that allows to isolate the observed effect from other impacts. The lab

implementation is also great for testing the concepts, that may have an impact on the live channels carrying real-life user traffic. The lab set-up was used for four primary goals:

- transceiver characterization (explained in paper IX),

- exploring the symbol rate variable probing behavior in different OSNR regimes (papers III, V, VII, IX),

- suitable performance profile investigations for OSaaS characterization (paper I), and

- required service margin investigations in varied OSNR and channel load conditions (papers VII, IX).

The lab installations in the ADVA Gdynia lab and Open Ireland CONNECT lab used the same setup, as illustrated on the Fig. 10 with only a few differences in the used fiber length and exact ROADM modules. The signals from PLT ports and ASE-loading were inserted to the lab OLS through colorless add/drop, utilizing an 8:1 splitter followed by an optical amplifier to compensate for the insertion losses. Two variable optical attenuators (VOAs) were used in the scheme – VOA-1 was used to enable and disable the ASE-load and VOA-2 was used to decrease the Tx power to the OLS. The set up used two flex-grid ROADMs at both ends of the single hop link: in Gdynia, ADVA 9ROADM-96C modules in combination of 40-km fiber spools were used, and in CONNECT lab, Lumentum ROADMs in combination with 25-km fiber spools were used. To enable single-ended measurements, the OSaaS spectrum was looped back at the add/drop port of the far-end ROADM. All lab-based OLS systems used a ITU-T G.652.D compatible standard single mode fibers.

The spectral allocation of the lab systems in Gdynia and CONNECT lab is illustrated on Fig. 10, Right. In Gdynia lab, OSaaS service configurations (b) and (c) from Fig. 7 were implemented, providing five adjacent 75-GHz wide MCs or a single 375-GHz wide MC. For the testing and equalization purposes, five PLT ports with a 75-GHz step between the central frequencies were commissioned within the OSaaS. The ports were configured to 200-Gbit/s 69-GBd DP-QPSK signal format and set to 0 dBm transmit (Tx) power per OTSi.
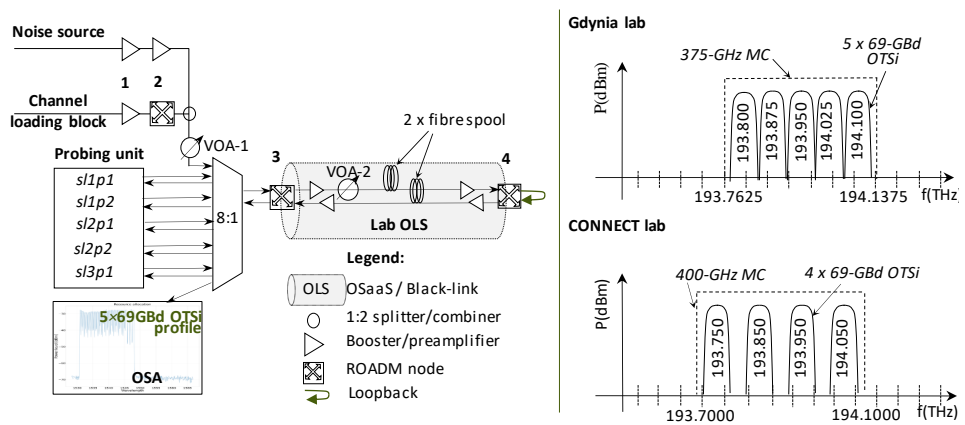

Fig. 10. *General test setup and spectral assignment used in the labs*

The ROADM Tx powers in Gdynia lab were set to -18.7 dBm Tx power per MC for a 5×75-GHz MC OSaaS configuration and – 11.7 dBm Tx power for a single 375-GHz MC OSaaS configuration.

In Open Ireland CONNECT lab, OSaaS service configuration (c), providing a single 400-GHz wide MC was used. For the testing and equalization purposes, four PLT ports with a 100-GHz step between the central frequencies were commissioned within the OSaaS, each configured to 200-Gbit/s 69-GBd DP-QPSK signal format and 0 dBm transmit (Tx) power per OTSi. The ROADM Tx powers in Open Ireland lab were set to -11 dBm Tx power per 400-GHz MC OSaaS configuration. In addition to OLS ROADMs, two additional ROADMs were used to create ASE-loaded dummy channels. For this, the booster in the first ROADM was transmitting a continuous ASE noise over the full C-band. This was shaped into 37.5-GHz wide ASE-loaded dummy channels by the Wavelength Selective Switch (WSS) in the second ROADM, with a 50-GHz spacing between the central frequencies of the dummy channels. The ASE-loaded channel plan for channelized noise at the Tx port of the second ROADM and enabled or disabled 400-GHz channel blocks in the OLS in CONNECT lab are illustrated on the Fig. 11. A set of screen captures from Optical Spectrum Analyzer are also added for increased clarity how the spectrum in the PLT receiver looked during the testing. Precise description of the noise- and channel loading block is given in [137].
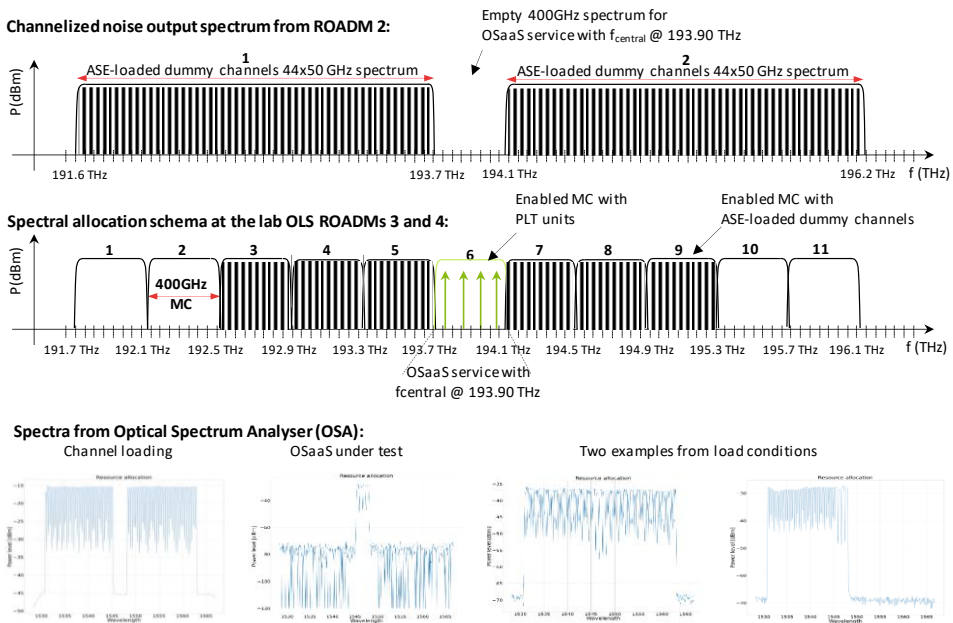

Fig. 11. *Channel allocation plan for ROADM 2 and ROADM 3 and 4 in the CONNECT lab and some received spectra examples from OSA*

4.5 Test set-ups in production networks

To verify the feasibility of the proposed theoretical concepts and solutions, include the uncertainties that may rise from live production networks, and demonstrate the variety in real-life infrastructures, four production networks were used for testing:

- Tele2 Estonia's long-haul flex-grid, Raman-enabled network with links up to 5738 km, (papers I, II, IV, V, VII),
- Funet's long-haul flex-grid, Raman-enabled network with links up to 1673 km, (paper VI),
- Tele2 Estonia's regional-haul fixed-grid network with links up to 1302 km, (papers III, V),
- and HEAnet's flex-grid metro network, with links up to 128 km, (papers VII, IX),

The tested networks used different infrastructure installations (buried and arial cables) and WDM technologies, but all networks used ITU-T G.652.D compliant fibers. The selection of the specific infrastructure was based on the experiment goal. For example, the feasibility of channel probing method for achievable capacity estimations was initially verified in Tele2 Long-Haul network, that is fully coherent, dispersion compensation-free network with a very low to-the-line transmit powers in each of the consecutive amplification sites on links spanning up to 5738 km. This provides the closest testing environment to Poggiolini's Gaussian Noise Model [138]: a dispersion uncompensated linear medium, long enough for dispersion to accumulate. Due to a great alignment between the expected capacity and actually achievable capacity, the method was also tested outside of the ideal conditions: in legacy WDM systems, that use channel filters, dispersion compensation modules and are in general, shorter in reach. For this, Tele2-s regional WDM system was used.

Next, filtering penalty at the service edges, wavelength-dependent performance variations and power fluctuations from the OLS were investigated in long haul networks. The OSaaS characterization concepts were verified in Tele2 long-haul network, providing a single long link, that was shortened by looping the signal back from intermediate ROADMs. The concatenation of the GSNR profiles was verified in Funet's network.

Finally, the margin allocation derived in the lab environment was tested out in HEAnet metro network.

To stay realistic, the data to describe the real-life was limited to the link length, and the type of MC configuration used to implement the OSaaS lightpath. To extend the transmission distance and to allow single-ended measurements at the test-site, the spectrum services were looped back at the add/drop port of the far-end ROADMs in all the tested live networks. Link acronyms for Tele2 networks are combined from the link name and the looped length of the link. Table 3 assigns the link data to the research papers used in this thesis.

The geographic presentation of these links is based on the information available on the operator homepage and is presented on Fig. 12. As the OSaaS end user only sees the OSaaS as a black box, the transparent OSaaS tunnels on the links are presented with yellow arrows. Further details about the system layouts and production systems can be found in the relevant papers (see Table 3).

Table 3: Data about the live network links used in this work

Link	Acronym	Looped length (km)	MC configuration	Used in papers
Tele2 R	A-4	3		III, V
Tele2 R	B-70	70		III, V
Tele2 R	A-144	144		III, V
Tele2 R	A-241	241		III, IV, V
Tele2 R	C-284	284		III, IV, V
Tele2 R	A-382	382	1 x 100-GHz for capacity estimation	III, V
Tele2 R	B-485	485		III, V
Tele2 R	B-621	621		III, V
Tele2 R	A-675	675		III, V
Tele2 R	B-822	822		III, V
Tele2 R	B-1182	1182		V
Tele2 R	B-A-1302	1302		V
Tele2 LH	LH-1016	1016	1 x 100-GHz for capacity estimation 1 x 400-GHz for spectral sweep, 1 x 375-GHz for characterization 5 x 75-GHz for characterization	II, V
Tele2 LH	LH-1792	1792		I, II, IV, V, VIII, XI
Tele2 LH	LH-2943	2943		II, V
Tele2 LH	LH-3751	3751		I, II, V, VIII, XI
Tele2 LH	LH-5738	5738		I, II, V, VIII
Funet LH	Hämeenlinna	282	1 x 300-GHz for GSNR profile concatenation	VI
Funet LH	Stockholm	1161		VI
Funet LH	Kajaani 2	1673		VI
HEAnet M	TCD-2 short	2	1 x 400-GHz for OSaaS margin detection	VII, IX
HEAnet M	DCU-2	28		IX
HEAnet M	DCU-1	30		IX
HEAnet M	TCD-2 long	128		VII, IX

Regardless of different link lengths, native channel load and underlying WDM technology, the test setup for all the live networks was the same in principle: transceiver unit with one or more characterized network ports was used to probe the link under test.

Similarly to the lab environment, the transceiver units were interconnected to the network OLS using a colorless add/drop, utilizing an 8:1 splitter followed by an optical amplifier to compensate for the insertion losses. Only the experiments held in Tele2's regional-haul network used a single transceiver port, connected directly to the nominal 100-GHz fixed filter receive port at the channel filter connected to add/drop port of the ROADM.

Fig. 13 presents the OSaaS configurations and spectral allocations used in different tested live networks, as they would appear in a single DWDM system spectrum in the C-band. The light grey dotted line depicts the noise profile of one of the possible Raman-amplified OLS implementations. A 75-GHz OTSi spacing was used in Tele2 and

Funet long-haul networks, and a 100-GHz OTSi spacing was used in Tele2's fixed grid network and HEAnet's flex-grid metro network. The MC configurations in OLS were following the OTSi spacing, and where possible, one wide MC was configured.
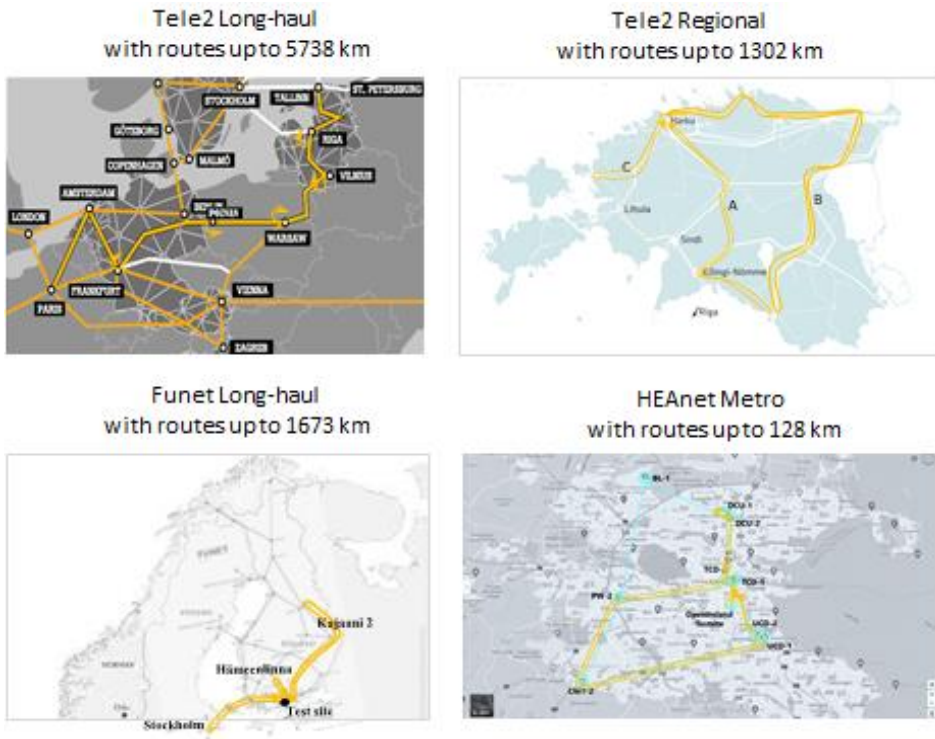

Fig. 12. Geographical layouts of the networks as presented at the operator homepage
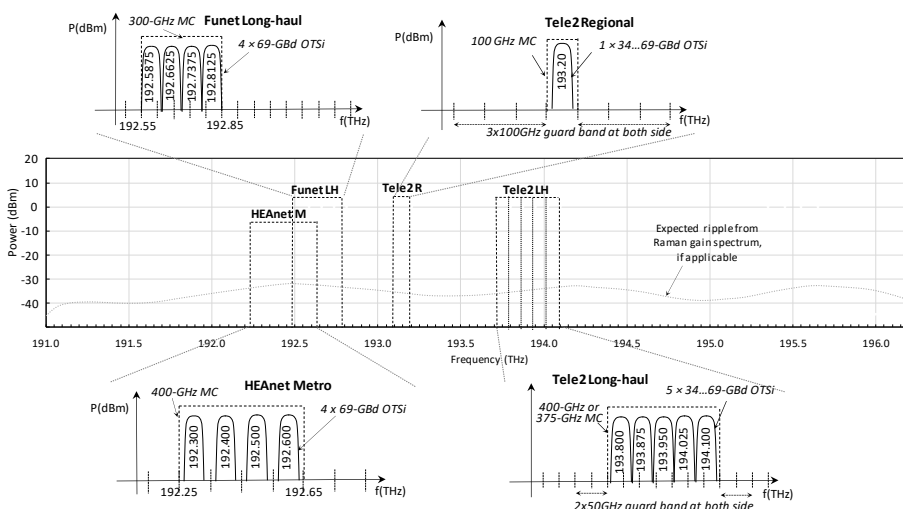

Fig. 13. Tested OSaaS configurations with MC mask and used OTSi spacing data per tested OLS

For equalization purposes, 200-Gbit/s 69-GBd DP-QPSK signal format with 0 dBm output power per OTSi was used. This power defined the set point for the Power Spectral Density of the test setup and was maintained in case of PLT configuration changes in variable symbol rate probing scenarios by adjusting the Tx power of the transceiver. The same method was used to maintain the PSD also in wide-band MC configurations (c). The ROADM Tx powers were derived from the nominal 50 GHz or 100 GHz channel power levels in the network.

4.6 Replicability and transferability

In OSaaS use cases, the end user sees the OLS as a black box. Due to the implementation specifics of the live networks (cable infrastructure, fiber standards, WDM technology and components), each network and spectral slot within the OLS is unique. Therefore, variation in estimated performance should be expected when using the probing over an OSaaS spectrum, even if the exact same type of components, configurations, and span lengths, as introduced in the test setups, are used. However, the channel probing concepts and trends in estimated results should be universal, as long ITU-T G.652.D compatible fibers are used.

5 OSAAS SPECIFIC PERFORMANCE ESTIMATIONS

To make efficient use of spectral resources, a thorough understanding of spectrum performance is required. Using a commonly accepted metric/measure benefits both the OSaaS service provider and the end-user. While OSNR alone is not sufficient in detecting the channel performance and achievable capacity [8], since it only provides the linear component of the noise, also GSNR must be evaluated. However, in majority of the use cases, OLS data to calculate the GSNR using proprietary, or open QoT estimation tools is not available to the end user. Since GSNR cannot be measured directly, a work-around has been proposed by the SubOptic OpenCable working group [131], to get as close estimate to the GSNR as possible.

   This chapter introduces channel probing method, also known as inverse back-to-back method, or B2B^{-1}, to experimentally estimate the OSaaS performance without any knowledge about the OLS and it`s components.

5.1 Background of Channel Probing method

Achieving more control over spectral efficiency and achievable capacity have been some of the most important factors in the increasing demand for OSaaS. Selecting the best transceiver configuration out of hundreds of modulation format and symbol rate combinations provided by the future S-BVT transceivers can be a time-consuming task. To reduce the time, a *Generalized* Signal to Noise Ratio (GSNR) of the lightpath can be estimated. GSNR considers all optical distortions that impact the optical signal, including ASE noise, nonlinear distortions, as well as any transceiver impairments. However, capturing this value cannot be performed over direct measurements, as no measurement tool exists to do so. Although off-line QoT estimation tools or open-access initiatives target precise link performance estimations through calculations [125-127], the computation of exact per-wavelength performance requires detailed knowledge about the underlying infrastructure and system components. This includes data about gain profiles of the amplifiers, polarization-dependent loss and gain, filtering penalties, OLS channel allocation plan and load. This content is often unavailable or outdated. In addition, data describing the OLS design in great detail is mostly handled as business-sensitive information and hence not shared with the end customers. To overcome this, an experimental method to characterize any open system with OSNR and GSNR has been proposed by the SubOptic Open Cables Working Group. The existing variations for these metrics alongside with a comprehensive characterization guide using Inverse Back-to-Back Method to characterize the submarine cable links are explained in [8], with the latest recommendation published as [9]. Further specifics about the test schema and achievable precision are discussed in [132]. The method requires a coherent S-BVT transceiver, that is characterized with Q-over-OSNR curves in the linear domain, but as well against any performance impairments caused by test wavelength, chromatic dispersion, and PMD. In this work, we refer to a characterized transceiver as Probing Light Transceiver (PLT). Considering the fairly constant and uninterrupted environment of the subsea systems, the estimation accuracy provided by a precisely characterized PLT unit is well worth the characterization effort.

However, terrestrial networks are often more prone to dynamic changes caused by changes in traffic load and exposure to temperature changes compared to submarine systems. In addition, the amplifiers are often operated in a constant gain regime and adding a probing light transceiver (PLT) together with adjacent neighboring channels as proposed in [8, 9 and 132] may cause spectral hole burning in lightly populated terrestrial systems, as the idle spectral parts in the conventional brownfield terrestrial systems are not ASE loaded or filled with dummy channels. This means, that also the amplifier's gain spectrum in terrestrial brownfield systems may differ between beginning-of-life and end-of-life. Furthermore, if the transceivers used for OSaaS characterization are not fully characterized against the performance impairments caused by test wavelength, chromatic dispersion, and PMD, it can cause bias in the estimations. Therefore, the exact procedure based on the work by SubOptic Open Cable working group must be modified for the usage in brownfield terrestrial systems.

While this section provides some historical background information about the channel probing concept, section 5.2 provides the theoretical background, capabilities, and achievable accuracy of the method. Furthermore, adjustments to the original channel probing technique are discussed to estimate the GSNR in brownfield terrestrial systems.

In general, channel probing in transparent optical networks is not a new concept. Probes called active supervisory or dummy lightpaths were used already in the early 2000's to estimate the link availability and performance in transparent optical networks [139-141]. These lightpaths used intensity-modulated direct-detection (IMDD) transceivers as the probing light and were commissioned to extract availability and pre-FEC BER performance data from the network link. However, the perspective of link performance estimation precision, accuracy and usage-scenarios in optical networks has been significantly widened by the concept of using the characterized digital signal processor (DSP)-based modern S-BVT transceivers as the probing light.

The very first attempt to use a back-to-back characterized coherent transceiver to capture the link performance was performed by Torrengo et al in 2011 [142], when they introduced the first lab experiment to verify the predecessor of the GN model [143]. The GN model by Poggiolini [138] poses that both components, the linear ASE noise, and nonlinear impairments (NLI) contributing to the *Generalized* OSNR would have a Gaussian distribution in case of non-dispersion compensated spans in the optical networks. This led to a symbol rate independent GSNR to become a widely used optical link QoT metric, when the model was verified also through simulations [144,145]. Due to the disaggregated networking implementations over the trans-Atlantic and trans-Pacific links, the channel probing concept was first adopted in the optical submarine network community. References [146-148] introduce the GSNR as the primary link characteristic and provide instructions for transceiver characterizations to perform accurate GSNR measurements. Since 2017, characterized coherent transceivers to estimate the link GSNR have been used in many studies, from optical link characterization [149, 150] and network automation [151,152] to linear OSNR estimations [153-155], but it was only after the more intense insights to GSNR-based link characterization through characterized transceivers, provided in [8], when the topic gained real momentum.

5.2 OSaaS specific channel probing

In this sub-section a general overview of the channel probing method introduced in [8] is given and the method is adjusted to terrestrial brownfield networks. By adjusting the symbol rate, frequency, and power of the PLT configuration, we estimate the GSNR of the spectrum slot, detect the possible filtering effects, capture wavelength dependent performance variations, and operation regime within the terrestrial brownfield OSaaS. Then, primary error sources of the method are discussed and recommendations for margin allocation to compensate for probing inaccuracies are given.

5.2.1 General concept of Channel Probing

To evaluate the channel performance, either GOSNR or GSNR of the link must be known. ITU-T Recommendation 977.1 [113] defines the theoretical GOSNR as per equation (2), where the $OSNR_{ASE}$, $OSNR_{NLI}$ and $OSNR_{GAWBS}$ are the OSNR components from ASE noise, nonlinear distortions, and Guided Acousto-optic Wave Brillouin Scattering, respectively:

$$\frac{1}{GOSNR_{est,link}} = \frac{1}{OSNR_{ASE}} + \frac{1}{OSNR_{NLI}} + \frac{1}{OSNR_{GAWBS}} \qquad (2).$$

While the GOSNR per (2) can be calculated, the calculations require comprehensive and detailed knowledge about the OLS components commissioned on the link, which is often not available in disaggregated networking scenarios. This may cause major drawbacks in estimating the channel performance with conventional methods, as direct measurements of the GOSNR and GSNR are not possible due to the nonlinear component they include.

Reference [8] proposes, that close estimations of the actual channel performance in optical networks are possible through the channel probing process. For this, a characterized probing-light is inserted into the network in the corresponding channel location, and Q-value is used to estimate the respective Generalized Optical Signal to Noise Ratio (GOSNR) ($GOSNR_{est,link}$) of the link based on the Q-over-OSNR curve from transceiver characterization. While the estimated $GOSNR$ consist of all the optical distortions that impact the optical signal as per (2), the estimated $GOSNR$ from the channel probing is not the actual, real GOSNR of the link, but only it's projection/approximation in the linear space. This is caused by the fact that any measured Q value from the real-life networks is compared to the polynomial fitting from the linear domain, projecting all the link induced impairments into linear domain, too. However, as also the typical, required (O)SNR from the system specification documentation, required for margin estimations, is defined in linear domain, the GOSNR estimations from channel probing can be used to estimate of the spectrum performance and achievable capacity on the link. The estimated $GOSNR_{est,link}$ is then normalized to the symbol rate of the Probing Light Transceiver (PLT) signal to obtain the estimated GSNR of the link ($GSNR_{est,link}$) as per equation (3), where the 12.5 GHz is a reference bandwidth and BW is the PLT bandwidth in GHz:

$$GSNR_{est,link} = \frac{12.5}{BW} * GOSNR_{est,link} \qquad (3).$$

According to [113], the GSNR of the link can be expressed as (4), where SNR_{ASE} is the linear noise from amplified spontaneous emission, SNR_{NLI} is the nonlinear noise from intra channel and inter channel interference, SNR_{GAWBS} is the Guided Acousto-optic Wave Brillouin Scattering, SNR_{modem} is the impairments introduced by the modem technology and used unit, and SNR_i is any additional impairment that can be caused by filtering, environmental aspects, or other:

$$\frac{1}{GSNR_{est,link}} = \frac{1}{SNR_{ASE}} + \frac{1}{SNR_{NLI}} + \frac{1}{SNR_{GAWBS}} + \frac{1}{SNR_{modem}} + \frac{1}{SNR_i} \qquad (4).$$

If the modem penalties and impairments from filtering, environmental aspects, and other are not precisely characterized during transceiver characterization process, they could not be subtracted from $GSNR_{est,link}$ and the actual GSNR of the link cannot be derived [8]. This is often the case in real-life terrestrial brownfield use cases, as PLT characterization in such detail requires customized measurement set-up to record transceiver performance dependance from polarization mode dispersion, chromatic dispersion, and used frequency per each of the modulation format and symbol rate combinations characterized for channel probing. As a consequence, the estimated $GSNR_{est,link}$ becomes dependent from the exact transceiver module that was used for probing. However, the estimates can be used for the same transceiver type, and the error from implementation penalties between transceivers can be minimized by avoiding probing activity at high Q values, where the variation between transceivers is the highest.

After the derivation of $GSNR_{est,link}$, GSNR implementation margin can be estimated for any modulation format and symbol rate combination by subtracting the required GSNR ($GSNR_{req}$), available from the S-BVT transceiver system specification documentation from the $GSNR_{est,link}$ as per (5).

$$GSNR_{margin} = GSNR_{est,link} - GSNR_{req} \qquad (5).$$

If the $GSNR_{margin}$ calculation result according to (5) is positive, the configuration is expected to work and all calculations resulting in a negative GSNR implementation margin, are expected to not to work over the probed link.

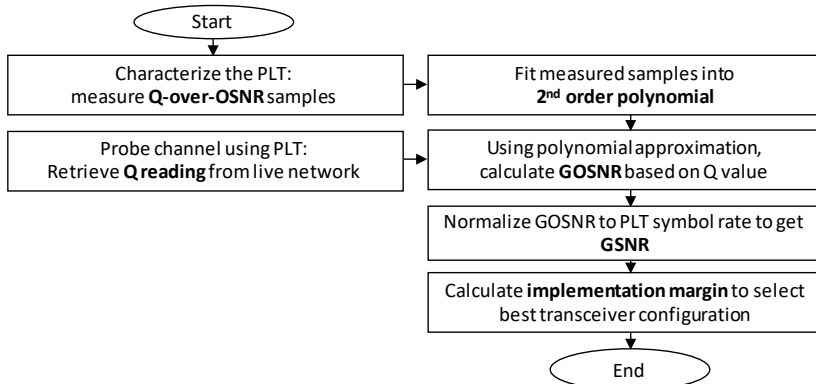The general channel probing process is explained on Fig. 14.

Fig. 14. *General channel probing concept*

5.2.2 Symbol rate variable channel probing

Generic channel probing method introduced in 5.2.1 can provide reliable spectrum performance estimations within the exact bandwidth covered by the PLT configuration. Unfortunately, ROADMs, channel multiplexers or grating based dispersion compensation modules in the optical networks can introduce bandwidth narrowing effect. While the mild penalty from bandwidth narrowing can be compensated in the transceivers, any significant bandwidth limitation could cause the degradation of achievable performance. This effect can introduce a bias in $GSNR_{est,link}$ estimations when only a single PLT configuration is used to estimate the $GSNR_{est,link}$. To investigate this phenomenon and its impact on the achievable capacity predictions on the link, all of the pre-characterized PLT configurations from Table 2 were used. During probing, a constant power spectral density-based probing regime was used to estimate the $GSNR_{est,link}$ of the wide-band and bandwidth limited OSaaS in Tele2 long-haul and regional-haul network. We refer to this extension of the channel probing method as a symbol rate variable channel probing.

In networks without bandwidth limitations, probing operated with constant PSD should return constant GSNR estimations regardless of the required bandwidth of the PLT configuration. Fig. 15, top presents the original probing results from the long-haul dispersion compensation free network with a colorless add/drop. The x-axis presents the link length in kilometers and the y-axis the estimated GSNR, obtained by using different PLT configurations. As visible, all measurement results regardless of the PLT configuration are concentrated within ±0.4 dB around the probable GSNR of the link with no distinguishable pattern based on symbol rate or the modulation format of the PLT unit.

As these random variations are likely introduced by the fast fluctuations and measurement errors (reading and accuracy), the actual $GSNR_{est,link}$ is probably an average
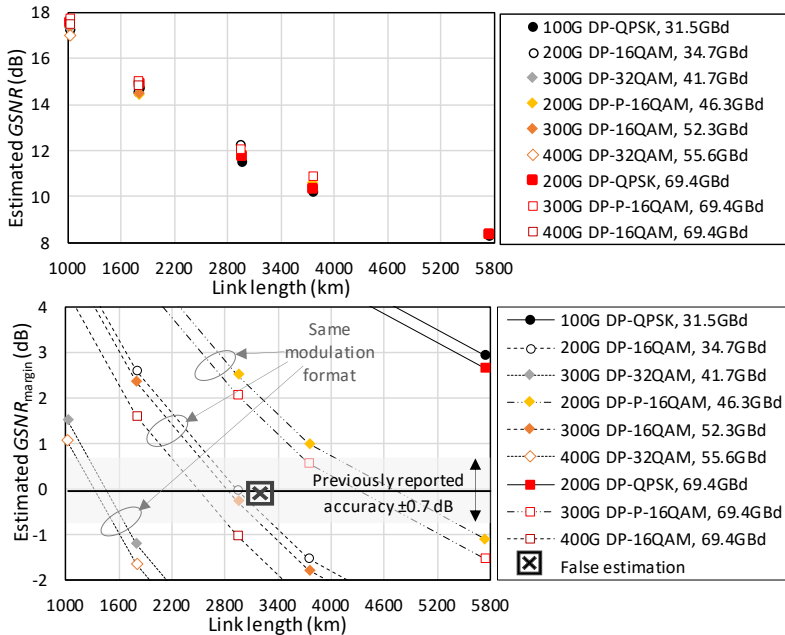

Fig. 15. Top: Results from symbol rate variable channel probing and
Bottom: GSNR_margin estimations for a long-haul network

estimated value from all the working PLT configurations. The average $GSNR_{est,link}$ can be then further used to derive $GSNR_{margin}$ as per equation (5). Fig. 15, bottom presents the $GSNR_{margin}$ estimations based on the averaged $GSNR_{est,link}$ from all working PLT configurations in long-haul network. Cross mark close to the near-zero margin estimation indicates the false estimation, which occurs when the measured verification signal condition did not match the estimated signal condition. Here, the x-axis presents the link length in kilometers and the y-axis the estimated $GSNR_{margin}$ for different PLT configurations. Different marker styles refer to different symbol rates and line styles distinguish different modulation formats. The chart is zoomed in for the area near zero implementation margin, where the probability of false estimations is highest. Using symbol rate variable channel probing, 0.05 dB in $GSNR_{margin}$ accuracy in the long-haul network was achieved compared to a single probe-configuration estimation, reported as 0.7 dB in [93]. This can be attributed to the averaging effect over multiple available GSNR estimations from the same network link, which allows to average out the small time-dependent performance fluctuations between each individual GSNR estimation.

Modern flex-grid networks with colorless add/drop are generally robust to bandwidth limitations, or these can be overcome by simple reconfigurations in the ROADMs. Bandwidth narrowing, however, is a problem in legacy fixed-filter systems. In case of significant bandwidth limitation, high symbol rate signals are subject to stronger narrow band filtering and using a wideband probing signal results in underestimating the link GSNR that would be achievable for lower symbol rate signals. Using narrow band probing configurations would create the illusion of a link with a high GSNR not achievable for higher symbol rate signals.

This effect can be assessed with GSNR penalty, which is a systematic decrease in estimated GSNR, caused by the variation in PLT symbol rate, modulation format, frequency, or power setting. As theoretical, calculated GSNR values for the link are often not available for the OSaaS end user, GSNR penalty for the specific configuration under interest can be calculated as a GSNR estimation difference between the highest performing PLT configuration and the configuration under interest, measured on the same transmission link. To verify the symbol rate dependent changes in GSNR estimations caused by bandwidth limitation and eliminate the GSNR estimation differences due to non-linear behavior, back-to-back measurements (with 0-km fiber length) to characterize the filtering penalty were carried out in Tele2 network, emulating the link A-4 in Tele2 regional haul network.
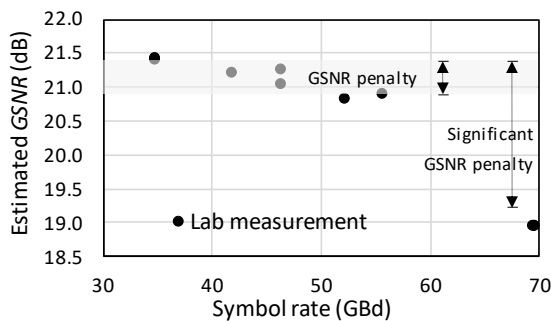

Fig. 16. Symbol rate variable probing for filtering penalty characterization

This link includes two flex-grid ROADM modules and three arrayed waveguide grating (AWG) based fixed-grid multiplexer modules and defines the minimum filtering penalty on all the links in the regional-haul network. Fig. 16 presents the results of the back-to-back (B2B) measurements for the symbol rate dependency of the estimated GSNR. The x-axis presents the symbol rate of the PLT configuration, and the y-axis present the estimated GSNR. While the estimated GSNR decreases up to 0.6 dB compared to the highest performing PLT configuration at 34.5 GBd for the symbol rates up to 55.5 GBd, PLT configurations with 69.4 GBd experience significantly higher GSNR penalty, reaching almost up to 2.5 dB. This behavior can be explained with a bandwidth limitation penalty from the AWG based channel filter modules (3-dB bandwidth of 80 GHz) and ROADMs.

The probing results from the symbol rate variable channel probing in Tele2 regional-haul network are presented in Fig. 17 (a). The x-axis presents the link length in kilometers and the y-axis the estimated GSNR in dBs. As expected, the link GSNR estimations by different PLT configurations are highly scattered for the legacy regional-haul links due to symbol
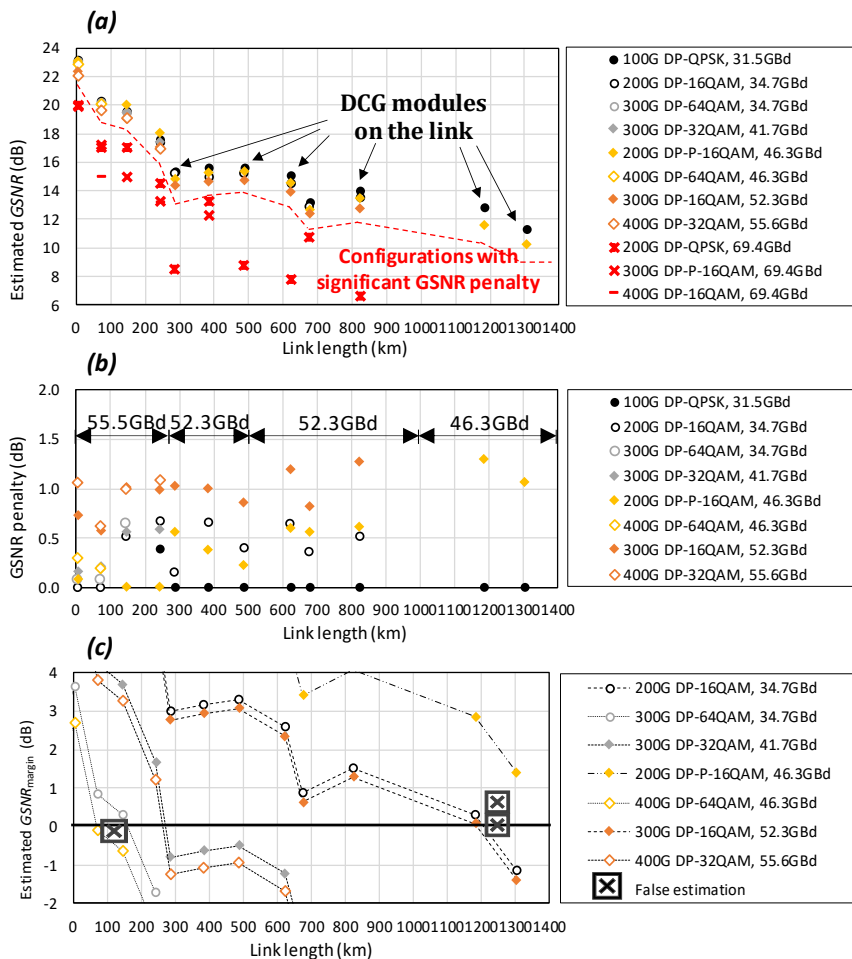

Fig. 17. *(a) Results from symbol rate variable channel probing, (b) GSNR penalty and symbol rate cap and (c) GSNR$_{margin}$ estimations for a regional-haul network*

rate dependent GSNR penalty caused by bandwidth narrowing. As a result, the average estimated GSNR value is only a statistical number in bandwidth limited regional-haul network and further analyses on the original probing results are required to estimate the $GSNR_{est,link}$.

According to results on Fig. 17 (a), PLT configurations with equal symbol rate experience similar penalties from the system and estimate the link GSNR with ±0.35 dB accuracy, regardless of the modulation type for up to 55.5 GBd signals, whereas a change to 69.4 GBd symbol rate in the PLT configuration resulted in a great variance in the estimated GSNR. While the maximum variance between the estimated GSNR on links shorter than 500 km is below 0.7 dB for the probe settings between 31.5 and 46.3 GBd and below 1.1 dB for the probes up to 55.6 GBd, it quickly grows up to 7.1 dB for the probes including 69.4 GBd. For the links up to 1000 km, these figures are 0.7 dB, 1.3 dB and 7.5 dB, respectively. In addition to the bandwidth limitation penalty from the channel filter modules and ROADMs for the Dispersion Compensated Fiber (DCF)-based links, additional penalty from DCG modules (3-dB bandwidth of 60 GHz) is captured on the links including grating-based dispersion compensation modules. For the two longest links in regional-haul network, only two PLT configurations were working, having a GSNR penalty of 1.3 dB between the 31.5 and 46.3 GBd configurations.

Fig. 17 (b) presents GSNR penalty for the PLT configurations compared to the best performing PLT configuration, excluding the configurations experiencing severe filtering penalty. The x-axis presents the link length in kilometers and the y-axis the estimated GSNR penalty in dBs. As visible from the figure, the longer the link, the higher the GSNR penalty even for same PLT configurations. This can be explained with cascaded filtering from multiplexers, ROADMs, and DCG modules that decrease the effective bandwidth of the OSaaS.

In order to estimate the best possible transceiver configuration for the narrow-band OSaaS offering at hand, it becomes essential to identify the highest usable symbol rate on the link – a symbol rate cap. To identify the symbol rate cap for the link, two criteria must be met:

- it must be acquired through working PLT configuration with the highest symbol rate and
- it does not experience significantly higher GSNR penalty compared to the other working PLT configurations on the link.

According to our tested OSaaS services on Fig. 17 (a) and filtering penalty analyses on Fig. 17 (b), four of the shortest links have a symbol rate cap at 55.6 GBd. That is decreased to 52.3 GBd for links up to 1000 km and only 46.3 GBd for the longest two links. As visible from the Fig. 17 (b), the absolute values of the GSNR penalty itself are not consistent along the links nor important as long the two criteria for the symbol rate cap identification are met. All configurations exceeding the symbol rate cap should be removed from the pool of possible transceiver configurations before the $GSNR_{margin}$ calculation. In Fig. 17 (a), this means leaving out all high symbol rate configurations marked with red.

Then, the average estimated $GSNR_{est,link}$ can be calculated for the narrow-band OSaaS link, using the GSNR estimation results from PLT configurations with smaller and equal symbol rate than the symbol rate cap. The best transceiver configuration can be selected

as per highest line rate from all possible configurations returning positive implementation margin as per equation (5).

Fig. 17 (c) presents the achievable accuracy of the $GSNR_{margin}$ estimation in legacy network together with the verification signal condition. The x-axis presents the link lengths in kilometers, and the y-axis estimated $GSNR_{margin}$ in dB-s for the different PLT configurations. Different marker styles refer to different symbol rate regimes and line styles distinguish different modulation formats. The chart is zoomed in for the area near zero implementation margin and cross marks placed near the $GSNR_{margin}$ marker indicate the correctness of the estimation.

Following the identification of the symbol rate cap and applying this to original data from symbol rate variable channel probing, the selection of the best possible transceiver configuration was achieved with the estimation accuracy better than 0.10 dB for the links up to 822 km and 0.32 dB on the links up to 1302 km on the regional-haul network. The most likely cause for the two false positive $GSNR_{margin}$ estimations on the link B-1182 km, where probably caused by the small number of working PLT configurations, which may have not contributed enough for the required averaging effect, to achieve accurate $GSNR_{est,link}$ estimation. However, considering the margin values generally implemented for network robustness against ageing and slow performance changes, the achieved result is an accurate measure of the network performance at a current moment.

5.2.3 Channel probing with frequency sweep

It is well known that the performance across the optical spectrum provided by a DWDM systems is not constant and can vary depending on the channel location in the spectrum. This is caused by the loss profile of the fibers, gain profiles of the amplifiers, and loss profiles of different modules used in DWDM networks. To capture the possible performance variations over the wider spectral slots used for wide-band OSaaS, generic channel probing procedure from [8] must be further modified. For this, the central frequency of the PLT must be changed systematically to cover the available spectrum slot dedicated for OSaaS. With a suitably selected frequency step increments, a selection of OSaaS services from Tele2 regional (A-241, C-284) and long-haul (LH-1792) production networks were probed for concept verification.

A 100-GHz narrow-band spectrum service was investigated on routes A and C, whereas a 400-GHz wide-band service was used on route LH. The channel performance on all routes was tested with reduced number of probes from Table 2, utilizing only 200-Gbit/s 69-GBd DP-QPSK, 200-Gbit/s 46-GBd DP-P-16QAM, and 200-Gbit/s 34-GBd DP-16QAM probing signals. To obtain comparable results, constant power spectral density was maintained for all PLT configurations. The spectrum performance was evaluated by a GSNR, captured with 6.25 GHz frequency steps over the allocated spectrum.

Fig. 18, top shows the channel probing results from routes A and C. While the nominal media channel width on route A and C is 100 GHz, the large predicted GSNR difference between the three modulation formats reveals that the usable effective optical bandwidth must be much smaller. Given that a 6.25-GHz central frequency mismatch of a 34.5-GBd signal already causes a noticeable penalty, we can conclude that the effective optical channel bandwidth is lower than 50 GHz. On route A-241, up to 2 dB degradation in the estimated GSNR is observed for a 200-Gbit/s 34-GBd DP-16QAM signal

configuration in case of 18.75-GHz offset. With the same offset, 200-Gbit/s 46-GBd DP-P-16QAM and 200-Gbit/s 69-GBd DP-QPSK signal formats are already experiencing outage as the attainable GSNR is insufficient.

In addition to severe filtering penalty for the 200-Gbit/s 69-GBd DP-QPSK signal format, the results for Route C-284 on Fig. 18, top also indicate a misalignment of the nominal central frequency. Without sweeping, this misalignment could have been left undiscovered and already a small fluctuation in the transceiver wavelength could cause a severe degradation of the service quality, especially with 46-GBd DP-P-16QAM modulation that generally requires higher margin than a 200-Gbit/s 69-GBd DP-QPSK signal. To increase the robustness, the transceiver frequency should be fine-tuned to minimize frequency misalignment and to obtain the best spectrum performance.

Fig. 18, bottom presents the GSNR variation over the LH-1792 link in a single 400-GHz media channel and a 5×75 GHz adjacent media channel configuration, the latter effectively providing a 375 GHz wide spectrum slot. The representation of the estimated GSNR over the OSaaS spectrum slot can be called the GSNR profile. GSNR profile helps the wide-band OSaaS end users to evaluate the impact of the wavelength dependent performance variations on achievable throughput in the OSaaS spectrum. It demonstrates the severity of filtering at the media channel edges and any ripple/tilt in the OSaaS
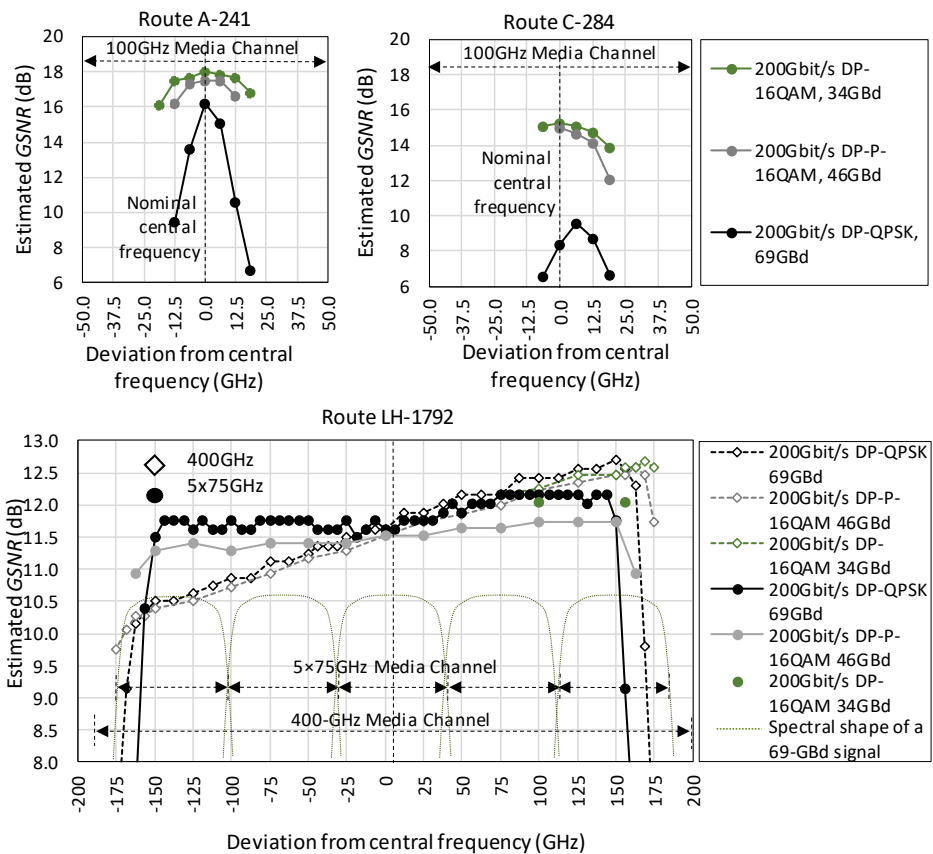

Fig. 18. Top: Channel probing sweep results from route A and C, **Bottom:** from route LH

52

performance over the spectrum. In general, GSNR profiles captured with the smallest bandwidth and frequency increment provided by the PLT unit present the best insights to intra-spectrum performance. This is because wide-band PLT configurations may fail to detect any dips in the spectrum caused by adjacent concatenated media channels. Similarly, wider frequency step may not capture the smaller performance changes in the spectrum. This is illustrated with the coarse sample set of the DP-P-16QAM modulation format data set on Fig. 18 (c). GSNR profile captured with the smallest frequency increments enables OSaaS customers to decide the best possible transceiver configurations for any part of the spectrum, to maximize the OSaaS throughput.

According to measurements on wide-band OSaaS demonstrated on Fig. 18, bottom, all three modulation formats predict a similar GSNR performance with a maximum deviation of 0.25 dB in $GSNR_{est,link}$ for the single 400-GHz wide spectrum configuration, and up to 0.53 dB $GSNR_{est,link}$ difference between the captured $GSNR_{est,link}$ datapoints for the coarse sample set of the OSaaS with 5×75 GHz configuration. Higher deviation in results in this case can be attributed to a time dependent variation in the network performance, as the samples in this case were collected on different days. Based on the GSNR profiles, 400-GHz single MC and 5×75 GHz adjacent MC OSaaS configurations have a different wavelength dependent performance that is caused by the different OSaaS configuration, and thus, intra-OSaaS signal power equalization schemes.

The most evident is a 2.5-dB GSNR tilt over the 400-GHz single MC OSaaS configuration that leads the DP-16QAM probe configuration, requiring generally higher GSNR to lack sufficient margin to work at the lower part of the spectrum slot. Although this difference can be reduced to 0.3 dB GSNR tilt when operating 5×75 GHz MC OSaaS configuration, it reveals that the signal degradation caused by underlying infrastructure cannot fully be diminished with equalization. This can be attributed to the Raman-enabled amplification scheme of the Tele2 long-haul network link, which produces a spectral ripple in the amplified C-band region with peak performances following the Raman pump locations and valleys in the between areas. Although the equalization at the ROADM nodes helps to balance out the ripple, the underlying effects from the longest hops on the infrastructure are still detectable in estimated $GSNR_{est,link}$. Based on the longest span examples, the signals travelling in the valley part of the spectrum are more prone to linear OSNR depletion in the end of the links due to reduced effectiveness of the Raman amplification in the valley areas of the spectrum, resulting in overall reduced power levels and OSNR. The signals travelling at the peak parts of the spectrum are more prone to nonlinear effects, as their power levels in the beginning of each new network span after the equalizing ROADM are generally higher than average. While the ripple effect may not be relevant for medium-haul distances, it does create a performance difference between different spectral locations on the longer links.

Based on the estimated GSNR and GSNR implementation margins at different parts of the spectrum of the LH-1792 link, 300-Gbit/s 69-GBd DP-P-16QAM modulation could be used at the lower end of the spectrum, while 300-Gbit/s 52-GBd DP-16QAM signal configuration is possible at the higher end. For the 5×75 GHz media channel configuration, regardless of the 0.3 dB Q-value difference over the spectrum service, the achieved GSNR allows only 300-Gbit/s 60-GBd DP-16QAM/DP-P-16QAM hybrid configuration to be used over the whole 5×75 GHz spectrum. Furthermore, in comparison with a single 400-GHz MC configuration, the 200-Gbit/s 34-GBd DP-16QAM PLT

configuration in 5×75-GHz media channel configuration only works for a few central frequencies over the tested spectral slot, experiencing post-FEC errors on the rest of the tested frequencies.

Although for the current link both configurations resulted in the same usable capacity carried within the tested wide-band OSaaS service, longer links may introduce a difference in total achievable bandwidth between two configurations. At any case, the GSNR performance information obtained by this measurement could be used for a power pre-emphasis at the transmitter to equalize the signal performance across the spectral slot and increase the service margins.

5.2.4 Channel probing with power adjustments

Reference [156] explains how the maximum channel performance is reached at an optimal power, where the amplified spontaneous emission noise power is twice the nonlinear noise power. In many terrestrial brown-field production networks, per channel to-the-line launch powers are optimized per amplifier output, by dividing the maximum amplifier output power with the number of end-of-life channels. More often than not, this figure is rarely adjusted according to the specific span lengths between two amplifier stations or even less likely, according to the total link length. And although the available simulation or planner tools enable to estimate the non-linear penalty per link, the opportunity is mostly used in the commissioning stage of the new network and forgotten in operation state. While the new, high-performing transceivers enable to overcome the small degradations or changes implemented after the initial commissioning, the non-optimized power-to-the-line may reduce service performance when it comes to long, concatenated links in such networks.

Simplest way to detect the optimum operation regime per channel is to increase the individual channel powers to see when the top of the SNR vs. power (or "bell") curve is achieved. Unfortunately, within power limited networks, this could lead to amplifier saturation or performance degradation on neighboring channels due to spectral hole burning effect. Therefore, a method that depends only on the maximum total power allowed by the spectrum slot is required.

This can be achieved by comparing the results received from symbol rate variable channel probing with constant PSD to the constant signal power measurements. Measurements with constant signal power use only the highest allowed total signal power for all tested symbol rates (effectively, increasing the PSD for the narrower signal formats). In both cases, the total power per probing activity stays equal or below the maximum allowed power per spectral slot and reference power used during the network equalization.

A selection of links on the Tele2 regional-haul network route A were analyzed by comparing the design-based PSD-based GSNR estimations to design-based signal power-based GSNR estimations. The operation regime detection results are presented on Fig. 19. The solid lines are the probing results with single, constant signal power for all PLT configurations and dotted lines are the same PLT configurations tested with PSD adjusted power levels. Different shades/colors refer to different link lengths. The visible symbol rate dependent tilts on the GSNR estimations on the lines measured with constant PSD refer to filtering penalty from the route. As a reference, also one link from
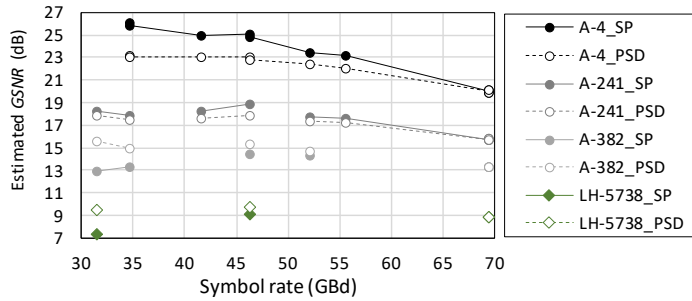
Fig. 19. *Detection of the operation regime on different links*

the Tele2 long-haul network is included on the Fig. 19, presented with diamond marker shape. For each of the links, the reference PSD and reference total allowed signal power per carrier is at 69.4 GBd, where the measurement lines for the constant PSD and constant signal power meet.

The operation regime of the specific configuration can be detected by comparing the estimated GSNR values for the constant PSD and constant signal power line.

For the shorter links (black and dark grey lines), probing with constant signal powers provides better GSNR performance than probing with constant PSD. This means, the signals still do benefit from increased launch power, hence working in the linear regime. For the longest link in regional-haul network (light grey) and long-haul network (green), the constant signal power probing provides worse GSNR estimations than the constant PSD probing. This indicates that, with constant signal power, the increased PSD of individual narrowband signals is too high, and the signal power is above the optimum operation point between ASE noise and nonlinear distortions. This means, a reduction of the signal power at the specific OTSi should be considered, if applicable from receiver sensitivity perspective at the intermediate ROADM nodes of far end S-BVT transceiver.

It is worth mentioning that while the simple operation regime detection is sufficient in narrow band OSaaS configurations, wide-band OSaaS offerings may experience operation regime differences in different spectral parts of the OSaaS service. This has an increased probability in cases where high ripple or tilt is captured through the spectral sweep exercise. It is therefore recommended to carry out operation regime detection over the spectral range of the OSaaS service to characterize the spectral slot for highest usable power levels.

By detecting the operation regime, operators can adjust the to-the-line power levels per channel and per link to increase the service margins. This helps to increase the tolerance against random fluctuations in network performance that can lead to outages when channels are operated at the BER threshold. Based on our example, the $GSNR_{margin}$ can be improved up to 2.5 dB for 31.5-GBd and 34.7-GBd signal configurations depending on the link. For the 46.3-GBd and 52.0-GBd signal configurations, the improvement is less significant, reaching only 0.8 dB. However, the improvement in such magnitude is helpful, when operated in low-margin regime.

5.3 Accuracy aspects of the method

The accuracy of the $GSNR_{est,link}$ is defined as the difference between the estimated GSNR and the real GSNR of the link. While the characterization errors, OLS equalization and PLT data reading errors contribute to systematic error, random errors of the $GSNR_{est,link}$ are caused by performance fluctuations in time.

While the industry has accepted channel probing method as a relatively straight-forward method to experimentally characterize the service, fully characterized transceivers are not often available for the task. This means that the operators are relying on average performance data curves provided by the vendors or are obligated to capture the Q-over-OSNR curves themselves. This requires time to go through multiple PLT configurations and, while simple in theory, may cause some confusion in calculating the OSNR, when working with fixed resolution optical spectrum analyzer (OSA) and high symbol rate signal formats. Furthermore, due to manufacturing and component impairments, each of the transceivers may have a slightly different performance, suggesting the exercise should be carried out every time a new transceiver is used for the OSaaS characterization. For daily operations, this may seem like too much hustle, and operators are willing to use a good-enough fitted curve with the smallest likelihood to overestimate the performance.

Depending on the PLT unit and network conditions during the test period, the probing method user must make all efforts to minimize the systematic and random error sources possibly impacting the accuracy and precision of the estimation. Knowing the impact and causes of the individual probing errors allows to reduce the error magnitude and leads to a more accurate result interpretation. Fig. 20 explains the estimation errors in estimating the true GSNR value of the link.

The systematic error is primarily caused by inadequate PLT characterization. This can be caused by the bias from transmitter and receiver noise, wrong OSNR reading during characterization or poor polynomial fitting. The results of such errors lead to the Q-over-OSNR curve to be shifted left or right on the OSNR scale, which is directly transferred to the estimated GSNR. Also, the performance differences between the PLT and actually commissioned transceiver unit contribute to the systematic error.

If multiple recorded Q-over-OSNR curves exist for a specific transceiver type, reference [153] suggests using the average curve. Based on their example, the standard
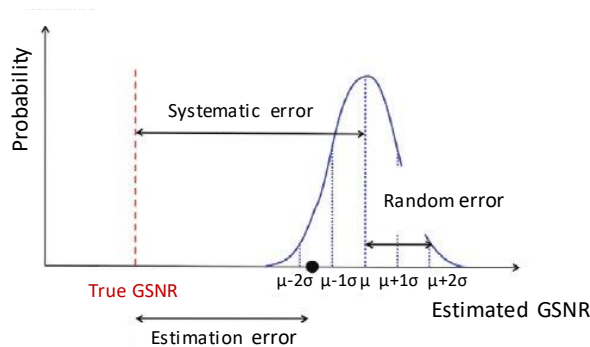

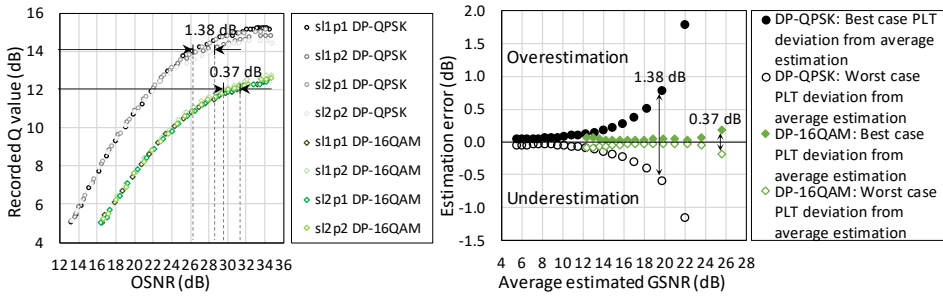*Fig 20.* Error sources in GSNR estimation using channel probing

Fig 21. *Characterization curves from four transceivers for 69 GBd DP-QPSK and 34 GBd DP-16QAM signal formats and possible estimation error*

deviation (σ) of the estimated OSNR based on seven tested transceivers increased with the estimated OSNR and reached 0.7 dB at 24.05 dB OSNR. However, if minimum GSNR overestimation is desired, the best-performing curve from the transceiver characterization activity should be used. As the final estimated GSNR is achieved with the inversion, the best curve is likely to give the most modest link GSNR estimation.

To illustrate the possible GSNR estimation error caused by the usage of non-fitted transceiver characterization curves, Fig. 21 displays four S-BVT transceivers, each characterized with Q-over-OSNR curves for 200-Gbit/s 69-GBd DP-QPSK and 200-Gbit/s 34-GBd DP-16QAM modulation format/symbol rate configurations, as recommended in [8]. The left side of the Fig. 21 presents four individual sets of transceiver-specific Q-over-OSNR datapoints, generated in Open Ireland CONNECT testbed under linear conditions using the characterization setup. Although similar to the eye, the same, 14.0 dB Q-value required up to 1.38 dB higher OSNR for the worst performing PLT unit for 200-Gbit/s 69-GBd DP-QPSK signal format and achieving 12.0 dB Q-value required up to 0.37 dB higher OSNR for the 200-Gbit/s 34-GBd DP-16QAM signal format. This means that using a non-transceiver-specific curve may generate a potential GSNR estimation error.

The magnitude of this error is based on the four characterized PLT transceivers used in this work is presented on the right-hand plot of Fig. 21. The y-axis presents the potential GSNR estimation error in dB. The 0-line presents the average normalized estimated GSNR from all four PLT units, and the x-axis represents the GSNR. The markers on the plot represent the maximum over- and underestimation among all four transceivers, compared to the mean estimated GSNR value calculated over all the PLT estimations. Black markers present 200-Gbit/s 69-GBd DP-QPSK, and green markers the 200-Gbit/s 34-GBd DP-16QAM signal configuration. The potential GSNR estimation error from using the non-transceiver specific curves is the difference between the curves and is dependent on the implementation penalties between the original transceiver used to create the Q-over-OSNR curve and the actual PLT unit used for probing activity. If the original PLT transceiver used for characterization curve creation was better-performing, then underestimation occurs, as the original transceivers required lower OSNR to achieve the same Q-value. If the original transceiver was performing worse than the PLT used for probing, overestimation occurs. At Q value 14.0 dB and at average estimated GSNR of 19.79 dB, the maximum variance in estimated GSNR is 1.38 dB depending on the used non-transceiver-specific curve for the 200-Gbit/s 69-GBd DP-QPSK signal. At Q value

14.5 dB and average estimated GSNR of 22.00 dB, the estimation variation between different curves grows quickly to 2.90 dB. Errors in such magnitude can make a remarkable difference for the operators [137].

To obtain meaningful performance data from the channel probing procedure, infrastructure-related error sources in channel probing should be minimized, too. For OSaaS use cases implemented with a different media channel width than the nominal grid of the OLS system, the systematic error with the potentially highest deviation magnitude is caused by the service equalization with nominal design-based power levels in the ROADMs. To avoid this, the OSaaS services must be equalized using the maximum allowed power spectral density in the OLS. Depending on the OLS functions and capabilities, that may require some manual ROADM output power set-point adjustments to fit the OSaaS media channel width and design-based power spectral density of the OLS. The equalization is even more challenging, when several OTSi are used within a single wide-band media channel. In addition to equalization, specific spectral location under test, impact of link channel load and degradation caused by optical filtering may impact the systematic error in GSNR estimations. Furthermore, the actual performance estimations on field are dependent on the probing setup: the setup implementing a loopback at the add/drop port of the far end ROADM doubles the optical distance travelled by the probing signal. In strictly linear environments, that adds a 3 dB degradation to the $GSNR_{est,link}$ of the single direction of the link. The estimation error may be induced, if the transmit and receive directions in the network are with different performance due to very long spans at the beginning of one direction, that may deplete the OSNR early on the link. A second option for channel probing is using a transceiver pair similarly to a regular service operation in the network. However, even if both involved transceivers are characterized, it is not clear how to combine the two characterization curves of the involved transceivers for maximum probing accuracy. These specifics remain a task for future studies.

The additional bias from the actual performance can be caused also by the short-term and long-term network performance variations, that may impact the Q reading between the PLT test and the commissioning of the final transceiver unit(s). However, it can be argued if the bias caused by the delays in commissioning should be accounted as a probing error.

In general, the only random errors in channel probing can be caused by the fast network performance fluctuations. These fluctuations may be caused by PLT or OLS component, or environment instabilities that create cumulative bursts of errors, which influences the Q-value reading during the probing. Random errors contribute to reduced precision of the probing activity but can be overcome with longer measurement periods or performing multiple measurements per single PLT configuration.

As a conclusion, the channel probing method-based service characterization is only valid for the time of the measurement and various changes in the network may change the performance of the spectrum slot. In addition to PLT characterization-related estimation inaccuracies, various time-dependent variations must be accounted for. Leaving aside the fast power fluctuations and slow long-term aging, OSaaS characterization with a single probe sweep method, as proposed in [133], requires margin estimations to compensate for measurement related errors, future addition or removal of neighboring channels, and changes in general channel load.

5.4 Accuracy of the estimated $GSNR_{est,link}$/$GSNR_{margin}$

As the theoretical GSNR calculations are often not available for OSaaS use cases and no direct measurement tool to capture GSNR exists, the verification of the estimated $GSNR_{est,link}$ accuracy has to be also addressed indirectly. To verify the accuracy of the estimated $GSNR_{est,link}$, near zero-margin PLT configurations can be used as verification signals.

For this, a GSNR implementation margin ($GSNR_{margin}$) from equation (5) can be used. If the $GSNR_{margin}$ calculation result is positive, the configuration is expected to work over the probed link. All calculations resulting in a negative GSNR implementation margin are expected to not to work. Contradiction between the estimated $GSNR_{margin}$ and the actual signal state indicate the false $GSNR_{est,link}$ estimation.

The theoretical background of the method is the following: in the case of a linear operation, the GSNR margin can be viewed as a difference between the existing link OSNR and required link OSNR. Assuming, that the measured noise power in nominal 0.1 nm bandwidth in dBm remains the same, the margin can be increased or decreased by adjusting the power of the commissioned signal in dBm, as it effectively changes the OSNR of the Channel under Test (CuT) [137]. When the signal bandwidth is fixed, noise conditions are constant, and the minimum required OSNR for the specific configuration is known, the reduction of the commissioned signal power to the minimum signal power required to satisfy the required OSNR should bring us close to the pre-FEC BER threshold. Therefore, the validity of the estimated $GSNR_{margin}$ can be assessed by comparing the $GSNR_{margin}$ with the relative power difference between commissioned signal power and minimum required signal power to meet the zero-margin, corresponding to pre-FEC BER threshold.

For this, we first use transceiver-specific characterization curves for 200-Gbit/s 69-GBdDP-QPSK and 200-Gbit/s 34-GBd DP-16QAM PLT configurations to detect the candidate GSNR of the link. In order to avoid overestimation, the lowest estimation is used as the $GSNR_{est,link}$. Then, the required GSNR for the configuration is subtracted from the $GSNR_{est,link}$, and the estimated $GSNR_{margin}$ for various PLT configurations can be calculated as per equation (5). Configurations which have close-to-zero margins are selected as verification signals for further testing. For this, the PLT unit is configured to the configuration under interest and the power levels of the verification signal configurations were adjusted to achieve a 5.0 dB Q-value reading, exactly corresponding to the pre-FEC BER threshold and zero $GSNR_{margin}$.

Results from the margin verification activity from four live links in HEAnet metro network are presented in Fig. 22. The y-axis of the figure presents the $GSNR_{margin}$ estimation error with the zero-line on the plot corresponding to a zero margin, based on the $GSNR_{est,link}$. The x-axis presents all tested PLT configurations. If all the calculated margin estimations from (5) would be correct, the power adjustments in the same amount as the margin would position all the readings closely around the zero-line. Crossing the zero-margin line should change the working state of the signal. As the original state of these configurations was either below or above the FEC threshold, the arrows on the figure present the direction and amount of the power adjustment in dBm performed. If the arrow is facing up, the configuration was originally not working, and it's power was increased.
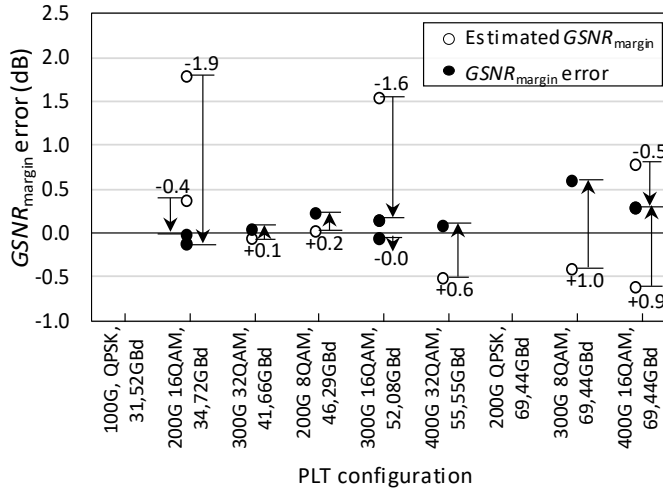
Fig. 22. Margin estimation error per PLT configuration from four HEAnet live links

For some PLT configurations, it was possible to adjust the power levels for two live network links. In this case, the specific configuration on Fig. 22 has two estimated $GSNR_{margin}$ markers per PLT configuration. Calculated GSNR margins based on (5) are marked with transparent markers, regardless if the channels were originally working or not. Probing results for power-adjusted verification signals are marked with black markers. The difference in the estimated adjustment power and required power to reach the pre-FEC BER threshold is the margin error. When the $GSNR_{est,link}$ overestimation is avoided, and lowest $GSNR_{est,link}$ is selected for the calculations, the margin verification brings us close to the zero-margin line for narrow-band signal formats. The results stay well within the probing error caused by the probing granularity (usually 0.1 dB in power adjustment increments or 0.1 dB in Q value), and only the high symbol-rate channels experience a lower margin estimation accuracy, as the margin error reaches up to 0.6 dB in error magnitude. While the most probable reason for the margin error is caused by the error in $GSNR_{est,link}$ estimations, the PLT implementation impairments, not characterized for the high-symbol rate PLT configurations, may also be the reason for the margin misalignments.

5.5 Validity of the estimation results

According to [8], $GSNR_{est,link}$ obtained from the probing measurement can be defined as the ratio between the power of useful signal divided by the sum of the powers of all noise sources and can be expressed as (4). Therefore, without characterizing propagation associated penalties such as CD, PMD and PDL associated with the test, the real GSNR of the link, consisting of the SNR_{ASE}, SNR_{NLI} and SNR_{GAWBS} component only, is not available. However, the $GSNR_{est,link}$ estimations are valid for the $GSNR_{margin}$ estimations for the same modem type. In [8, 9], the characterization process of the PLT unit is explained and in [9, 132], the standard deviation and accuracy for the different pre-FEC BER readings and its impact on the achievable throughput estimation dependent on a performance variability of different PLT units is explained. These references conclude that a better GSNR

estimation accuracy is achieved at lower Q values since the transceiver performance variation is much smaller in that region.

Leaving aside the PLT unit dependent penalties, equation (4) is valid in optical systems, where fiber propagation impairments caused by the interplay of loss, chromatic dispersion and Kerr nonlinearity can be approximated as additive white Gaussian noise (AWGN) [138]. This raises the question of GSNR metric reliability in short spans, dispersion compensated spans and spans experiencing high nonlinear penalty. Therefore, it is important to note that the estimated $GSNR_{est,link}$ from the channel probing is not the actual, real GSNR of the link, but its projection/approximation in the linear space, where the Q-over-OSNR characterization of the PLT unit is performed. Therefore, any measured Q value from the real-life networks is compared to the polynomial fitting from the linear domain, projecting all the link induced impairments into linear domain, too. As also the typical, required GSNR from the system specifications is only defined for linear working regime, the $GSNR_{margin}$ estimations lead us to similarly accurate estimations in each of the tested network scenarios (including short and dispersion compensated links).

Although channel probing provides reliable end-to-end GSNR estimations, as discussed above, the estimation results are only valid for the infrastructure configuration and network load during the probing activity. As OSaaS characterization is mostly performed once during the service handover, margins to accommodate the future degradations from possible daily fluctuations, ageing effects and network load/condition changes must be considered. For this, two options exist:

- incorporate additional margins as per [121] to the initial estimated $GSNR_{margin}$ to increase the robustness of the OSaaS live traffic or
- implement continuous probing.

While the first is a fixed measure and only protects the OSaaS user within the degradation range set by margin, the later provides continuous performance estimations from the network. When data from continuous probing is used to train the machine learning (ML) algorithm, performance changes in OLS can be predicted and notifications can be sent to OSaaS user in case of abnormal changes [157, XII].

5.6 Conclusions

This chapter presented how a channel probing concept from [8] and [132] can be extended and modified, to capture various performance nuances present in narrow- and wide-band OSaaS configurations implemented in brown-field terrestrial DWDM systems. Through the employment of symbol rate variable probing, sweep procedure and operation regime detection, the capture of the OSaaS performance was demonstrated without any need for detailed OLS related information.

Using symbol rate variable extended channel probing, a GNSR estimation accuracy of 0.05 dB was achieved for a OSaaS service implemented in flex-grid, dispersion uncompensated long-haul system. Furthermore, the usability of the method has been verified in the fixed-grid, dispersion compensated legacy network, where channel probing was believed to be not usable before. A GSNR estimation accuracy of 0.32 dB has been achieved for a narrow-band OSaaS service configurations prone to filtering

penalty from multiplexer, grating based dispersion compensation and ROADM modules. The high precision of the probing accuracy can be accounted on multiple $GSNR_{est,link}$ estimations from different PLT configurations used in a constant power spectral density mode. This approach allows to average out the errors from channel probing procedure and use mean value from all estimations as a final estimated $GSNR_{est,link}$.

The chapter also introduced the spectral sweep procedure to capture the GSNR profile that gives insights to OSaaS bandwidth and configuration. Specific for wide-band services, the sweep procedure can highlight the wavelength dependent performance variations, a spectral ripple/tilt within the service, or capture the filtering penalty at the service edges. Furthermore, frequency sweep can be also exercised on a narrow-band OSaaS service to detect the bandwidth limitations and central frequency misalignments in the OLS components.

Furthermore, the usefulness of the operation regime detection has been demonstrated. Knowing the operation regime can help adjusting power levels and perform GSNR-based pre-emphasis to maximize service margins.

In addition, the chapter provided a comprehensive overview of error sources related to channel probing method in terrestrial systems, highlighting the primary causes for systematic and random errors and stressing the importance to always use transceiver-specific characterization curves when performing channel probing. The magnitudes of the errors dependent on the latter were demonstrated based on four characterized transceivers used in this work.

Finally, the estimation error was experimentally verified in HEAnet network through depleting the $GSNR_{margin}$. This demonstrated that the achievable estimation error in the tested networks was slightly PLT symbol rate dependent, and reached up to 0.6 dB.

Based on the performance data acquired from the proposed channel probing toolkit, spectrum users and OLS system operators can take fully informed decisions on how to leverage their spectral resources in the most efficient way. Together with the automation and continuous probing perspective in the operation phase of the OSaaS, using the live transponders, further improvements on the performance monitoring capabilities of the OSaaS can be achieved. As a conclusion, channel probing provides a feasible method to capture the performance related aspects in the OSaaS use cases.

6 OSAAS CHARACTERIZATION

The primary motivation for OSaaS service characterization is to provide end-customers with up-to-date input for achievable capacity calculations over the OSaaS spectral slot without revealing business-sensitive data about the OLS system and its components. As OSaaS is fundamentally different from leased line capacity services and dark fiber rental, a 24-hour BER test or Optical Time Domain Reflectometer (OTDR) testing is not feasible for this new service type. Even capturing the received noise spectrum power spectral density over the OSaaS would not help, as it does not enable to estimate the achievable capacity. The potential and accuracy of ASE-loaded OSNR profiles was investigated in [133], but the risk of causing possible problems to the neighboring channels through loading high amounts of power into the OSaaS spectrum makes it unfeasible for the use. Furthermore, the OSNR component may not be sufficient to reliably estimate the achievable capacity in the longer systems which accumulate nonlinear impact from the medium even in case of operating each span in a linear regime. This means, an entirely new service characterization method must be agreed upon, to reliably describe the OSaaS performance for commercial offerings.

Together with the thresholds for secure operation, the OSaaS characterization must include the following list of data:

- OSaaS service boundary frequencies,
- allowed power thresholds,
- accurate performance values for achievable capacity estimations within the spectrum slot,
- precise capture of the possible wavelength-dependent performance variations within the provided OSaaS bandwidth,
- precise indication of the effective service bandwidth and filtering penalty at the MC edges,
- presentation of possible nonlinear regimes within the provided OSaaS bandwidth,
- list all possible required margins for safe end-of-life operations.

For simplified overview, these requirements can be presented in the table, presenting the required thresholds and values. Without depending on any QoT estimation tool, the example of a handover documentation for a 400-GHz OSaaS service today would look as brought in Table 4. The following sub-chapters will focus on each of the rows not available today and explain the necessity, derivation and accuracy of the items proposed to be included in the handover documentation. It provides reader with necessary information about wavelength dependent performance variations within the service, as well as possible filtering penalty and nonlinear operation regime within the OSaaS. The chapter also discusses margin allocation to accommodate impact from direct neighboring channels, end of life channel loads, and fast and slow performance fluctuations in the network. Finally, the chapter presents an end-to-end performance estimation example in multi-domain, multi-operator environments based on the service characterization data.

Table 4: OSaaS handover documentation with service specifications and margins

OSaaS parameters per OLS system	Value	Min	Max
Optical Bandwidth (GHz), start and stop frequency (THz)	400	193.75	194.15
Total power (dBm)	9	-1	9
PSD (dBm/GHz)	-23	-33	-20
OSNR ($f_{central}$) (dB)	20	17	20
GSNR ($f_{central}$) (dB)	Not available		
Wavelength dependent GSNR variance (dB)			
Operation regime in different parts of spectrum			

Margins:
    Slow performance fluctuations (dB)
    Fast performance fluctuations (dB)
    Enabling direct neighbors (dB)
    End-of-life spectral load(dB)
    Aging (dB)
	Not available		

The test setups used to derive the results in this chapter are as follows: the examples and analyses of the GSNR-based profiles presented in 6.1 are captured in Tele2 pan-European long-haul network and ADVA Gdynia lab in Poland. The service margins derivation for enabling direct neighboring channel and end-of-life channel loads in 6.2 is performed in Open Ireland CONNECT lab and verified in HEAnet production network in Dublin, Ireland. The standard deviation-based service margins to compensate for fast and slow performance variations in the network are derived from Tele2 long-haul network. Finally, the concatenated profiles are tested in Funet production network in Finland. All tested network setups are described in Chapter 4.

6.1 GSNR profile

Reference [133] concludes, that in terrestrial brownfield systems, Generalized Signal to Noise (GSNR)-based characterization profiles for OSaaS are preferred over Amplified Spontaneous Emission (ASE)-loaded Optical Signal to Noise (OSNR)-based profiles. This conclusion is mainly driven by three factors: possibly high inaccuracy of the OSNR-based profiles in lightly populated DWDM systems, high probability to cause impact on neighboring channels when suddenly lighting up a big portion of the spectrum with ASE-load, and high accuracy and relatively small amount of needed measurement equipment in case of GSNR-based profiles.
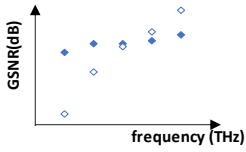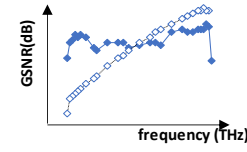
In essence, a GSNR profile is a performance profile, that presents measured GSNR data over the full bandwidth of the OSaaS spectrum. Based on this data, users can make weighted decisions on the achievable capacity at any part of the OSaaS spectrum.

To capture the GSNR profiles, characterized transceiver(s) to use channel probing technique are required. With a single probing light unit (PLT), single-probe frequency sweep method can be used, while in case of multiple simultaneously available PLT units, multiple-probe scenario can be used to record the coarse GSNR profile. Theoretically,

also receive power profile can be considered for OSaaS characterization, but as it does not allow to estimate the service performance and achievable capacity, it cannot be used as a stand-alone profile. However, the Rx power data can provide additional information on signal performance and is therefore collected together with the Q-value required for GSNR estimations.

An overview of the two GSNR profile types, the required resources to capture them, and their theoretical capabilities to characterize OSaaS are given in Table 5. For the use in service handover documentation, these profiles should be complemented with a margin set to indicate possible degradations from fast and slow performance fluctuations, network ageing, enabling the direct neighboring channels or changes in general channel load in the OLS system. To derive margins for the fast and slow performance fluctuations and network ageing, a long-term performance monitoring is preferred in a continuous probing mode. However, margins for performance degradation from enabled direct neighboring channels and end-of-life channel loads can be also derived experimentally. This is covered in chapter 6.2.
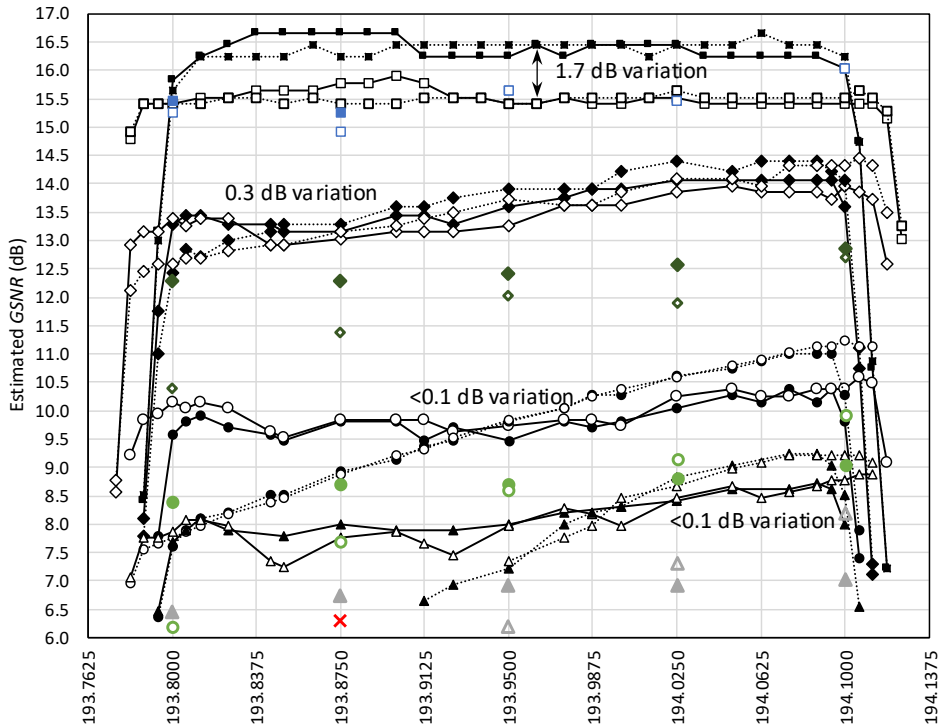
Table 5: Available GSNR profiles and their capabilities to characterize OSaaS

	Multiple-probe GSNR profile	Single-probe sweep GSNR profile
Example profiles from a 375-GHz OSaaS spectrum with - 5×75-GHz configuration (b), and - 1×375-GHz configuration (c)	 ◆ Multiple-probe GSNR profile for (b) ◇ Multiple-probe GSNR profile for (c)	 ◆ Single-probe GSNR profile for (b) ◇ Single-probe GSNR profile for (c)
Required equipment to record	Multiple characterized PLT units	Single characterized PLT unit
Minimum resolution	As per MC bandwidth	As per PLT unit bandwidth
Captured effects: - General accuracy - Wavelength-dependency - Effective service bandwidth - NL regime	Dependent on PLT configuration Y Y Y, when Rx power profile is available	Dependent on PLT configuration Y Y Y, when Rx power profile is available

6.1.1 General accuracy of the GSNR profile

The first aspect we address is the accuracy of the GSNR profiles. Fig. 23 presents the GSNR profiles for three link lengths from Tele2 long-haul network and one from the Gdynia lab. The links are configured based on (b) and (c) implementation scenarios from Fig. 7 with either 5×75-GHz MC configuration or 1×375 GHz MC configuration. Then, symbol-rate variable channel probing with 100-Gbit/s DP-QPSK 31.5-GBd and 200-Gbit/s 69.4-GBd DP-QPSK PLT configurations is performed.

As visible from Fig. 23, the variation between the profiles recorded with narrow-band and wide-band PLT configurations deviate up to 1.7 dB for the high OSNR lab setup, while it is less than 0.3 dB for the LH-1792 link and even less for two longer links on the production network. In addition, the 200-Gbit/s 69.4-GBd DP-QPSK PLT configuration is delivering higher GSNR estimations compared to its 100-Gbit/s 31.5-GBd DP-QPSK counterpart at high-OSNR links.

Fig. 23. *GSNR profiles for the lab link and three long-haul production links*

To explain this, a separate measurement in the lab OLS in Gdynia was carried out by varying the VOA-2 attenuator to alter the effective OSNR of the link. For GSNR comparison purposes, constant Tx PSD was maintained during the measurements. Results from these measurements are illustrated in Fig. 24. The x-axis presents the OSNR of the lab OLS in dB, recorded under 0.1 nm reference bandwidth conditions by the DSP of the PLT unit, when configured as 200-Gbit/s 69.4-GBd DP-QPSK. As the perceived OSNR of the OLS varies with the PLT symbol rate, when the Tx PSD is kept constant, the values on the x-axis only present fixed conditions for the noise loading of the OLS, and not the true OSNR of the lab link. For additional reference, the VOA-2 attenuation settings for noise loading in dB are presented on the secondary x-axis. The y-axis presents the estimated GSNR deviation in dB. Different lines correspond to characterized PLT configurations, color-coded and grouped by the symbol rate. The exercise revealed less than 0.2 dB of variation between the estimations available from three PLT configurations working at 16.9 dB of OSNR. For the 24.9 dB OSNR setting, the variation between the same three PLT settings was to almost 1.9 dB. At the same time, the maximum Rx PSD deviation between the various PLT configurations fluctuated randomly between 0.3 and 0.7 dBm/GHz over the full OSNR range, showing no correlation with the increasing variation within the GSNR estimations. This lab exercise supports the test results from the live network, where the variation within GSNR estimation results, retrieved with different PLT configuration grows with link OSNR. The most probable reason for the high estimation variation at high OSNR can be accounted to the saturation regime of the high-symbol-rate PLT configurations at high signal quality, explained in detail in [8]. This is more likely to happen when operating a high-symbol-rate PLT configuration, as the implementation impairments and penalties of the PLT units flatten the Q-over-OSNR PLT characterization curves. This can introduce more than 10-fold change in the estimated GOSNR with only a marginal change in the Q-value. As the 200-Gbit/s 69.4-GBd DP-QPSK signal format is robust towards noise, its saturation OSNR is the lowest compared to other high symbol rate PLT configurations. Consequently, the primary challenge related to reliable GSNR profile capture is the selection of a suitable PLT configuration.
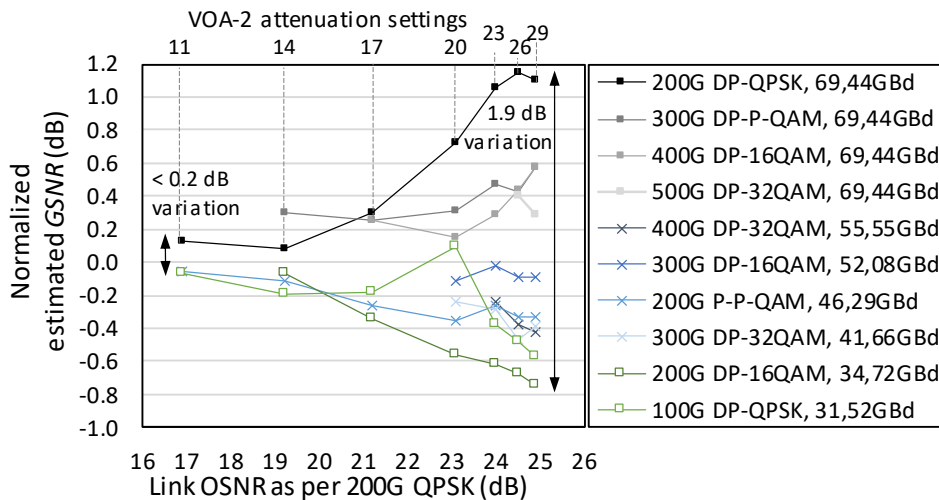

Fig. 24. GSNR estimations on various PLT and OLS OSNR configurations

Based on our work, we recommend the use of 200-Gbit/s 34.5-GBd DP-16QAM as PLT at high OSNR and 100-Gbit/s 31.5-GBd DP-QPSK as PLT at low OSNR for optimal performance capture in flex-grid networks. If only one PLT configuration is desired to perform the channel probing, 200-Gbit/s DP-P-16QAM is a good candidate due to its low required GSNR and relatively narrow signal bandwidth.

6.1.2 Wavelength-dependent variation over the OSaaS bandwidth

The second aspect under interest is to identify any wavelength-dependent variations within the tested OSaaS implementations. Fig. 23 shows, that the flattest performance within the OSaaS spectrum is captured on the lab OLS. The estimation deviation for the same PLT configuration is ±0.15 dB around the mean estimated GSNR value over the OSaaS bandwidth, independent of the OSaaS configuration. This can be attributed to the EDFA-only amplification scheme and relatively short link length in lab OLS. The links in the production network, however, were characterized with a pronounced GSNR variation over the OSaaS spectrum. The variation was explicitly evident for the single 375-GHz MC OSaaS configuration, reaching 2.5 dB for the shortest, 1792 km link, and up to 8.5 dB for the longest, 5728 km link. For the tested links, the GSNR variation aligned well with the Raman ripple caused by the Raman gain profile. As mentioned in chapter 4 describing the test setups, the detected Raman ripple in the spectrum is dependent on Raman implementation. Raman implementations with higher number of pumps cause less ripple, but each added pump adds to the cost of the equipment. In any case, the areas between the pumps will have a smaller effective gain and hence experience higher effective span loss. This causes the signals to have a lower OSNR and, if operated in the linear regime, also lower GSNR. Due to this variation, the LH-5738 link has part of the spectrum working below the minimum required GSNR value for any modulation-format/symbol-rate combination to work and hence being unusable for data transmission. At the same time, the better performing part at the higher frequencies of the GSNR profile on LH-5738 link is flattened. This can be attributed to the optimum operation point on the link, as further explained in section 6.1.4. In general, PSD-based intra-MC equalization, as in OSaaS configuration (d) should minimize the variation in the GSNR profile caused by the Raman gain spectrum. Unfortunately, this is a relatively new function and not available in many brown-field installations.

Regardless of the 5×75-GHz configuration, that should contribute to a better equalization over the 375-GHz OSaaS bandwidth, the impact of the ripple introduced by the Raman gain spectrum is still evident in the GSNR profile. In addition to that, the 5×75-GHz GSNR profile has distinguishable dips between the adjacent 75-GHz MCs. This is explicitly evident when probing with narrower PLT configurations. Fig. 25 explains the ripple formation based on PSD distribution in three locations on the ROADM link: equalized Tx PSD transmitted to-the-line (TTL) after the initial signal add, Rx PSD after the link and equalized Tx PSD TTL to the next ROADM link. As Rx PSD after the link is impacted by the intrinsic Raman gain profile on the line and the equalization of the spectrum only happens with the defined increments of the MCs, the 75-GHz dedicated spectral width in the 5×75-GHz configuration still has a pronounced tilt formation even within the MC. As the effective PLT bandwidth is swept over the full spectrum of the OSaaS, it still picks up the low-performing areas of the spectrum due to the power ripple
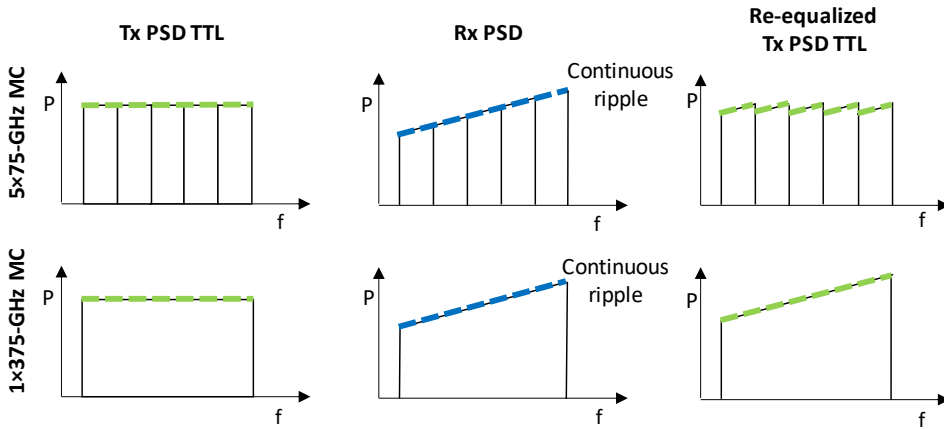
Fig. 25. *Explanation of the dip formation*

caused by the Raman amplification. If the spectrum is swept with a high symbol rate PLT configuration, the dips in the spectrum are less distinguishable due to the broader bandwidth of the PLT configuration and hence a higher averaging effect. As the primary goal of the OSaaS characterization is to describe the spectrum as precisely as possible, narrower PLT configurations are preferred.

For both tested OSaaS configurations, the variation in the estimated GSNR recorded by the multiple-probe scenario follows the slope of the single-probe sweep profile. Deviations are primarily explained by different insertion losses from the add/drop structures that were not flattened by the equalization process in ROADMs in a wide-band OSaaS scenario. Compared to the GSNR values recorded by the single-probe sweep, the GSNR values recorded by the multiple-probe scenario are degraded due to enabled neighboring channels. This can be attributed to linear and nonlinear crosstalk from neighboring channels, mainly caused by the used 75-GHz spacing between the central frequencies of the OTSi, which is not optimal for the 69-GBd signals.

6.1.3 Effective service bandwidth

Another benefit of a narrow-band PLT configuration is the precise capture of the effective service bandwidth at the service edges. Fig. 23 showcases how the OTSi-s located at the OSaaS spectrum edges experience increased filtering penalty from the ROADM modules with increasing length of the route. When comparing the performance of central frequencies closest to the service boundaries (193.8 and 194.1 THz), we see that operation of a 200-Gbit/s 69-GBd DP-QPSK signal format experiences some penalties from the filtering already on the shortest live network link.

This is a known effect, and many works in the literature address this from different angles [158-160]. This penalty from narrow-band filtering results in a reduced GSNR estimation close to service edges, as the approximation of the GSNR in channel probing method accounts for all impairments from the transmission medium. Here, the simplicity of the channel probing can help to make weighted decisions on the OTSi configurations to be used at the service edges in a black-box scenario.

6.1.4 Operation regimes estimation

As mentioned in section 6.1 it is possible to make assumptions on the operation regime when both GSNR profile and Rx power are recorded during the channel probing activity. Fig. 26 demonstrates these profiles using a 100-Gbit/s DP-QPSK PLT for OSaaS configurations (b) and (c) on link LH-3752. Similarly to Fig. 23, solid lines represent the 5×75-GHz configuration and dotted lines the 375-GHz MC configuration. Black lines mark the estimated GSNR values in dB, with a primary axis on the left, and green lines mark the recorded Rx power, presented as Rx PSD, with the values on the secondary axis (in dBm/GHz). Following both lines over the OSaaS bandwidth, presented on the x-axis, we expect to see a steady GSNR growth with increasing power when operating in the linear regime. However, we can see that starting from 194.00 THz, further growth in power does not introduce the same increase in GSNR. This indicates that the link under test operates around the optimum power. However, for our tested long-haul links, there was no change in the operation regime, where the additional power would introduce a reduction in GSNR, indicating the nonlinear operation.
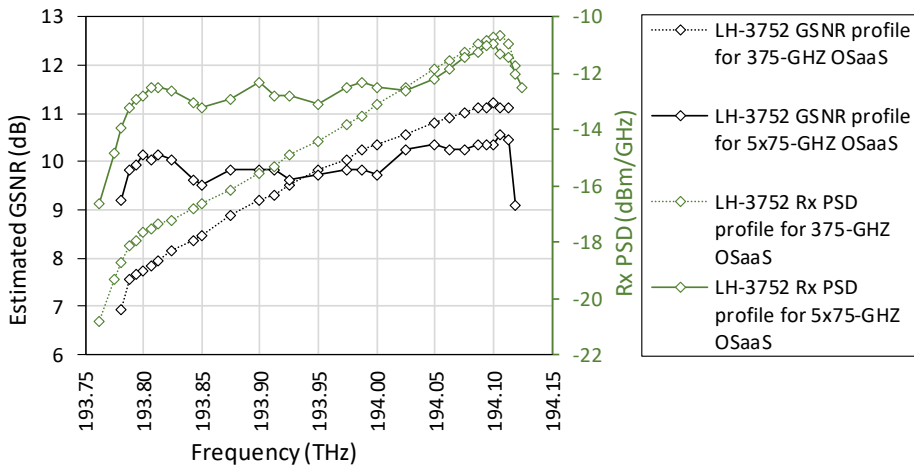

Fig. 26. *Rx PSD vs GSNR profiles for the LH-3752 link*

6.2 Time dependent performance margins

In this sub-chapter, we utilize long-term telemetry data collection from Tele2 long-haul network to derive service margins to cover for time-dependent performance fluctuations in a wide-band OSaaS. For this, a single 375-GHz wide-band OSaaS was implemented in Tele2 Raman-enabled long-haul network. The three provided links with a looped length of 1792 km, 3752 km, and 5837 km utilized a standard single-mode fiber and used aerial Optical Power Ground Wires on the Baltic part of the network. The probing signals were pre-emphasized between -3.0 dBm and +3.0 dBm to partially compensate for the Raman ripple effect within the allocated spectrum, discussed in 6.1.2. To capture the maximum changes in the link performance, automatic power equalization on the link compensation was disabled.

The telemetry data collection illustrated in Fig. 9 was arranged considering a regular OSaaS end customer monitoring capability. This means, that the system-related monitoring data, collected by the provider's Network Management System (NMS), is not accessible to the OSaaS end-user and only the telemetry data collected from the transceiver equipment operated by the end-user, can be used for margin derivation. The telemetry data was automatically retrieved from the transceivers using automated telemetry scripts based on the vendor specific NETCONF commands. The data was retrieved every 30 seconds and included forty parameters per OTSi, including current Q-value and optical receive (Rx) power. The retrieved data was stored in a time-series database (InfluxDB) and visualized using a Grafana dashboard with an option to export as comma-separated values (CSV) for further processing.

6.2.1 Slow performance fluctuations

The primary noticeable pattern in the recorded data was the slow drift with a 24-hour/daily pattern, which was surrounded by fast performance fluctuations. The longer the link, the more pronounced was the daily pattern. To analyze the magnitude of the variations and hence, derive the service margins for slow performance drift, averaging over a two-hour time window was performed to eliminate the impact from fast performance variations, limiting the dataset to 301 unique data points per transceiver and link, as presented on Fig. 27, top. As visible from the figure, the worst performance on the first link was on the OTSi operated at the best possible spectral position at 194.100 THz within the OSaaS (see Fig. 13 for Raman ripple). This is caused by the signal pre-emphasis at the transmit end, where 194.100 THz was suppressed by -3 dBm and the transmit power of the 193.800 THz increased by +3 dBm, with other signals adjusted in between. By the end of second link, the performance over the spectrum has equaled out and varies only ±0.5 dB around the mean Q-value. On the longest link, however, the amount of pre-emphasis at the transmit end is not enough. This leaves three transceivers operated at the lower performing area of the OSaaS performing below the Q-value threshold. Transceivers operating below the Q-threshold were discarded from the analysis. Then, the standard deviation (σ) was calculated based on the averaged values to derive service margins based on 6×σ which would cover 99.7% of the performance variations caused by the slow drift. These margins were compared to the maximum and minimum detected Q-values in dB from the link. Assuming the ideal normal distribution of the 301 data points, 0.3% would lead to less than one data point being outside of the found margins. The derived average service margins to compensate for the slow performance drift based on a 6×σ for the Q-value were 0.87 dB, 1.45 dB, and 1.56 dB for the 1792-km, 3752-km, and 5738-km links respectively and are able to compensate majority of the operation points within the daily slow drift. Differences between the link performances and transceivers are presented in Fig. 27, bottom. The colors of the curves refer to the monitored link and style the used transceiver frequencies. The black and red standard deviation values on the figure stand for the best-performing transceiver on the 1792-km link and worst-performing transceiver on the 5738-km link.
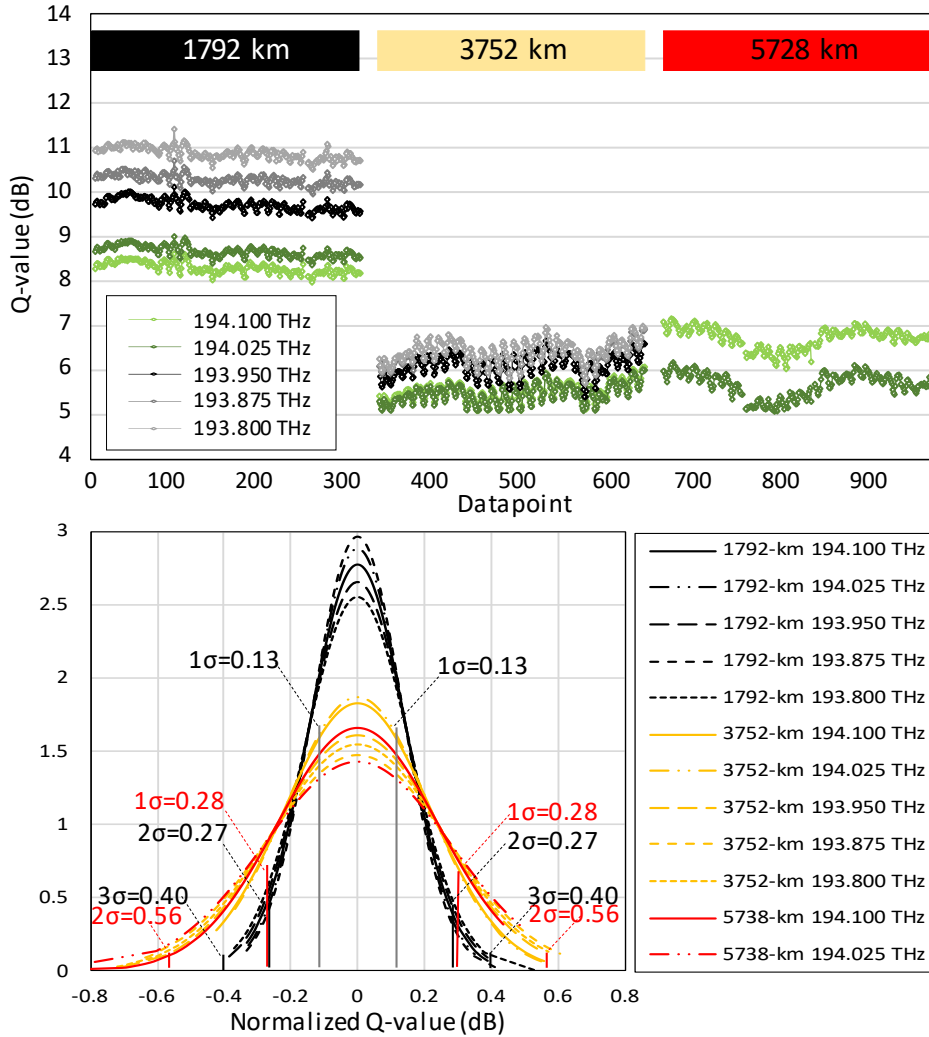
Fig. 27. Top: *Averaged slow drift in Q-value for all links,*
Bottom: *Normalized Q distribution on all links*

6.2.2 Fast performance fluctuations

Additionally, an hour-long raw data consisting of 124 data points per transceiver was used to calculate the standard deviation for fast performance fluctuations in the network for each of the transceivers. Similarly, to the slow drift, the standard deviations were calculated per transceiver and per link length.

Based on all five ports, the per-link average service margins to compensate for the fast power fluctuations based on 6×σ were 0.32 dB, 0.345 dB, and 0.44 dB for the 1792-km, 3752-km and 5738-km links respectively. Comparing the per transceiver performance, the derived margins were higher for the transceivers working with lower Rx power levels. This emphasizes that wide-band OSaaS should be operated together with power spectral density-based spectrum equalization schemas when possible.

Fig. 28 summarizes the total required margins to compensate for slow and fast performance variations in the tested long-haul network. The results per link length are marked with bar colors. As the signals operated in the lowest-performing area of the OSaaS spectrum were performing under the Q-threshold, the margins on the longest link could not be derived for transceivers working at 193.950, 193.875 and 193.800 THz. These are marked with N/A bars on the figure. The total margin consisting of two components is marked on the top of the bars.

According to Fig. 28, the margins required by the transceivers on the shortest link are within close range regardless of the high variance in the received Q-value. This may be caused by almost equal Rx powers on the link due to pre-emphasis. However, as the impact from pre-emphasis is lessened with the growing link length, the deviation in margin requirements is also increasing. This means, OSaaS operation in a single wide-band MC configuration over Raman-enabled long-haul networks requires margin adjustments to compensate for wavelength-dependent variations. This is specifically crucial for wide-band OSaaS operated in Raman-enabled long-haul networks.

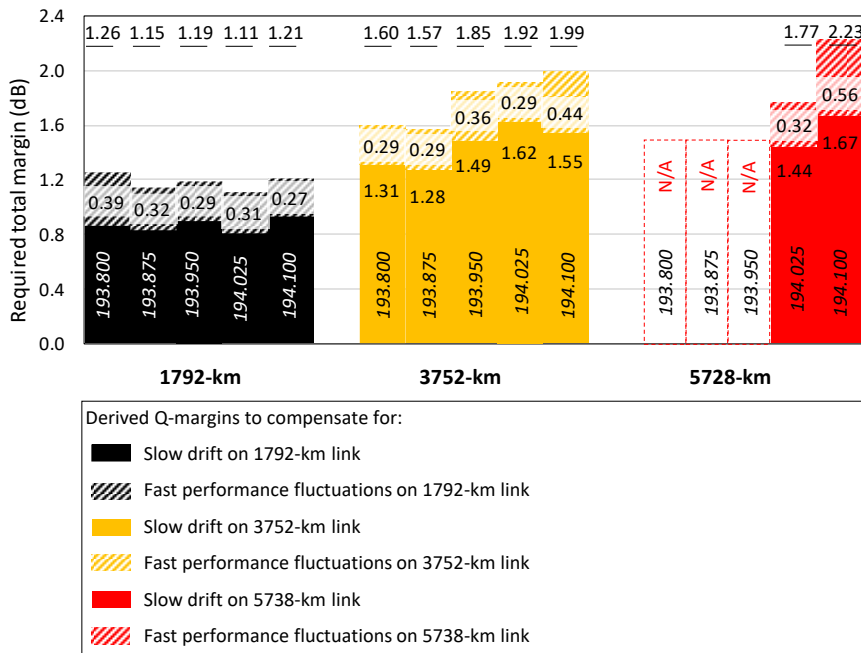**Fig. 28.** *Total margin requirements based on 6×σ for link lengths and individual transceivers*

6.3 Channel load dependent performance margins

In this section, we derive OSaaS service margins to cover future degradations from neighboring channel impact and end-of-life system deployment. For this purpose, we focus on the 200-Gbit/s 69-GBd DP-QPSK signals, which show the highest sensitivity to neighboring channels.

In order to do so, a test setup was installed in Open Ireland CONNECT lab to enable channelized ASE-loading to the OLS system together with the CuT. The test setup is introduced on Fig. 10 and spectral allocation for ASE-loaded spectrums on Fig. 11. Further details about the test setup can be found from [137]. The setup allowed to collect channel probing data over nine different channel loading conditions, which included systematically enabling and disabling 400-GHz spectral slots in the OLS. The central 400-GHz spectral slot was used for four probing transceivers, commissioned to 200-Gbit/s 69-GBd DP-QPSK signal format.

Fig. 29 presents the raw data from the GSNR estimations from gradually filled spectrum exercise. The y-axis presents the absolute values for candidate GSNR estimations based on the measurements with different PLT configurations of a single transceiver. The four shaded areas present the OLS conditions after modifying the
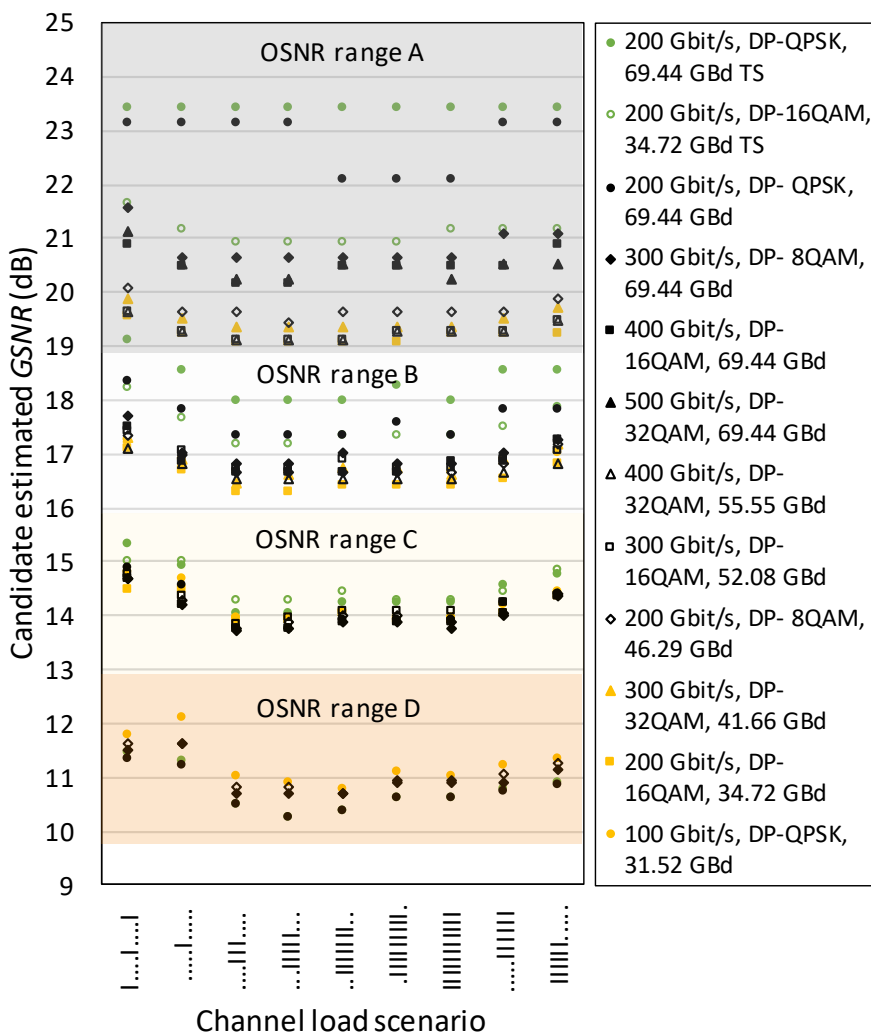

Fig. 29. Raw data from the channel probing in Open Ireland lab for
non-transceiver specific and transceiver-specific curves

VOA-2 in the test setup, leading to four received OSNR regimes as perceived by 200-Gbit/s 69-GBd DP-QPSK in a single channel (i.e. …..I…..) load condition: 30 dB (A), 27 dB (B), 23 dB (C), and 19 dB (D), respectively.

The x-axis presents nine symbols for channel load conditions, where each "I" and "." stands for enabled or disabled channelized ASE-loaded 400-GHz OSaaS service block. Simultaneously with the margin derivation, Fig. 29 presents the error caused by the usage of non-transceiver-specific characterization curves compared to the transceiver-specific characterization curves, discussed in section 5.3. The probing results received with transceiver-specific characterization curves, exactly matching the PLTs actual performance, are presented with green filled bullets for 200-Gbit/s 69-GBd DP-QPSK configuration and green transparent bullets for 200-Gbit/s 34-GBd DP-16QAM configuration. The results retrieved by using non-transceiver-specific characterization curves are presented with black and orange markers for high and low symbol rate configurations.

In Fig. 29, the minimum variation over all estimated GSNRs is at 14 dB GSNR, and the highest variation is observed near 21 dB GSNR. This also reveals that the two primary formats, 200-Gbit/s DP-QPSK and 200-Gbit/s DP-16QAM, recommended for channel probing in [8], often present the most extremes of the estimated GSNR values from symbol-rate variable probing. At high GSNR, high-symbol-rate signals are unreliable because a small change in Q leads to a large change in estimated GSNR, while the low-symbol-rate signals underestimate the GSNR of the link. The same trend can also be observed between GSNR estimations using transceiver-specific curves from the characterization exercise. As visible from Fig. 29, the transceiver-specific curves provide higher GSNR estimations at higher OSNRs compared to the non-transceiver-specific curves. As the link setup and OSNR is unchanged, and the Q value read out from the PLT unit remained the same, the difference in the observed performance difference between the non-transceiver-specific and transceiver-specific curves is only illusive, demonstrating a perfect example of a systematic probing error. This means the general performance of the used PLT unit used in this exercise is slightly lower than that of the PLT unit used to create the original, non-transceiver-specific characterization curves. Although the estimations of 200-Gbit/s DP-QPSK curves are pointing to a similar GSNR range, having a maximum of 1.0 dB of estimation difference at 27 dB OSNR, the 200-Gbit/s DP-16QAM curves have a slightly higher deviation in between the estimated link GSNR, reaching up to 2.0 dB at 30 dB OSNR. This showcases the need to use the correct characterization curves whenever possible, but specifically at high OSNRs.

6.3.1 Neighboring channel impact

Based on Fig. 29, all channel load conditions were tested for two OSaaS fill scenarios – enabling only one carrier within the OSaaS, and enabling all four OTSi within the OSaaS, repeated for all OSNR conditions. These results are presented on Fig. 30, by displaying the required per-channel margin to compensate for enabling the direct neighboring channels within the OSaaS for various channel load and OSNR scenarios. All four PLT units within the 400-GHz OSaaS under test were configured as 200-Gbit/s 69-GBd DP-QPSK configuration and a PLT unit installed in sl2p1 was used as a CuT. The shaped channels from ASE noise loading were used for end-of-life spectrum fill, which allocated up to 88%

of the spectrum in the lab OLS. In total, nine channel-load scenarios for spectrum fill were tested. The x-axis in Fig. 30 presents the used channel load scenario and the y-axis the required GSNR margin in dB. The required GSNR margin is calculated by subtracting the CuT performance with enabled neighbors from standalone performance for every channel load condition. Line colors refer to different OSNR regimes similarly to Fig. 29. In general, the higher the spectrum allocation, the lower the impact from the addition of the direct neighboring channels. The highest required safety margin to enable direct neighboring channels based on our lab study is 0.92 dB, when operating the spectrum with 100 GHz channel spacing within the OSaaS. For real-life use-cases, this margin can be rounded up to the nearest full digit, 1.0 dB.

In addition to the lab environment, neighboring channel impact was tested on four routes in HEAnet metro network with OSNRs between 17.0 dB and 24.5 dB, using a PLT unit installed in sl1p2. The results obtained were similar to the margin requirements derived in the systematic lab study and are included in Fig. 30 with the cross marks above scenario I….I….I, which is the closest to real-life network channel load. However, although the highest required margin in dB from production network aligns with the lab-derived margin expectations, the individual margin requirements per OSNR regime do not align
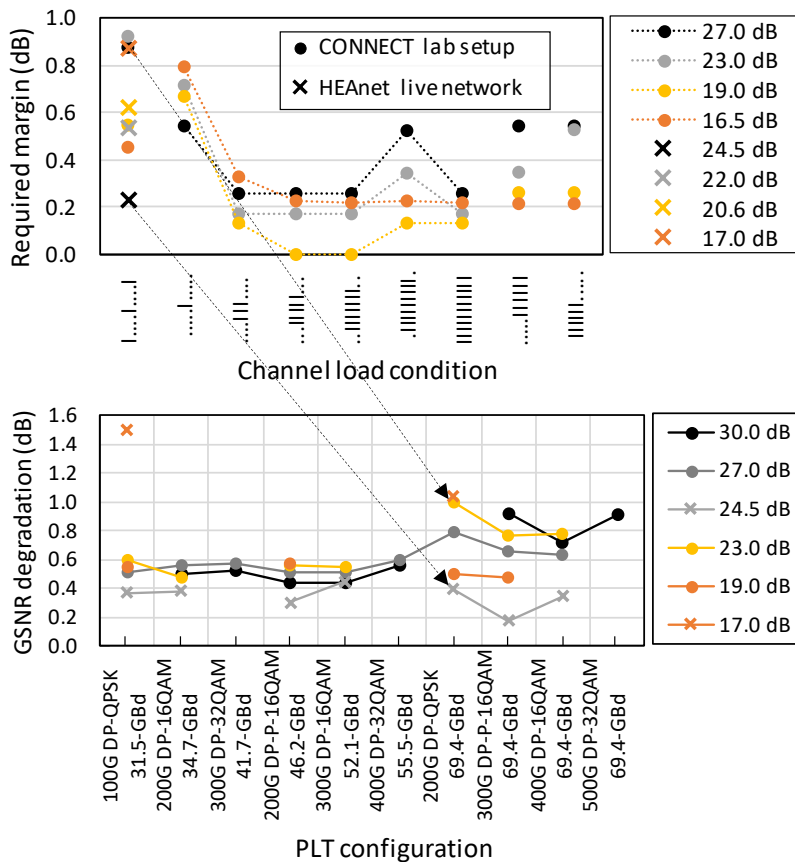

Fig. 30. *Minimum required OSaaS service margins to accommodate:*
Top: *direct neighboring channels,*
Bottom: *Direct neighboring channels when operated with different PLT configurations*

for lab and live environments. This can be caused by the usage of different PLT units for the tests in lab and live environments. In real life use cases, even a small change in spectral allocation, OLS components, or amplifier response may have an impact on the performance and margins. Therefore, the derived margins in this work only present one possible set of the required margins and further studies with long-term data collection from different lab and production networks are required to verify the margins that operators can commit to.

6.3.2 End-of-life channel loads

According the OSaaS survey introduced in Section 3.2, terrestrial systems are often operated with lightly populated spectrums and usage of ASE-loaded power balancing or dummy channels is not common. This means, with the cumulative addition of services into the lightly populated spectrum, the performance of the signals is expected to degrade compared to the initial, beginning-of-life performance.

Fig. 31 illustrates the required margins to allocate end-of-life (EOL) channel loads and consists of two graphs. The top graph presents the required end-of-life GSNR margin for the CuT installed at sl2p1 at a certain loading condition compared to the worst CuT performance over all loading conditions. The lowest performing loading condition is preferred over maximum channel load, because the worst performance often occurred with loading conditions ….III…. to .IIIIIIII. and not the full load. This may be due to the
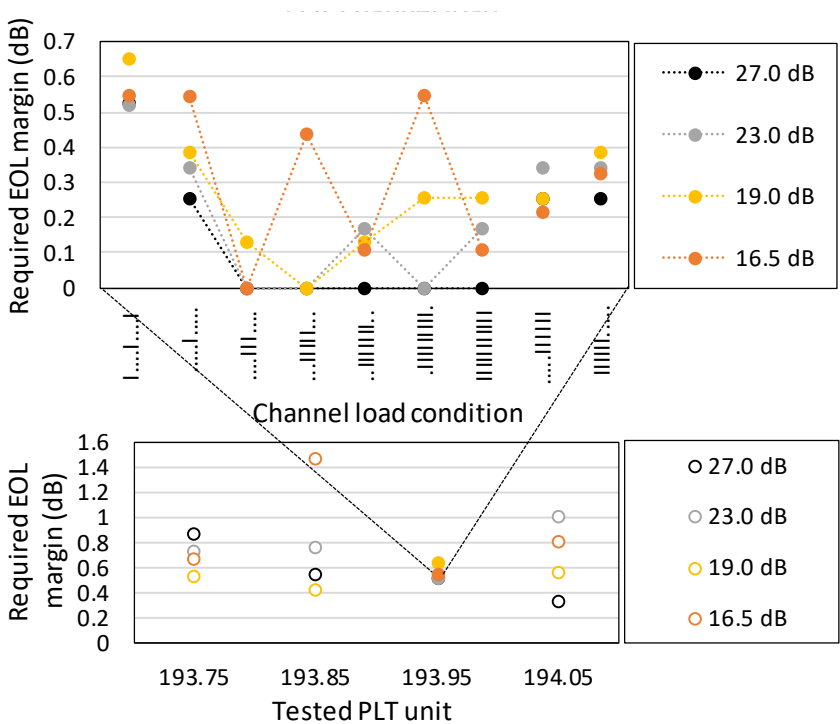

Fig.31. *Minimum required OSaaS service margins to accommodate:*
Top: EOL channel loads,
Bottom: EOL channel loads as seen by other tested PLT units

changes in amplifier operation regime, but the causes may be different for different OLS systems. Similarly to Fig. 29, the x-axis represents different channel load conditions and the y-axis the required margin. Line and marker styles present the OSNR conditions as on Fig. 29. Based on the results from the systematic lab study utilizing the PLT unit installed in sl2p1, 200-Gbit/s 69-GBd DP-QPSK signal configuration requires up to 0.65 dB margin allocation to cover end-of-life channel loads in the spectrum. However, different PLT units may have different margin requirements.

The bottom graph of the Fig. 31 presents only the maximum required EOL margin per OSNR regime over all loading conditions as required by different tested PLT units operated within a single 400-GHz OSaaS. The PLT units were configured with a 100-GHz spacing between the central wavelengths, starting with 193.75 THz for the sl1p1 and ending with 194.05 THz for the PLT unit installed in sl2p2. The graph is showcasing a more than two-fold difference between a relatively moderate, up to 0.65 dB EOL margin requirement for the PLT unit installed in sl2p1 (at 193.95 THz) compared to a 1.46 dB margin requirement for a PLT unit installed in sl1p2 (193.85 THz).

6.4 Concatenated GSNR profiles

In this section, we investigate the accuracy of the concatenated GSNR profiles in OSaaS implementation scenarios in multi-operator, multi-vendor, multi-domain environments when the GSNR profiles for the individual network segments are available. For this, two long-haul and one regional-haul link from the Funet production network are individually characterized and the estimation for the concatenated link performance is computed. Then, the links are transparently interconnected, and the actual end-to-end performance of the merged link is captured by channel probing. Finally, the estimation accuracy is calculated.

First, all routes were characterized by their GSNR profile, using a single-probe sweep and multiple probe capture. For long links 200-Gbit/s 69-GBd DP-QPSK and 100-Gbit/s 31-GBd DP-QPSK signal configurations was used for single-probe sweep, and 200-Gbit/s 69GBd DP-QPSK and 200-Gbit/s 34-GBd DP-16QAM signal configuration was used for the shorter link. For multiple probe GSNR profile, 200-Gbit/s 69-GBd DP-QPSK was used on all four probes. Fig. 32 presents the individual GSNR profiles along with receive power spectral densities for the multiple-probe and single-probe sweep results from three different network segments. The first route, Kajaani 2 with 1673 km, is the longest route characterized. The link features a power adjustment algorithm, that interferes with maintaining the desired constant transmit power spectral density along the route, rising the power levels for narrow-band probes. This results in up to 3 dB higher power spectral density for narrow-band signals that causes them to operate slightly in non-linear regime at the peak side of the spectrum slot (192.55 THz). Unlike the Kajaani 2 link, the GSNR profiles of the 1161-km long Stockholm link follow the 1.8 dB tilt of the received PSD and both probe configurations work in the linear regime over the full media channel bandwidth. Both of the longer links have a maximum deviation between the wide-band and narrow-band probe estimations below 0.6 dB for the estimated GSNR. The last link, Hämeenlinna with 282 km, has a high OSNR, not preferred for channel probing due to larger probing error due to saturation regimes of the probes [8]. The GSNR profiles recorded by the two probe configurations differ up to 2.0 dB. The channel probing
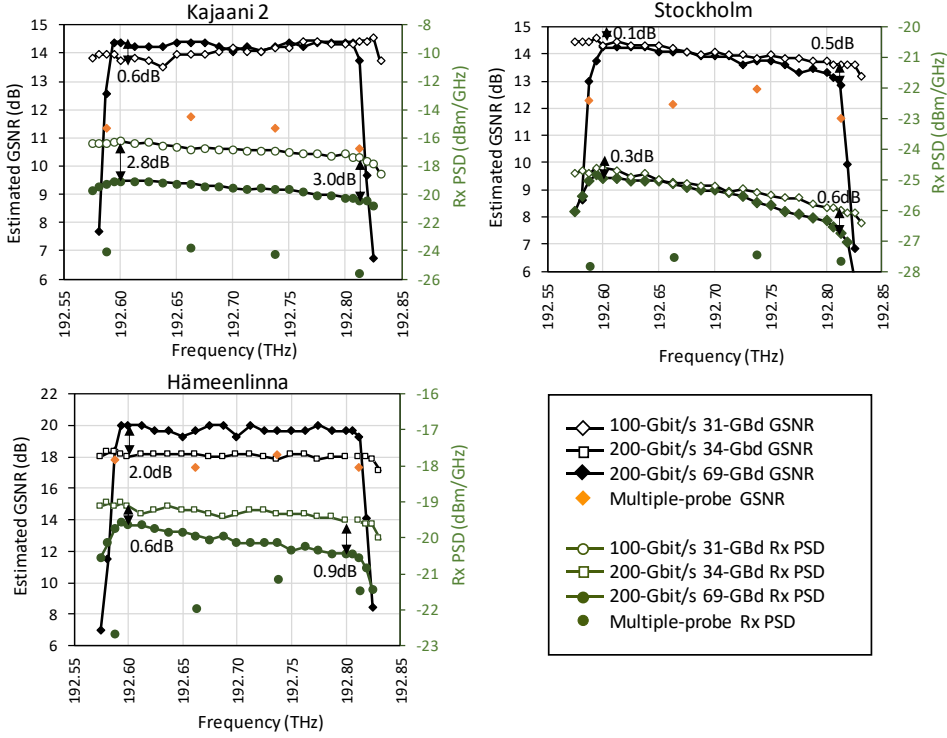
Fig. 32. *Individual GSNR and Rx power spectral density profiles for the routes*

accuracy is further degraded by the enabled power adjustments on the link that is causing the up to 0.9 dB difference in received power spectral density.

The GSNR estimations for the concatenated routes are calculated according to (6):

$$\frac{1}{GSNR_{TOT}} = \frac{1}{GSNR_1} + \frac{1}{GSNR_2} + \cdots \qquad (6).$$

First, two longer routes were concatenated, reproducing a service scenario with two independent OSaaS providers. The GSNR profile estimations and channel probing results for the concatenated segments are visualized in Fig. 33 left. Then, the 260-km Hämeenlinna segment was added to the chain, illustrating the scenario with three service providers. The GSNR profile from the concatenated estimations and end-to-end channel probing results with absolute values for the 3-provider scenario are presented in Fig. 33 right. The estimation error for both, single-probe, and multiple simultaneous 200-Gbit/s 69-GBd DP-QPSK probe scenarios for the two concatenated end-to-end links is presented on Fig. 34. Fig. 34 reveals that the computed GSNR-profiles tend to underestimate the performance of the concatenated links compared to the actual measured GSNR profile of the links, regardless of the probing method used. This means, that the actual performance was better than the one computed based on the individual GSNR profiles of the segments. This makes sense, as the simple total of all the summed components as per (6) included also the add/drop paths of each individual segment. For our tested links, the underestimation is in the range of 0.4 to 1.4 dB compared to the real performance
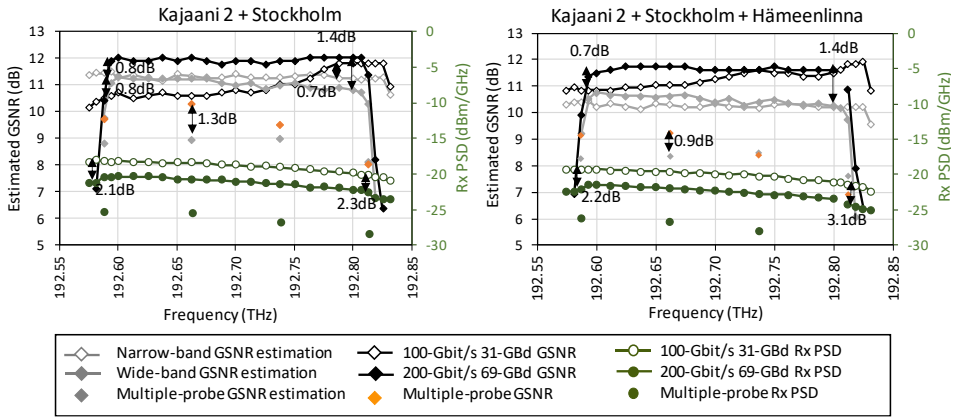
79

Fig. 33. *Comparisons of the GSNR estimations and channel probing results*

of the concatenated link. The only exception is the 100-Gbit/s 31-GBd DP-QPSK probe for the concatenated Kajaani 2 and Stockholm link. The overestimation of the computed GSNR profile is likely caused by the fact, that the actual measured performance of the narrow-band signal experiences a noticeable degradation in the Raman peak side of the spectrum. This is caused by the increased nonlinearities from the higher accumulated to-the-line launch powers on concatenated links, degrading the measured performance of the concatenated link. Similar impact is also visible on the 3-provider concatenated link, but in a smaller degree, thus leaving all computed GSNR profiles to underestimate the actual link performance in a similar degree. One of the possible reasons for this is the conservative input GSNR profile for the Hämeenlinna link, effectively lowering the computed GSNR for the whole concatenated link.

Regardless of the generally lower values of the coarse GSNR profile provided by the multiple simultaneous probes, the estimation error is also less than ±1.4 dB between the computed estimations and measurements. Due to higher robustness against the power adjustments on the link, the estimations results are in better alignment with the valleys and peaks within the spectral slot. Probes working in the valley part of the spectrum report slightly higher estimation accuracy compared to probes working at the peak of
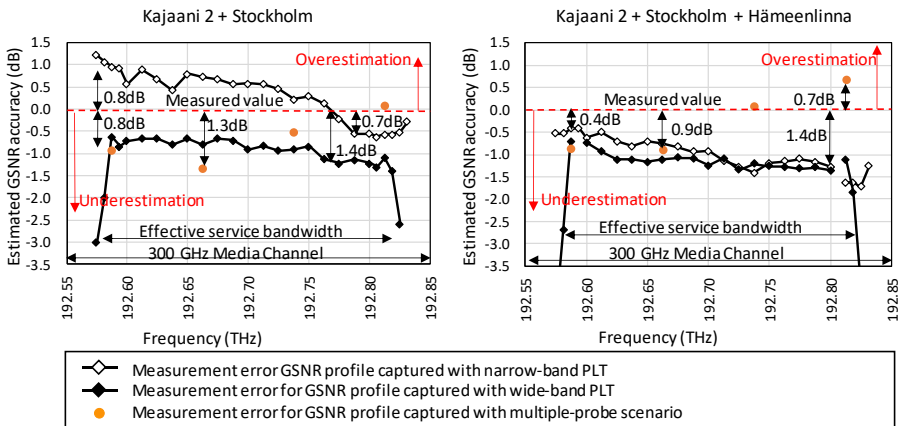

Fig. 34. *Estimation accuracy for different probing scenarios*

the spectrum slot. This can be explained with higher accumulated to-the-line transmit powers that contribute to higher nonlinear penalty, which cannot be estimated using (6).

In general, the accuracy of channel probing is very vulnerable to power adjustments at any point in the OLS, including the daily performance fluctuations on the link. In addition, the method is reliable only in linear operation within the effective bandwidth of the media channel. In addition to the power adjustments on the link, the selected calculation method for concatenated GSNR profiles may create bias in long-haul systems. In long-haul systems, a general droop method, proposed in [113] may reduce the error, as it accounts for the gradual degradation of the signals from all interconnected links. Finally, non-transceiver-specific characterization curves used in this exercise could contribute to the high error in the estimations. To avoid that, one single characterized probe, the golden transceiver, should be always used for the GSNR profile capture.

With all the downsides listed, the achieved ±1.4 dB accuracy for a 3-segment multi-vendor, multi-domain, multi-operator environment end-to-end performance estimation is a good estimate compared to non-existent estimates available without the GSNR profiles. Further work on this topic can benefit from using the general droop model and characterized probes.

6.5 Conclusions

Chapter 6 has presented clear guidelines for OSaaS characterization and allocated margins. The details and nuances of the two GSNR-based characterization methods were discussed in Section 6.1. By using the implementation scenarios (b) and (c) from Fig. 7, differences between the profiles and their capabilities to capture the customer expectations for the OSaaS characterization, listed in the introduction of chapter 6 were showcased. The required service margins to accommodate fast and slow performance variation in the OLS were derived using the telemetry data collected from the end user transceivers, and margins to accommodate direct neighbors and end-of-life channel loads in lightly populated terrestrial DWDM systems were investigated in Open Ireland CONNECT lab. Furthermore, the feasibility of the GSNR profile-based end-to-end link performance computation was demonstrated for concatenated multi-operator, multi-vendor, multi-domain environments, emulated in Funet long-haul network.

Section 6.1 demonstrated, that for capturing the wavelength-dependent variations, the GSNR profile recorded with a single-probe sweep is the simplest solution to describe the required aspects of the service. The proposed characterization has great potential to simplify network planning in disaggregated environments. Especially in the purchase and pre-handover stages this method will enable accurate throughput estimations at any part of the spectrum. Further benefits of the OSaaS characterization with GSNR profiles include automated path calculations in low-margin networks for service re-routing or restoration.

Section 6.2 has experimentally derived the standard deviation-based OSaaS margins, utilizing the long-term telemetry data from a 375-GHz wide-band OSaaS consisting of five 200-Gbit/s 69-GBd DP-QPSK signals operated on a Raman-enabled pan-European network. The used method is applicable for any OLS, and only requires the telemetry data collected from the end-user transceivers. Based on the worst-performing transceiver, the maximum total margin of 1.26, 1.99 and 2.23 dB is required to facilitate

stable operation of the commissioned services within a wide-band OSaaS over 1792-km, 3752-km and 5738-km links, respectively. The examples brought in the work are specifically valuable for operators operating Raman enabled networks and plan to provide wide-band OSaaS services. In future systems, continuous probing in combination with machine learning algorithms can be used to continuously monitor performance deviations and compare the current values to the OSaaS characterization in hand-over documentation. This would allow operators and end-users to detect possible performance degradations caused by ageing or changes in the OLS utilization and take relevant actions to avoid any loss of transported data.

Section 6.3 has explained the experimental derivation of the margin set to accommodate the performance degradations form enabled neighboring channels and end-of-life channel loads. Based on the systematic measurements in the Open Ireland CONNECT lab, a 1.0 dB GSNR margin is required to cover degradation from enabling direct neighboring carriers, and an additional 1.5 dB margin allocation is required to compensate for the end-of-life channel load conditions in the case of 200-Gbit/s 69-GBd DP-QPSK signal configuration operation. However, as the margins are dependent on PLT configuration [135], the margins derived in this work would be applicable only for the operation with 200-Gbit/s 69-GBd DP-QPSK signal configuration. This means, further work should be performed to specify required service margins for other signal configurations that can be operated within the OSaaS.

In section 6.4, the GSNR profile-based end-to-end performance estimations for two- and three-provider scenarios were investigated. A maximum estimation error of ±1.4 dB was found between the calculation-based and end-to-end probing-based performance estimations. In service procurement scenarios where the OLS is treated as a black-box, this error magnitude can be justified as a rough estimation for long-haul links of 3000 km and more. Further accuracy improvements can be achieved by using characterized golden transceivers for the individual link characterizations and disabling any link power adjustments during the initial service characterization time.

Finally, the OSaaS characterization table from the introduction of the Chapter 6 can be filled in, as the first guideline for the minimum margins to be provided. A comprehensive example of the handover documentation for the 1792-km link to complement GSNR profile is presented in Table 6. To improve the accuracy of the proposed margins and provide margins that operators could commit to in their OSaaS handover documentation, further studies utilizing fully automated lab setups to gather data from various OLS setups, PLT units, and configurations should be executed. The first attempts to fully automize the Open Ireland CONNECT lab environment and showcase the ML-Based DWDM System Margin Estimation is investigated in [XI].

Table 6: OSaaS handover documentation with service specifications and margins

OSaaS parameters per OLS system	Value	Min	Max
Bandwidth (GHz), start and stop frequency (THz)	375	193.7625	194.1375
Total power (dBm)	8.75	-0.25	8.75
PSD (dBm/GHz)	-7.5	-17.5	-7.5
OSNR ($f_{central}$) (dB)		22.9	
GSNR ($f_{central}$) (dB)		13.8	
Wavelength dependent GSNR variance (dB)	<2.5dB		
Operation regime in different parts of spectrum	Linear		
Margins:			
Slow performance fluctuations (dB)	0.87	0.81	0.94
Fast performance fluctuations (dB)	0.32	0.27	0.39
Enabling direct neighbors (dB)		1.00	1.50
End-of-life spectral load (dB)		1.00	1.50
Aging (dB)			

7 OSAAS IN MULTI-DOMAIN, MULTI-OPERATOR NETWORKS

In modern optical communication systems, systems implemented on one fiber pair can typically provide up to 4800 GHz of optical spectrum within the DWDM system's C-band. Conventionally, this bandwidth is lit by the system operator using optical transceivers that act as demarcation interfaces as they provide capabilities to adjust signal parameters like power levels, signal bandwidth, and frequency to guarantee the expected service performance. This is in perfect alignment with the primary expectations for the traditional telecommunication service for both parties: while the operator is solely responsible for operating the system and guaranteeing the end-to-end service continuity, the end user is solely responsible for paying the bill.

With Optical Spectrum as a Service, however, the operator is expected to transfer the ownership, and thus the control of such demarcation interfaces to the customer, and only provide open, direct access to the spectrum of its all-optical OLS. The drawback here is that the uncontrolled light signals from the customer that are inserted into the OLS can enable high-quality transmission but can also negatively impact the performance of the other carriers within the OSaaS and in the worst case, the availability of the whole OLS system. Such change in control has negative impact on the network integrity. Surely, the contract for OSaaS can define the limits for power, bandwidth, or other thresholds and regulate the use and distribution of the confidential business- or even worse, mission-critical infrastructure-related data. However, these obligations are set on paper and often hard to fulfill with currently available technical solutions. The control uncertainties described above may detriment the end-to-end provisioning using Software Defined Networking (SDN) orchestrators in multi-domain, multi-operator environments due to security restrictions [161-163]. Furthermore, the simple disaggregated service model for OSaaS blurs the customer-provider responsibility boundaries due to a lack of dedicated demarcation points, as the end-customer signals may interrupt the provider's network performance. Alternative to the software-based solutions [164], the missing demarcation points at the domain borders of multi-domain, multi-vendor, multi-operator environments can be solved by using a dedicated vendor independent demarcation device.

7.1 Network Domain Interface Device

To address the painful customer-provider control dilemma and missing demarcation interfaces at the domain borders, this section proposes a completely vendor-, domain-, operator- and OLS-technology independent Network Domain Interface Device (NeDID) to police the end-customer signals. Fig. 35 illustrates the usage scenario for NeDIDs providing a discrete demarcation point between the domains. The NeDID can be operated as a standalone unit, but modules interconnected over the external management channel allow to create a transparent optical overlay network that can be operated by a single wholesale operator or shared among the consortium of network resource owners. As the new NeDID allows secure resource sharing, it increases the OSaaS attractiveness also among operators, who so far have not considered providing telecommunication services as their core business (mission-critical power-, gas- or water utilities). This creates the opportunity for overlay network providers to negotiate the
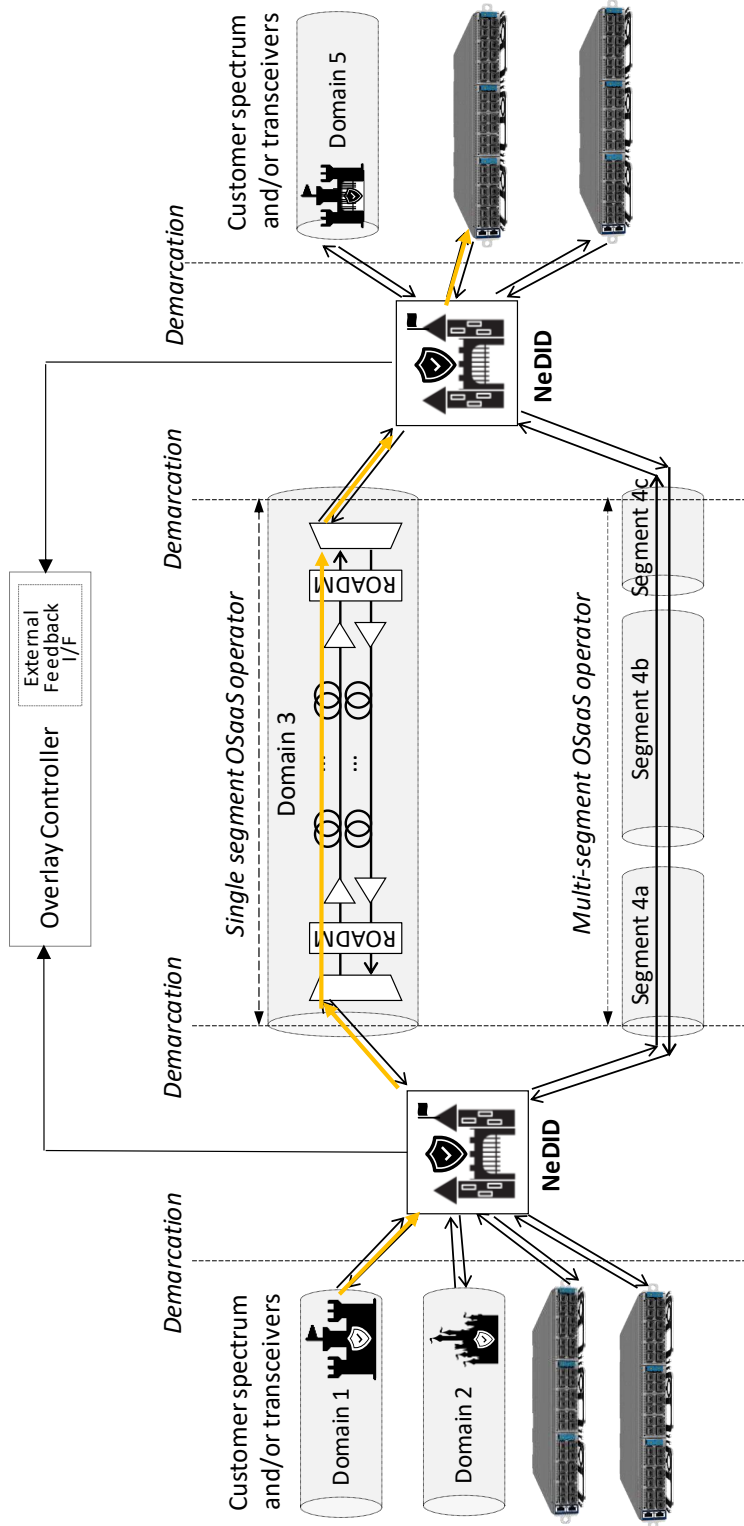
Fig. 35. *Multi-domain, multi-operator environment with NeDIDs and transparent optical overlay network concept.*

resources and manage them in a secure and controlled way without interfering with any physical threshold in the involved underlying networks nor ever needing an access to the management system of the underlying optical network resources. This leaves a total control over their networks and resources for operators participating in resource sharing. The handover of any resources to be connected to the NeDID is based on contracts. The interconnected spectral resources are characterized using a single-probe sweep method described in [133]. The dedicated spectral slot performance will be monitored and policed by the NeDID during the overlay network operation.

Unique for the NeDID, the input signals to the NeDID are treated equal, independent of their origin, be it bundled signals from different network domains, a sub-spectrum, individual wavelengths from customer transceivers or sensory interfaces, used for infrastructure monitoring. The NeDID monitors, polices, and adjusts the incoming signals according to the next domain-specific rule sets and thresholds assigned on the NeDID output port. These rule sets and thresholds are dependent on the next-domain OLS technology – it's grid, allowed power spectral density (PSD), required guard bands, and other domain-specific rules that would be applied for native signals in the domain. These rules are agreed during contract negotiations with the resource providers and also apply to optional sensory signals, including Amplified Spontaneous Emission (ASE) noise or channel probes, that can be used to characterize the end-to-end OSaaS service.

To guarantee the interworking and signal integrity between the domains, each of the NeDID contains a basic set of interworking functions:

- receive filtering to ensure signals are transmitted only inside the assigned spectrum of the OSaaS within the next domain,
- treats all incoming signals equally (no customer port distinguishment),
- very fast shutdown of (certain rogue) signals,
- amplification, power leveling per power spectral density (PSD) or total power, and power limitation of the outgoing spectrums as per domain-specific predefined rule sets and thresholds, and
- potential ASE noise insertion and dummy channel insertion for amplifier control/balancing/saturation.

Each of the NeDID also includes a built-in controller that hosts the contractually agreed rule set and threshold database applicable for different signals, domains, or sub-domains interconnected to the NeDID. Based on this database, the controller decides the incoming signal treatment depending on the outgoing signal direction. It also provides a feedback loop from far-end NeDID to pre-emphasis signals within the allowed thresholds to achieve optimized receiver performance and switch or reroute the OSaaS service. The controller also provides a real-time, µs-range streaming telemetry function with a subscription that can collect data from all ports on the device.

The signal flow diagram within the NeDID is pictured in Fig. 36. All signals entering through the West interface (I/F) are monitored and based on the policing rules, treated in the multiple input-multiple output Wavelength Selective Switch (WSS) block, providing filtering and routing functions. This is followed by the Erbium-doped fiber amplifier (EDFA) and variable optical attenuator (VOA) array, providing amplification and
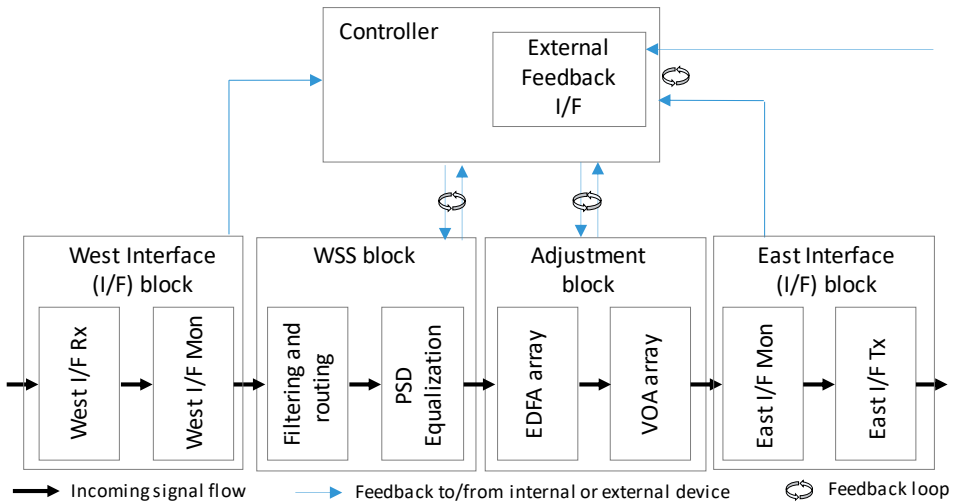
Fig. 36. *The basic signal flow diagram for NeDID*

attenuation functions for all the signals leaving the block, based on the thresholds and requirements of the next domain.

Finally, the signals are monitored for the final time before leaving the NeDID to the next domain. Internal and external feedback loops between the blocks and the controller within a single NeDID and between the individual NeDID entities, using the external feedback interface (I/F) allow signal adjustments when daily power fluctuations or power- or signal quality-based pre-emphasis is detected.

7.2 Transparent Optical Overlay Networks

According to the OSaaS survey introduced in Section 3.2, carried out among 25 participants operating telecommunication networks worldwide, 56% of them would be willing to share their spectrum resources with a third-party or wholesale retailer if the signal handover could be implemented safely and control over the OLS components would remain at the hands of the resource owner only. Today, caused by the uncertainties related to OSaaS demarcation and handover, the operators prefer to provide either leased lines and other higher-layer services or share optical infrastructure on a purely physical level – sharing the telecommunication ducts or individual fiber strands within the existing cables. The space between the higher-layer services and the physical infrastructure has remained untouched due to signal safety and system control reasons. The NeDID, with the functions mentioned above, enables to close this gap and change how the optical resources in already lighted DWDM systems are shared.

In order to accommodate light from end-users or share the spectral resources with a wholesale retailer, it is imperative for the infrastructure owners to maintain the control over the shared physical resources. The first step entails a safe signal handover implementation at operator's network edge nodes.

The distinguishing aspect when using NeDID is that the resource owner is not required to actively participate in sales, service handover, or service monitoring activities but

would still have the monthly revenue from the rented spectral resources. This creates an opportunity for a few new operation modes. The simplest case would be a single operator's standalone operation of the NeDID. The NeDID allows to individually control the incoming signals to one domain/line system, so a single interested operator can control the signal parameters entering its OLS and dedicate parts of its system for optical spectrum sharing. A single operator model is similar to the disaggregated optical networking model today, where the OLS and transceivers may come from different vendors but are operated by the same operator. With the NeDID, the operator would be ready to accept bundled signals within a wide-band OSaaS configurations as (b), (c), and (d) from Fig. 7 that often consist of individual carriers with different configurations that are difficult to control and police with conventional ROADM modules. Secondly, the concatenation of multi-operator domains would create opportunities for new business models. A consortium-based business model can be used with two or more interested partners with a common goal of selling an end-to-end spectrum. In addition, a single wholesale carrier model can be used, where a single carrier's carrier would buy the available resources from different operators and operate the transparent optical overlay network on top of the available resources.

Wide-scale implementation of the optical spectrum services requires precise performance characterization of the available spectral resources and guaranteeing signal integrity in a timely manner. The new NeDID and transparent optical overlay concept target these missing functions on a photonic layer. The NeDID can provide a channel probing-based option to characterize the spectral resources, continuously monitor the signals entering the NeDID, police and adjust the signals entering the next domain according to the preset thresholds and calculate service level agreement performance. In consortium and wholesale models, the optical resource providers are responsible for keeping the OLS performance as stable as possible, but it is the NeDID operator who is responsible for blocking out the rouge signals, suppressing fast power transients, adjusting the power levels of the signals for next domain, and calculating the available resources' compatibility to the contractual service level agreement documentation.

The NeDIDs are managed independently from any underlying OLS resource using a well-known protocols such as NETCONF/RESTCONF with open data models. Regardless of the business model used, the NeDID operator has access to all the monitoring and performance data collected and calculated by the NeDID card – collected from multiple input and output ports monitoring, adjustment, and service level agreement (SLA) compatibility calculations. The access to the NeDID configurations and streaming telemetry can be shared with an OLS provider or end-to-end OSaaS end-user. In this case, only a single domain- or service-related information would be available for the restricted user.

A significant value brought by the continuous monitoring through streaming telemetry is the reduction of time and effort, spent on fault localization in multi-domain, multi-operator environments. Often, fault localization in these complex network infrastructures is complicated due to reduced visibility beyond the domain borders. SDN orchestrators are not yet commonly used in live network consortiums, and their future use may be limited due to conflicting control expectations. In NeDID operations, the fault localization is performed based on streaming telemetry available from the monitoring sections of the device. The failing OLS segment can be quickly identified, and protection switching can be triggered in case of agreed protection resources. For priority traffic

within transparent overlay networks, also restoration is an option. However, compared to protection switching, it may introduce longer computation times to find available resources. In addition, the performance and latency of the new route may not be suitable for the end user. After protection switching, the traffic is monitored, and unavailability time is immediately calculated for the affected services with the root cause of the fault included. This may be an outage in any of the involved OLS or a change in power levels. Continuous telemetry data collection in the cards would enable learning the hard and soft failures in the transparent overlay networks and improve predicting the required service margins, which are required to cover the daily and yearly fluctuations, ageing, changes in channel loads, etc.

Fig. 37 presents a possible implementation of the NeDID and transparent optical overlay networks based on the Nordic and Baltic regions in Europe. The mesh grid presents the underlying physical optical infrastructure and colored domains the overlay network segments operated by a single wholesale operator A and a consortium B. There
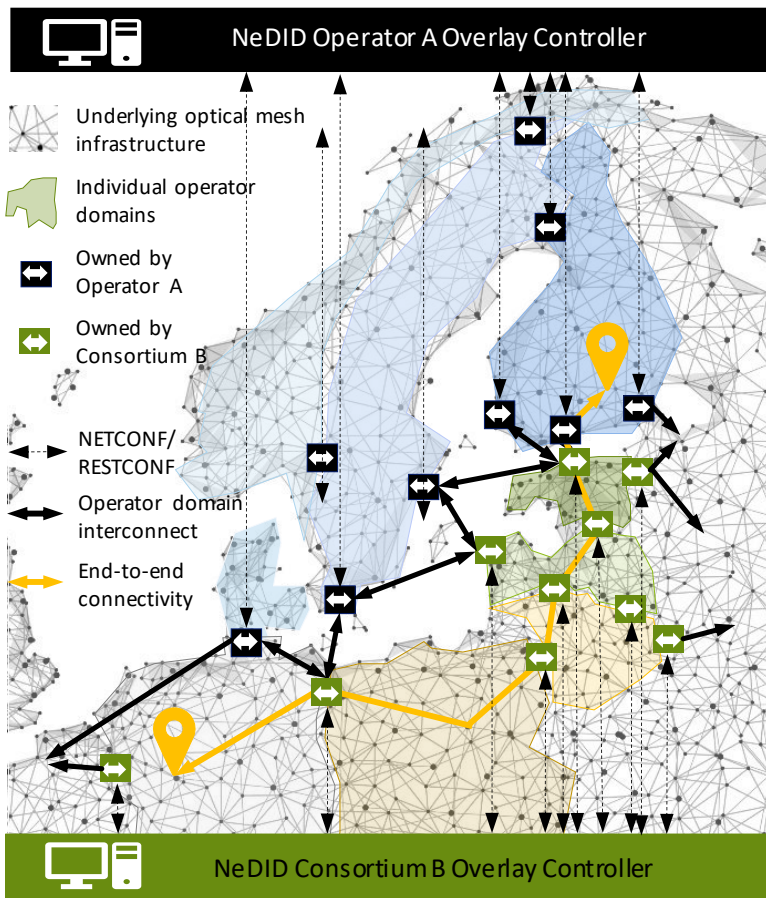
Background map: © Anttoniart – stock.adobe.com

Fig. 37. The operation of NeDID devices in multi-vendor, multi-operator environment based on the Nordics and Baltics.

may be multiple overlapping layers of such optical networks, operated by competitive infrastructure operators to operator A and consortium B, each layer interconnected at the primary internet exchange points or mutually used network edge sites. The NeDID card ownership is marked with black for operator A and green for consortium B, each operating their own Overlay Controller to maintain control within their optical overlay network. The primary benefit of the optical overlay network is that due to the introduction of the NeDIDs, consortium B members can act as they own their end-to-end WDM network, covering the interconnected region. Adding the NeDID at the endpoints of the interconnection links between operator A and consortium B allows transparent end-to-end connectivity between the optical infrastructures, operated by multiple operators. The significant differentiation compared to many other overlay networks is, that the spectrum resources from different underlaying networks participating in the end-to-end connectivity obtain a physical layer in the involved optical underlay networks. Therefore, the transparent optical overlay network concept will be a fully transparent mesh network interconnecting various optical infrastructures across the regions without violating any of the system thresholds in the interconnected underlay spectrum resources. In addition to many benefits of such service model, introduced in Chapter 1, the transparent overlay networks may also simplify providing the Network on Demand services [165,166], without the need to request the availability for each of the requested resources nor violating any of the thresholds in the physical layer.

7.3 Optimization potential

In this section, we propose network optimization use-cases that focus on the throughput optimization potential based on the data acquired through the spectrum probing process.

7.3.1 OLS-dependent optimization potential

Section 5.2.2 explained how OSaaS services implemented in fixed-grid networks may experience narrowband filtering on signal formats using higher symbol rates, and hence, accommodating a wider bandwidth in the OLS spectrum. This significantly reduces the benefits of S-BVT transceivers, as the higher symbol rate signals, typically requiring smaller OSNR and GSNR than the narrow-band signals with the same data rate, cannot be used. This causes losses in achievable capacity on link. In this section, we explain how symbol rate variable channel probing in narrow-band/fixed-grid OSaaS implementations (configuration (a) from Fig. 7) can be used to estimate the impact of filtering penalty on the total achievable capacity on the link and drive OLS optimization decisions.

To illustrate this, we use the symbol rate variable channel probing results from the Tele2 fixed-grid 10-Gbit/s optimized regional-haul network from section 5.2.2. First, the achievable throughput for current link configuration is estimated based on $GSNR_{est,link}$ and $GSNR_{margin}$. The achievable capacity in a bandwidth limited OSaaS scenario is illustrated with black bars on Fig. 38. Then, the potential throughput increase is estimated based on the PLT configuration that did not experience bandwidth limitation: 200-Gbit/s 34-GBd DP-16QAM or 100-Gbit/s 31-GBd DP-QPSK. These throughput calculations, indicating the achievable throughput gain from a system without any filtering penalty, are shown with
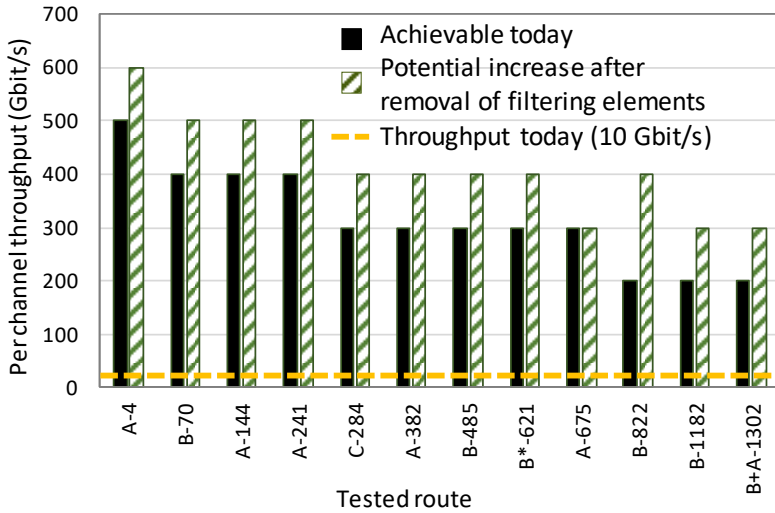
Fig. 38. *Achievable and potential throughput estimations*

green bars on Fig. 38. While only a small increase can be achieved due to moderate filtering effects on short distances, up to 100% increase can be achieved on links with additional filtering penalty caused by the DCG-based dispersion compensation modules.

For some links, getting rid of filtering elements would only bring performance improvement in service margin, but not a change in the maximum achievable line rate (link length 675 km). However, considering the average increase per channel, the total throughput increase would aggregate to 4-Tbit/s capacity gain, over the scenario of just implementing S-BVT transceivers in the network.

This type of analyses can be used to make network upgrade decisions like adding colorless access structures to the existing ROADMs and swapping older, optical microelectron-mechanical systems (MEMS)-based ROADMs to Liquid Crystal on Silicon (LCoS)- based ROADMs. However, caution must be taken when swapping DCG based dispersion modules to DCF-based modules, as this could increase the nonlinear penalty from Shelf Phase Modulation (SPM) on the link and deplete the expected benefits from swapping the modules on the longer links (675-km link example). If possible, in the long run, going dispersion uncompensated and fully coherent also on the old legacy infrastructure links should be considered as an option instead.

7.3.2 Time-dependent optimization potential

While the primary usage scenario for the channel probing method in this work is the characterization of the OSaaS performance in disaggregated networking scenarios, the initial spectrum characterization only covers the QoT performance at the time of the characterization. To overcome that, continuous channel probing utilizing commissioned transceivers carrying also the live traffic could be used to monitor the changes in OSaaS service performance. These changes could be caused by fast, slow (daily) or even yearly variations in the network, added crosstalk penalty from changed channel load in the neighboring spectrum or other. Continuous channel probing enables spectrum end users to learn about the daily and yearly changes in the network performance and use the

gained knowledge in running higher capacities during the network peak performance times. This can be useful in data-center connectivity. According to our observations over the 10-month test-period, daily changes on a LH-3752 link during the summertime, impacted the estimated link GSNR on average 1.5 dB per 24 h period, while the performance fluctuations during the colder months reached at most 0.4 dB in amplitude per 24 hours. Since a better performance was observed during the colder night-time, users can optimize their higher-capacity demanding database back-ups to be run at night-time. On the observed link, 1.5 dB of GSNR difference would allow to switch from the default 200-Gbit/s 69-GBd DP-QPSK signal configuration to 200-Gbit/s 58-GBd DP-QPSK/DP-P-16QAM hybrid modulation and therefore reduce the required bandwidth from 75 GHz to 62.5 GHz per carrier, resulting in 2.56 Tbit/s capacity gain over C-band.

The benefits of continuous channel probing can also be used by the OLS operator. Probes operated inside the guard-band channels can be treated as a network monitoring point to perform OSaaS service policing in addition to general network performance monitoring and fault detection. Single characterized transceiver can be used to monitor multiple links. For this, an optical switch could be used to send the probing signal into different channel locations in multi-domain disaggregated network environments, providing ms-range switching time on already pre-provisioned lightpaths compared to reconfigurations in the ROADMs. These usage scenarios require additional research to provide solutions that reduce the investments costs per monitoring point.

Furthermore, continuous channel probing or performance data collection can be used for machine learning based fault prediction [157], [XII]. The data allows the operators to quickly react to degrading performance and schedule a predictive maintenance, to avoid unscheduled service down-time, that can be costly to the operator and may cause application level interruptions to the end user, even if the optical paths are protected.

7.4 Conclusions

The ever-increasing pace in digitalization of all aspects of life is demanding operators to think outside of the box when it comes to providing high-capacity international connectivity with decreasing cost per bit. Regardless of how fast the new optical fiber infrastructure is deployed, there are always areas with scarce resources. Therefore, smart ways to safely share the optical spectrum within the existing systems could provide a feasible way to increase the availability of the end-to-end paths and decrease the overall cost per bit.

This chapter introduced a new, vendor-, domain-, OLS technology and operator-independent Network Domain Interface Device that can be used to police the incoming signals and adjust them to the requirements and thresholds of the next domain. If more than one such card is used, a transparent optical overlay network can be created that allows using resources dedicated to such overlay network in a flexible and safe manner. This paves the way for higher utilization in existing optical networks, as it allows sharing the resources also for operators who do not operate optical networks as their core business. The increased flexibility to choose between a higher number of

paths also enables to create protection paths for individual OTSi within the OSaaS and for the full OSaaS lightpath, possibly helping to justify new investments into the physical layer infrastructures for operators with less populated systems that are nearing end-of-life.

Furthermore, this chapter also introduced OLS and time-dependent optimization potential in the existing systems, providing input data for network upgrades, time-dependent performance utilization, and increased monitoring capabilities.

8 CONCLUSION

Living in the information age, where many aspects of life depend on availability and quality of the broadband connection, the optical networks are evolving together with the society's need for connectivity. Today, Dense Wavelength Division Multiplexing (DWDM) technology forms the digital backbone of the interconnected World. Implemented on top of physical infrastructure consisting of fiber optic cables and co-location sites, the layout, geographical location, and access of the fibers define which areas can be connected and DWDM technology defines the achievable capacity, operational flexibility and cost per bit/s. With the dawn of elastic optical networks, growing trend of network disaggregation, and modern sliceable bandwidth-variable transceivers, Optical Spectrum as a Service (OSaaS) service model is gaining attraction. In this service model, the service provides provide an open slot in the DWDM spectrum, which enables end users to commission 3rd party transceivers, not native to the DWDM system, on top of the acquired spectrum. While providing many benefits from reduced amount of equipment required to build the end-to-end connectivity to increased availability, technically, the service is not yet mature for wide-scale implementation in production networks. This is caused by the lack of demarcation functions, that in leased line service model were provided by the transceiver cards operated by the service provider. The missing demarcation points launch an avalanche of problems, starting from service characterization, signal policing and calculating the service availability based on the agreed service level agreement. Furthermore, as the exact configuration of the OSaaS lightpath defines the wavelength-dependent variations within the service, that are difficult to assess without having a comprehensive overview about the OLS components, the implementation of the wide-band OSaaS in the production networks is put on hold.

The goal of this thesis was to investigate the root problems of the OSaaS implementations in open disaggregated transport networks. The focus of this work was set on terrestrial brown-field systems, to help network providers achieve higher spectrum utilization rates and flexibility in their networks. The focus on brownfield networks was selected due to the wide geographical coverage they have. This means, the brownfield adjusted solutions would allow the operators and end customers to benefit from the new service model in most timely manner.

The thesis approached four primary problems raised in 1.2 and proposes solutions that are applicable for terrestrial brownfield optical networks. The primary contributions of the thesis are the following:

a) For the first time, a structured, underlying physical infrastructure independent overview of the possible OSaaS implementation configurations was provided. To give the end-user and service provider a clear picture of the benefits and concerns when deciding which OSaaS configuration to implement, the operational aspects related to each of the implementations were discussed.

b) A comprehensive channel probing toolkit optimized for terrestrial brownfield DWDM systems was derived in order to capture all related OSaaS related performance nuances.

c) A clear OSaaS characterization method is presented alongside with the required service margins, required to overcome fast- and slow performance fluctuations, enabling neighboring channels, and end-of-life channel loads in the networks.

d) Finally, a Network Domain Interface Device alongside with a transparent Optical Overlay Networks concept was introduced. The device provides a set of interworking functions, like service policing, telemetry data collection, and service level agreement compatibility calculations. The transparent overlay networks concept proposes a market-changing new service model for optical networks, enabling higher flexibility and transparency in future optical networks. In addition, OLS and time-dependent system optimization perspective is given.

Due to the experimental nature of the derived concepts and verifications in live production networks, the contributions of the thesis enable the operators to take weighted decisions and measurable steps in implementing OSaaS in their production networks. As a result, higher network efficiency can be achieved, be it as easy as confidently allow IP-over-DWDM traffic into the networks or interconnecting multiple network and operator domains to implement an end-to-end connectivity between geographically diverse datacenter locations.

The performance estimation methods used in this work can also be used by scientists working on neighboring fields like QoT aware routing algorithms in elastic optical networks, network planning, service margins, and ML assisted predictive maintenance. The co-operation can significantly improve the efficient resource allocation in the networks and pave the way for Spectrum on Demand services, which would have a positive impact both on the implementation cost of the end-to-end connectivity and overall environmental impact to achieve net-zero emissions by 2050.

Based on the information presented in this work, further work initiatives have been already started and include:

- Continuous telemetry collection to enable uninterrupted performance tracking in optical networks implementing OSaaS service type. These works include X, XI, [157] and XII,

- Golden Transceiver initiative for automation of the S-BVT transceiver characterization,

- OLS-specific capacity analyses based on symbol rate variable channel probing in HEAnet fixed-grid long-haul network to drive network optimization decisions and,

- First NeDID prototype creation alongside with scientists from Trinity College Dublin and Politecnico di Milano.

As a final conclusion from this work, Optical Spectrum as a Service implementation in brownfield terrestrial systems can be challenging today, but the challenges can be overcome by the technical solutions proposed in this thesis. As a result, the terrestrial brownfield systems can be transformed into open disaggregated transport networks, capable of transporting modern, flexible, and efficient service types as Optical Spectrum as a Service.

References

1. E. Riccardi, A. Pagano, E. Hugues-Salas, G. Zervas, D. Simeonidou, A. D'Errico, M. Bohn, A. Napoli, D. Rafique, M. Nölle, and J.K. Fischer, "Sliceable bandwidth variable transponders for elastic optical networks: the idealist vision," In 2015 Fotonica AEIT Italian Conference on Photonics Technologies, pp. 1-4 (2015)

2. N. Sambo, A. Giorgetti, F. Cugini and P. Castoldi, "Sliceable Transponders: Pre-Programmed OAM, Control, and Management," in Journal of Lightwave Technology, vol. 36, no. 7, pp. 1403-1410 (2018)

3. M. Svaluto Moreolo, J.M. Fàbrega, and L. Nadal, "Sliceable BVT evolution towards programmable multi-Tb/s networking," Electronics, 8(12), p. 1476, (2019)

4. A. Napoli and V. Curri, "Introduction to the JOCN Special Issue on Open Optical Networks," Journal of Optical Communications and Networking, 12, OON1-OON3 (2020)

5. S. Barguil, V. Lopez and J. P. Fernandez-Palacios Gimenez, "Towards an Open Networking Architecture," 2020 International Conference on Optical Network Design and Modeling (ONDM), pp. 1-3 (2020)

6. E. Riccardi, P. Gunning, Ó. G. de Dios, M. Quagliotti, V. López and A. Lord, "An Operator view on the Introduction of White Boxes into Optical Networks," in Journal of Lightwave Technology, vol. 36, no. 15, pp. 3062-3072, (2018)

7. K. Grobe, C. Fürst, A. Autenrieth, and T. Szyrkowiec, "Flexible spectrum-as-a-service," in TERENA Networking Conference (TNC) (2014)

8. E. Rivera-Hartling, P. Pecci, and M. Priyanth, "Subsea open cables: a practical perspective on the guidelines and gotchas," in Proceedings Suboptic, Plenary (2019)

9. E.R. Hartling, A. Pilipetskii, D. Evans, E. Mateo, M. Salsi, P. Pecci, and P. Mehta, "Design, Acceptance and Capacity of Subsea Open Cables," Journal of Lightwave Technology, 39(3), pp.742-756 (2021)

10. S. Buscaglione, "GÉANT infrastructure evolution under GN4-3N," in TERENA Networking Conference (TNC) (2021)

11. "Spectral grids for WDM applications: DWDM frequency grid," ITU-T Recommendation G.694.1 (10/2020), [available online, last accessed 16th of November 2022] https://www.itu.int/rec/T-REC-G.694.1/en

12. OpenReach, (2012), "Openreach launches Optical Spectrum Access service with ADVA Optical Networking gear," press release (January 30th, 2012)

13. R. Velc, R. Vohnout, J. Vojtěch, P. Škoda, B. Belter, P. Ridlichowski, and C. Tziouvaras, "Pre-Commercial Procurement in Optical Networking domain," In 18th International Conference on Transparent Optical Networks (ICTON), pp. 1-4 (2016)

14. H. Wessing, K. Bozorgebrahimi, J. Vojtech, P. Skoda, and E. Camisard, Deliverable D13. 1 Research and Study Network Technologies–White Paper, 2016

15. A. Colmenero, A.M.F. DTU, D.C. Mur, D. Schmitz, F. Panken, H.Y. DTU, I. Demirkol, K. Boudjemaa, R. Tuminauskas, R. Smets, and Z. Ołtuszyk, Deliverable D13. 2 Blueprint of Services and Research Plan for Future Work, 2016

16. Colt, (2018), "Colt Spectrum brings cost effective Dark Fibre alternative to ultra-high bandwidth customers," press release (May 8th, 2018)

17. L. Fischer; J. Qvist, "Spectrum Sharing for Next Generation Networks", Technology Exchange Conference (2019)

18. ADVA, (2020), "ADVA unlocks network potential with spectrum as a service," press release (March 12th, 2020)

19. GEANT, (2021), "Moldovan and Ukrainian R&E communities benefit from new 'spectrum' link with GÉANT," press release (October 4th, 2021)

20. "Generic functional architecture of the optical media network," ITU-T Recommendation G.807, [available online, last accessed 16th of November 2022], https://www.itu.int/rec/T-REC-G.807/en

21. "Optical interfaces for coarse wavelength division multiplexing applications," [available online, last accessed 16th of November 2022], https://www.itu.int/rec/T-REC-G.695/en

22. "Multichannel DWDM applications with single-channel optical interfaces," [available online, last accessed 16th of November 2022], https://www.itu.int/rec/T-REC-G.698.1/en

23. "Amplified multichannel dense wavelength division multiplexing applications with single channel optical interfaces," [available online, last accessed 16th of November 2022], https://www.itu.int/rec/T-REC-G.698.2/en

24. O. Gerstel, M. Jinno, A. Lord, and S. J. B. Yoo, "Elastic optical networking: A new dawn for the optical layer?," IEEE Communications Magazine, vol. 50, no. 2, pp. s12-s20 (2012)

25. P. Layec, A. Morea, F. Vacondio, O. Rival and J. Antona, "Elastic optical networks: The global evolution to software configurable optical networks," in Bell Labs Technical Journal, vol. 18, no. 3, pp. 133-151 (2013)

26. L. Nadal, J.M. Fàbrega, M. Svaluto Moreolo, F. Javier Vílchez, R. Casellas, R. Muñoz, R. Vilalta, and R. Martínez, "Programmable disaggregated multi-dimensional S-BVT as an enabler for high capacity optical metro networks," Journal of Optical Communications and Networking, 13, C31-C40 (2021)

27. J. Santos, N. Costa, and J. Pedro, "On the Impact of Deploying Optical Transport Networks Using Disaggregated Line Systems," Journal of Optical Communications and Networking, 10, A60-A68 (2018)

28. H. Wessing, P. Skoda, M. Nordal Petersen, A. Pilimon, P. Rydlichowski, G. Roberts, R. Smets, J. Radil, J. Vojtech, R. Lund, Z. Zhou, C. Tziouvaras, and K. Bozorgebrahimi, "Alien Wavelengths in National Research and Education Network Infrastructures Based on Open Line Systems: Challenges and Opportunities, " Journal of Optical Communications and Networking, 11, 118-129 (2019)

29. M. Newland, R. Schmogrow, M. Cantono, V. Vusirikala, and T. Hofmeister, "Open optical communication systems at a hyperscale operator [Invited]," Journal of Optical Communications and Networking, 12, C50-C57 (2020)

30. C. Xie, L. Wang, L. Dou, M. Xia, S. Chen, H. Zhang, Z. Sun, and J. Cheng, "Open and disaggregated optical transport networks for data center interconnects [Invited]," Journal of Optical Communications and Networking, 12, C12-C22 (2020)

31. Nord Pool Market Data, last accessed December 2022, [available online, last accessed November 16th, 2022], https://www.nordpoolgroup.com/en/Market-data1/#/nordic/chart

32. European Commission, 2050 long-term climate strategy, [available online, last accessed November 16th, 2022], https://climate.ec.europa.eu/eu-action/climate-strategies-targets/2050-long-term-strategy_en

33. Rcrwireless, (2019), "Consortium selects Alcatel Submarine Networks to deploy Indigo subsea system," press release (April 6th, 2017).

34. ESI Africa, (2019), "Submarine cable to deepen telecom infrastructure in West Africa," press release (Oct 4th, 2019).

35. Ciena, (2021). "Telxius offers managed spectrum on Dunant and Marea powered by Ciena," press release (April 7th, 2021).

36. K. Peterman, (2019), "What are public communication technologies? ", blog post (February 9th, 2019), [available online, last accessed November 16th, 2022], https://medium.com/@katharyn.peterman/what-are-public-communication-technologies-1b3fb4e9ba3e

37. G.P. Agrawal, "Optical communication: its history and recent progress," Optics in our time, pp.177-199 (2016)

38. P.J. Winzer, D.T. Neilson, and A.R. Chraplyvy, "Fiber-optic transmission and networking: the previous 20 and the next 20 years [Invited]," Optics Express 26, 24190-24239 (2018)

39. I. Bertschek, W. Briglauer, K. Hüschelrath, B. Kauf, and T. Niebel, "The economic impacts of broadband internet: A survey," Review of Network Economics, 14(4), pp. 201-227 (2015)

40. M.T. Majeed, T. Ayub, "Information and communication technology (ICT) and economic growth nexus: A comparative global analysis," Pakistan Journal of Commerce and Social Sciences (PJCSS), ISSN 2309-8619, Johar Education Society, Pakistan (JESPK), Lahore, Vol. 12, Iss. 2, pp. 443-476 (2018)

41. C. Mercado, G. Dedene, E. Peters, and R. Maes, "Toward a dynamic, systemic, and holistic theory for strategic value creation in ICT-based services," in A Focused Issue on Competence Perspectives on New Industry Dynamics (2012)

42. A. Atieh, P. Perez, R. Andrew, and F. Sheikh "More services, less fiber: The commercial and network architecture impact of a black-link approach to the sharing of optical fiber infrastructure for the deployment of triple play services," Proc. SPIE 6022, Network Architectures, Management, and Applications III, 60220C (2005)

43. A. Atieh, P. Perez, R. Andrew and F. Sheikh, "A "black-link" approach for sharing optical fiber infrastructure and enabling multi-services," 2006 Optical Fiber Communication Conference and the National Fiber Optic Engineers Conference, paper JThB98 (2006)

44. D. Ventorini, E. Moura, L. Paraschis, O. Gerstel, M. Silva, K. Wollenweber, A.J. Silvério, P. Prado, H. Júnior, L. Augusto, L. and C.H. Silva, "Demonstration and evaluation of IP-over-DWDM networking as "alien-wavelength" over existing carrier DWDM infrastructure," in National Fiber Optic Engineers Conference, paper NME3 (2008)

45. P.R. Morkel, A. Färbert, A. Schwandner, G. Schubert, G. Rozensweig, J.J. Maki, A. Hotchkiss, M. Ding, G. Sun, and S. ElAhmadi, "Integrated IP-Optical Networks. Demonstration of DWDM Router-to-Router IP Transport Over 574 km SMF Fiber Link Using 11.1 Gbit/s OTN Pluggable Interface with Integrated G.709 and FEC," in Optical Fiber Communication Conference/National Fiber Optic Engineers Conference, paper NME4 (2008)

46. S. Harren, M. Kayser, E. Klaproth, T. Hallan, A. Hotchkiss, S. Nathan, S. ElAhmadi, and S. N. ElAhmadi, "Elimination of DWDM Transponders over a Deployed IP over DWDM Network Using Novel DWDM XFP Transceivers with Integrated G.709 and Forward Error Correction," in Optical Fiber Communication Conference and National Fiber Optic Engineers Conference, paper NThF4, (2009)

47. V. Vraciu, O. Rusu, P. Gasner, and M. Bărbulescu, "100 Gbps alien wavelength installation in a production DWDM network," in RoEduNet Conference 13th Edition: Networking in Education and Research Joint Event RENAM 8th Conference, pp. 1-4 (2014)

48. K. Slavicek and V. Novak, "Introduction of alien wavelength into CESNET DWDM backbone," in 6th Int. Conf. on Information, Communications and Signal Processing, pp. 1-5 (2007)

49. R. Nuijts and L.L. Bjørn, "40 Gb/s alien-wavelength experiment over 1000 km of G.655 (TWRS) transmission fiber between Amsterdam and Copenhagen," in TERENA Networking Conference (2010)

50. D.Z. Chen and M.F. Lane, "Emerging Network Need for Alien Wavelength Management," in Optical Fiber Communication Conference and Exposition and The National Fiber Optic Engineers Conference, paper NTuD5 (2007)

51. O. Gerstel, R. Cassata, L. Paraschis, and W. Wakim, "Operational Solutions for an Open DWDM layer," in Optical Fiber Communication Conference and National Fiber Optic Engineers Conference, paper NThF1 (2009)

52. S. Melle, G. Bennett, C. Liou, C. Villamizar, and V. Vusirikala, "Alien wavelength transport: an operational and economic analysis," in National Fiber Optic Engineers Conference, paper NThF2 (2009)

53. R.S. Tucker, R. Parthiban, J. Baliga, K. Hinton, R.W. Ayre, and W.V. Sorin, "Evolution of WDM optical IP networks: A cost and energy perspective," Journal of Lightwave Technology, 27(3), pp. 243-252 (2009)

54. N. Amaya, I. Muhammad, G.S. Zervas, R. Nejabati, D. Simeodinou, Y.R. Zhou, and A. Lord, "Experimental demonstration of a gridless multi-granular optical network supporting flexible spectrum switching," in Optical Fiber Communication Conference and Exposition and the National Fiber Optic Engineers Conference, pp. 1-3 (2011)

55. M. Jinno, B. Kozicki, H. Takara, A. Watanabe, Y. Sone, T. Tanaka, and A. Hirano, "Distance-adaptive spectrum resource allocation in spectrum-sliced elastic optical path network [topics in optical communications]," IEEE Communications Magazine, 48(8), pp. 138-145 (2010)

56. Y. Wang, X. Cao, Q. Hu and Y. Pan, "Towards elastic and fine-granular bandwidth allocation in spectrum-sliced optical networks," Journal of Optical Communications and Networking, vol. 4, no. 11, pp. 906-917 (2012)

57. H.C. Le, N. T. Dang and N. Duc Nguyen, "Impact of optical regeneration on dynamic elastic optical networks," 2017 International Conference on Advanced Technologies for Communications (ATC), pp. 11-15 (2017)

58. N. Amaya, M. Irfan, G. Zervas, K. Banias, M. Garrich, I. Henning, D. Simeonidou, Y.R. Zhou, A. Lord, A., K. Smith, and V.J.F. Rancano, "Gridless optical networking field trial: flexible spectrum switching, defragmentation and transport of 10G/40G/100G/555G over 620-km field fiber," Optics express, 19(26), pp. B277-B282 (2011)

59. K.I. Kitayama, M. Sasaki, S. Araki, M. Tsubokawa, A. Tomita, K. Inoue, K. Harasawa, Y. Nagasako, and A. Takada, "Security in photonic networks: Threats and security enhancement," Journal of Lightwave technology, 29(21), pp. 3210-3222 (2011)

60. J. Vojtěch, V. Smotlacha, S. Šíma and P. Škoda, "Photonic services," in 14th International Conference on Transparent Optical Networks (ICTON), pp. 1-4 (2012)

61. J. Vojtech, V. Smotlacha, P. Skoda, S. Sima, J. Radil and M. Hůla, "Photonic services enables real-time applications over long distances," 3rd International Conference on Photonics, pp. 231-234 (2012)

62. J. Vojtech, V. Smotlacha, P. Skoda, A. Kuna, M. Hula, and S. Sima, "Photonic services, their enablers and applications," Proc. SPIE, vol. 8516, 85160H, 2012.

63. L. Altmanová, "Photonic services: Challenge for users and for networkers," the GN3 project report (2013)

64. R. Kunze, "A framework for Management and Control of optical interfaces supporting G.698.2," Internet Engineering Task Force Internet-Draft (2011)

65. A. Lord, P. Wright, and Y. R. Zhou, "Alien waves: technology, benefits and standardization," in International Conference on Photonics in Switching (PS), pp. 1-3 (2012)

66. M. Gunkel, A. Mattheus, A. Napoli, G. Meloni, F. Fresi and T. Rahman, "Elastic Black Link for future vendor independent optical networks," Optical Fiber Communications Conference and Exhibition (OFC), pp. 1-3 (2015)

67. M. Gunkel, A. Mattheus, F. Wissel, A. Napoli, J. Pedro, N. Costa, T. Rahman, G. Meloni, F. Fresi, F. Cugini, N. Sambo, and M. Bohn, "Vendor-Interoperable Elastic Optical Interfaces: Standards, Experiments, and Challenges [Invited]," Journal of Optical Communications and Networking, 7(12), B184-B193 (2015)

68. R. Kunze, E.G. Grammel, D. Beller, E. Galimberti, and J. Meuric, "A framework for management and control of DWDM optical interface parameters," IETF draft-ietf-ccamp-dwdm-if-mng-ctrlfwk-06 (2017)

69. "Architecture of optical transport networks," [available online, last accessed November 16th, 2022], https://www.itu.int/rec/T-REC-G.872-201210-S/en

70. H. Wessing, P. Skoda, M.N. Petersen, A. Pilimon, P. Rydlichowski, G. Roberts, R. Smets, J. Radil, J. Vojtech, R. Lund, Z. Zhou, C. Tziouvaras, and K. Bozorgebrahimi, "Alien Wavelengths in National Research and Education Network Infrastructures Based on Open Line Systems: Challenges and Opportunities," Journal of Optical Communications and Networking, 11, pp. 118-129 (2019)

71. Y.R. Zhou, K. Smith, M. Wilkinson, R. Payne, A. Lord, T. Bennett, and M. Frankel, "Coherent 100G field trial over installed fiber links: Investigating key network scenarios and applications," Journal of Optical Communications and Networking, 4(11), pp. B35-B41 (2012)

72. A.M. Fagertun, S. Ruepp, M.N. Pedersen, and B. Skjoldstrup, "Field Trial of 40 Gb/s Optical Transport Network using Open WDM Interfaces," in 18th OptoElectronics and Communications Conference held jointly with 2013 International Conference on Photonics in Switching, paper TuPQ_5 (2013)

73. Y.R. Zhou, K. Smith, R. Payne, A. Lord, G. Whalley, T. Bennett, E. Maniloff, S. Alexander, and D. Boymel, "Real-Time Gridless 800G Super-channel Transport Field Trial over 410km Using Coherent DP-16 QAM," in Optical Fiber Communication Conference, paper Tu2B-3 (2014)

74. Y.R. Zhou, K. Smith, R. Payne, A. Lord, L. Raddatz, M. Bertolini, T. Van De Velde, C. Colombo, E. Korkmaz, M. Fontana, and S. Evans, "1.4Tb Real-Time Alien Superchannel Transport Demonstration over 410km Installed Fiber Link Using Software Reconfigurable DP-16QAM/QPSK," in Optical Fiber Communication Conference: Postdeadline Papers, paper Th5A.9 (2014)

75. Y.R. Zhou, K. Smith, R. Payne, A. Lord, J. Hopewell, J. Weatherhead, J. Chen, J. Yao, W. Liu, C. Zhao, Y. Xiong, Z. Xiao, and P. Du, "Field Demonstration of up to 3Tb/s Real-Time Superchannel Transport over 359km Using a Fully Managed Flexible Grid Infrastructure with Net Spectral Efficiency of 5.97bit/s/Hz," in Optical Fiber Communication Conference, paper Tu3H.4 (2015)

76. Y. Loussouarn, E. Pincemin, M. Song, S. Gauthier, Y. Chen, and Z. Shengqian, "400 Gbps Real-Time Coherent Nyquist-WDM DP-16QAM Transmission over Legacy G.652 or G.655 Fibre Infrastructure with 2 dB Margins," in Optical Fiber Communication Conference, paper W3E3 (2015)

77. M. Channegowda, R. Nejabati, M. Rashidi Fard, S. Peng, N. Amaya, G. Zervas, D. Simeonidou, R. Vilalta, R. Casellas, R. Martínez, R. Muñoz, L. Liu, T. Tsuritani, I. Morita, A. Autenrieth, J.P. Elbers, P. Kostecki, and P. Kaczmarek, "Experimental demonstration of an OpenFlow based software-defined optical network employing packet, fixed and flexible DWDM grid technologies on an international multi-domain testbed," Optical Express 21, pp. 5487-5498 (2013)

78. P. Layec, A. Morea, F. Vacondio, O. Rival and J. Antona, "Elastic optical networks: The global evolution to software configurable optical networks," in Bell Labs Technical Journal, vol. 18, no. 3, pp. 133-151 (2013)

79. A. Martinez, M. Yannuzzi, V. Lopez, D. Lopez, W. Ramirez, R. Serral-Gracia, X. Masip-Bruin, M. Maciejewski, and J. Altmann, "Network management challenges and trends in multi-layer and multi-vendor settings for carrier-grade networks," IEEE Communications Surveys & Tutorials, 16(4), pp.2207-2230 (2014)

80. F. Cugini, N. Sambo, F. Paolucci, F. Fresi and P. Castoldi, "Adaptation and monitoring for elastic alien wavelengths," 21st European Conference on Networks and Optical Communications (NOC), pp. 82-87 (2016)

81. F. Paolucci, N. Sambo, F. Cugini, and P. Castoldi, "Demonstration of effective OAM for alien wavelength and transport network," in Optical Fiber Communication Conference, paper W2A.31 (2017)

82. E. Palkopoulou, I. Stiakogiannakis, D. Klonidis, K. Christodoulopoulos, E. Varvarigos, O. Gerstel, and I. Tomkos, "Dynamic cooperative spectrum sharing in elastic networks," in Optical Fiber Communication Conference and Exposition and the National Fiber Optic Engineers Conference, pp. 1-3 (2013)

83. L.H. Bonani, A. dos Santos Tozetti, F. Callegati and W. Cerroni, "Routing issues on spectrum sharing and partitioning for flexible optical networks," 16th International Conference on Transparent Optical Networks (ICTON), pp. 1-4 (2014)

84. S. Talebi, F. Alam, I. Katib, M. Khamis, R. Salama, and G.N. Rouskas, "Spectrum management techniques for elastic optical networks: A survey," Optical Switching and Networking 13, pp. 34-48 (2014)

85. B.C. Chatterjee, N. Sarma and E. Oki, "Routing and Spectrum Allocation in Elastic Optical Networks: A Tutorial," in IEEE Communications Surveys & Tutorials, vol. 17, no. 3, pp. 1776-1800, (2015)

86. Y. Qiu, "An efficient spectrum assignment algorithm based on variable-grouping mechanism for flex-grid optical networks," Optical Switching and Networking, 24, pp. 39-46 (2017)

87. J. Santos, N. Costa, and J. Pedro, "On the Impact of Deploying Optical Transport Networks Using Disaggregated Line Systems," Journal of Optical Communications and Networking. 10, A60-A68, (2018)

88. T. Ahmed, S. Rahman, S. Ferdousi, M. Tornatore, A. Mitra, B.C. Chatterjee, and B. Mukherjee, "Dynamic routing, spectrum, and modulation-format allocation in mixed-grid optical networks," Journal of Optical Communications and Networking. 12, 79-88, (2020)

89. K. Perlicki, "Impact of alien wavelength on wavelength division multiplexing transmission quality," Photonics Letters of Poland, vol. 4, no. 3, pp. 118-120, (2012)

90. GÉANT, "Optical reach of photonic services," Milestone MJ1.2.3, [available online, last accessed November 16th, 2022], https://geant3.archive.geant.org/Media_Centre/Media_Library/Media%20Librar y/GN3-13-162_MJ1.2.3_White-Paper_Optical-Reach-of-Photonic-Services_v3.pdf

91. N. Sambo, A. Sgambelluri, M. Secondini, M. N. Petersen, A. M. Fagertun, and G. Roberts, "Alien wavelength modeling tool and field trial," in International Conference on Photonics in Switching (PS), pp. 339-341 (2015)

92. T. Horvath, P. Munster, M. Latal and N. -H. Bao, "Photonic Services with Sensor System in One Fibre with 100-GHz DWDM Grid," in ELEKTRO, pp. 1-4, (2020)

93. K. Kaeval, K., D. Rafique, K. Blawat, K. Grobe, H. Grießer, J.P. Elbers, P. Rydlichowski, A. Binczewski, and M. Tikas, "Exploring channel probing to determine coherent optical transponder configurations in a long-haul network," in Optical Fiber Communications Conference and Exhibition, pp. 1-3 (2020)

94. K. Kaeval, H. Grießer, K. Grobe, J.P. Elbers, M. Tikas and G. Jervan, "Channel Performance Estimations with Extended Channel Probing," in Photonic Networks; 21th ITG-Symposium, pp. 1-5 (2020)

95. K. Kaeval, T. Fehenberger, J. Zou, S.L. Jansen, K. Grobe, H. Grießer, J.P. Elbers, M. Tikas, and G. Jervan, "QoT assessment of the optical spectrum as a service in disaggregated network scenarios," Journal of Optical Communications and Networking, 13, E1-E12 (2021)

96. K. Kaeval, J.P. Elbers, K. Grobe, M. Tikas, T. Fehenberger, H. Grießer, G. Jervan, "Black-Box Assessment of Optical Spectrum Services," in Optical Fiber Communications Conference and Exhibition, pp.1-3 (2021)

97. M. Newland, R. Schmogrow, M. Cantono, V. Vusirikala, and T. Hofmeister, "Open optical communication systems at a hyperscale operator [Invited]," Journal of Optical Communications and Networking. 12, C50-C57 (2020)

98. A. Lord, Y.R. Zhou, P. Wright, P. Willis, C. Look, G. Jeon, S. Nathan, and A. Hotchkiss, "Managed alien wavelength service requirements and demonstration," in 37th European Conference and Exhibition on Optical Communication, pp. 1-3 (2011)

99. A.M. Fagertun and B. Skjoldstrup, "Flexible transport network expansion via open WDM interfaces," International Conference on Computing, Networking and Communications (ICNC), pp. 385-389 (2013)

100. H.W. DTU, K. Bozorgebrahimi, A. Tzanakaki, and B. Belter, Deliverable D12. 3 (DJ1. 1.1) Future Network Architectures, (2016), [available online, last accessed November 16th, 2022], https://geant3plus.archive.geant.net/Documents/D12-3_DJ1-1-1_Future-Network-Architectures.pdf

101. A. Colmenero, A.M.F. DTU, D.C. Mur, D. Schmitz, F. Panken, H.Y. DTU, I. Demirkol, K. Boudjemaa, R. Tuminauskas, R. Smets, and Z. Ołtuszyk, Deliverable D13. 2 "Blueprint of Services and Research Plan for Future Work". [available online, last accessed November 16th, 2022], https://ec.europa.eu/research/participants/documents/downloadPublic?documentIds=080166e5a89985d4&appId=PPGMS

102. L. Alahdab, E. Le Rouzic, C. Ware, J. Meuric, A. Triki, J.L. Augé, and T. Marcot, "Alien Wavelengths Over Optical Transport Networks," Journal of Optical Communications and Networking. 10, 878-888 (2018)

103. F. Paolucci, R. Emmerich, A. Eira, N. Costa, J. Pedro, P. Wilke Berenguer, C. Schubert, J. K. Fischer, F. Fresi, A. Sgambelluri, and F. Cugini, "Disaggregated edge-enabled C+L-band filterless metro networks," Journal of Optical Communications and Networking. 12, 2-12 (2020)

104. G. Roberts, P. Skoda, G. Vuagnin, P. Bolletta, J. Vojtech, K. Boudjemaa, K. Bozorgebrahimi, C. Tziouvaras, "Milestone M7.2 (M38) SCS Service Definition" 2020, [available online, last accessed November 16th, 2022], https://resources.geant.org/wp-content/uploads/2022/02/M7-2_SCS-Service-Definition.pdf

105. A.M. Fagertun, S. Ruepp and B. Skjoldstrup, "CAPEX/OPEX benefits of alien wavelengths for the next generation optical internet," International Conference on Optical Network Design and Modeling (ONDM), pp. 122-127 (2015)

106. V. Kamalov, V. Dangui, T. Hofmeister, B. Koley, C. Mitchell, M. Newland, J. O'Shea, C. Tomblin, V. Vusirikala, and X. Zhao, "Lessons learned from open line system deployments," in Optical Fiber Communications Conference and Exhibition, pp. 1-3 (2017)

107. Lightwave Online, (2017), "Open optical line system pros and cons at the Open Optical Conference," press release (November 7th, 2017).

108. M. Filer, J. Gaudette, M. Ghobadi, R. Mahajan, T. Issenhuth, B. Klinkers, and J. Cox, "Elastic optical networking in the Microsoft cloud," Journal of Optical Communications and Networking, 8(7), pp. A45-A54 (2016)

109. B. Clouet, J. Pedro, N. Costa, M. Kuschnerov, A. Schex, J. Slovak, D. Rafique, and A. Napoli, A., "Networking aspects for next-generation elastic optical interfaces," Journal of Optical Communications and Networking, 8(7), pp. A116-A125 (2016)

110. M. Filer, H. Chaouch, and X. Wu, "Toward transport ecosystem interoperability enabled by vendor-diverse coherent optical sources over an open line system," Journal of Optical Communications and Networking, 10(2), pp. A216-A224 (2018).

111. K. Bozorgebrahimi, "Spectrum sharing – lessons from workshop", TERENA Networking Conference (2019)

112. C. Xie, L. Wang, L. Dou, M. Xia, S. Chen, H. Zhang, Z. Sun, and J. Cheng, "Open and disaggregated optical transport networks for data center interconnects [Invited]," Journal of Optical Communications and Networking, 12, C12-C22 (2020)

113. "Transverse compatible dense wavelength division multiplexing applications for repeatered optical fibre submarine cable systems," ITU-T Rec. G. 977.1, [available online, last accessed November 16th, 2022], https://www.itu.int/rec/T-REC-G.977.1-202010-I/en

114. "Generic functional architecture of the optical media network – Amendement 1," ITU-T Rec. G.807 Appendix 1, [available online, last accessed November 16th, 2022], https://www.itu.int/rec/T-REC-G.807-202101-I!Amd1/en

115. "Cloud computing – Functional requirements of Network as a Service," ITU-T Rec. Y.3512, [available online, last accessed November 16th, 2022], https://www.itu.int/rec/T-REC-Y.3512/en

116. P. Krummrich, "Mastering power transients—a prerequisite for future optical networks. In Optically Amplified WDM Networks", Academic Press, pp. 155-200 (2012)

117. O. Leclerc, "Towards transparent optical networks: still some challenges ahead," 2005 IEEE LEOS Annual Meeting Conference Proceedings, pp. 418-419 (2005)

118. M. Bolshtyansky and G. Cowle, "Spectral Hole Burning in EDFA under various channel load conditions," 2009 Conference on Optical Fiber Communication, pp. 1-3 (2009)

119. F. Buchali, V. Lauinger, M. Chagnon, K. Schuh, and V. Aref, "CMOS DAC supported 1.1 Tb/s/λ DWDM transmission at 9.8 bit/s/Hz over DCI distances," Journal of Lightwave Technology, 39(4), pp. 1171-1178 (2020)

120. F. Buchali, V. Aref, R. Dischler, M. Chagnon, K. Schuh, H. Hettrich, A. Bielik, L. Altenhain, M. Guntermann, R. Schmid, and M. Möller, "128 GSa/s SiGe DAC implementation enabling 1.52 Tb/s single carrier transmission," Journal of Lightwave Technology, 39(3), pp. 763-770, 2020

121. Y. Pointurier, "Design of low-margin optical networks", Journal of Optical Communications and Networking, 9(1), pp. A9-A17 (2017)

122. D. Semrau, E. Sillekens, P. Bayvel, and R.I. Killey, "Modeling and mitigation of fiber nonlinearity in wide-band optical signal transmission [Invited]," Journal of Optical Communications and Networking. 12, C68-C76 (2020)

123. D.F. Grosz, A. Agarwal, S. Banerjee, D.N. Maywar and A.P. Kung, "All-Raman ultralong-haul single-wideband DWDM transmission systems with OADM capability," in Journal of Lightwave Technology, vol. 22, no. 2, pp. 423-432, (2004)

124. K. Grobe, M. Eiselt, "Wavelength Division Multiplexing: A Practical Engineering Guide 1st Edition", John Wiley & Sons, p. 295, fig. 6.40 (2013)

125. B.D. Taylor, G. Goldfarb, S. Bandyopadhyay, V. Curri and H. Schmidtke, "Towards a Route Planning Tool for Open Optical Networks in the Telecom Infrastructure Project," Optical Fiber Communications Conference and Exposition, pp. 1-3 (2018)

126. A. Ferrari, M. Filer, K. Balasubramanian,Y. Yin, E. Le Rouzic, J. Kundrát, G. Grammel, G. Galimberti, and V. Curri, "GNPy: an open source application for physical layer aware open optical networks," Journal of Optical Communications and Networking, 12(6), pp.C31-C40 (2020)

127. A. Ferrari, J. Kundrát, E. Le Rouzic, M. Filer, A. Campanella, A. D'Amico, K. Balasubramanian, Y. Yin, O. Havliš, M. Hažlinský, and J. Vojtěch, "The GNPy Open Source Library of Applications for Software Abstraction of WDM Data Transport in Open Optical Networks," In Proc. of 6th IEEE Conference on Network Softwarization (NetSoft), pp. 386-394 (2020)

128. ADVA TeraFlex™, [available online, last accessed November 16th, 2022], https://www.adva.com/en/products/open-optical-transport/fsp-3000-open-terminals/teraflex

129. "Forward error correction for high bit-rate DWDM submarine systems," ITU-T G.975.1 (02/04), [available online, last accessed November 16th, 2022], https://www.itu.int/rec/T-REC-G.975.1/en

130. T. Yoshida, M. Mazur, J. Schröder, M. Karlsson and E. Agrell, "Performance Monitoring for Live Systems With Soft FEC and Multilevel Modulation," in Journal of Lightwave Technology, vol. 38, no. 11, pp. 2912-2921, (2020)

131. "SubOptic Open Cables Working Group," [available online, last accessed November 16th, 2022], https://suboptic.org/

132. A.C. Meseguer, P. Plantady, A. Calsat, S. Dubost, J.C Antona, and V. Letellier, "Automated full C-band technique for fast characterization of subsea open cable G-SNR," In Asia Communications and Photonics Conference (pp. S4B-5). Optical Society of America, (2019)

133. K. Kaeval, S.L. Jansen, F. Spinty, K. Grobe, H. Griesser, T. Fehenberger, M. Tikas, and G. Jervan, "Characterization of the Optical Spectrum as a Service," Journal of Optical Communications and Networking, 14(5), pp. 398-410, (2022)

134. K. Kaeval, J. Myyry, K. Grobe, H. Grießer, and G. Jervan, "Concatenated GSNR Profiles for End-to-End Performance Estimations in Disaggregated Networks." in Optical Fiber Communications Conference and Exhibition, pp. 1-3 (2022)

135. Kaeval, K., Slyne, F., Troia, S., Kenny, E., Pedreño-Manresa, J., Patri, S., Grobe, K., Grießer, H., Jervan, G., "Service Margins for Optical Spectrum Services", European Conference on Optical Communication (2022)

136. Kaeval, K., Patri, S.K., Pedreno-Manresa, J., Grobe, K., Elbers, J.P., Grießer, H., Tikas, M., Jervan, G., "Service Margins for Wide-Band Optical Spectrum Services Implemented in Long-Haul Raman-Enabled Networks", Optical Fibre Communication Conference, 2023, pp. W3H-6

137. Kaeval, K., Slyne, F., Troia, S., Kenny, E., Grobe, K., Griesβer, H., Kilper, D.C., Ruffini, M., Pedreño-Manresa, J., Patri, S.K., and Jervan, G., "Employing Channel Probing to Derive End-of-Life Service Margins for Optical Spectrum Services", Journal of Optical Communications and Networking, 15, C63-C73 (2023)

138. P. Poggiolini, "The GN model of non-linear propagation in uncompensated coherent optical systems," Journal of Lightwave Technology, 30(24), pp. 3857-3879 (2012)

139. D.C. Kilper, R. Bach, D.J. Blumenthal, D. Einstein, T. Landolsi, L. Ostar, M. Preiss, and A.E. Willner, "Optical performance monitoring," in Journal of Lightwave Technology, vol. 22, no. 1, pp. 294-304 (2004)

140. C. Mas, I. Tomkos and O.K. Tonguz, "Failure location algorithm for transparent optical networks," in IEEE Journal on Selected Areas in Communications, vol. 23, no. 8, pp. 1508-1519 (2005)

141. V.Y. Wen, V.W. S. Chan and L. Zheng, "Efficient fault-diagnosis algorithms for all-optical WDM networks with probabilistic link failures," in Journal of Lightwave Technology, vol. 23, no. 10, pp. 3358-3371 (2005)

142. E. Torrengo, R. Cigliutti, G. Bosco, A. Carena, V. Curri, P. Poggiolini, A. Nespola, D. Zeolla, and F. Forghieri, "Experimental validation of an analytical model for nonlinear propagation in uncompensated optical links," Optics express, 19(26), pp. B790-B798 (2011)

143. P. Poggiolini, A. Carena, V. Curri, G. Bosco, and F. Forghieri, "Analytical modeling of nonlinear propagation in uncompensated optical transmission links," IEEE Photonics technology letters, 23(11), pp.742-744 (2011)

144. R. Borkowski, A. Caballero, V. Arlunno, D. Zibar, and I.T. Monroy, "Robust cognitive-GN BER estimator for dynamic WDM networks," In Proc. of The European Conference on Optical Communication (ECOC), pp. 1-3, 2014

145. O.V. Sinkin, C.R. Davidson, H. Wang, L. Richardson, J.X. Cai, D. Kovsh, D.G. Foursa, B. Bakhshi, G. Mohs, and A.N. Pilipetskii, "Effective signal to noise ratio performance metric for dispersion-uncompensated links," In Proc. of 2015 European Conference on Optical Communication (ECOC), pp. 1-3, 2015

146. M. Enright, "Open cables and integration with terrestrial networks," in Proceeding of SubOptic 2016, WE2A-4, 2016

147. R. Hadaway, E.R. Hartling, P. Mehta, M. Hubbard, D. Evans, L. Berg, and M. Hinds, "Submarine cable upgrades," In Undersea Fiber Communication Systems, pp. 577-603, 2016

148. P. Pecci, S. Dupont, S. Dubost, S. Ruggeri, O. Courtois, and V. Letellier, "Experimental characterization of submarine "open cable" using Gaussian-noise model and OSNRwet parameter," In Optical Fiber Communications Conference and Exhibition (OFC), pp. 1-3, 2017

149. J. Slovak, W. Schairer, M. Herrmann, K. Pulverer, and E. Torrengo, "Benefits of performance awareness in coherent dynamic optical networks," In Optical Fiber Communication Conference, paper W4A-1 (2018)

150. C. Delezoide, K. Christodoulopoulos, A. Kretsis, N. Argyris, G. Kanakist, A. Sgambelluri, N. Sambo, P. Giardina, G. Bernini, D. Roccato, and A. Percelsi, "Field trial of marginless operations of an optical network facing ageing and performance fluctuations," In European Conference on Optical Communication (ECOC), pp. 1-3, 2018

151. S. Oda, M. Miyabe, S. Yoshida, T. Katagiri, Y. Aoki, T. Hoshida, J.C. Rasmussen, M. Birk, and K. Tse, "A learning living network with open ROADMs," Journal of Lightwave Technology, 35(8), pp. 1350-1356, 2017

152. M. Filer, M. Cantono, A. Ferrari, G. Grammel, G. Galimberti, and V. Curri, "Multi-vendor experimental validation of an open source QoT estimator for optical networks," Journal of Lightwave Technology, 36(15), pp. 3073-3082 (2018)

153. Y.R. Zhou, K. Smith, J. Weatherhead, P. Weir, A. Lord, J. Chen, W. Pan, D. Tanasoiu, and S. Wu, "Demonstration of a Novel Technique for Non-Intrusive In-Band OSNR Derivation Using Flexible Rate Optical Transponders Over a Live 727 km Flexible Grid Optical Link," Journal of Lightwave Technology, 35(20), pp. 4399-4405 (2017)

154. M. Cantono, J.L. Auge, and V. Curri, "Modelling the impact of SRS on NLI generation in commercial equipment: An experimental investigation," In Optical Fiber Communication Conference, paper M1D-2, (2018)

155. D. Gariépy, S. Searcy, G. He, S. Tibuleac, M. Leclerc, and P. Gosselin-Badaroudine, "Novel OSNR measurement techniques based on optical spectrum analysis and their application to coherent-detection systems," Journal of Lightwave Technology, 37(2), pp. 562-570 (2018)

156. E. Grellier, and A. Bononi, "Quality parameter for coherent transmissions with Gaussian-distributed nonlinear noise," Optics Express, 19(13), pp. 12781-12788 (2011)

157. I. Dick, "Machine Learning based Fault Detection Algorithms or Long-Haul Elastic Optical Networks", Master Thesis, Technical Universität München

158. Pan, J. and Tibuleac, S., "Filtering and crosstalk penalties for PDM-8QAM/16QAM super-channels in DWDM networks using broadcast-and-select and route-and-select ROADMs," Optical Fiber Communications Conference and Exhibition, 2016, pp. 1-3

159. B. Shariati, M. Ruiz, J. Comellas, and L. Velasco, "Learning from the optical spectrum: failure detection and identification," Journal of Lightwave Technology, 37(2), pp. 433-440, 2019

160. C. Pulikkaseril, L.A. Stewart, M.A. Roelens, G.W. Baxter, S. Poole, and S. Frisken, "Spectral modeling of channel band shapes in wavelength selective switches," Optics express, 19(9), pp. 8458-8470, 2011

161. V. Lopez, O.G. de Dios, L.M. Contreras, J. Foster,H. Silva, L. Blair, J. Marsella, T. Szyrkowiec, A. Autenrieth, C. Liou, and A. Sasdasivarao, "Demonstration of SDN orchestration in optical multi-vendor scenarios," In 2015 Optical Fiber Communications Conference and Exhibition (OFC), 2015, March, pp. 1-3, IEEE

162. O.G. De Dios, R. Casellas, F. Paolucci, A. Napoli, L. Gifre, S. Annoni, S. Belotti, U. Feiste, D. Rafique, M. Bohn, and S. Bigo, "First demonstration of multi-vendor and multi-domain EON with S-BVT and control interoperability over Pan-European testbed". In 2015 European Conference on Optical Communication (ECOC) (pp. 1-3). 2015, September. IEEE

163. A. Aguado, M. Davis, S. Peng, S., M.V. Alvarez, V. López, T. Szyrkowiec, A. Autenrieth, R. Vilalta, A. Mayoral, R. Muñoz, and R. Casellas, "Dynamic virtual network reconfiguration over SDN orchestrated multitechnology optical transport domains," Journal of Lightwave Technology, 34(8), pp. 1933-1938, 2016

164. Y. Li, W. Mo, S. Zhu, Y. Shen, J. Yu, P. Samadi, K. Bergman, and D.C. Kilper, 2017. "tSDX: enabling impairment-aware all-optical inter-domain exchange," Journal of Lightwave Technology, 36(1), pp. 142-154

165. C. Zhang, R. Jing, J. Li, Y. Ma, X. Huo, Y. Zhao, and J. Zhang, "Field trial of bandwidth on demand services based on hierarchical control over multi-domain OTN networks," Journal of Optical Communications and Networking, 7(11), pp. 1057-1063

166. Y. Li, Y. Zhao, J. Zhang, X. Yu, H. Chen, R. Zhu, Q. Zhou, C. Yu, and R. Cui, "First field trial of Virtual Network Operator oriented network on demand (NoD) service provisioning over software defined multi-vendor OTN networks". Optical Fiber Technology, 33, pp. 22-29, 2017

Acknowledgements

Different people have different goals in life. Some want to travel the world, some want to climb a mountain top, and some want to pursue a PhD degree. I wanted to do the latter since I can remember. However, enrolling in a PhD program after 13 years of work on field was definitely not a common path. Regardless, my time as a PhD student has provided me some immensely valuable experiences, that I'm sure I would have not gained anywhere else. During this 4-year time period, I have met the most amazing people and had great fun in working with the state-of-the art technologies and networks.

First of all, I would like to thank my supervisor professor **Gert Jervan**, who encouraged me to enroll in a PhD program already in 2010 when I took a course in TalTech with him to investigate System Dependability aspects in Optical Networks for a Pan-European high-capacity transmission link. Secondly, I would like to thank the CTO of ADVA Optical Networking, **Christoph Glingener**, who planted an idea to pursue my PhD degree in ADVA's Advanced Technology team. And the stars must have been aligned, when **Jörg-Peter Elbers** proposed me the topic I had been interested in for a decade – Optical Spectrum Services in Open Disaggregated Transport Networks. A mere decade later, I was finally enrolled in an industrial PhD program, with the most supporting and patient co-supervisors on Earth, **Helmut Grießer** and **Klaus Grobe**, to guide me through the academic research. Thank you, ADVA, for hosting me during my research and introducing me to the fantastic team of ADVA Advanced Technology and ADVA family: **Danish Rafique, Sai Kireet Patri, Jose-Juan Pedreno-Manersa, Jasper Müller, Kamil Blawat, Tobias Fehenberger, Jim Zou, Achim Autenrieth, Florian Spinty**, and **Vincent Sleiffer**. Thank you for your fruitful discussions, support, and dedication. It has been a pleasure and an honor to work with you!

I would also like to thank our amazing customers, who have opened their networks for this exciting research, starting with **Marko Tikas, Vitali Tulko** and **Marina Pärnsalu** from Tele2 Estonia, **Jani Myyry** from Funet and **Eoin Kenny** from HEAnet. Your co-operation and help in verifying the Optical Spectrum Services concepts in production network environment has been extremely valuable. In addition, I would like to thank our partners from HAPT consortium, **Frank Slyne**, **Marco Ruffini** and **Dan Kilper** from Trinity College Dublin and **Sebastian Troia** from Politecnico di Milano, whose help was invaluable in automizing the test-scenarios in Open Ireland CONNECT lab, and heavy-lifting the papers discussing the service margins.

In addition, I would like to express my deepest gratitude and love to my dearest friends, **Sander Lars Jansen, Gerlinde Bedö, Ashley Tödtheide** and **Victor Welman**. There were days when the sun only raised because of you. Thank you for your unconditional love and friendship that you have shared with me. There are no words to express my feelings for you. I love you to the moon and back.

And finally, I would like to express my gratitude to my **friends and family in Estonia**, who impatiently waited for all these four years for me to return back home. Thank you for supporting me in this roller-coaster that pursuing a PhD sometimes is.

Abstract

Optical Spectrum Services in Open Disaggregated Transport Networks

Modern society depends on broadband connectivity to access digital environments like the Internet, cloud applications, digital databases, video streams, broadcasts, and continuous access to the Internet of Things. While wireless communication technologies are still prevalent in the access space, the backbone of such connectivity is provided over fiber optical communication networks. To increase the capacity and throughput of a single backbone communication link, Dense Wavelength Division Multiplexing technology on top of fiber infrastructure has been widely used since the 1990s. Traditionally, these systems have been fixed to use proprietary transceivers to light up the wavelengths and provide capacity. This has been challenged by the emerging disaggregation trend in optical transport networks, empowered by the Sliceable Bandwidth Variable Transceivers (S-BVT). With the hope for higher flexibility and spectral efficiency in the networks, operators are willing to provide future-proof Optical Spectrum as a Service (OSaaS) instead of classical capacity services. Differentiated from the conventional capacity services, where the transceivers operated by the service provider functioned as a demarcation point in the network, in OSaaS service model, an end customer is granted direct access to the spectral resources in the provider's DWDM system. If the desired spectrum is continuously available in all included network segments, OSaaS can be operated over thousands of kilometers without signal regeneration at the domain end nodes. This can provide significant benefits compared to traditional network architecture: reduced capital investments into the expensive transponder and demarcation equipment, reduced energy consumption, reduced requirements for human resources to maintain the service, and reduced electronic waste products and utilization costs at the end of the equipment lifetime. However, the new service type introduces several uncertainties, starting with the uniform characterization of the service during handover, quality of transmission estimations, and incoming customer spectrum policing, which can have a severe impact on the underlying network's integrity.

This thesis defines, how Optical Spectrum Services can be configured in the Open Optical DWDM networks and provides insights into the operational complexities related to each of the configurations. The thesis also provides a solution to experimentally define the service performance during the handover, using a channel probing method to capture a Generalized Signal to Noise based performance profile. The proposed method enables to reliably identify wavelength-dependent performance variations, possible filtering penalties, and the operation regime of the optical spectrum services, which are demonstrated in the work. In addition, service margins to cover for enabling direct neighboring channels, and end-of-life channel loads are derived in a systematic lab study. Furthermore, based on the telemetry data, service margins to cover the fast and slow performance fluctuations in the networks are derived, using standard deviation. Finally, the underlying network integrity questions are addressed, and vendor-, domain-, operator- and DWDM network's technology-independent Network Domain Interface Device (NeDID) is introduced. The NeDID includes a comprehensive set of interworking

functions to enable monitoring and policing of the bundled signals at the edges of the domains. Furthermore, enabled by the safe resource sharing in optical layer-zero networks, provided by NeDID, a new Transparent Optical Overlay model is introduced. Included examples demonstrate the reduction of the required equipment to implement end-to-end connectivity over multi-domain, multi-operator environments, reducing the CAPEX and OPEX costs, CO_2 production over the service lifecycle, and waste products after the end-of-life. In addition, it reduces the secondary costs related to manpower and maintenance activities, required to operate, and maintain the equipment and services. Finally, sharing the optical spectrum in a safe manner may increase the availability of the capacity between the service endpoints, as more infrastructure providers would consider resource sharing, effectively increasing the number of paths between two endpoints, and therefore, the possibility to reroute service in case of service interruptions.

In a conclusion, the thesis has used an experimental approach to address the operational concerns that have prevented the wide-scale OSaaS implementation in brownfield terrestrial DWDM systems. Simple and straightforward solutions to characterize the service are provided alongside the novel Transparent Optical Overlay concept, enabled by Network Domain Interface Device. Due to the experimental nature of the derived concepts and verifications in live production networks, the contributions of the thesis enable the operators to take weighted decisions and measurable steps in implementing OSaaS in their production networks. As a result, higher network efficiency can be achieved, be it as easy as confidently allowing IP-over-DWDM traffic into the networks or interconnecting multiple networks and operator domains to implement end-to-end connectivity between geographically diverse datacenter locations. As a consequence, the terrestrial brownfield systems can be transformed into open disaggregated transport networks, capable of transporting modern, flexible, and future-proof service types as Optical Spectrum as a Service.

Lühikokkuvõte

Optilise spektri teenused avatud lainepikkustihendus võrkudes

21. sajandi ühiskond käsitleb pidevalt kättesaadavat lairibaühendust elutähtsa teenusena. Ilma selleta kas puudub või on häiritud juurdepääs elu osaks saanud rakendustele nagu Internet, digitaalsed andmebaasid, nõudmisel video-vood ja kõrgkvaliteetsed ühisedastusel põhinevad ülekanded, pilverakendused ja pidev juurdepääs asjade interneti platvormidele. Kui juurdepääsutehnoloogiate seas domineerib jõuliselt traadita side, siis ülekandevõrgud baseeruvad kiudoptilistel infrastruktuuril. Tõstmaks selliste võrkude sidemahtu ja efektiivsust, kasutavad sideoperaatorid 1990 aastate algusest lainepikkustihendusel põhinevat multipleksimise tehnoloogiat, mis võimaldab ühe infovoo asemel kasutada paralleeledastuse põhimõtet ning korraga ühes fiibripaaris edastada kümneid üksteisest sõltumatuid infovooge. Traditsiooniliselt kasutasid sellised edastussüsteemid süsteemi tootjate poolt toodetud transiivereid, mis lõpp-kliendi seadmelt saabuva optilise signaali elektriliseks konverteerisid, et signaal seejärel sobiva võimsuse ja lainepikkusega optilisse lainepikkustihendusel põhinevasse ülekandevõrku multipleksida. Selline toimimine tagab teenuse pakkumisel selged vastutuspiirid – teenuse pakkuja vastutab saja protsendiliselt teenuse toimivuse eest ning teenuse tarbija arve maksmise eest. Sellist turvalist edastusviisi on aga kõigutamas uued tehnoloogilised lahendused ümberkonfigureeritavate transiiverite näol (*Sliceable Bandwidth Variable Transceivers* (S-BVT)), lubades lõppkasutajale suuremat paindlikkust spektri kasutamisel ning operaatorile tulu ilma kallitesse transiiveritesse investeerimata.

Optilise spektri teenused erinevad fundamentaalselt klassikalistest mahupõhistest ülekandevõrgu teenustest, sest transiiverite valik ja opereerimine usaldatakse teenuse lõppkasutajale. Teenuse pakkuja vaid avab kokku lepitud spektri osa ülekandevõrgus, ning vastutab signaali optilise võimendamise eest vahevõimenduspunktides ning signaali ruutimise eest. Sellisel viisil saab lõppkasutaja ühe transiiveripaariga edastada infot üle tuhandete kilomeetrite, kui sama edastusspekter on saadaval kõikides läbitavates võrgusegmentides. Sellisel opereerimisel on mitmeid eeliseid klassikaliste teenuslahenduste ees, sest väiksem kogus vajalikke transiivereid vähendab kapitali investeeringute vajadust, energiatarbimist, vajab väiksemat hooldusmeeskonda transiiverite hooldamiseks ning vähendab peale seadmete eluea lõppu ka utiliseerimist vajavate seadmete hulka. Samas on uue teenusmudeli puhul ka hulgaliselt määramatust – kuidas teenust täpselt karakteriseerida, kuidas üheselt hinnata selle jõudlust ning kuidas hoida kliendilt saabuv mitmeid optilisi kandjaid sisaldav valgussiignal etteantud parameetrite piires.

Käesolev doktoritöö pakub juhendeid, kuidas Optilise Spektri Teenuseid lainepikkustihenduse võrkudes konfigureerida ning kirjeldab, kuidas erinevad konfigurtsioonid opereerimise keerukust mõjutavad. Töö pakub mõõtmistel põhineva lahenduse spektri teenuste jõudluse hindamiseks teenuse üle andmisel, kasutades kanali uurimise meetodit *(channel probing)*, kus teada olevate parameetritega valgussiignal sisestatakse lainepikkustihendusvõrgu spektrisse ning spektri kaugemas otsas oleva vastuvõtja abil hinnatakse vastuvõetud signaali kvaliteedi alusel kanali jõudlust.

Peamiseks jõudluse parameetriks selles töös on üldistatud signaali ja müra suhe *(Generalized Signal to Noise Ratio (GSNR))*, mis sisaldab endas kiudoptilise ülekandemeediumi, võrgukomponentide, kui ka saatja-vastuvõtja transiiveri poolt põhjustatud ebatäiuseid. Süstemaatiliselt mõõte-transiiveri kesksagedust muutes on võimalik salvestada *GSNR*-profiil, mis võimaldab usaldusväärselt määratleda lainepikkusest sõltuvad jõudluse erinevused, võimalikud filtreerimise kaod ja optiliste spektri teenuste opereerimise reziimi. Lisaks määrab töö laborikatsete abil minimaalsed teenuse marginaalid, mis tulenevad vahetute kõrvalsageduse aktiveerimisest ning maksimaalsest kanalite hulga aktiveerimisest sidesüsteemis. Marginaalide määramiseks lühiajaliste ja päevase kestusega teenuse jõudluse kõikumiste vastu kasutab töö statistilist standard hälvet, kasutades töös toodud näidetes pikaajalist teenuse jõudluse kauglugemise andmestikku. Lõpetuseks pakub töö lahenduse infrastruktuuri turvalisuse küsimustele, pakudes välja seadmetootja, domeeni, operaatori ja lainepikkustihendus tehnoloogiast sõltumatu võrgu domeeni liidese seadme *(Network Domain Interface Device (NeDID))*. NeDID sisaldab kõikehõlmavat funktsionaalsuste kogumit domeenidevahelise ühilduvuse tagamiseks, sisaldades nii seadet läbivate signaalide seire, kohandamise, kui ka kontrolli funktsioone. Tulenevalt uuest turvalisest spektri ressursside jagamise ja opereerimise võimekusest optiliste ülekandevõrkude füüsilisel tasemel pakub töö välja ka uue, läbipaistva optilise ülemkihi teenuskontseptsiooni *(Transparent Optical Overlay service model)*. Uue teenusekontseptsiooni baasil toob töö näiteid vähendatud seadmete hulga vajadusest mitme domeeni ja mitme operaatoriga võrkude keskkonnas, vähendades otseselt nii kapitali kui ka opereerimiskulusid, CO_2 emissioone üle teenuse eluea ning ka utiliseerimist vajavate seadmete hulka teenuse eluea lõpus. Lisaks kaudsete kulude minimeerimisele, mis on seotud hooldusmeeskonna töö korraldamisega võimaldab turvaline optilise spektri ressursi jagamine kaaluda teenuse pakkumist ka operaatorite seas, kellele sideteenuste pakkumine ei ole põhiärisuunaks. See suurendab võimalike varuteede hulka ükskõik millisele teenusele kahe lõpppunkti vahel ning avaldab seega positiivset mõju teenuse, võrkude ja digitaalsete platvormide kättesaadavusele.

Kokkuvõttena saab öelda, et käesolev doktoritöö pakub ülekandevõrkude operaatoritele mõõtmistel põhineva lahenduse senini optilise spektri teenuse rakendamist piiranud probleemidele. Spektri jõudluse kaardistamiseks kasutatav optilise valguskanali uurimise meetod võimaldab operaatoritel täpselt defineerida teenuse kvaliteet teenuse üle andmise hetkel ning läbipaistva optilise ülemkihi kontseptsioon koos NeDID seadmega pakub lahenduse füüsilise kihi probleemidele. Tulenevalt töö eksperimentaalsest käsitlusviisit saavad operaatorid pakutud kontseptsioone koheselt rakendada, et teha samme optilise spektri teenuse pakkumiseks oma ülekandevõrkudes, olgu teenuse pakkumise eesmärgiks kas kõrgem võrgu kasutusefektiivsus või turvalise IP-side võimaldamine üle lainepikkustihendusvõrkude. Kasutades töös pakutud meetodeid ning seadistamis-konfiguratsioone, on võimalik igast produktsioonis olevast maismaa ülekandevõrgust vormida avatud ülekandevõrk, mis võimaldab efektiivse ja tulevikukindla optilise spektri teenuse transporti.

Appendix 1

Publication I

Kaeval, K., Jansen, S.L., Fehenberger, T., Spinty, F., Grobe, K., Grieβer, H., Tikas, M., and Jervan, G., "Characterization of the Optical Spectrum as a Service", *Journal of Optical Communications and Networking*, Vol. 14, No. 5, (2022).

Characterization of the Optical Spectrum as a Service

KAIDA KAEVAL[1,2,*], SANDER LARS JANSEN[1], FLORIAN SPINTY[1], KLAUS GROBE[1], HELMUT GRIESSER[1], TOBIAS FEHENBERGER[1], MARKO TIKAS[3], GERT JERVAN[2]

[1] ADVA Optical Networking SE, Martinsried, Germany
[2] Tallinn University of Technology, Tallinn, Estonia
[3] Tele2 Estonia, Tallinn, Estonia
*Corresponding author: kkaeval@adva.com

Encouraged by the emerging disaggregation trend in optical transport networks, operators are willing to offer flexible and future-proof Optical Spectrum as a Service (OSaaS) instead of classical capacity services. To define this modern service in commercial offerings, a commonly accepted, reliable and easy-to-use service characterization method has to be developed. This is explicitly challenging in terrestrial brown-field, black-box scenarios, where Open Line System (OLS) data is unavailable or outdated to employ calculation or simulation-based methods. The objective of this work is to identify a characterization method that reliably captures wavelength-dependent performance variations, possible filtering penalties, and the operation regime of the optical spectrum services.

First, all OSaaS configuration options in the OLS are systemized into four primary configurations and their operational aspects are discussed. Then, two of the most used OSaaS configurations are tested in the lab and in a live network environment, providing links up to 5738 km in length. Generalized Signal To Noise Ratio (GSNR) profiles are captured with channel probing method, using a single-probe sweep and multiple simultaneous probes. Then, the accuracy and suitability of the Amplified Spontaneous Emission (ASE) loaded Optical Signal To Noise Ratio (OSNR) profile is tested in a lab environment. Finally, we discuss required time and hardware resources to characterize the service and bring out the pros and cons for each investigated profile. In conclusion, we propose a single-probe sweep as a reliable and easy-to-use method to characterize the OSaaS in terrestrial brown-field networks.

http://dx.doi.org/10.1364/JOCN.99.099999

1. INTRODUCTION

Regardless of how fast new fibre infrastructure is deployed, there will always be areas with scarce fibre resources that benefit from infrastructure sharing. Combined with the ever-growing need for capacity and continuous pressure to lower the cost per bit, service operators are impelled to innovate and implement new service models. Over the years, establishing connectivity between two end-points in the network has been possible through different service models [1]. Fig. 1 shows the different models for a service provider to provide connectivity to a customer. From the customer perspective, the simplest model is leased capacity, where the investments, operational aspects and service performance assurance are the responsibility of the service provider. At the other end of the responsibility scale lays dark fibre lease, where the service provider only provides rack space and guaranteed power along the fibre route. The customer is responsible for the whole network life-cycle from OLS system planning, commissioning and operation to upgrade or possible decommissioning. However, as the leased capacity model may not be cost effective, when high capacity is required, dark fibre may not be available for purchase. With the emerging disaggregation trend, enabled by the flex-grid technology and sliceable transceivers, Optical Spectrum as a Service (OSaaS) positions as an attractive service model to fill the gap on the responsibility scale.

Motivated by the potential to lower the investment and operational cost, OLS operators are ready to open up their networks for a wide range of configurations including capacity indefeasible rights of use (IRU), managed and unmanaged OSaaS [2-10]. While the infrastructure sharing is common in submarine systems [11-13], the implementation in terrestrial, brown-field systems requires additional attention starting from service characterization and ending with operational aspects.
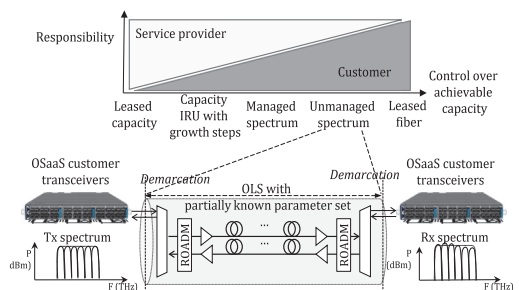

Fig 1. Service models with their responsibility distribution and OSaaS concept

In essence, an OSaaS is a transparent lightpath connecting two end-points in a single or multi-domain optical network. Differentiated from an alien wavelength service, it is capable of transporting multiple carriers over a predetermined spectrum slot. If the desired spectrum is continuously available in all included network segments, OSaaS can be operated over thousands of kilometres without signal regeneration at the domain end nodes. Avoiding unnecessary regeneration can provide significant benefits compared to traditional network architecture: reduced capital investments into the expensive transponder and demarcation equipment, reduced energy consumption, reduced requirements for human resources to maintain the service, and reduced electronic waste products and utilization costs at the end of the equipment lifetime.

Whereas in the managed OSaaS service model the end-customer has control over the transponder equipment selection, the operation of the transponders and OLS is performed by the service provider. In the unmanaged OSaaS service model, the end-user of the service is granted direct access to the portion of the optical spectrum in the OLS, which is limited with total usable power and power spectral density within the spectrum slot. This enables end-users to freely select and operate transceiver equipment, select desired networking margins and have complete control over the connectivity's life cycle from installation to decommissioning, without the need to operate and maintain the OLS. With sufficient operation margin [14], the customer can traverse transparently the complete end-to-end distance from core-to-core or core-to-access without the intermediate 3R regeneration at the domain borders. This not only avoids unnecessary regeneration, it also reduces the total number of active equipment and thereby reduces power consumption and increases reliability. However, this freedom for the end-customer increases the vulnerability of the OLS, which grows linearly with the portion of the third-party light inserted into the OLS spectrum.

To set the ground for the discussions in this paper, let us first navigate through the literature providing information about the historical evolution of spectrum services.

The first work in literature addressing the operation of third-party equipment over an OLS dates back to the early 2000s. Enabled by the so-called "black-link" approach, introduced in ITU-T recommendations G.695, G.698.1 and G.698.2 [15-17], various demonstrations were reported: optical fibre infrastructure sharing to enable triple-play services [18,19], IP-over-WDM [20-23] and alien wavelength services [24,25]. Reference [26] proposed a parameter set for an alien wavelength service and [27, 28] discussed the motivation and operational challenges for implementing alien wavelengths over an open Dense Wavelength Division Multiplexing (DWDM) system. Different switching modes for alien wavelengths with wavelength and waveband granularity were discussed in [29]. With the advent of flex-grid systems in the early 2010s, more effort was put into understanding the spectral transfer function [30], spectrum resource allocation [31,32], wavelength-dependent performance variations in the network [33,34] and security aspects [35] of alien wavelength services. To stress that the service model fits for various applications, alien wavelength services were also called photonic services [36-39]. In time, more focus was put on standardization efforts of the "black-link" [40-44], which represents the physical medium, or the media channel as per ITU-T recommendation G.872, introduced in October 2012 [45].

With the clear vision for disaggregated networking and motivated by the need to operate real-time applications over DWDM networks, the national research and education network (NREN) community has been continuously at the forefront of the developments of alien wavelength and alien spectrum services. Reference [46] lists many trials and experiments that investigate various aspects of alien services, from spectrum sharing between different NRENs to the development of advanced photonic services. Many transponder upgrade installations and achievable capacity demonstrations using new sliceable transceivers are actually alien wavelength configurations, as the transceivers were managed separately from the OLS system components [47-52]. With the increasing motivation to use alien wavelengths in production networks, disaggregated networking gains further traction. Various papers discuss the control and management questions over elastic, multi-vendor, multi-domain environments [53-57]. The dominant trend from fixed-grid networks towards elastic flex-grid networks triggers investigations in the spectrum assignment and routing domain [58-64]. Simultaneously, Quality of Transmission (QoT) estimations in a black-link scenario are investigated [65-73]. Several works also cover the architecture, topological use-cases, and requirements for such alien services [74-80], including the ITU-T recommendation G.807 [81] that defines the generic functional architecture of the optical media network. References [82-86] report multiple benefits and increased efficiency in using third party transponders over an existing OLS. Many papers discuss the implementations in terrestrial and submarine networks [87-90], including ITU-T recommendation G.977.1 [91], providing guidelines for physical layer specifications for DWDM applications on dispersion-unmanaged repeatered optical fibre submarine cable systems. However, the authors are not aware of any publications that aim to provide a systematic overview on the possible OLS configurations to formulate the lightpath for OSaaS nor how these configurations impact the performance of the alien wavelength, or optical spectrum in disaggregated network scenarios.

This paper aims to describe, systematize, and discuss the OLS configurations suitable for OSaaS service implementations in terrestrial, brown-field network scenarios and compare different options to characterize the service for commercial offerings. For characterization, three measurement-based methods are used: Amplified Spontaneous Emission based Optical Signal to Noise Ratio profiles, referred to as ASE-loaded OSNR profiles, and Generalized Signal to Noise Ratio (GSNR) based profiles, captured with a channel probing technique [71, 90], using a single-probe sweep and multiple-probe scenarios. Together with the data required for GSNR profile generation, the receive (Rx) power profile is also captured at the probing unit. However, as a stand-alone profile, the Rx profile is not considered suitable for OSaaS characterization as it does not allow to estimate the service performance and achievable capacity. GSNR-based profiles are captured in a production network environment, providing links up to 5738 km. Both GSNR profiles and ASE-loaded OSNR profiles are captured for the lab environment. Finally, the individual capability of each profile to satisfy the characterization requirements is evaluated based on the captured profiles.

The rest of the paper is organized as follows. Second chapter discusses service configuration options for OSaaS and their impact on performance and operational aspects. Based on customer expectations, this chapter also sets the requirements for OSaaS service characterization. The third chapter introduces the characterization methods and test setups used in this work. The fourth section provides the experimental results from the lab and production network for the GSNR profiles and compares them to the end-customer expectations to OSaaS characterization. The fifth section introduces results for ASE-loaded OSNR profiles, followed by the profile`s suitability analyses for OSaaS characterization. The sixth section discusses required time and hardware resources and compares the benefits of the available profiles. The last section provides conclusions and take-aways from this work.

2. OSAAS CONFIGURATION, CHARACTERIZATION AND OPERATION

As per ITU-T Recommendation G.807 [81], describing the generic functional architecture of the optical media network, the spectral slot or a lightpath allocated for the OSaaS is called a Media Channel (MC). Single or multiple MC-s form the primary building block(s) for OSaaS configurations. The wavelength service(s) inside the MC are referred to as Optical Tributary Signal(s) (OTSi). OTSi can be directly operated inside the MC, or alternatively a dedicated Network Media Channel (NMC) per OTSi can be configured. Although the OSaaS can be operated in all DWDM systems, the available service configurations depend on the add/drop architecture and ROADM technology used. In general, four OSaaS configurations exist. The overview of the OSaaS concept and the four primary configuration options for the transport of five 69-GBd OTSi is illustrated in Fig. 2.

The only configuration option available in fixed-grid networks or OLS systems using older ROADM technologies (not liquid crystal on silicon) and networks utilizing channelized dispersion compensation gratings (DCG) for chromatic-dispersion compensation is a narrow-band OSaaS (a). Although this configuration has been successfully used for alien wavelength services in the past, the configuration is not optimum for modern, variable symbol-rate transceivers. Modern transceivers, typically operated with symbol rates of 60 GBd or higher, may experience a narrowband filtering performance penalty on fixed-grid networks [70]. The benefits of high baud-rate transceivers are better utilized when colourless add/drop structures and dispersion-compensation-free OLS are used. Without any channelized component in the OLS, continuous spectrum as per OSaaS configurations (b), (c) and (d) can be provided to the end-user. In fixed-grid ROADMs, 50 GHz or 100 GHz channel spacing from ITU-T Recommendation G.694.1 [92] can be used to combine multiple adjacent MC-s into a wide-band OSaaS configuration (b). Flex-grid ROADMs can use any multiples of the 6.25 GHz increments to configure wide-band OSaaS (b), or allocate a single wide-band MC covering the full OSaaS bandwidth. Depending on the capabilities of the ROADM, MC can be equalized as per total signal power (configuration (c)) or power spectral density (PSD) (configuration (d)). However, the latter is used only in the newest OLS implementations.

As total signal power from alien carriers increases the vulnerability of the OLS system, it is important to have maximum control over the individual OTSi used within the OSaaS services. OSaaS configurations with adjacent narrow-band MC-s have a smaller power per MC and are therefore simpler to control and operate. Wide-band MC-s without intra-MC PSD-based equalization may lead to scenarios, where total
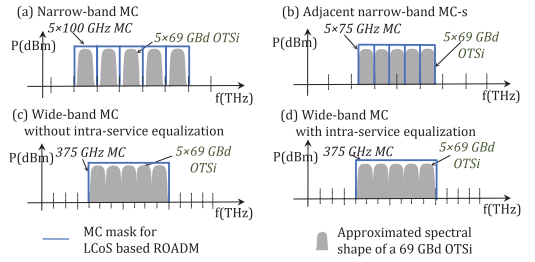

Fig 2. Four configuration options for OSaaS

dedicated power per MC is used on a single OTSi within the MC. This may cause spectral hole burning (SHB) or other effects that may impact the performance of the neighbouring spectral parts. However, with careful operations, wide-band configurations enable the implementation of various networking techniques, like GSNR-based signal pre-emphasis, low-margin networking [14], or flexible spectral allocation within the OSaaS service. As a downside, wide-band OSaaS configurations are more prone to wavelength-dependent performance variations. A single wide-band MC may incorporate a pronounced ripple or tilt effect from the EDFA and Raman gain spectrum, reaching up to 1 dB peak-to-peak ripple per span [93, 94]. This is especially evident on longer transparent links, where the OLS spectrum is not adjusted after each span [95]. The effect can lead to a large power ripple and tilt within the OSaaS bandwidth, resulting in performance variations. This will complicate the achievable capacity calculations within the OSaaS, as the GSNR required for that exercise is not constant over the service bandwidth. While a single MC with an intra-PSD PSD-based equalization scheme and multiple adjacent narrow-band MC-s in a flex-grid system would significantly suppress the ripple and tilt effect from the transmission medium, they may not get rid of the effect entirely.

While off-line QoT estimation tools or open-access initiatives target precise performance estimations [96-99], the calculations of the actual per-wavelength performance requires detailed knowledge on the underlying infrastructure and system components. This includes data about gain profiles of the amplifiers, polarisation-dependent loss and gain, filtering penalties, OLS channel allocation plan and load. This content is often unavailable or outdated. In addition, data describing the OLS design in great detail is mostly handled as business-sensitive information and hence not shared with the end-customers.

The motivation for OSaaS service characterization is to provide end-customers with up-to-date input for achievable capacity calculations

	ASE-loaded OSNR profile	Multiple-probe GSNR profile	Single-probe sweep GSNR profile
Example profiles from a 375-GHz OSaaS spectrum with 5×75 GHz configuration (b) and 1×375 GHz configuration (c)	Rx power of (b) — OSNR profile for (b) / Rx power of (c) — OSNR profile for (c)	◆ Multiple-probe GSNR profile for (b) / ◇ Multiple-probe GSNR profile for (c)	◆ Single-probe GSNR profile for (b) / ◇ Single-probe GSNR profile for (c)
Required equipment to record	Noise source, OSA	Multiple characterized PLT units	Single characterized PLT unit
Minimum resolution	As per Optical Spectrum Analyser	As per MC bandwidth	As per PLT unit bandwidth
Captured effects: - General accuracy - Wavelength dependent variations - Effective service bandwidth - NL regime	Dependent on OLS utilization Y Y N	Dependent on PLT configuration Y Y Y, when Rx power profile is available	Dependent on PLT configuration Y Y Y, when Rx power profile is available

Table 1 Available profiles and their capabilities to characterize OSaaS

over the OSaaS spectral slot without revealing business-sensitive data about the OLS system and its components. Together with the thresholds for secure operation, the OSaaS characterization includes:

- OSaaS service boundary frequencies,
- allowed power thresholds,
- accurate performance values for achievable capacity estimations within the spectrum slot,
- precise capture of the possible wavelength-dependent performance variations within the provided OSaaS bandwidth,
- precise indication of the effective service bandwidth and filtering penalty at the MC edges,
- presentation of possible nonlinear regimes within the provided OSaaS bandwidth.

To characterize the OSaaS, ASE-loaded OSNR profiles or GSNR profiles covering the whole OSaaS bandwidth can be used. While ASE-loaded OSNR profiles require ASE-noise generator and Optical Spectrum Analyser (OSA) to record, GSNR profiles rely on the availability of the characterized transceiver to use channel probing technique [71, 90]. With a single probing light unit (PLT), single-probe sweep method can be used, while multiple-probe scenario uses multiple simultaneously available PLT units to record the coarse GSNR profile. An overview of the profiles, required resources and their theoretical capabilities to characterize OSaaS are given in Table 1. For the use in service handover documentation, these profiles can be further complemented with a margin set to indicate possible degradations from daily and yearly performance fluctuations, network ageing or channel load changes.

3. TEST SETUP

To select the best method to characterize the OSaaS, in addition to the single-probe sweep explored in [67], in this work, also coarse multiple-probe GSNR profiles and an ASE-loaded OSNR profiles are investigated. To implement a stable measurement environment and avoid random fluctuations caused by changing environmental conditions, a test setup consisting of a 40 km ITU-T G.652D span and two ROADMs was set up in the lab. To evaluate the impact of the route length and the capability of the GSNR profiles to capture the wavelength-dependent performance variations from the OLS as well as the filtering penalty on service edges,

Lab set-up

Test-site **Long-haul production network**

Fig. 3 General test setup and assigned routes

Tele2 Estonia's long-haul flex-grid, Raman-enabled pan-European production network was used.

The OSaaS service topologies implemented in lab and production networks are shown in Fig. 3. Link acronyms, as given in the following figures, are combined from the link name and the looped length of the link. The signals for channel probing and ASE-loading were inserted through colourless add/drop, utilizing an 8:1 splitter for both, live and lab networks. Two variable optical attenuators (VOA) were used in the scheme – VOA-1 was used to enable and disable the ASE-load and VOA-2 was used to add noise to the OLS. To extend the transmission distance and to allow single-ended measurements at the test-site, the spectrum services were looped back at the add/drop port of the far-end ROADMs. OSaaS service configurations (b) and (c) from Fig. 2 were implemented in the OLS, providing five adjacent 75-GHz wide MC-s and a single 375-GHz wide MC, respectively. For equalization purposes, five 69-GBd OTSi were used, each configured to 200-Gbit/s 69-GBd DP-QPSK signal format. The PLT transmit (Tx) power per OTSi was set to 0 dBm. The ROADM Tx powers were set similarly for the lab and production network. -18.7 dBm Tx power per MC was used in a 5×75-GHz MC OSaaS configuration and - 11.7 dBm Tx power was used in a single 375-GHz MC OSaaS configuration. The underlying fibre infrastructure for the lab and production network segments conforms to the SSMF ITU-T 652.D standard.

All routes were then individually characterized with the GSNR profiles, utilizing the Inverse Back-to-Back (BtoB-1) method, following the guidelines from references [90, 91]. The test set-up was customized for OSaaS scenarios in brown-field terrestrial systems as per [71], and used a single-probe sweep and a coarse multiple-probe scenario, employing five probing light transceivers (PLT) located at central frequencies 193.800, 193.875, 193.950, 194.025 and 194.100 THz. Individual performance estimations are obtained by comparing the measured Q value from live networks to the Q-over-OSNR polynomial fitting of the PLT from the linear domain, and normalized to PLT symbol rate. The estimated SNR_{TOT} obtained from the BtoB-1 method can be defined as the ratio between the power of useful signal divided by the sum of the powers of all noise and impairment sources – such as ASE (SNR_{ASE}), nonlinear impairments (SNR_{NLI}), noise arising from the specific PLT unit modem technology used (SNR_{modem}), and other modem and line impairments from enabled neighbouring channels, narrow-band filtering or other (SNR_i), evaluated wholly in the signal bandwidth and expressed as:

$$\frac{1}{SNR_{TOT}} = \frac{1}{SNR_{ASE}} + \frac{1}{SNR_{NLI}} + \frac{1}{SNR_{modem}} + \frac{1}{SNR_i} (1).$$

As SNR_{TOT} accounts for all impairments, it allows the end-user to calculate achievable capacity over the link for the same modem type, even, if SNR_{modem} impairments are not separately evaluated. Hence, SNR_{TOT} in this work is used as the closest available approximation to the actual GSNR of the link.

In addition to the Q-value required for GSNR estimation, the optical receive (Rx) power from the system was captured for each recorded frequency for analyses of the operation-regime.

The PLT-s were implemented on an ADVA reconfigurable TeraFlex transceivers, providing 100 Gbit/s to 600 Gbit/s capacity per carrier by adjusting the modulation format and symbol rate. Both OSaaS configurations were characterized with 100-Gbit/s DP-QPSK 31.5-GBd and 200-Gbit/s DP-QPSK 69.4-GBd PLT configurations. Constant PSD was maintained in the system by adjusting the Tx power of the PLT. For the sweeping procedure described in [70], 12.5-GHz steps were used over the OSaaS spectrum, except for the service edges, where 6.25-GHz steps were employed for increased accuracy.

Finally, the suitability of the ASE-loaded OSNR profile was evaluated for the characterization of the OSaaS service. As ASE-loading on a 375-GHz OSaaS service would instantly allocate nearly 8% of the total end-
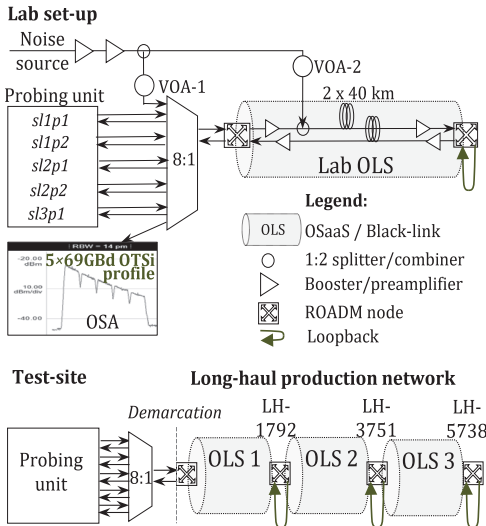
of-life power of the OLS, the test was carried out in a lab environment to avoid any unexpected impact to the live channels. High and low OSNR scenarios were investigated for 5×69-GBd OTSi and ASE-loaded OLS.

The initial setup for the lab tests was equalized with 5×69-GBd OTSi, each configured as a 200-Gbit/s 69-GBd DP-QPSK PLT. To enable ASE-loading, the OTSi-s were disabled and a variable optical attenuator (VOA-1) was enabled. The OLS was then re-equalized to regain -18.7 dBm and -11.7 dBm transmit Tx power in the ROADMs for 5×75-GHz and single 375-GHz MC OSaaS configurations. Then, a spectral image consisting of 16400 power samples in dBm over the full C-band was captured with an Optical Spectrum Analyser (OSA) for the ASE-loaded Rx profile (P_{TOT}), consisting of both, ASE power (P_{ASE}) and system noise component of the re-equalized OLS (N). This was followed by disabling the ASE loading and repeating the spectral image capture only for the respective system noise profile N. These two Rx profiles form the raw data for the ASE-loaded OSNR profile ($OSNR_{ASE}$) calculations as per (2). For P_{TOT}, the collected power samples were integrated over the 75-GHz MC effective signal bandwidth. To derive the OSNR for the commonly used reference bandwidth 0.1 nm [100], the power samples from the noise profile N were first integrated over the 0.1 nm (12.5 GHz) bandwidth ($N_{0.1nm}$) and a correction coefficient was used to obtain the total power over the media channel, to derive P_{ASE} from P_{TOT}. The $OSNR_{ASE}$ calculated per (2) is expressed in dB for reference bandwidth 0.1nm.

$$OSNR_{ASE} = \frac{P_{TOT} - \frac{75}{12.5} * N_{0.1nm}}{N_{0.1nm}} \quad (2).$$

After recording the ASE-loaded OSNR profiles for high and low OSNR scenarios, VOA-1 was disabled and 5×69-GBd OTSi PLT ports were enabled again. This was followed by the channel probing in the system. Finally, the system was equalized back to initial setup by using equalization with 5×69-GBd OTSi to attain the original default system configuration. Finally, channel probing was carried out to compare the performance difference caused by the ASE-loaded and 5×69-GBd OTSi loaded lab OLS equalization.

4. RESULTS FOR GSNR PROFILE CAPTURES

First, the GSNR and Rx power profiles were recorded in the lab and the production network for the single-probe sweep and multiple-probe scenarios.

Fig. 4 represents the results for OSaaS configurations (b) and (c), where the x-axis presents the central frequency of the PLT in THz over the spectral range of the OSaaS and the y-axes the estimated GSNR in dB. GSNR profiles recorded with single-probe sweep are illustrated by marker-line combinations. Solid lines mark the 5×75-GHz configuration, and dotted lines the single 375-GHz MC configuration. For both configurations, filled markers stand for a 200-Gbit/s DP-QPSK 69.4-GBd PLT configuration and unfilled markers for a 100-Gbit/s DP-QPSK 31.5-GBd PLT configuration. Coarse profiles, captured with multiple simultaneous PLT units are illustrated with coloured markers. The GSNR was estimated instantly after the OSaaS was equalized by a 5×69-GBd OTSi. For multiple-probe GSNR profiles, filled markers stand for a 5×75-GHz OSaaS configuration and empty markers for a 375-GHz configuration.

A. General accuracy of the GSNR profile

The first aspect we address is the accuracy of the GSNR profiles. As visible from Fig. 4, the variation between the profiles recorded with narrow-band and wide-band PLT configurations deviate up to 1.7 dB for the high OSNR lab setup, while it is less than 0.3 dB for the LH-1792 link and even less for two longer links on the production network. In addition, the 200-Gbit/s 69.4-GBd DP-QPSK PLT configuration is delivering higher GSNR estimations compared to its 100-Gbit/s 31.5-
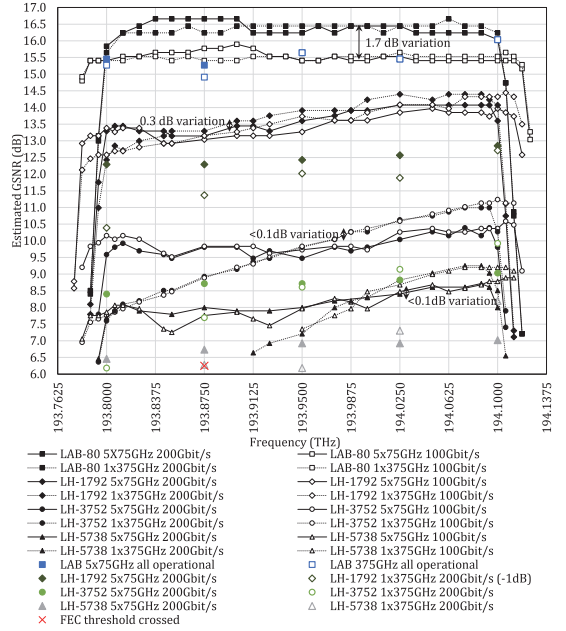

Fig. 4 GSNR profiles for the lab link and three long-haul production links

GBd DP-QPSK counterpart at high-OSNR links. To explain this, a separate measurement in the lab OLS was carried out by varying the VOA-2 attenuator to alter the effective OSNR of the link. For GSNR comparison purposes, constant Tx PSD was maintained during the measurements. Results from these measurements are illustrated in Fig. 5. The x-axis presents the OSNR of the lab OLS in dB, recorded under 0.1 nm reference bandwidth conditions by the digital signal processor (DSP) of the PLT unit, when configured as 200-Gbit/s DP-QPSK 69.4-GBd. As the perceived OSNR of the OLS varies with the PLT symbol rate, when the Tx PSD is kept constant, the values on the x-axis only present fixed conditions and noise loading of the OLS, and not the true OSNR of the lab link. For additional reference, the VOA-2 attenuation settings for noise loading in dB are presented on the secondary x-axis in dB. The y-axis present the estimated GSNR deviation in dB. Different lines correspond to characterized PLT configurations, colour-coded and grouped by the symbol rate. DP-P-16QAM stands for a proprietary partial-16QAM modulation format, used to transmit 3 bits per symbol (as 8QAM).

Less than 0.2 dB of variation was observed between the estimations available from three PLT configurations working at 16.9 dB of OSNR.
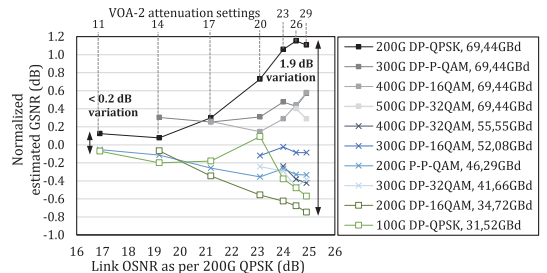

Fig. 5 GSNR estimations on various PLT and OLS OSNR configurations

For the 24.9 dB OSNR setting, the variation between the same three PLT settings grew to almost 1.9 dB. At the same time, the maximum Rx PSD deviation between the various PLT configurations fluctuated randomly between 0.3 and 0.7 dBm/GHz over the full OSNR range, showing no correlation with the increasing variation within the GSNR estimations. This lab exercise supports the test results from the live network, where the variation within GSNR estimation results, retrieved with different PLT configuration grows with link OSNR. The most probable reason for the high estimation variation at high OSNR can be accounted to the saturation regime of the high-symbol-rate PLT configurations at high signal quality, explained in detail in [90]. This is more likely to happen when operating a high-symbol-rate PLT configuration, as the implementation impairments and penalties of the PLT units flatten the Q-over-OSNR PLT characterization curves. This can introduce more than 10-fold change in the estimated GOSNR with only a marginal change in the Q-value. As the 200-Gbit/s 69.4-GBd DP-QPSK signal format is robust towards noise, its saturation OSNR is the lowest compared to other high symbol rate PLT configurations. Consequently, the primary challenge related to reliable GSNR profile capture is the selection of a suitable PLT configuration. Based on our work, we recommend the use of 200-Gbit/s 34.5-GBd DP-16QAM as PLT at high OSNR and 100-Gbit/s 31.5-GBd DP-QPSK as PLT at low OSNR for optimal performance in flex-grid networks. If only one PLT configuration is desired to perform the channel probing, 200-Gbit/s DP-P-16QAM is a good candidate due to its low required GSNR and relatively narrow signal bandwidth.

B. Wavelength-dependent variation over the OSaaS bandwidth

The second aspect under interest was to identify any wavelength-dependent variations within the tested OSaaS-s. Fig. 4 shows, that the flattest performance within the OSaaS spectrum is captured on the lab OLS. The estimation deviation for the same PLT configuration is ±0.15 dB around the mean estimated GSNR value over the OSaaS bandwidth, independent of the OSaaS configuration. This can be attributed to the EDFA only amplification scheme and relatively short link length in lab OLS. The links in the production network, however, were characterized with a pronounced GSNR variation over the OSaaS spectrum. The variation was explicitly evident for the single 375-GHz MC OSaaS configuration, reaching 2.5 dB for the shortest, 1792 km link, and up to 8.5 dB for the longest, 5728 km link. For our tested links, the GSNR variation aligned well with the slope of the recorded Rx power profile caused by the Raman gain profile. As the Raman pump power is transferred to lower frequencies in the spectrum, the ripple is defined by the pump locations in the spectrum. Areas between the pumps will have a smaller effective gain and hence experience higher effective span loss. This causes the signals to have a lower OSNR and, if operated in the linear regime, also lower GSNR. Due to this variation, the LH-5738 link has part of the spectrum working below the minimum required GSNR value for any modulation-format/symbol-rate combination to work and hence being unusable for data transmission. At the same time, the better performing part at the higher frequencies of the GSNR profile on LH-5738 link is flattened. This can be attributed to the optimum operation point on the link, as further explained in section 4D. In general, PSD-based intra-MC equalization, as in OSaaS configuration (d) should minimize the variation in the GSNR profile caused by the Raman gain spectrum. Unfortunately, this is a relatively new function and not available in many brown-field installations.

Regardless of the 5×75-GHz configuration, that should contribute to a better equalization over the 375-GHz OSaaS bandwidth, the impact of the ripple introduced by the Raman gain spectrum is still evident in the GSNR profile. In addition to that, the 5×75-GHz GSNR profile has distinguishable dips between the adjacent 75-GHz MCs. This is explicitly evident when probing with narrower PLT configurations. Fig. 6

explains the ripple formation based on PSD distribution in three locations on the ROADM link: equalized Tx PSD transmitted to-the-line (TTL) after the initial signal add, Rx PSD after the link and equalized Tx PSD TTL to the next ROADM link. As Rx PSD after the link is impacted by the intrinsic Raman gain profile on the line and the equalization of the spectrum only happens with the defined increments of the MCs, the 75-GHz dedicated spectral width in the 5×75-GHz configuration still has a pronounced tilt formation even within the MC. As the effective PLT bandwidth is swept over the full spectrum of the OSaaS, it still picks up the low-performing areas of the spectrum due to the power ripple caused by the Raman amplification. If the spectrum is swept with a high symbol rate PLT configuration, the dips in the spectrum are less distinguishable due to the broader bandwidth of the PLT configuration and hence a higher averaging effect. As the primary goal of the OSaaS characterization is to describe the spectrum as precisely as possible, narrower PLT configurations are preferred.

For both tested OSaaS configurations, the variation in the estimated GSNR recorded by the multiple-probe scenario follows the slope of the single-probe sweep profile. Deviations are primarily explained by different insertion losses from the add/drop structures that were not flattened by the equalization process in ROADMs. Compared to the GSNR values recorded by the single-probe sweep, the GSNR values recorded by the multiple-probe scenario are degraded due to enabled neighbouring channels. This can be attributed to linear and nonlinear crosstalk from neighbouring channels, mainly caused by the used 75-GHz spacing between the central frequencies of the OTSi, which is not optimal for the 69-GBd signals.

C. Effective service bandwidth

Another benefit of a narrow-band PLT configuration is the precise capture of the effective service bandwidth at the service edges. Fig. 4 showcases how the OTSi-s located at the OSaaS spectrum edges experience increased filtering penalty from the ROADM modules with increasing length of the route. When comparing the performance of central frequencies closest to the service boundaries (193.8 and 194.1 THz), we see that operation of a 200-Gbit/s DP-QPSK 69-GBd signal format experiences some penalties from the filtering already on the shortest live network link.

This is a known effect, and many works in the literature address this from different angles [101-103]. This penalty from narrow-band filtering results in a reduced GSNR estimation close to service boundaries, as the approximation of the GSNR in channel probing method accounts for all impairments from the transmission medium. Here, the simplicity of the channel probing can help to make weighted decisions on the OTSi configurations to be used at the service edges in a black-box scenario.
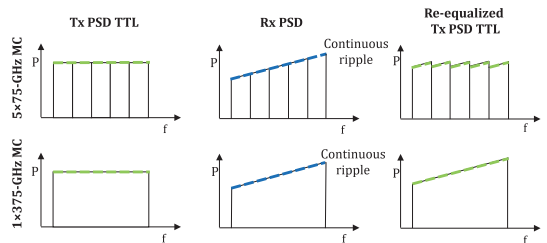

Fig. 6 Explanation of the dip formation

D. Operation regimes estimation

As mentioned in section 4B, it is possible to make assumptions on the operation regime when both, GSNR profile and Rx power, are recorded during the channel probing activity. Fig. 7 demonstrates these profiles using a 100-Gbit/s DP-QPSK PLT for OSaaS configurations (b) and (c) on link LH-3752. Similarly to Fig. 4, solid lines represent the 5×75-GHz configuration and dotted lines the 375-GHz MC configuration. Black lines mark the estimated GSNR values in dB, with a primary axis on the left, and green lines mark the recorded Rx power, presented as Rx PSD, with the values on the secondary axis (in dBm/GHz). Following both lines over the OSaaS bandwidth, presented on the x-axis, we expect to see a steady GSNR growth with increasing power when operating in the linear regime. However, we can see that starting from 194.00 THz, further growth in power does not introduce the same increase in GSNR. This indicates that the link under test operates around the optimum power. However, for our tested long-haul links, there was no change in the operation regime, where the additional power would introduce a reduction in GSNR, indicating the nonlinear operation.
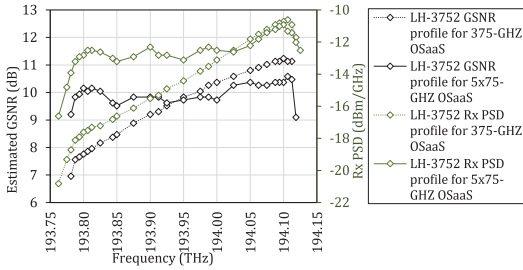

Fig. 7 Rx PSD vs GSNR profiles for the LH-3752 link

5. RESULTS FOR ASE-LOADED OSNR PROFILE CAPTURE

This section investigates the usability of the ASE-loaded OSNR profiles to characterize the OSaaS service. By varying VOA-2 of the lab setup, the OSaaS performance was evaluated at both high and low OSNR. Fig. 8 presents the Rx power (P_{Rx}) and system noise floor profiles for the lab OLS equalized with ASE-loading and 5×69-GBd OTSi. The x-axis present the frequency in THz, the primary y-axis the recorded power in dBm and the secondary y-axis the calculated OSNR in dB for the individual MCs under 0.1 nm reference bandwidth measurement conditions. High OSNR cases are marked with dark olive lines for the ASE-loaded Rx powers, and dark blue lines for the 69-GBd OTSi Rx powers, captured by the OSA. For low OSNR, bright green lines mark Rx powers recorded for ASE-loading, and bright blue lines the same for the 5×69-GBd OTSi loaded scenario. OSaaS configurations (b) and (c) were tested, marked with a solid line for the 5×75-GHz configuration and a dotted line for the 375-GHz OSaaS configuration. Black and grey lines present the OLS noise floor for high and low OSNR scenarios for ASE- and 5×69-GBd OTSi loaded systems.

A. General accuracy of the ASE-loaded OSNR profile

First, we analyse the accuracy of the ASE-loaded OSNR profile by comparing the results with a 5×69-GBd OTSi based OSNR profile. Although the captured Rx power profiles for the ASE and 5×69-GBd OTSi loaded measurements in Fig. 8 look similar, the variation is revealed when the respective OSNR profiles are calculated as per (2). Despite the same set-points per MC in the OLS ROADMs, the received PSD for the ASE-load and 5×69-GBd OTSi at the central frequencies is different. OSNR calculations as per (2) reveal that the slight power differences perceived in Rx powers adds up to 0.55 dB difference in calculated OSNR. This is demonstrated by the stand-alone OSNR
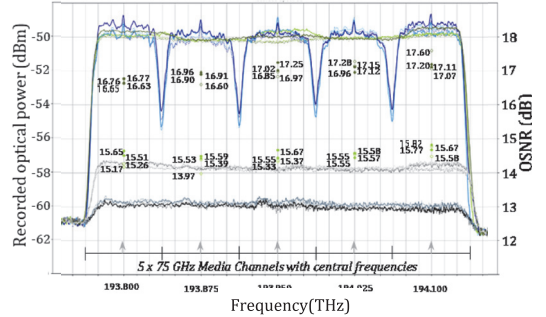

Rx profile for 5x75 GHz and 1x375 GHz, High OSNR, 5×69-GBd OTSi load
Rx profile for 5x75 GHz and 1x375 GHz, High OSNR, system noise
Rx profile for 5x75 GHz and 1x375 GHz, High OSNR, re-eq. ASE-load
Rx profile for 5x75 GHz and 1x375 GHz, High OSNR, re-eq. system noise
Rx profile for 5x75 GHz and 1x375 GHz, Low OSNR, 5×69-GBd OTSi load
Rx profile for 5x75 GHz and 1x375 GHz, Low OSNR, system noise
Rx profile for 5x75 GHz and 1x375 GHz, Low OSNR, re-eq. ASE-load
Rx profile for 5x75 GHz and 1x375 GHz, Low OSNR, re-eq. system noise
♦ ◇ OSNR of the 5x75 GHz and 1x375 GHz, High OSNR, 5×69-GBd OTSi load
● ○ OSNR of the 5x75 GHz and 1x375 GHz, High OSNR, re-eq. ASE-load
♦ ◇ OSNR of the 5x75 GHz and 1x375 GHz, Low OSNR, 5×69-GBd OTSi load
● ○ OSNR of the 5x75 GHz and 1x375 GHz, Low OSNR, re-eq. ASE-load

Fig. 8 P_{Rx} and OSNR profiles for ASE and 5×69-GBd OTSi loaded OLS

markers in Fig. 8. Dark olive bullets mark the OSNRs per-MC based on the ASE-loading and dark olive diamonds mark the calculated OSNRs per MC based on the 5×69-GBd OTSi load. Filled markers stand for OSNR calculations for the 5×75-GHz OSaaS configuration and transparent markers for the 1×375-GHz OSaaS configuration. The primary cause for this deviation is the flat shape of the ASE-load and used 0.19 roll-off factor of the 69-GBd OTSi.

Additional bias from the designed OLS performance may be introduced by the system equalization with ASE noise. Fig. 9 compares the estimated Generalized OSNRs (GOSNRs) for the same lab OLS equalized with ASE-loading and 5×69-GBd OTSi. Similarly to OSNR, the GOSNR is expressed in dB per 0.1 nm noise bandwidth. Based on our test results, the GOSNR of the lab OLS equalized with ASE-loading is approximately 1.75 dB better for the low OSNR and 1.20 dB better for the high OSNR scenario compared to the lab OLS equalized with 5×69-GBd OTSi. As the signal shape of the ASE-loading and OTSi is different, the Wavelength Selective Switch (WSS) within the ROADM may adjust differently in ASE-loaded and OTSi-loaded equalization. This results in biased performance when the ASE-load is switched to the OTSi load in the service production phase. For example, when the ASE-load fixes the WSS to a lower attenuation, the switch from ASE-load to OTSi in service production phase may saturate the amplifiers if OLS is fully utilized with channels.
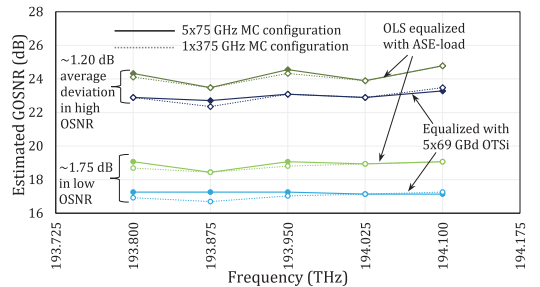

Fig. 9 Estimated GOSNR from channel probing for lab OLS equalized with ASE-load and 5×69-GBd OTSi

The inability to assure correct design-based Tx powers per MC after the ROADM equalization impacts also the multiple-probe scenario. Increased insertion losses from the add/drop structures may hinder the equalization process in the ROADMs. Channels not meeting their design based Tx powers may be therefore transmitted to the line with lower Tx powers. To avoid degraded performance it may cause, amplification right after the add/drop structures to compensate for any insertion losses is recommended.

Lastly, the calculated OSNR values, retrieved with ASE-loaded OSNR profiling method, are 17.0 dB and 15.3 dB under 0.1nm reference bandwidth measurement conditions for our high and low OSNR use-cases. These deviate remarkably from the 23.0 dB and 17.1 dB GOSNR values, estimated under same conditions by the channel probing for the same lab OLS configurations. This bias can be attributed to the amplifier operation point, power distribution, and gain profile changes, but also to spectral hole burning, when large amounts of signal power are switched off in the spectrum to record the system noise floor. Similar bias can be introduced in live networks, where the OLS spectrum is underutilized. Apart from under-utilization, the accuracy of ASE-loaded OSNR profiles can be impaired by power adjustment algorithms of the OLS. These algorithms readjust the power levels according to the total power at the amplifier output port or any other point in the OLS, creating the bias in the OSNR profile. Only short-term power transients do not play a critical role in the OSNR profile capture, when sufficient amount of measurement iterations are performed for averaging.

Overall it can be concluded that while ASE-loaded OSNR profile is a suitable characterization method in theory, there are many practical challenges in the implementation. While the ASE loading process can be improved by increasing the noise power gradually to reduce the impact to live traffic on the OLS, the accuracy of this method is impaired by too many variables to be considered as a reliable characterization method for an OSaaS implemented in the underutilized OLS systems.

B. Wavelength-dependent variation, effective service bandwidth and operation regimes estimation

Although the accuracy of ASE-loaded OSNR profile does not position it as a first choice for OSaaS characterization, let us review the suitability of this method to cover the remaining set of OSaaS characterization requirements.

First, we review the wavelength-dependent performance variations. Similarly to the single-probe sweep, ASE-loaded OSNR profile only covers the wavelength-dependent performance variations induced by the ROADMs and OLS, as the ASE-loading is performed through a single port in the add/drop structures.

Secondly, we focus on the effective service bandwidth. Fig. 8 shows that the shape of the ASE-load and the 5×69-GBd OTSi are slightly cut by the OSaaS service edge for the MC with central frequency at 193.8 THz. This may also be the cause for the lowest recorded OSNR compared to other MC-s within the OSaaS service. Due to the granularity of the ROADMs, the OTSi-s are not always perfectly symmetrically positioned over the spectrum, and this may result in uneven performance on two service edges. The precise detection of the effective service bandwidth is the primary benefit of the ASE-loading and the respective Rx power profile. However, calculating the OSNR as per (2) will average out some of the useful data from the raw Rx power data in addition to possibly biased OSNR estimations based on 5.A.

Lastly, the ASE-loaded method is only providing the linear OSNR component of the OLS performance. As knowledge about the nonlinear component helps the optimum operation power selection, specifically in long-haul systems spanning thousands of kilometres, the OSNR profile alone does not enable to estimate if the carriers within OSaaS are transmitted in linear or non-linear operation regime. Furthermore, the OSNR profile alone does not enable to directly estimate the achievable

capacity within the spectrum slot, that is one of the primary goals for OSaaS characterization, as it requires accounting for both, the linear and nonlinear components of the OLS performance .

6. DISCUSSION

The primary characterization of the OSaaS is carried out before the service handover and very often in the purchase phase of the service. From the operational perspective, characterization completed with minimum time, manpower and special equipment requirements is preferred, when all characterization requirements from Chapter 2 are met.

Considering, that the time to install PLT units for channel probing or EDFA-s for ASE-loading at site are similar for all three characterization methods proposed in this paper, the method that takes the longest to measure is the single-probe sweep. As only one characterized PLT transceiver is used, each measurement point in the spectrum needs time for power-on delay, DSP stabilization and averaging. The time constraints required for automated GSNR profile measurement are defined by:

$$t_{\text{req}} = \frac{BW}{f_{\text{req\_stepmin}}} * \left(t_{f_{\text{change}}} + t_{\text{stab}} + t_{\text{read}} \right) \ (3),$$

where BW is the MC bandwidth in GHz, $f_{\text{req\_stepmin}}$ is the frequency increment of the sweep in GHz, $t_{f_{\text{change}}}$ is the power-on delay after a frequency change in seconds, t_{stab} is the stabilization time after the frequency change in seconds, and t_{read} the reading time in seconds to minimize random fluctuations. Using the smallest frequency increment and accounting 60 seconds for $t_{f_{\text{change}}}$, t_{stab} and t_{read}, the GSNR profile characterization of a 375-GHz MC service would take 50 minutes. Compared to 24-hour bit-error-ratio (BER) test, which is generally required for handover of capacity-based services, this is remarkably shorter. However, compared to capturing optical time domain reflectometer (OTDR) traces required for leased fibre handover documentation, the 50-minute probing time counts as long. To reduce probing times, $f_{\text{req\_stepmin}}$ can be increased at the central area of the MC if a single wide-band MC configuration is used for OSaaS.

When multiple PLT units are available, the OSaaS service can be characterized with decreased granularity. In this case, with a single PLT configuration, the characterization data with a 75-GHz granularity can be retrieved in less than a minute, considering the simultaneous reading from all PLT units. However, this characterization would miss the possible dips between the adjacent MC edges, unless each of the PLTs is swept simultaneously from one edge of the MC to the other, collecting the GSNR data over the full spectrum. With this, the multiple-probe scenario has the potential to provide data about the various insertion losses from the add/drop structures as well as the full spectral profile, with reduced time requirements compared to single-probe sweep. Most importantly, it provides information about the magnitude of the GSNR degradation induced by enabled neighbouring channels. However, as the method requires multiple PLT-s for the characterization, it comes as a disadvantage in case the hardware is not available. For the future, the authors propose to use multi-carrier transceivers to characterize the OSaaS service, if the sub-carrier performance can be individually characterized and later used for channel probing. In this case, the narrow-band subcarriers would allow precise evaluation of the wider spectrum chunks in one probing activity.

The quickest approach to characterize the OSaaS would be to capture the ASE-loaded OSNR profile with noise generation equipment and an optical spectrum analyser. The time constraints required to capture both, the ASE-loaded Rx power and the system noise floor are around 1 minute. The calculation of the $OSNR_{ASE}$ profile is then performed as per (2). This may take additional time as the data needs to be read out from the equipment and processed accordingly. Similarly to the GSNR

profiles, the ASE-loaded OSNR profile captures a moment in the network, and daily changes or component ageing in the networks will impact the accuracy of the profile. As per our investigations, the OSNR profile in a lightly loaded DWDM systems may be highly impacted by the changes in the amplifier operation point or ROADM equalization. Therefore, a deviation between the expected performance based on characterization data and actual OLS performance may occur.

Regarding the profiles abilities to capture desired OSaaS characteristics, listed in Chapter 2, each profile had some benefits and shortfalls. As for the accuracy, the most accurate performance over the spectrum is provided by the multiple-probe GSNR profile, as it also includes the neighbouring-channel impact. However, this profile needs multiple PLT units to record, which may not be easily available. The best overview of the wavelength-dependent variation is provided by a single-sweep GSNR profile, as it includes the continuous performance estimations for the entire OSaaS spectrum. The neighbouring-channel impact here can be estimated by margins. As the ASE-loaded Rx profile is captured with the high-resolution OSA, it provides the highest resolution compared to any other profile and is therefore the best candidate to describe the physical filtering of the spectrum slot. From this perspective, the ASE-loaded Rx profile is also the best in capturing small OLS performance variations within the MC bandwidth, such as power dips, ripple or tilt. However, this data is mostly averaged out when the normalized OSNR is calculated.

From the precision perspective and general fulfilment of the OSaaS characterization requirements, GSNR profiles are better candidates for OSaaS service description despite the longer time-frames needed for profile recording. As hardware availability is often the limiting factor, the sweep-based GSNR profile is probably the most interesting algorithm for service providers, delivering the required characterization for OSaaS with minimum hardware requirements.

7. CONCLUSIONS

Over the recent years, Optical Spectrum as a Service (OSaaS) has become an attractive service model for customers demanding high capacity, future proof network resources. For implementation, various configuration options exist. To allow service quality and performance estimations in the purchase phase or before service handover, a reliable service characterization method is required. In black-box scenarios, where vendor-specific planning tools and software-based QoT estimation tools lack information about the OLS implementation, OLS-independent GSNR and power profiles can be used to characterize the service.

In this paper, we have systemized the service configurations and discussed their impact on the service operation from both customer and OLS operator viewpoints. We have proposed three service characterization profiles to capture the wavelength-dependent variations in the spectrum, the filtering penalty at the service edges and the operation regime within the OSaaS service. We have tested the profiles in the lab environment and on a long-haul production network and analysed their pros and cons in describing the relevant OSaaS performance aspects. In addition, we have reviewed the measurement time required for each individual method.

In summary, we have proposed the GSNR profile with a single-probe sweep as the simplest solution to describe the required aspects of the service. The proposed characterization has great potential to simplify network planning in disaggregated environments. Especially in the purchase and pre-handover stages this method will enable accurate throughput estimations at any part of the spectrum [104].

Further benefits of the OSaaS characterization with GSNR profiles include automated path calculations in low-margin networks for service re-routing or restoration. However, it should be noted that some additional margin is required to overcome possible GSNR degradations from neighbouring channels and network aging. In future systems, continuous probing in combination with machine learning algorithms can be used to continuously monitor performance deviations compared to the OSaaS characterization in hand-over documentation. This would allow operators and end-users to detect possible performance degradations caused by aging or changes in the OLS utilization and take relevant actions to avoid any loss of transported data.

References

1. S. Buscaglione, "GÉANT infrastructure evolution under GN4-3N," in TERENA Networking Conference (TNC) (2021).
2. OpenReach, (2012), "Openreach launches Optical Spectrum Access service with ADVA Optical Networking gear," press release (January 30th, 2012).
3. K. Grobe, C. Fürst, A. Autenrieth, and T. Szyrkowiec, "Flexible spectrum-as-a-service," in TERENA Networking Conference (TNC) (2014).
4. R. Velc, R. Vohnout, J. Vojtěch, P. Škoda, B. Belter, P. Ridlichowski, and C. Tziouvaras, "Pre-Commercial Procurement in Optical Networking domain," In 18th International Conference on Transparent Optical Networks (ICTON) (2016), pp. 1-4.
5. H. Wessing, K. Bozorgebrahimi, J. Vojtech, P. Skoda, and E. Camisard, Deliverable D13. 1 Research and Study Network Technologies—White Paper, 2016.
6. A. Colmenero, A.M.F. DTU, D.C. Mur, D. Schmitz, F. Panken, H.Y. DTU, I. Demirkol, K. Boudjemaa, R. Tuminauskas, R. Smets, and Z. Ołtuszyk, Deliverable D13. 2 Blueprint of Services and Research Plan for Future Work, 2016.
7. Colt, (2018), "Colt Spectrum brings cost effective Dark Fibre alternative to ultra-high bandwidth customers", press release, 08/05/2018
8. L. Fischer; J. Qvist, "Spectrum Sharing for Next Generation Networks", Technology Exchange Conference (2019)
9. ADVA, (2020), "ADVA unlocks network potential with spectrum as a service," press release (March 12th, 2020).
10. GEANT, (2021), "Moldovan and Ukrainian R&E communities benefit from new 'spectrum' link with GÉANT", press release, 04/10/2021.
11. Rcrwireless, (2019), "Consortium selects Alcatel Submarine Networks to deploy Indigo subsea system," press release (April 6th, 2017).
12. ESI Africa, (2019), "Submarine cable to deepen telecom infrastructure in West Africa," press release (Oct 4th, 2019).
13. Ciena, (2021). "Telxius offers managed spectrum on Dunant and Marea powered by Ciena," press release (April 7th, 2021).
14. Y. Pointurier, "Design of low-margin optical networks", Journal of Optical Communications and Networking, 9(1), pp.A9-A17 (2017).
15. "Optical interfaces for coarse wavelength division multiplexing applications," https://www.itu.int/rec/T-REC-G.695/en.
16. "Multichannel DWDM applications with single-channel optical interfaces," https://www.itu.int/rec/T-REC-G.698.1/en.
17. "Amplified multichannel dense wavelength division multiplexing applications with single channel optical interfaces," https://www.itu.int/rec/T-REC-G.698.2/en.
18. A. Atieh, P. Perez, R. Andrew, and F. Sheikh "More services, less fiber: The commercial and network architecture impact of a black-link approach to the sharing of optical fiber infrastructure for the

deployment of triple play services," Proc. SPIE 6022, Network Architectures, Management, and Applications III, 60220C (2005).

19. A. Atieh, P. Perez, R. Andrew and F. Sheikh, "A "black-link" approach for sharing optical fiber infrastructure and enabling multi-services," 2006 Optical Fiber Communication Conference and the National Fiber Optic Engineers Conference, 2006, paper JThB98.

20. D. Ventorini, E. Moura, L. Paraschis, O. Gerstel, M. Silva, K. Wollenweber, A.J. Silvério, P. Prado, H. Júnior, L. Augusto, L. and C.H. Silva, "Demonstration and evaluation of IP-over-DWDM networking as "alien-wavelength" over existing carrier DWDM infrastructure, " in National Fiber Optic Engineers Conference, 2008, paper NME3.

21. P. R. Morkel, A. Färbert, A. Schwandner, G. Schubert, G. Rozensweig, J. J. Maki, A. Hotchkiss, M. Ding, G. Sun, and S. ElAhmadi, "Integrated IP-Optical Networks. Demonstration of DWDM Router-to-Router IP Transport Over 574 km SMF Fiber Link Using 11.1 Gbit/s OTN Pluggable Interface with Integrated G.709 and FEC," in Optical Fiber Communication Conference/National Fiber Optic Engineers Conference, 2008, paper NME4.

22. S. Harren, M. Kayser, E. Klaproth, T. Hallan, A. Hotchkiss, S. Nathan, S. ElAhmadi, and S. N. ElAhmadi, "Elimination of DWDM Transponders over a Deployed IP over DWDM Network Using Novel DWDM XFP Transceivers with Integrated G.709 and Forward Error Correction," in Optical Fiber Communication Conference and National Fiber Optic Engineers Conference, 2009, paper NThF4.

23. V. Vraciu, O. Rusu, P. Gasner, and M. Bărbulescu, "100 Gbps alien wavelength installation in a production DWDM network," in RoEduNet Conference 13th Edition: Networking in Education and Research Joint Event RENAM 8th Conference, 2014, pp. 1-4.

24. K. Slavicek and V. Novak, "Introduction of alien wavelength into CESNET DWDM backbone," in 6th Int. Conf. on Information, Communications and Signal Processing, 2007, pp. 1-5.

25. R. Nuijts and L. Lange Bjørn, "40 Gb/s alien-wavelength experiment over 1000 km of G.655 (TWRS) transmission fiber between Amsterdam and Copenhagen," in TERENA Networking Conference, 2010.

26. D. Z. Chen and M. F. Lane, "Emerging Network Need for Alien Wavelength Management," in Optical Fiber Communication Conference and Exposition and The National Fiber Optic Engineers Conference, 2007, paper NTuD5.

27. O. Gerstel, R. Cassata, L. Paraschis, and W. Wakim, "Operational Solutions for an Open DWDM layer," in Optical Fiber Communication Conference and National Fiber Optic Engineers Conference, 2009, paper NThF1.

28. S. Melle, G. Bennett, C. Liou, C. Villamizar, and V. Vusirikala, "Alien wavelength transport: an operational and economic analysis," in National Fiber Optic Engineers Conference, 2009, paper NThF2.

29. R.S. Tucker, R. Parthiban, J. Baliga, K. Hinton, R.W. Ayre, and W.V. Sorin, "Evolution of WDM optical IP networks: A cost and energy perspective," Journal of Lightwave Technology, 27(3), pp.243-252, 2009.

30. N. Amaya, I. Muhammad, G.S. Zervas, R. Nejabati, D. Simeodinou, Y.R. Zhou, and A. Lord, "Experimental demonstration of a gridless multi-granular optical network supporting flexible spectrum switching," in Optical Fiber Communication Conference and Exposition and the National Fiber Optic Engineers Conference, 2011 , pp. 1-3.

31. M. Jinno, B. Kozicki, H. Takara, A. Watanabe, Y. Sone, T. Tanaka, and A. Hirano, "Distance-adaptive spectrum resource allocation in spectrum-sliced elastic optical path network [topics in optical communications]," IEEE Communications Magazine, 48(8), pp.138-145, 2010.

32. Y. Wang, X. Cao, Q. Hu and Y. Pan, "Towards elastic and fine-granular bandwidth allocation in spectrum-sliced optical networks," Journal of Optical Communications and Networking, vol. 4, no. 11, pp. 906-917, 2012.

33. N. Amaya, M. Irfan, G. Zervas, K. Banias, M. Garrich, I. Henning, D. Simeonidou, Y.R. Zhou, A. Lord, A., K. Smith, and V.J.F. Rancano, "Gridless optical networking field trial: flexible spectrum switching, defragmentation and transport of 10G/40G/100G/555G over 620-km field fiber," Optics express, 19(26), pp.B277-B282, 2011.

34. O. Gerstel, M. Jinno, A. Lord, and S. J. B. Yoo, "Elastic optical networking: A new dawn for the optical layer?," IEEE Communications Magazine, vol. 50, no. 2, pp. s12–s20, 2012.

35. K.I. Kitayama, M. Sasaki, S. Araki, M. Tsubokawa, A. Tomita, K. Inoue, K. Harasawa, Y. Nagasako, and A. Takada, "Security in photonic networks: Threats and security enhancement," Journal of Lightwave technology, 29(21), pp.3210-3222, 2011.

36. J. Vojtěch, V. Smotlacha, S. Šíma and P. Škoda, "Photonic services," in 14th International Conference on Transparent Optical Networks (ICTON), pp. 1-4, 2012.

37. J. Vojtech, V. Smotlacha, P. Skoda, S. Sima, J. Radil and M. Hůla, "Photonic services enables real-time applications over long distances," 3rd International Conference on Photonics, 2012, pp. 231-234.

38. J. Vojtech, V. Smotlacha, P. Skoda, A. Kuna, M. Hula, and S.Sima, "Photonic services, their enablers and applications," Proc. SPIE, vol. 8516, 85160H, 2012.

39. L. Altmanová, "Photonic services: Challenge for users and for networkers," the GN3 project report, 2013.

40. R. Kunze, "A framework for Management and Control of optical interfaces supporting G.698.2," Internet Engineering Task Force Internet-Draft, 2011.

41. A. Lord, P. Wright, and Y. R. Zhou, "Alien waves: technology, benefits and standardization," in International Conference on Photonics in Switching (PS), 2012, pp. 1-3.

42. M. Gunkel, A. Mattheus, A. Napoli, G. Meloni, F. Fresi and T. Rahman, "Elastic Black Link for future vendor independent optical networks," Optical Fiber Communications Conference and Exhibition (OFC), 2015, pp. 1-3.

43. M. Gunkel, A. Mattheus, F. Wissel, A. Napoli, J. Pedro, N. Costa, T. Rahman, G. Meloni, F. Fresi, F. Cugini, N. Sambo, and M. Bohn, "Vendor-Interoperable Elastic Optical Interfaces: Standards, Experiments, and Challenges [Invited]," Journal of Optical Communications and Networking, 7(12), B184-B193, 2015.

44. R. Kunze, E.G. Grammel, D. Beller, E. Galimberti, and J. Meuric, "A framework for management and control of DWDM optical interface parameters," IETF draft-ietf-ccamp-dwdm-if-mng-ctrlfwk-06, 2017.

45. "Architecture of optical transport networks," https://www.itu.int/rec/T-REC-G.872-201210-S/en

46. H. Wessing, P. Skoda, M.N. Petersen, A. Pilimon, P. Rydlichowski, G. Roberts, R. Smets, J. Radil, J. Vojtech, R. Lund, Z. Zhou, C. Tziouvaras, and K. Bozorgebrahimi, "Alien Wavelengths in National Research and Education Network Infrastructures Based on Open Line Systems: Challenges and Opportunities," Journal of Optical Communications and Networking. 11, 118-129 (2019).

47. Y.R. Zhou, K. Smith, M. Wilkinson, R. Payne, A. Lord, T. Bennett, and M. Frankel, "Coherent 100G field trial over installed fiber links: Investigating key network scenarios and applications," Journal of Optical Communications and Networking, 4(11), pp.B35-B41, 2012.

48. A. M. Fagertun, S. Ruepp, M. N. Pedersen, and B. Skjoldstrup, "Field Trial of 40 Gb/s Optical Transport Network using Open WDM Interfaces," in 18th OptoElectronics and Communications Conference held jointly with 2013 International Conference on Photonics in Switching, 2013, paper TuPQ_5.

49. Y. R. Zhou, K. Smith, R. Payne, A. Lord, G. Whalley, T. Bennett, E. Maniloff, S. Alexander, and D. Boymel, "Real-Time Gridless 800G Super-channel Transport Field Trial over 410km Using Coherent DP-16 QAM," in Optical Fiber Communication Conference, 2014, paper Tu2B-3.

50. Y. R. Zhou, K. Smith, R. Payne, A. Lord, L. Raddatz, M. Bertolini, T. Van De Velde, C. Colombo, E. Korkmaz, M. Fontana, and S. Evans, "1.4Tb Real-Time Alien Superchannel Transport Demonstration over 410km Installed Fiber Link Using Software Reconfigurable DP-16QAM/QPSK," in Optical Fiber Communication Conference: Postdeadline Papers, 2014, paper Th5A.9.

51. Y. R. Zhou, K. Smith, R. Payne, A. Lord, J. Hopewell, J. Weatherhead, J. Chen, J. Yao, W. Liu, C. Zhao, Y. Xiong, Z. Xiao, and P. Du, "Field Demonstration of up to 3Tb/s Real-Time Superchannel Transport over 359km Using a Fully Managed Flexible Grid Infrastructure with Net Spectral Efficiency of 5.97bit/s/Hz," in Optical Fiber Communication Conference, 2015, paper Tu3H.4.

52. Y. Loussouarn, E. Pincemin, M. Song, S. Gauthier, Y. Chen, and Z. Shengqian, "400 Gbps Real-Time Coherent Nyquist-WDM DP-16QAM Transmission over Legacy G.652 or G.655 Fibre Infrastructure with 2 dB Margins," in Optical Fiber Communication Conference, 2015, paper W3E3.

53. M. Channegowda, R. Nejabati, M. Rashidi Fard, S. Peng, N. Amaya, G. Zervas, D. Simeonidou, R. Vilalta, R. Casellas, R. Martínez, R. Muñoz, L. Liu, T. Tsuritani, I. Morita, A. Autenrieth, J.P. Elbers, P. Kostecki, and P. Kaczmarek, "Experimental demonstration of an OpenFlow based software-defined optical network employing packet, fixed and flexible DWDM grid technologies on an international multi-domain testbed," Optical Express 21, 5487-5498, 2013.

54. P. Layec, A. Morea, F. Vacondio, O. Rival and J. Antona, "Elastic optical networks: The global evolution to software configurable optical networks," in Bell Labs Technical Journal, vol. 18, no. 3, pp. 133-151, 2013

55. A. Martinez, M. Yannuzzi, V. Lopez, D. Lopez, W. Ramirez, R. Serral-Gracia, X. Masip-Bruin, M. Maciejewski, and J. Altmann, "Network management challenges and trends in multi-layer and multi-vendor settings for carrier-grade networks," IEEE Communications Surveys & Tutorials, 16(4), pp.2207-2230, Fourthquarter 2014.

56. F. Cugini, N. Sambo, F. Paolucci, F. Fresi and P. Castoldi, "Adaptation and monitoring for elastic alien wavelengths," 21st European Conference on Networks and Optical Communications (NOC), 2016, pp. 82-87.

57. F. Paolucci, N. Sambo, F. Cugini, and P. Castoldi, "Demonstration of effective OAM for alien wavelength and transport network," in Optical Fiber Communication Conference, 2017, paper W2A.31.

58. E. Palkopoulou, I. Stiakogiannakis, D. Klonidis, K. Christodoulopoulos, E. Varvarigos, O. Gerstel, and I. Tomkos, "Dynamic cooperative spectrum sharing in elastic networks," in Optical Fiber Communication Conference and Exposition and the National Fiber Optic Engineers Conference, 2013, pp. 1-3.

59. L. H. Bonani, A. dos Santos Tozetti, F. Callegati and W. Cerroni, "Routing issues on spectrum sharing and partitioning for flexible optical networks," 16th International Conference on Transparent Optical Networks (ICTON), 2014, pp. 1-4

60. S. Talebi, F. Alam, I. Katib, M. Khamis, R. Salama, and G.N. Rouskas, "Spectrum management techniques for elastic optical networks: A survey," Optical Switching and Networking 13, pp.34-48, 2014.

61. B. C. Chatterjee, N. Sarma and E. Oki, "Routing and Spectrum Allocation in Elastic Optical Networks: A Tutorial," in IEEE Communications Surveys & Tutorials, vol. 17, no. 3, pp. 1776-1800, thirdquarter 2015.

62. Y. Qiu, "An efficient spectrum assignment algorithm based on variable-grouping mechanism for flex-grid optical networks," Optical Switching and Networking, 24, pp.39-46, 2017.

63. J. Santos, N. Costa, and J. Pedro, "On the Impact of Deploying Optical Transport Networks Using Disaggregated Line Systems," Journal of Optical Communications and Networking. 10, A60-A68, 2018.

64. T. Ahmed, S. Rahman, S. Ferdousi, M. Tornatore, A. Mitra, B.C. Chatterjee, and B. Mukherjee, "Dynamic routing, spectrum, and

65. K. Perlicki, "Impact of alien wavelength on wavelength division multiplexing transmission quality," Photonics Letters of Poland, vol. 4, no. 3, pp. 118–120, 2012.

66. GÉANT, "Optical reach of photonic services," Milestone MJ1.2.3 [Online]. Available: https://geant3.archive.geant.org/Media_Centre/Media_Library/Media%20Library/GN3-13-162_MJ1.2.3_White-Paper_Optical-Reach-of-Photonic-Services_v3.pdf.

67. N. Sambo, A. Sgambelluri, M. Secondini, M. N. Petersen, A. M. Fagertun, and G. Roberts, "Alien wavelength modeling tool and field trial," in International Conference on Photonics in Switching (PS), 2015, pp. 339–341.

68. T. Horvath, P. Munster, M. Latal and N. -H. Bao, "Photonic Services with Sensor System in One Fibre with 100-GHz DWDM Grid," in ELEKTRO, 2020, pp. 1-4.

69. K. Kaeval, K., D. Rafique, K. Blawat, K. Grobe, H. Grießer, J.P. Elbers, P. Rydlichowski, A. Binczewski, and M. Tikas, "Exploring channel probing to determine coherent optical transponder configurations in a long-haul network," in Optical Fiber Communications Conference and Exhibition, 2020, pp. 1-3.

70. K. Kaeval, H. Grießer, K. Grobe, J. -P. Elbers, M. Tikas and G. Jervan, "Channel Performance Estimations with Extended Channel Probing," in Photonic Networks; 21th ITG-Symposium, 2020, pp. 1-5.

71. K. Kaeval, T. Fehenberger, J. Zou, S.L. Jansen, K. Grobe, H. Grießer, J.P. Elbers, M. Tikas, and G. Jervan, "QoT assessment of the optical spectrum as a service in disaggregated network scenarios," Journal of Optical Communications and Networking. 13, E1-E12, 2021.

72. K. Kaeval, J.P. Elbers, K. Grobe, M. Tikas, T. Fehenberger, H. Grießer, G. Jervan, "Black-Box Assessment of Optical Spectrum Services," Optical Fibre Conference, 2021, pp.1-3

73. M. Newland, R. Schmogrow, M. Cantono, V. Vusirikala, and T. Hofmeister, "Open optical communication systems at a hyperscale operator [Invited]," Journal of Optical Communications and Networking. 12, C50-C57, 2020.

74. A. Lord, Y.R. Zhou, P. Wright, P. Willis, C. Look, G. Jeon, S. Nathan, and A. Hotchkiss, "Managed alien wavelength service requirements and demonstration," in 37th Annual Conference and Exhibition on Optical Communication, 2011, pp. 1-3.

75. A. M. Fagertun and B. Skjoldstrup, "Flexible transport network expansion via open WDM interfaces," International Conference on Computing, Networking and Communications (ICNC), 2013, pp. 385-389.

76. H.W. DTU, K. Bozorgebrahimi, A. Tzanakaki, and B. Belter, Deliverable D12. 3 (DJ1. 1.1) Future Network Architectures, 2016.

77. A. Colmenero, A.M.F. DTU, D.C. Mur, D. Schmitz, F. Panken, H.Y. DTU, I. Demirkol, K. Boudjemaa, R. Tuminauskas, R. Smets, and Z. Ołtuszyk, Deliverable D13. 2 "Blueprint of Services and Research Plan for Future Work". Available online : https://www.geant.org/Projects/GEANT_Project_GN4-1/Documents/D13-2_Blueprint-of-Services-and-Research-Plan-for-Future-Work.pdf

78. L. Alahdab, E. Le Rouzic, C. Ware, J. Meuric, A. Triki, J.L. Augé, and T. Marcot, "Alien Wavelengths Over Optical Transport Networks," Journal of Optical Communications and Networking. 10, 878-888, 2018.

79. F. Paolucci, R. Emmerich, A. Eira, N. Costa, J. Pedro, P. Wilke Berenguer, C. Schubert, J. K. Fischer, F. Fresi, A. Sgambelluri, and F. Cugini, "Disaggregated edge-enabled C+L-band filterless metro networks," Journal of Optical Communications and Networking. 12, 2-12, 2020.

80. G. Roberts, P. Skoda, G. Vuagnin, P. Bolletta, J. Vojtech, K. Boudjemaa, K. Bozorgebrahimi, C. Tziouvaras, "Milestone M7.2 (M38) SCS Service Definition" 2020, available online:

modulation-format allocation in mixed-grid optical networks," Journal of Optical Communications and Networking. 12, 79-88, 2020.

https://www.geant.org/Resources/Documents/M7-2_SCS-Service-Definition.pdf#search=spectrum%20service

81. "Generic functional architecture of the optical media network," ITU-T Recommendation G.807, https://www.itu.int/rec/T-REC-G.807/en.

82. A. M. Fagertun, S. Ruepp and B. Skjoldstrup, "CAPEX/OPEX benefits of alien wavelengths for the next generation optical internet," International Conference on Optical Network Design and Modeling (ONDM), 2015, pp. 122-127.

83. V. Kamalov, V. Dangui, T. Hofmeister, B. Koley, C. Mitchell, M. Newland, J. O'Shea, C. Tomblin, V. Vusirikala, and X. Zhao, "Lessons learned from open line system deployments," in Optical Fiber Communications Conference and Exhibition, 2017, pp. 1-3.

84. Lightwave Online, (2017), "Open optical line system pros and cons at the Open Optical Conference," press release (November 7th, 2017).

85. M. Filer, J. Gaudette, M. Ghobadi, R. Mahajan, T. Issenhuth, B. Klinkers, and J. Cox, "Elastic optical networking in the Microsoft cloud," Journal of Optical Communications and Networking, 8(7), pp.A45-A54, 2016

86. B. Clouet, J. Pedro, N. Costa, M. Kuschnerov, A. Schex, J. Slovak, D. Rafique, and A. Napoli, A., "Networking aspects for next-generation elastic optical interfaces," Journal of Optical Communications and Networking, 8(7), pp.A116-A125, 2016.

87. M. Filer, H. Chaouch, and X. Wu, "Toward transport ecosystem interoperability enabled by vendor-diverse coherent optical sources over an open line system," Journal of Optical Communications and Networking, 10(2), pp.A216-A224, 2018.

88. K. Bozorgebrahimi, "Spectrum sharing – lessons from workshop", TERENA Networking Conference (2019).

89. C. Xie, L. Wang, L. Dou, M. Xia, S. Chen, H. Zhang, Z. Sun, and J. Cheng, "Open and disaggregated optical transport networks for data center interconnects [Invited]," Journal of Optical Communications and Networking. 12, C12-C22, 2020.

90. E. Rivera-Hartling, P. Pecci, and M. Priyanth, "Subsea open cables: a practical perspective on the guidelines and gotchas," in Proceedings Suboptic, 2019, Plenary.

91. "Transverse compatible dense wavelength division multiplexing applications for repeatered optical fibre submarine cable systems," ITU-T Rec. G. 977.1, online https://www.itu.int/rec/T-REC-G.977.1-202010-I/en.

92. "Spectral grids for WDM applications: DWDM frequency grid," ITU-T Rec. G.694.1, online https://www.itu.int/rec/T-REC-G.694.1-202010-I/en.

93. D. Semrau, E. Sillekens, P. Bayvel, and R.I. Killey, "Modeling and mitigation of fiber nonlinearity in wide-band optical signal transmission [Invited]," Journal of Optical Communications and Networking. 12, C68-C76, 2020.

94. D. F. Grosz, A. Agarwal, S. Banerjee, D. N. Maywar and A. P. Kung, "All-Raman ultralong-haul single-wideband DWDM transmission systems with OADM capability," in Journal of Lightwave Technology, vol. 22, no. 2, pp. 423-432, 2004.

95. K. Grobe, M. Eiselt, "Wavelength Division Multiplexing: A Practical Engineering Guide 1st Edition", John Wiley & Sons, p. 295, fig. 6.40, 2013.

96. B. D. Taylor, G. Goldfarb, S. Bandyopadhyay, V. Curri and H. Schmidtke, "Towards a Route Planning Tool for Open Optical Networks in the Telecom Infrastructure Project," Optical Fiber Communications Conference and Exposition, 2018, pp. 1-3.

97. A. Ferrari, M. Filer, K. Balasubramanian,Y. Yin, E. Le Rouzic, J. Kundrát, G. Grammel, G. Galimberti, and V. Curri, "GNPy: an open source application for physical layer aware open optical networks," Journal of Optical Communications and Networking, 12(6), pp.C31-C40, 2020.

98. A. Ferrari, J. Kundrát, E. Le Rouzic, M. Filer, A. Campanella, A. D'Amico, K. Balasubramanian, Y. Yin, O. Havliš, M. Hažlinský, and J. Vojtěch, "The GNPy Open Source Library of Applications for Software

Abstraction of WDM Data Transport in Open Optical Networks," In Proc. of 6th IEEE Conference on Network Softwarization (NetSoft), 2020, pp. 386-394.

99. Facebook, (2016), "An open approach for switching, routing, and transport," blog post (November 11th, 2016)

100. "Optical system design and engineering considerations," ITU-T Supplement 39, https://www.itu.int/rec/T-REC-G.Sup39-201602-I/en.

101. Pan, J. and Tibuleac, S., "Filtering and crosstalk penalties for PDM-8QAM/16QAM super-channels in DWDM networks using broadcast-and-select and route-and-select ROADMs," Optical Fiber Communications Conference and Exhibition, 2016, pp. 1-3.

102. B. Shariati, M. Ruiz, J. Comellas, and L. Velasco, "Learning from the optical spectrum: failure detection and identification," Journal of Lightwave Technology, 37(2), pp.433-440, 2019.

103. C. Pulikkaseril, L.A. Stewart, M.A. Roelens, G.W. Baxter, S. Poole, and S. Frisken, "Spectral modeling of channel band shapes in wavelength selective switches," Optics express, 19(9), pp.8458-8470, 2011.

104. K. Kaeval, J. Myyry, K. Grobe, H. Grießer, and G. Jervan, "Concatenated GSNR Profiles for End-to-End Performance Estimations in Disaggregated Networks." in Optical Fiber Communications Conference and Exhibition, 2022, pp. 1-3.

Publication II

Kaeval, K., Rafique, D., Blawat, K., Grobe, K., Grießer, H., Elbers, J.P., Rydlichowski, P., Binczewski, A. and Tikas, M., 2020, March. "Exploring channel probing to determine coherent optical transponder configurations in a long-haul network", *Optical Fibre Communication Conference 2020*, pp. 1–3.

The paper is included in the proceedings of the Optical Fiber Communication Conference 2020, held in San Diego/online, 8–12 March 2020.

Exploring Channel Probing to Determine Coherent Optical Transponder Configurations in a Long-Haul Network

Kaida Kaeval[1], Danish Rafique[1], Kamil Bławat[1], Klaus Grobe[1], Helmut Grießer[1], Jörg-Peter Elbers[1], Piotr Rydlichowski[2], Artur Binczewski[2], Marko Tikas[3]

[1] *ADVA Optical Networking SE, Martinsried, Germany*
[2] *Poznan Supercomputing and Networking Center, Poznan, Poland*
[3] *Tele2 Estonia, Tallinn, Estonia*
kkaeval@advaoptical.com

Abstract: We use channel probing to determine the best transponder configurations for spectral services in a long-haul production network. An estimation accuracy better than ±0,7dB in GSNR margin is obtained for lightpaths up to 5738km. © 2020 The Author(s).

OCIS codes: 060.2330 Fiber Optics Communications; 060.2360 Fiber Optics Links and Subsystems; 060.1660 Coherent communications

1. Introduction

Facilitated by flexgrid-capable reconfigurable optical add/drop multiplexers (ROADMs) and digital signal processor (DSP) enabled coherent transponders, optical Spectrum as a Service (OSaaS) ideas are gaining popularity in dense wavelength division multiplexing (DWDM) networks [1]. OSaaS allows operators to share unused fiber capacity with customers and other operators, thereby increasing network utilization and reducing infrastructure costs.

To characterize a spectral slot on an optical lightpath, a measure for the attainable transmission performance is required. While the optical signal-to-noise ratio (OSNR) is a common performance criterion, it does not consider the impact of fiber nonlinearities. To account for these effects, the use of a generalized OSNR (GOSNR) was proposed [2]. Unfortunately, the GOSNR cannot be directly measured; it needs to be calculated from optical system parameters or inferred from indirect measurements. For subsea open cable systems, it has recently been suggested to use a test transponder to probe a subsea link and to derive the GOSNR distribution over wavelength from this measurement [3].

In this paper, we follow a similar approach for terrestrial long haul network and determine its applicability in a practical network context. We probe the optical channel with a transponder in a fixed reference configuration to estimate the GOSNR of a spectrum service in a long-haul network. By normalization of GOSNR to the symbol rate, a modulation format independent generalized signal-to-noise ratio (GSNR) is obtained. From the GSNR we then predict the best transponder configuration for different spectrum services delivering maximum capacity at highest spectral efficiency. We verify the accuracy of the method in Tele2 Estonia's terrestrial long-haul network between Tallinn and Frankfurt for lightpath lengths up to 5738km. A commercial coherent transponder offering highly flexible 100G-600G dual-polarization quadrature amplitude modulation (DP-QAM) modulation is used both for channel probing as well as for data transmission. Compared to previous work on automatic transponder configuration [4], we investigate the practicability of channel probing and configuration optimization on a large set of long-haul distances and modulation formats. We show that false positives can occur in predicting the best transponder configuration. Margins and/or an additional optimization step can be applied to solve this issue.

2. Method description

Following a back-to-back characterization of the probing light transponder (PLT), the channel probing method consists of two steps: Estimation of the channel performance in a spectrum slot by means of the GSNR derived from a reference measurement and selection of best modulation format/symbol rate combination for that lightpath. A back-to-back measurement of the Q-factor versus the OSNR for at least one modulation format/symbol rate combination is required to characterize the PLT. The logarithmic Q-over-OSNR characteristic is then fitted by a 2nd order polynomial and the resulting function is then inverted to estimate the OSNR from the Q-factor. For our tests, the Q-over-OSNR characteristics were taken with one PLT module, and the actual network probing was conducted with a second module, with no further cross-characterization between the modules.

In order to evaluate the actual channel performance of a lightpath at hand, the selected probing-light is inserted into the network in the respective spectral slot and the Q value is read out from the receiver to estimate the effective GOSNR. The GOSNR considers all optical distortions that impact the optical signal, including ASE noise, nonlinear distortions, etc. as well as any transceiver impairments. This value is then normalized to the symbol rate of the probe signal to obtain the GSNR. As second step, this GSNR is then compared to the typical GSNR values of different

modulation format/symbol rate combinations as per system specification. Note that specified typical vs. worst-case GSNR can vary, which must be considered when looking at estimations leading to close-to-zero margin. Margins can be added to the GSNR estimates to increase the robustness of the prediction to any fluctuations and ageing effects in the network [5].

3. Network and transceiver configurations for the verification tests

A coherent flex-grid network with a maximum physical path length of 2869 km and more than 6 Tbit/s of live traffic in service was used to investigate the feasibility of the method. Several optical lightpaths with lengths up to 5738 km, enabled by optical loopbacks in intermediate ROADM nodes, were investigated. We used four 100-GHz spectrum slots with the central frequencies 193.90 THz for the shortest lightpath 194.00 THz for a 1792-km path, 194.10 THz for a 2943-km path, and 194.20 THz for the three longest paths, respectively (see Figure 1). A passive 4×1 splitter/combiner was used in the add/drop path to insert and extract the signals.

After inserting the selected PLT into the respective links and estimating the GSNR, verification signals with different modulation format/symbol rate combinations were tested, keeping the power spectral density (PSD) constant for all signals under test. Then, margins were calculated between the PLT-estimated GSNR and typical specified GSNR per used modulation format/symbol rate as

$$\text{Margin} = \text{estimated GSNR} - \text{typical, specified GSNR} \qquad (1)$$

These margins were compared with the actual performance of the verification signals. If the margin estimation was positive, the verification signal was expected to work, leaving non-working channels as false positive results.
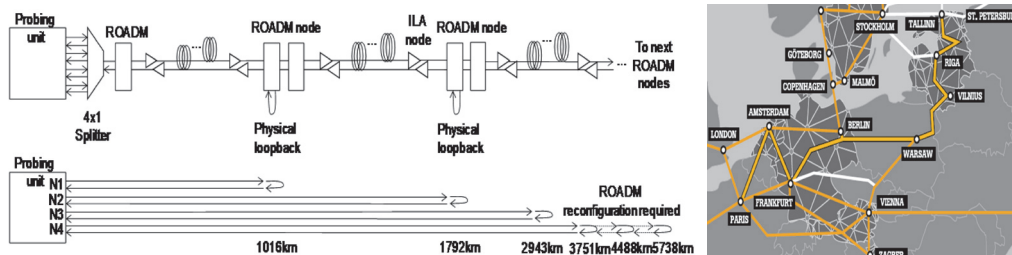
Figure 1. Test schema and network layout.

Although all conditions were held as stable as possible during the tests, certain variations in OSNR and polarization cannot be avoided in a live network with lightpaths of more than 5500 km in length. As such, we do not expect our method to deliver a perfect solution but rather a practical estimation.

4. Results and interpretation

We demonstrate the most important findings of our work in Figure 2. The main diagram shows the estimated GSNR margin on vertical axes over the different tested link lengths. All link performance estimations for the main diagram were retrieved using 200Gbit/s 69GBd DP-QPSK probing light that provided the best estimation accuracy over the other tested probing settings. Verification signals were selected with 0.5bit/symbol steps and 100G/200G/300G/400G data rates were tested. Different line styles refer to different data modulation formats/symbol rates and different colors to different line rates. The best transponder configuration for a given lightpath is the signal with the lowest GSNR margin, which is still working. As expected, the estimated GSNR margin decreases with increasing link length.

An estimation accuracy of better than ±0,7dB in GSNR margin is achieved for lightpaths up to 5738km. For low estimated GSNR margins some false positive results were estimated. These recorded estimation errors can be attributed to parameter changes in the photonic layer over the test period, slightly deviating performance of the PLT unit used in the tests compared to the characterized one, and the typical GSNR values used in Eqn. (1). The estimation errors were spread across all measurements, and no obvious correlation with modulation format, symbol rate or signal PSD was observed. For practical use, an additional operating margin would eliminate most of these errors. An additional fine-tuning step could also be applied to optimize the transponder configuration in the region where the estimated GSNR is low.

We also compared the link GSNR estimation accuracy when varying the symbol rates and constellation sizes of the probing light. In particular, the GSNR was estimated for: 34-GBd 100-Gbit/s DP-QPSK (PL1), 69-GBd 200-Gbit/s DP-QPSK (PL2), 69-GBd 300-Gbit/s DP-8QAM (PL4), 69-GBd 400-Gbit/s DP-16QAM (PL4) probing

signals. The results of these comparisons are presented as inserts for Figure 2. In these inserts, the shortest and longest links were chosen where all four probing light settings gave meaningful results, so A and B reflect a transmission distance of 1016km and 1792-km, respectively. We can see that the 34GBd 100Gbit/s DP-QPSK signal has the tendency to overestimate the lightpath GSNR, which leads to false positive results, while higher modulation formats are prone to estimation errors, most likely caused by the fact that higher constellations are more prone to noise. Overall, the inserts clearly show that the overall performance of the highest symbol rate with lowest constellation size (200Gbit/s 69GBd DP-QPSK) gave the best result.
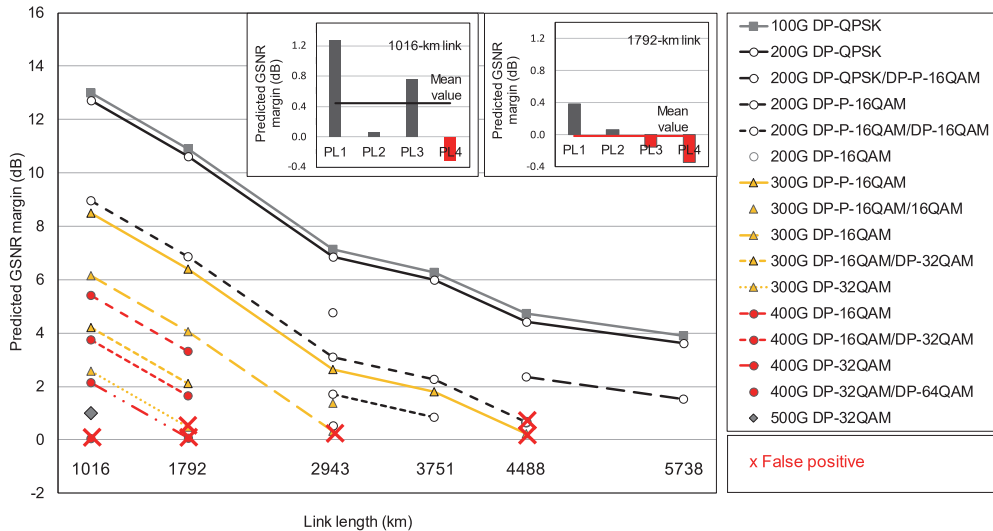
Figure 2. Predicted GSNR margin for different verification signal combinations with 200-Gbit/s PLT. The inserts A. and B. show the estimation deviation of the four different PLT settings.

5. Conclusions

Channel probing – including using data from already commissioned transponders – can be a cost-efficient approach in particular for quick link performance estimations. It can help eliminating uncertainty in simulations or calculations, which practically cannot consider all effects in reconfigurable and time-dependent networks.

In this paper, we investigated the performance of channel probing on a long-haul commercial network and showed consistent results for different symbol rates, modulation formats and link length combinations. Using a 200Gbit/s probing-light signal, an estimation accuracy of better than ±0,7dB in GSNR margin is achieved for lightpaths up to 5738km. For low estimated GSNR margins some false positive results were estimated. The errors fell well within both, the maximum network variations and the difference between typical vs. worst-case specifications.

6. References

[1] K. Grobe, et al., "Flexible Spectrum-as-a-Service," in Proc. TNC 2014, Paper 6A.

[2] P. Poggiolini, "The GN Model of Non-Linear Propagation in Uncompensated Coherent Optical Systems," JLT, vol. 30, no. 24, pp. 3857-3879, 2012.

[3] E. Rivera-Hartling, et al. "Subsea Open Cables: A Practical Perspective on the Guidelines and Gotchas," in Proc. Suboptic 2019, Plenary.

[4] B. Spinnler, et al., "Autonomous intelligent transponder enabling adaptive network optimization in a live network field trial," JOCN, Vol. 11, No. 9, 2019.

[5] C. Delezoide, et al., "Field Trial of Marginless Operations of An Optical Network Facing Ageing and Performance Fluctuations," in Proc. ECOC 2018, Paper W2A.56.

Publication III

Kaeval, K., Grieβer, H., K. Grobe, J. -P. Elbers, M. Tikas and G. Jervan, "Channel Performance Estimations with Extended Channel Probing," *ITG-PN 2020*, pp. 1–5.

Channel Performance Estimations with Extended Channel Probing

Kaida Kaeval
Advanced Technology
ADVA Optical Networking SE
Martinsried, Germany
kkaeval@adva.com

Helmut Grießer
Advanced Technology
ADVA Optical Networking SE
Martinsried, Germany
hgriesser@adva.com

Klaus Grobe
Global Sustainability
ADVA Optical Networking SE
Martinsried, Germany
kgrobe@adva.com

Jörg-Peter Elbers
Advanced Technology
ADVA Optical Networking SE
Martinsried, Germany
jpelbers@adva.com

Marko Tikas
Transmission Networks
Tele2 Estonia AS
Tallinn, Estonia
marko.tikas@tele2.com

Gert Jervan
Department of Computer Systems
Tallinn University of Technology
Tallinn, Estonia
gert.jervan@taltech.ee

Abstract— **We test the concept of extended channel probing in a Optical Spectrum as a Service scenario in coherent optimized flex-grid long-haul and 10Gbit/s OOK optimized 100-GHz fixed-grid dispersion managed legacy DWDM networks. An estimation accuracy better than ±0.1dB in GSNR implementation margin is obtained for both networks by using flexible coherent transceivers on lightpaths up to 822km on regional haul legacy network and up to 5738km on a long-haul network. We also explain, how to detect the operation regime of the channel by analyzing the received GSNR results from constant power spectral density (PSD) probing mode and constant signal power probing mode.**

Keywords—optical communications, Optical-Spectrum-as-a-Service, performance estimations, flexgrid, fixed-grid, throughput

I. INTRODUCTION

While coherent optimized DWDM networks are becoming the standard for long haul communication networks, many access and regional haul data transmission networks still rely on dispersion managed 10-Gbit/s OOK (on-off keying) optimized networks. While a lot of effort is put into upgrading these networks, full implementation of the decisions may take years and intermediate solutions are required by the operators to satisfy the growing need for capacity. One such solution is to enable coherent transmission over the legacy DWDM networks.

Considering the operation with design based signal power levels and sufficient guard bands to avoid interference with the existing 10Gbit/s OOK signals, possible filtering penalties from various multiplexers, Reconfigurable Optical Add Drop Multiplexers (ROADMs) or grating based dispersion compensation (DCG) modules may still complicate the selection of the best possible transponder configuration from thousands of available configurations provided by the modern flexible symbol rate and modulation format transponders to achieve the highest capacity per channel.

Although the Gaussian Noise model based channel probing method [1],[2] to estimate the channel performance is primarily performed over uncompensated coherent optimized networks, where several studies have shown successful results[2],[3],[4],[5], the concept is useful also in estimating the performance in dispersion compensated networks [7]. In this paper, we show how extended channel probing allows to improve the prediction accuracy from previously reported

0.7dB [5] to less than 0.1dB accuracy for both flex-grid uncompensated long-haul and fixed-grid dispersion compensated regional-haul networks in order to fully utilize the flexibility of the coherent transponders. We discuss the PSD based probing mode and propose an operation regime analysis to detect operation in the nonlinear regime.

II. EXTENDED CHANNEL PROBING

In order to evaluate the actual channel performance of a lightpath at hand, characterized probing-light is inserted into the network in the corresponding channel location and the bit error ratio (BER) estimation of the receiver, converted into a Q-value is used to estimate the respective effective Generalized OSNR (GOSNR). This value is then normalized to the symbol rate of the Probing Light Transceiver (PLT) signal to obtain the GSNR. However, the received GSNR value here would only be applicable to describe the spectrum performance for the exact covered bandwidth by the PLT configuration at the exact probed power regime.

To overcome this and get more insights to the performance of the network and spectral slot at hand, a set of PLT configurations with different modulation formats and symbol rates can be used. For the current work, eleven PLT configurations as listed in Tab. 1 were characterized by a back-to-back measurement of the Q-factor versus the OSNR in the lab. The logarithmic Q-over-OSNR characteristic was then fitted by a 2nd order polynomial to estimate the Generalized OSNR (GOSNR) from the Q-factor of each PLT configuration. This value was then normalized to the symbol rate of the PLT signal to obtain the GSNR.

Based on the estimated GSNR values from eleven PLT configurations, we calculate the average estimated GSNR based on the PLT configuration estimations, that do not experience severe penalties from filtering, making this method usable also in systems using fixed filter access or other filtering elements.

Finally, the GSNR implementation margin is estimated for a pool of usable transponder configurations, leaving out all configurations with higher symbol rate than the PLT with highest symbol rate configuration still working over the link. To calculate the GSNR implementation margin, we subtract the typically required GSNR margin according to the system specification from the estimated GSNR [5]. All calculations resulting in positive GSNR implementation margins are expected to work over the probed link.
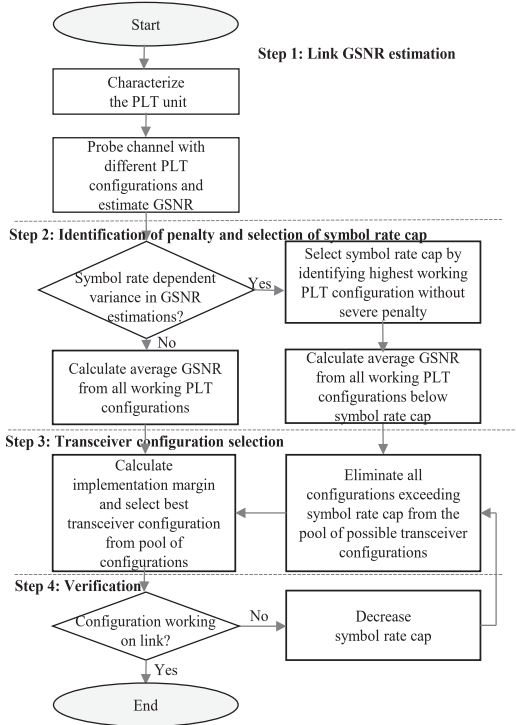
Fig. 1: Extended channel probing flowchart

Loopback location	DCM data	Looped link length(km)	Spans (back and forth)
LH SAL	DCM free	1016	14
LH KRUO	DCM free	1792	24
LH WAR	DCM free	2943	36
LH POZ	DCM free	3751	48
LH FRA	DCM free	5738	74
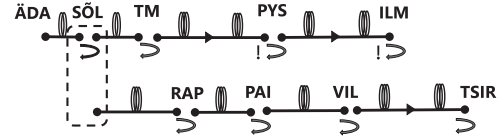
Loopback location	DCM data	Looped link length(km)	Spans (back and forth)
R SOL	DCM free	3	2
R TM	DCF only	70	4
R RAP	DCF only	144	4
R PAI	DCF only	241	6
R VIL	DCF only	382	8
R TSIR	DCF only	675	12
R PYS	DCF+DCG Mix	485	8
R ILM	DCF+DCG Mix	822	12

Fig. 2: Network links tested

By using the same probe configurations as verification signals, comparison of the estimated GSNR implementation margin to the actual performance of the verification signals was performed.

III. PROBING MODE

To start with extended channel probing, a switch from constant signal power setting to constant Power Spectral Density (PSD) power setting has to be performed. Although not as intuitive to work with, it has multiple benefits. Most important are the good alignment with power limited networking caused by the amplifier total output power and better comparability of the received GSNR results.

In case of a constant power distribution over the full C-band, the maximum usable PSD is defined by the maximum total power to the line from the amplifier output and total C-band bandwidth. As these values might have been optimized per link or hop, calculations for the suitable PSD in the production networks can be performed according to the ROADM output power-levels. When calculating the PSD for fixed-grid 10Gbit/s optimized legacy networks, the original channel power to the line can be divided with the 10Gbit/s bandwidth. That would also ensure the optimum performance with dispersion compensation fibres (DCF).

Network equalization should be performed with signal configuration with the highest symbol rate, regardless of possible penalties this signal format may experience due to filtering. The motivation here is to set the internal variable optical attenuators in the ROADM modules to a level that ensures that symbol rate changes during the probing activity

would not increase the total power levels per open optical cross-connect in the network. In our tests, we used 69GBd signals providing the highest power per channel.

As a consequence, the PSD based probing mode allows better comparability of the estimated GSNR values of each PLT configuration, as equal GSNR is expected at the receiver for the signal configurations with equal PSD in near-linear operation regime, where differences in results are mainly caused by transceiver implementation penalties, measurement errors or network fluctuations.

IV. TEST SET-UP AND INFRASTRUCTURE

The concept of extended channel probing shown in Fig. 1 was tested over two different production networks. A coherent optimized flex-grid long-haul network to verify the method and selected PSD based probing mode and a 10-Gbit/s optimized 100GHz-grid legacy regional-haul network with

TABLE. I: PLT configurations

Line rate	Modulation	Symbol rate
100Gbit/s	DP-QPSK	31.5GBd
200Gbit/s	DP-16QAM	34.7GBd
300Gbit/s	DP-64QAM	34.7GBd
300Gbit/s	DP-32QAM	41.7GBd
200Gbit/s	DP-8QAM	46.3GBd
400Gbit/s	DP-64QAM	46.3GBd
300Gbit/s	DP-16QAM	52.1GBd
400Gbit/s	DP-32QAM	55.6GBd
200Gbit/s	DP-QPSK	69.4GBd
300Gbit/s	DP-8QAM	69.4GBd
400Gbit/s	DP-16QAM	69.4GBd

dispersion compensation modules utilizing both, DCF and DCG modules. Network diagrams and link data is presented in Fig. 2, where links with exclamation mark loopbacks also included DCG modules.

First, a total of five links with link lengths from 1016km to 5738km in a long-haul pan-European coherent optimized flex-grid network were tested to verify the methods capability to return expected results in a network well suitable for the channel probing. Then, eight links with link lengths from 3km to 822km were tested in a regional haul DCM-based 10Gbit/s OOK optimized network.

Both networks utilize a different set of infrastructure components, like multiplexers, amplifiers, boosters and ROADMs, but are built on standard single mode fibres (SSMF ITU-T 652.D). This sets a good comparison for demonstrating the capabilities of extended channel probing for estimating additional aspects of the link performance at an Optical Spectrum as a Service scenario independent of the network infrastructure.

V. OVERALL RESULT ACCURACY

To better visualize the differences in probing in legacy networks and coherent optimized flexgrid networks, in Fig. 3, raw estimated GSNR data from the extended channel probing in both networks is shown. Markers with different styles refer to configurations with different symbol rates.

As visible in the inset of Fig. 3, the results are well aligned for the long haul network. Each PLT is contributing to the overall accuracy of the estimation and the average GSNR estimation over all PLT configurations allows us to reduce the error in GSNR implementation margin from previously reported 0.7dB [5] to 0.05dB. The reason is that, while small fluctuations in the network cause different BER readings, and thus the Q-value per each measurement also varies, the extended approach allows us to average out the variance in the results and get a better estimate for the link GSNR. GSNR implementation margins calculated from averaging GSNR values, together with the actual performance indication for the verification signals, are presented in Fig. 4. Different marker styles refer to different symbol rate regimes and line styles distinguish different modulation formats. The chart is zoomed in for the area near zero implementation margin and check or fail marks indicate, if the configuration worked in reality or not.
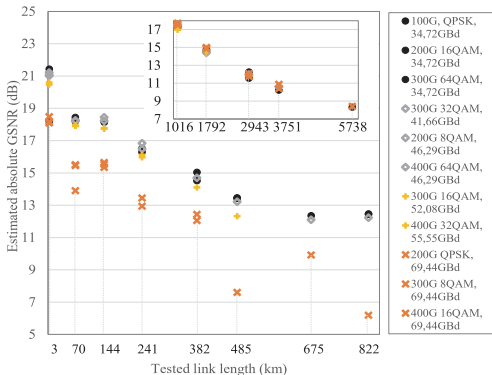

Fig. 3: Raw data from extended channel probing in regional haul network, estimated by different probe configurations. Inset presents the extended probing results for long-haul network.
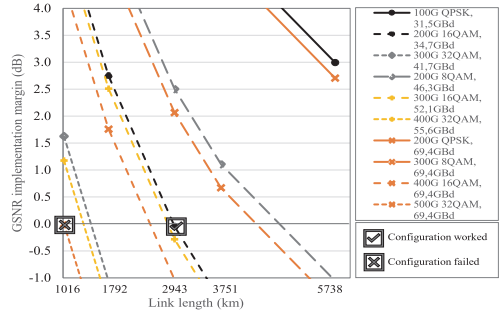

Fig. 4: GSNR implementation margin compared to channel actual performance in a long-haul network.

In contrast, for the legacy regional haul network it is relatively difficult to make any assumptions on the actual performance capabilities due to wide spread of the estimated GSNR values, reducing the average estimated GSNR value just as a statistical number. In this case, further analyses on the raw data are required to be able to decide the best performing modulation and symbol rate combination for the current spectral slot at hand.

VI. DETERMINING HIGHEST USABLE SYMBOL RATE

As high symbol rate signals are subject to stronger narrow band filtering, using a wideband probing signal results in underestimating the link GSNR that would be achievable for lower symbol rate signals. Using narrow band probing configurations would create the illusion of a link with a high GSNR not achievable for higher symbol rate signals.

In order to estimate the best possible modulation format and symbol rate combination in 10-Gbit/s optimized legacy networks, a bandwidth limitation caused by filtering penalty has to be identified.

According to our test results, when operated with system design based PSD powers, PLT configurations with equal symbol rate experienced similar penalties from the system and estimated the link GSNR with +/-0.35dB accuracy, regardless of the modulation type for up to 60GBd signals, whereas a change in the PLT symbol rate resulted in a great variance in the estimated GSNR.

From Fig. 3, we can see, that while the maximum difference between the estimated GSNR is below 0.7dB for the probe settings between 31.5 and 46.3GBd and below 1.1dB for the probes up to 55.6GBd, it quickly grows up to 7.1dB for the probes including 69.4GBd. This behaviour can be explained with a filtering penalty from the channel filter modules (3dB bandwidth of 80 GHz) and ROADMs for the DCF based links and additional penalty from DCG modules (3dB bandwidth of 60 GHz) for the 485-km and 822-km links.

To identify the bandwidth limitation and select the highest usable symbol rate on the link, we compare the estimated absolute GSNR values from the different probes and select the working probe with the highest symbol rate configuration that does not experience severe penalties from filtering. This symbol rate value (symbol rate cap) is essential in determining the best working modulation format and symbol rate configuration for the current link. Looking at Fig. 3, this means leaving out all high symbol rate configurations marked with "x" for the links with channel filter modules or with "+" for even smaller bandwidth due to DCG modules. Then, the
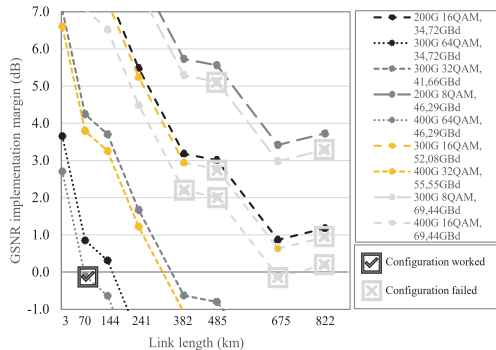
Fig. 5: GSNR implementation margin compared to channel actual performance in a regional-haul network.

Fig. 6: Operation regime estimation

average estimated GSNR can be calculated for the link as described for the long-haul network scenario and the implementation margin is calculated for all configurations with smaller and equal symbol rate than the highest working PLT configuration. Finally, the best transceiver configuration can be selected as per highest line rate from all possible configurations returning positive implementation margin[5]. Additional margins can be added to the GSNR estimations to increase the robustness of the prediction to any fluctuations and ageing effects in the network[6].

The results for the extended channel probing method with additional step considering the bandwidth limitation and symbol rate cap for the pool of possible transponder configurations are presented in Fig. 5. Similarly to Fig. 4, different marker styles refer to different symbol rates and line styles distinguish modulation formats. High symbol rate configurations not usable on the link and therefore left out from the GSNR implementation margin calculations are presented as light grey lines. The chart is zoomed in between -1 and +7dB GSNR implementation margin, to better illustrate the importance of the symbol rate limitation on the selection of the best working transceiver configuration. Similarly to Fig. 4, check or fail marks indicate if the configuration in reality worked or not. Light grey fail marks indicate the failing configurations exceeding the bandwidth limitations/symbol rate cap that were expected not to work.

Following the extended channel probing method, we were able to achieve the selection of the best possible modulation format and symbol rate combination on any link with an accuracy better than 0.1dB of GSNR implementation margin also in the dispersion managed legacy network. Considering the margin values usually implemented for network robustness against aging, slow changes in the network and infrastructure, the achieved result is an accurate measure of the network performance at a current moment.

VII. DETECTING OPERATION REGIME

In addition to the accurate GSNR estimations, extended channel probing allows to evaluate the operation regime of the channel. To this end, results received with constant PSD over different symbol rates are compared to the constant signal power measurements.

For the network equalized with the highest symbol rate signal, providing the highest to the line power as per network design, this initial power can be taken as a reference point
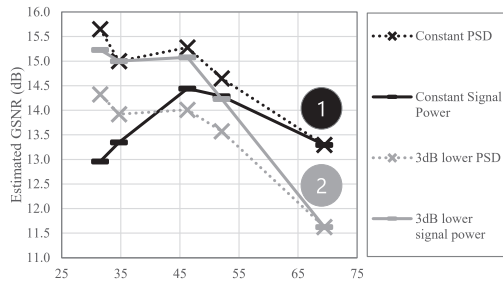
(reference point 1 in Fig. 6) for the operation regime test, regardless of the filtering penalty it experienced.

The 382-km link from our tests was analysed by comparing design based PSD mode GSNR estimations to design based signal power mode GSNR estimations. In both cases, the total power per probing activity stays equal or below the reference power used for the network equalisation. By comparing the estimated GSNR values for a black dotted, constant PSD line and a black solid, constant signal power line, we can see that signals perform better at constant PSD. This indicates that, with constant signal power, the increased PSD of individual narrowband signals is too high and the signal power is above the optimum balance between ASE noise and nonlinear distortions. For example, if we are operating in a linear regime, corresponding to a 3dB lower reference point signal power (reference point 2) the lines swap positions for narrower channels, and equal PSD delivers lower GSNR estimations than constant signal power mode. This means operation in the linear regime, as signals still do benefit from increased total signal powers.

This kind of analysis can be useful especially for longer links to adjust signal powers in the right direction to improve the performance for signal configurations operating at the BER threshold.

VIII. CONCLUSIONS

We use extended channel probing to improve the accuracy of the link GSNR estimations and to select the best possible transceiver configuration for coherent transponders operated on both, flex-grid coherent optimized and 10-Gbit/s optimized fixed-grid dispersion managed legacy DWDM systems. We show that eleven characterized probe configurations are sufficient to reliably select the best modulation format and symbol rate configuration for the transceivers and also derive useful information for network development and operation decisions.

In future studies, we want to investigate the minimum set of PLT configurations that can lead to a similar estimation accuracy.

REFERENCES

[1] P. Poggiolini, "The GN Model of Non-Linear Propagation in Uncompensated Coherent Optical Systems," IEEE J-LT, Vol. 30, No. 24, pp. 3857-3879, 2012.

[2]   E. Rivera-Hartling, et al., "Subsea Open Cables: A Practical Perspective on the Guidelines and Gotchas," in Proc. Suboptic 2019, Plenary.

[3]   B. Spinnler et al., "Autonomous intelligent transponder enabling adaptive network optimization in a live network field trial," JOCN, Vol. 11, No. 9, 2019.

[4]   Yu Rong Zhou et al., "Demonstration of a novel technique for non-intrusive in-band OSNR Derivation using flexible rate optical transponders over a live 727 km flexible grid optical link," IEEE J-LT, Vol. 35, No. 20, p. 4399-4405, 2017.

[5]   K. Kaeval et al., "Exploring Channel Probing to Determine Coherent Optical Transponder Configurations in a Long-Haul Network," in Proc. OFC 2020, Paper W1J.2.

[6]   Yvan Pointurier, "Design of low-margin optical networks," in Proc. OFC 2016, Tu3F.5.

[7]   K. Kaeval et al., "Extended Channel Probing to Estimate Achievable Throughput in Legacy DWDM Networks with Coherent Transmission," unpublished.

Publication IV

Kaeval, K., Elbers, J.P., Grobe, K., Tikas, M., Fehenberger, T., Grießer, H., Jervan, G., "Black-Box Assessment of Optical Spectrum Services," *Optical Fibre Communication Conference 2021*, pp. 1–3.

Black-Box Assessment of Optical Spectrum Services

Kaida Kaeval[1,2], Jörg-Peter Elbers[1], Klaus Grobe[1], Marko Tikas[3],
Tobias Fehenberger[1], Helmut Grießer[1], Gert Jervan[2]
[1] ADVA Optical Networking SE, Martinsried, Germany
[2] Tallinn University of Technology, Tallinn, Estonia
[3] Tele2 Estonia, Tallinn, Estonia
kkaeval@adva.com

Abstract: A spectral sweep process is introduced to discover performance issues in optical spectrum services. We detect filtering penalty, spectral ripple/tilt and channel crosstalk in field measurements, potentially leading to increased service robustness in low-margin networks. © 2021 The Author(s).

1. Introduction

Recently, optical spectrum is emerging as new service paradigm in high capacity optical DWDM networks [1]. Relying on open line systems (OLS), network operators can provide optical spectrum to customers who run traffic over it using their own DWDM terminals. To achieve the highest transmission capacity for a spectral slot at hand, customers need to choose the best transponder configuration that satisfies the minimum margin requirements [2]. While transmission impairments make an accurate performance evaluation challenging already for fixed-grid wavelength services [3], a flex-grid Optical Spectrum as a Service (OSaaS) scenario introduces even more variables.

Pre-characterized coherent transceivers have been proposed to estimate the Generalized Signal to Noise Ratio (GSNR) of optical lightpaths [4] and have been proven to reliably predict the Quality of Transmission (QoT) [5]. In this work, we adapt the frequency sweep procedure proposed in [6] and combine it with the Extended Channel Probing (ECP) method [7] to assess the performance of optical spectrum services in a black-box-scenario. We apply this approach to investigate the impact of narrow optical filtering, carrier frequency mismatch, spectral ripple/tilt, and adjacent channel crosstalk and discuss how to define spectrum services in a robust way.

2. System description and measurement set-up

Following the definitions in ITU-T Recommendation G.807 [8], we define an optical spectrum service as an optical media channel (MC) representing a transparent lightpath through an optical network on a predetermined frequency slot. A media channel supports zero or more optical tributary signals (OTSi) each of which may be carried in its own Network Media Channel (NMC). The MCs and NMCs can use guard bands to limit crosstalk between adjacent OTSi in and across adjacent MCs.

In real life scenarios, it is difficult to evaluate the media channel mask or channel transfer function determined by the cascade of optical filters along the lightpath. While ASE noise loading or attenuation profile measurements can determine the exact mask characteristics, they do not capture a possible GSNR variation over the media channel bandwidth.

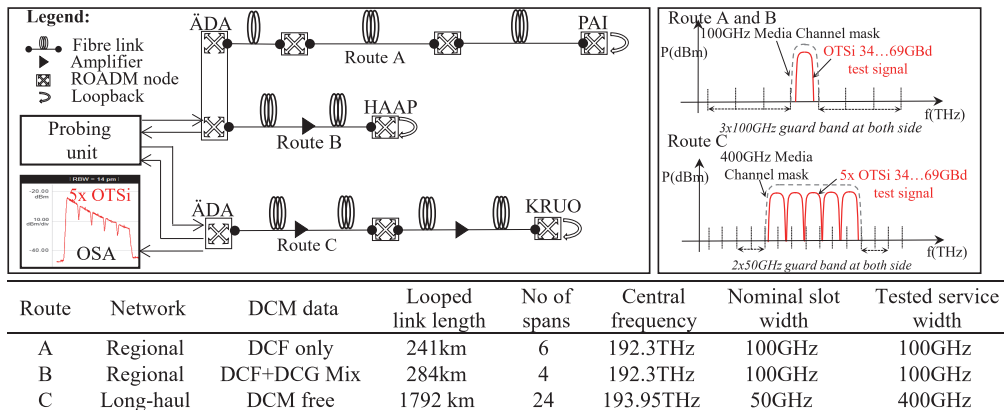| Route	Network	DCM data	Looped link length	No of spans	Central frequency	Nominal slot width	Tested service width
A	Regional	DCF only	241km	6	192.3THz	100GHz	100GHz
B	Regional	DCF+DCG Mix	284km	4	192.3THz	100GHz	100GHz
C	Long-haul	DCM free	1792 km	24	193.95THz	50GHz	400GHz

Fig. 1. General test set-up, spectral assignments and route data

To assess the feasibility of OSaaS offerings in field deployments, we tested optical spectrum services using MCs over three different routes in Tele2 Estonia's ROADM-based production network. The test set-up and available parameters of route A, B, and C are illustrated in Fig.1. To extend the transmission distance and to allow single-ended measurements in ÄDA, the spectrum services were looped back in the far end ROADMs.

The spectrum services on route A and B run over 10 Gb/s legacy DWDM links with fixed 100 GHz channel grid. Route A uses dispersion compensating fibers (DCFs) for optical dispersion compensation, whereas route B uses a mix of DCFs and dispersion compensating gratings (DCGs). In the terminal ROADMs in ÄDA, the optical user spectrum was added and dropped by arrayed waveguide grating (AWG) filters.

Route C runs over a dispersion-uncompensated long-haul DWDM link with flex-grid ROADMs optimized for 100 Gb/s transmission. Here, the optical user spectrum was added and dropped at a free terminal ROADM port using 8:1 splitter/combiner module in ÄDA without applying additional optical filtering.

A 100 GHz narrow-band spectrum service was investigated on routes A and B, whereas a 400 GHz wide-band service was used on route C. The channel performance on all routes was tested with 200 Gbit/s 69 GBd DP-QPSK, 200 Gbit/s 46 GBd DP-P-16QAM, and 200 Gbit/s 34 GBd DP-16QAM probing signals with root raised cosine (RRC) spectral shape (roll-off factor r = 0.19). To obtain comparable results, we maintain a constant ratio of signal power and symbol rate and adjust the signal power at each symbol rate accordingly when switching modulation formats. This is possible when the DWDM line systems and their amplifiers operate in constant gain mode. The system performance is evaluated by a generalized SNR (GSNR) which is derived from the measured Q-factor and normalized to the symbol rate [7]. By sweeping in 6.25 GHz steps over the allocated spectrum, we investigate the impact of filtering, frequency misalignment, spectral ripple/tilt effects and adjacent channel crosstalk from the perspective of an optical spectrum user.

3. Results and interpretation

Fig. 2 shows the results of the channel probing on the three different routes. While the nominal MC width on route A and B is 100 GHz, the large predicted GSNR difference between the three modulation formats reveals that the usable effective optical bandwidth must be much smaller. Given that a 6.25GHz mismatch of a 34GBd signal already causes a noticeable penalty, we can conclude that the effective optical channel bandwidth is lower than 50GHz. In Fig. 2a, up to 2dB degradation in the estimated GSNR is observed for a 200Gbit/s 34GBd DP-16QAM signal configuration in case of 18.75GHz offset. With the same offset, 200Gbit/s 46GBd DP-P-16QAM and 200Gbit/s 69GBd DP-QPSK signals are already experiencing outage as the attainable GSNR is insufficient.

The results in Fig. 2b also indicate a misalignment of the nominal center frequency on route B in addition to severe filtering penalty for the 200Gbit/s 69GBd DP-QPSK signal format. Without sweeping, this misalignment could have been left undiscovered and already a small fluctuation in the transceiver wavelength could cause a severe degradation of the service quality, especially with 46GBd DP-P-16QAM modulation, that generally requires higher margin and is more prone to filtering penalty, than a 200Gbit/s 69GBd DP-QPSK signal. To increase the robustness, the transceiver frequency should be fine-tuned to minimize frequency misalignment and to obtain the best media channel performance.
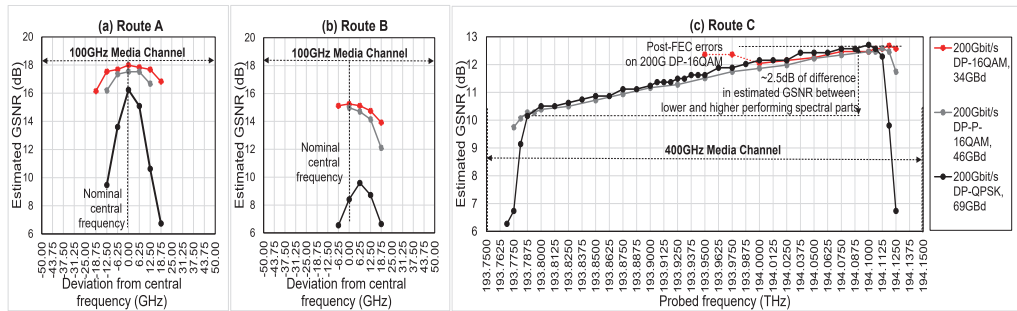

Fig. 2 Channel probing sweep results on a) route A, b) route B and c) route C

Fig.2c presents the GSNR variation over the 400GHz spectrum slot on route C. While all three modulation formats predict a similar GSNR performance, there is a 2.5 dB GSNR tilt over the media channel width and DP-16QAM (red line with extended dots) lacks sufficient margin to work at the lower 2/3 part of the slot. The knowledge of the GSNR

shape can help to maximize the total throughput of the spectral slot. Based on estimated GSNR and our example route, 300 Gbit/s 69GBd DP-P-16QAM modulation could be used at the lower end of the spectrum, while 300 Gbit/s 52 GBd DP-16QAM signals are possible at the higher end. The obtained GSNR information could also be used for a power pre-emphasis at the transmitter to equalize the signal performance across the spectral slot.

In colorless splitter/combiner based access architectures, there is a threat of impacting the neighboring channels, when signals are operated too close to the spectral slot borders and no guard-bands are used. Degradation is caused by power leakage into the neighboring slot. To investigate the severity of this scenario, we reconfigured the single 400 GHz media channel to five independent 75 GHz slots with one optical carrier per each slot. We then swept the central carrier frequency from one edge of the middle slot to the other edge.
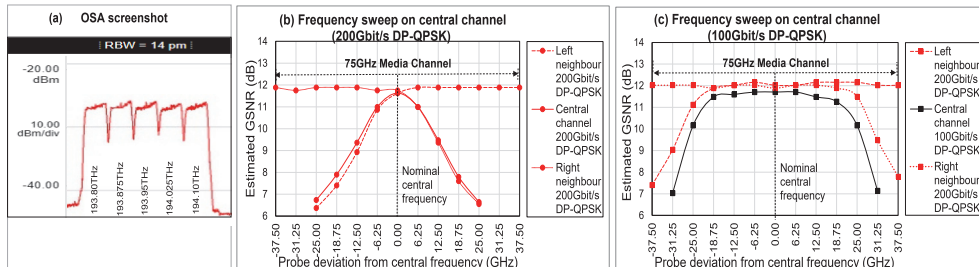
Fig. 3. Sweeping impact on the neighbouring channels in colourless directionless architectures

Fig. 3a illustrates the spectral arrangement of the signals for a crosstalk test with five 69GBd 200G DP-QPSK channels. Crosstalk is only noticeable between nearest neighbor channels. Fig. 3b shows that channels with equal symbol rates experience a similar penalty from decreased carrier spacing. This is understandable by the spectral symmetry. The spectral width of each signal is determined by its symbol rate (SR) and the roll-off factor r as (1+r)*SR and can be used to estimate how far channels need to be spaced apart to minimize crosstalk. A reduction of 6.25 GHz, 12.5 GHz and 18.75 GHz in channel spacing results in a degradation of the estimated GSNR by 0.8dB, 2.5dB and >4.4dB, respectively. Such degradation may not be acceptable in low-margin networks. In Fig. 3c, all side channels are maintained in 200Gbit/s 69GBd DP-QPSK format, while the central channel is reconfigured to 100G DP-QPSK modulation (solid black line). Due to the different symbol rate of the central channel, a spectral overlap with neighboring channels only happens at larger frequency offsets. At the same offset, the higher symbol-rate channels experience less crosstalk than the central channel due to their larger spectral width. Crosstalk becomes noticeable at 25GHz offset from the nominal central frequency of the test channel, where degradation in estimated GSNR is 1.2dB for 100Gbit/s 34GBd DP-QPSK channel and 0.9dB for 200Gbit/s 69GBd DP-QPSK neighbor. From our test results, it is recommended to run more robust signal configurations at the edges of a spectral slot to account for possible power or central frequency fluctuations in neighboring channels. Operators should also consider to allocate guard bands between media channels of different customers taking the maximum spectral width of transmitted signals into account.

4. Conclusions

We tested multiple Optical Spectrum as a Service (OSaaS) scenarios using a combined sweep and extended channel probing method. We verified that both parts of the procedure – frequency sweeping and symbol rate variable probing - do have their unique benefits in pin-pointing configuration issues and simplifying performance estimations. Based on this data, OSaaS users can take fully informed decisions, on how to leverage their spectral resources in the most efficient way without prior knowledge on the media channel envelope or impacting neighboring channels.

5. References

[1] ADVA, (2020), "ADVA Unlocks Network Potential With Spectrum As A Service ", press release, 12/03/2020
[2] Y. Pointurier, "Design of low-margin optical networks," JOCN, vol. 9, no. 1, pp. A9-A17, Jan. 2017
[3] A. P. Vela et al., "BER Degradation Detection and Failure Identification in Elastic Optical Networks," JLT, vol. 35, no. 21, Nov. 2017
[4] E. Rivera-Hartling et al., "Design, Acceptance and Capacity of Subsea Open Cables," in JLT, vol. 39, no. 3, Feb. 2021
[5] A. Ferrari et al., "GNPy: an open source application for physical layer aware open optical networks," JOCN, vol. 12, no. 6, 2020
[6] A. C. Meseguer et al., "Automated Full C-Band Technique for Fast Characterization of Subsea Open Cable G-SNR," in Proc. ACP2019, pp. 1-3, Chengdu, China
[7] K. Kaeval et al., "Channel Performance Estimations with Extended Channel Probing," in Proc. ITG-PN 2020, pp. 1-5, online.
[8] ITU-T Rec. G.807, online https://www.itu.int/rec/T-REC-G.807/en

Publication V

Kaeval, K., Fehenberger, T., Zou, J., Jansen, S.L., Grobe, K., Grießer, H., Elbers, J.P., Tikas, M., and Jervan, G., "QoT assessment of the optical spectrum as a service in disaggregated network scenarios", *Journal of Optical Communications and Networking*, 13, E1–E12 (2021).

QoT Assessment of the Optical Spectrum as a Service in Disaggregated Network Scenarios

KAIDA KAEVAL[1,2,*], TOBIAS FEHENBERGER[1], JIM ZOU[1], SANDER LARS JANSEN[1], KLAUS GROBE[1], HELMUT GRIESSER[1], JÖRG-PETER ELBERS[1], MARKO TIKAS[3], GERT JERVAN[2]

[1] *ADVA Optical Networking SE, Martinsried, Germany*
[2]*Tallinn University of Technology, Tallinn, Estonia*
[3]*Tele2 Estonia, Tallinn, Estonia*
Corresponding author: kkaeval@adva.com

The potential to operate third-party terminals over multi-domain transparent optical networks attracts operators and customers to implement Optical Spectrum as a Service (OSaaS). As infrastructure information cannot always be shared with OSaaS end customers, alternatives to off-line Quality of Transmission (QoT) estimation tools are required to assess the performance of the spectrum slot in order to estimate achievable throughput. In this paper, commercially available sliceable coherent transceivers are used to assess the Generalized Signal To Noise Ratio (GSNR) based QoT of the OSaaS in a live production network for both, narrow-band and wide-band OSaaS configurations. Extended channel probing based on symbol rate variability is combined with spectral sweeping and operation regime detection to characterize OSaaS implementations on 17 links with different underlying infrastructure configurations in order to maximize capacity and increase service margins in a low-margin operation regime. We achieve 0.05 dB estimation accuracy in GSNR for a wide-band spectrum services and 0.32 dB accuracy for narrow-band spectrum services. Based on the GSNR profile, spectral misalignment, spectral ripple and operation regime are detected and service margin improvements are demonstrated. Finally, we discuss the network optimization perspective based on acquired data from channel probing and propose use-cases for continuous channel probing in transparent optical networks.

http://dx.doi.org/10.1364/JOCN.99.099999

1. INTRODUCTION

With the high OSNR tolerance, automatic impairment mitigation and ultra-long reach of modern coherent transceivers, operators are eager to implement Optical Spectrum as a Service (OSaaS) [1, 2] in transparent optical networks. Unique for this service model, in OSaaS, the optical transceivers are owned and controlled by the service customer, whereas the open line system (OLS) is controlled by the network operator, creating the disaggregated networking environment in dense wavelength division multiplexing (DWDM) networks.

In essence, OSaaS is as a transparent lightpath connecting two endpoints in a single or multi-domain optical network, capable of carrying a single wavelength or multiple carriers over a predetermined spectrum. It is completely independent from the underlying infrastructure and can be applied to both, new flex-grid and legacy fixed-grid systems, as long as the end-to-end optical spectrum is available for the service. This allows transparent connections stretching thousands of kilometres between the terminal units, traversing multiple systems and operator domains, providing significant cost savings from both, investment and operational cost perspective.

In this paper, we refer to the spectral slot or a lightpath allocated for the OSaaS as a Media Channel (MC) as per ITU-T Recommendation G.807[3] and the wavelength service(s) inside it as Optical Tributary Signal (OTSi). The OTSi can be directly operated inside the MC, or a dedicated Network Media Channel (NMC) per OTSi can be configured. Depending on the access structures and ROADM functionalities on the OLS system, narrow-band or wide-band OSaaS can be configured. While fixed-grid access structures allow only narrow-band OSaaS configurations, typically used for "alien wavelength" services, systems with colourless access provide more options. Here, multiple adjacent narrow-band MCs or a single wide-band MC can be configured to form a wide-band OSaaS service. As signal power from alien carriers increases the vulnerability of the OLS system, narrow-band OSaaS is simpler to control and operate. However, wide-band configurations are preferred, when operation with high symbol rate signals or multiple carriers is desired to reduce the possible bandwidth narrowing effect.

A general OSaaS set-up with third-party terminals over the single and multi-domain open line system (OLS) is presented as scenario 1 and 2 in Fig. 1. While the most common usage scenario for OSaaS is a single vendor/domain scenario, the most benefits from OSaaS are obtained in
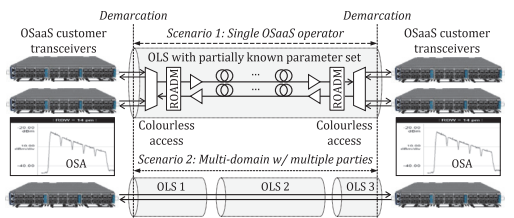
Media channel characteristic	Value	Min	Max
Allocated bandwidth (GHz)	400	193.75THz	194.15THz
Total allowed power (dBm)	9	-1	9
Allowed PSD (dBm/GHz)	-23	-33	-20
$OSNR_{0.1nm}$ @ $f_{central}$ (dB)	20	17	20
GSNR @ $f_{central}$ (dB)			
Wavelength-dependent performance variations		Not available	
Operation regime			

Fig 1. Top: General OSaaS set-up with third-party terminals over the single and multi-domain open line system (OLS), Bottom: partially available parameter set per OLS

a multi-domain environment. A perfect example of the multi-domain environment is formed by the national DWDM backbones of the small European Union countries that are connected together. A currently typical solution for the international connectivity in this scenario would require signal regeneration at the country borders, which can be avoided with OSaaS.

Contractually, OSaaS is described with the parameters listed at the bottom of Fig. 1. While the allocated bandwidth, total allowed power and power spectral density (PSD) define the input thresholds for the customer signal, the OSNR alone does not give a comprehensive overview about the achievable performance on the spectral slot. Essential characteristics to estimate the total achievable throughput of the OSaaS service, like GSNR, wavelength dependent performance variations and operation regime, are often not provided by the OLS operator.

To accurately estimate the highest achievable capacity per spectral slot and select the best suitable transceiver configuration out of thousands of possible configurations provided by the modern transceivers that still satisfy the minimum margin requirements [4], the user is required to account for all transmission impairments. This means accounting for any filtering penalties from various cascaded multiplexers, reconfigurable optical add/drop multiplexers (ROADMs) or even grating based dispersion compensation modules (DCGs) in fixed grid optical networks [5] to frequency-dependent spectral ripple caused by EDFA and Raman amplification profiles in wide-bandwidth flex-grid OSaaS scenarios. While the power-limited operation regime of the amplifiers sets the limits for the per-channel signal powers and optical power spectral density of the individual carriers, the launch powers set in the design phase of the link may not be the optimum for the selected route length. Multi-domain lightpath scenarios and any unpredictable time-varying changes in the QoT only add uncertainties to the quick yet reliable optimum performance-estimations exercise of the OSaaS. Furthermore, obtaining the knowledge about the OLS to accurately estimate the QoT in disaggregated networking scenarios may be a complicated task. As span lengths and precise system component parameters could reveal the achievable capacity and latency of the negotiated route, precise site locations along with system component data could increase the vulnerability to security related threats, making operators hesitating to share the data prior to contract signing.

To overcome the challenge, a channel probing method utilizing characterized coherent transceivers as a probing tool has been proposed to experimentally estimate the Generalized Signal to Noise Ratio (GSNR) of the lightpaths [5,6]. The usage of GSNR has proven to give reliable results in comparison with an offline GSNR based QoT estimation tool [7, 8] as well as on numerous field trials that introduce autonomous transceivers, combat routing challenges in infrastructure aware networking and estimate channel performance [9,10,11,12, 13,14]. Furthermore, the channel probing method is applicable for both OSaaS usage scenarios in Fig. 1 and can be, with small modifications to the procedure, successfully implemented to precisely capture the spectrum performance regardless of the underlying infrastructure.

The aim of this paper is to assess the unavailable OSaaS performance metrics and accordingly optimize the transceiver configurations to maximize the achievable throughput on the spectral slot allocated for OSaaS. To this end, we present a comprehensive study of OSaaS performance assessments in field deployments in a black-box-scenario [9]. We extend our previous work [15,16] with additional routes and network configurations to cover a wide variety of OSaaS configurations in live networks and propose a channel probing toolkit, consisting of symbol rate variable extended channel probing, frequency sweep and operation regime detection. Considering both flex-grid and fixed-grid production network infrastructures, we experimentally demonstrate that the proposed toolkit is able to derive OSaaS performance characteristics for any link with narrow-band or wide-band OSaaS deployment. Finally, we discuss how the knowledge acquired from channel probing can lead to increased capacity and service margins in low-margin networking scenarios.

The structure of this paper is as follows. Section 2 provides an overview about the generic channel probing concept to be used as a primary tool to characterize the OSaaS spectrum. In Section 3, general system description and test-setup is introduced, following with the results and findings explained in Section 4. The results section presents the media channel characteristics captured according to the adjusted channel probing parameters, followed by the discussion with some additional optimization possibilities in Section 5.

2. CHANNEL PROBING

Channel probing in transparent optical networks is not a new concept. Probes called active, supervisory or dummy lightpaths were used already in the early 2000's to estimate the link availability and performance in transparent optical networks [17,18,19]. These lightpaths used intensity-modulated direct-detection (IMDD) transceivers as the probing light and were commissioned to extract availability and pre-FEC bit error ratio (BER) performance data from the network link. However, the perspective of link performance estimation precision, accuracy and usage-scenarios in optical networks has been significantly widened with the concept to use characterized DSP-based modern sliceable transceivers as the probing light.

The very first attempt to use a back-to-back characterized coherent transceiver to capture the link performance was performed by Torrengo et al in 2011 [20], when they introduced the first lab experiment to verify the predecessor of the GN model [21]. The GN model by Poggiolini [22] poses that both components, the linear amplified spontaneous emission (ASE) noise and nonlinear impairments (NLI) contributing to the Generalized OSNR would have a Gaussian distribution in case of non-dispersion compensated spans. This led to a symbol rate independent GSNR to became a widely used optical link QoT metric, when the model was verified also through simulations [23,24]. Starting from 2016, the topic has gained attention in optical submarine networks as part of the implementations of disaggregated networking scenarios over the trans-Atlantic and trans-Pacific links, introducing GSNR as the primary link characteristic [25,26]

and proposing instructions for transceiver characterizations to perform accurate GSNR measurements. Since 2017, characterized coherent transceivers to estimate the link GSNR have been used in many studies, from optical link characterization [27,28,29,25] and network automation [13,30] to linear OSNR estimations [10, 31, 32], but it was only after the more intense insights to GSNR-based link characterization through characterized transceivers, provided in [5], when the topic gained real momentum.

A. General channel probing concept

To evaluate the actual channel performance of a lightpath at hand, a characterized probing-light with a fixed modulation format and symbol rate is inserted into the network in the corresponding channel location, and the pre-FEC BER estimation of the receiver, converted into a Q-value, is used to estimate the respective effective Generalized Optical Signal to Noise Ratio (GOSNR). The estimated GOSNR considers all optical distortions that impact the optical signal, including ASE noise, nonlinear distortions, as well as any transceiver impairments. This value is then normalized to the symbol rate of the Probing Light Transceiver (PLT) signal to obtain the estimated GSNR of the link ($GSNR_{est,link}$). Fig. 2 explains the general channel probing process.
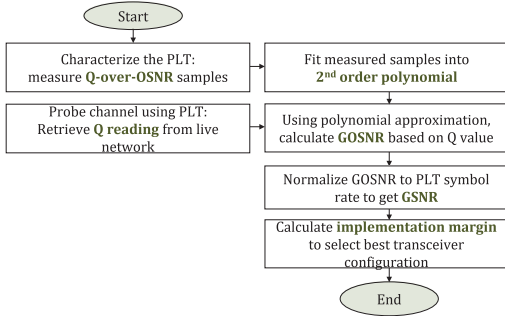

Fig 2. General channel probing concept

The accuracy of the $GSNR_{est,link}$ is defined as the difference between the estimated GSNR and the real GSNR of the link. While the characterization errors, OLS equalization and PLT data reading errors contribute to systematic error, random errors of the $GSNR_{est,link}$ are caused by performance fluctuations in time. To increase the accuracy, multiple $GSNR_{est,link}$ estimations from different PLT configurations used in a constant power spectral density mode, as per [15] can be captured. This allows to average out the errors from probing procedure and use mean value from all estimations as a final estimated $GSNR_{est,link}$.

GSNR estimations received from the channel probing form the original probing results for our spectrum QoT assessment and optimum transceiver configuration selection.

B. Accuracy of the method

To select the best possible transceiver configuration for the probed link, the GSNR implementation margin ($GSNR_{margin}$) is estimated for any tested modulation format/symbol rate configuration. To do so, typically required GSNR ($GSNR_{req}$) per configuration, available from the system specification documentation is subtracted from the estimated link GSNR ($GSNR_{est,link}$):

$$GSNR_{margin} = GSNR_{est,link} - GSNR_{req} \quad (1)$$

All calculations resulting in a positive GSNR implementation margin are expected to work over the probed link and all calculations resulting in a negative GSNR implementation margin, not to work.

As the theoretical GSNR calculations are often not available in OSaaS, the verification of the estimated $GSNR_{est,link}$ accuracy has to be also addressed experimentally. To verify the accuracy of the estimated $GSNR_{est,link}$, near zero-margin characterized PLT configurations can be used as verification signals by comparing the estimated $GSNR_{margin}$ from equation (1) to the actual performance of the PLT configuration over the tested link. Any contradiction between the estimation and real signal condition on the tested network link would indicate a false $GSNR_{est,link}$ estimation. The accuracy of the $GSNR_{est,link}$ is specified through the $GSNR_{margin}$, and is the absolute value of the highest false $GSNR_{margin}$ prediction. To increase the accuracy of the $GSNR_{margin}$ estimation, multiple $GSNR_{est,link}$ estimations per link can be captured to reduce random errors from the channel probing procedure and mean value from all estimations can be used as the final $GSNR_{est,link}$ estimation in equation (1).

According to [5], $GSNR_{est,link}$ obtained from the probing measurement can be defined as the ratio between the power of useful signal divided by the sum of the powers of all noise sources – such as ASE (SNR_{ASE}), NLI (SNR_{NLI}) and additional noise arising from the specific PLT unit modem technology used (SNR_{modem}) - evaluated wholly in the signal bandwidth and expressed as:

$$\frac{1}{GSNR_{est,link}} = \frac{1}{SNR_{ASE}} + \frac{1}{SNR_{NLI}} + \frac{1}{SNR_{modem}} \quad (2)$$

Therefore, without characterizing propagation associated penalties such as CD, PMD and PDL associated with the test, the real GSNR of the link, consisting of the SNR_{ASE} and SNR_{NLI} component only, is not available. However, $GSNR_{est,link}$ estimations are valid for the $GSNR_{margin}$ estimations for the same modem type. In [5, 33], the characterization process of the PLT unit is explained and in [10, 33], the standard deviation and accuracy for the different pre-FEC BER readings and its impact on the achievable throughput estimation dependent on a performance variability of different PLT units is explained. These references conclude that a better GSNR estimation accuracy is achieved at lower Q values since the transceiver performance variation is much smaller in that region.

Leaving aside the PLT unit dependent penalties, equation (2) is valid in optical systems, where fibre propagation impairments caused by the interplay of loss, chromatic dispersion and Kerr nonlinearity can be approximated as additive white Gaussian noise (AWGN) [22]. This raises the question of GSNR metric reliability in short spans, dispersion compensated spans and spans experiencing high nonlinear penalty. Therefore, it is important to note that the estimated $GSNR_{est,link}$ from our channel probing is not the actual, real GSNR of the link, but its projection/approximation in the linear space. Our probing results from 17 tested links show that the estimated $GSNR_{est,link}$ approximation is well usable for $GSNR_{margin}$ estimations. We attribute this to the fact, that the GN-model is meant to be used in the linear domain, where also the Q-over-OSNR characterization of the PLT unit is performed. Therefore, any measured Q value from the real-life networks is compared to the polynomial fitting from the linear domain, projecting all the link induced impairments into linear domain, too. As also the typical, required GSNR from the system specifications is only defined for linear working regime, the $GSNR_{margin}$ estimations lead us to similarly accurate estimations in each of the tested network scenarios (including short and dispersion compensated links).

C. GSNR estimation validity

In general, OSaaS characterization is performed once during the service handover. Although channel probing provides reliable end-to-end GSNR estimations, the estimation results are only valid for the infrastructure configuration and network load during the probing activity. There are two options to accommodate the future degradations from possible daily fluctuations, aging effects and network load/condition changes: a) incorporate additional margins as per [4] to

the initial estimated $GSNR_{margin}$ to increase the robustness of the OSaaS live traffic or b) implement continuous probing. While the first is a fixed measure and only protects the OSaaS user within the degradation range set by margin, the later provides continuous performance estimations from the network. When data from continuous probing is used to train the machine learning (ML) algorithm, performance changes in OLS can be predicted and notifications can be sent to OSaaS user in case of abnormal changes.

Any major change in the network (including power distribution change between channels, changes causing increased filtering penalty, reroute, etc) should be carried out during the maintenance window and followed by a new OSaaS characterization. Depending on the width of the spectrum slot, full characterization incorporating extended channel probing, frequency sweep and operation regime detection can take up to an hour for a 100-GHz OSaaS service. The time required is primarily dependent on the number of PLT configurations used and stabilization times of the commercial transceivers. The set of PLT configurations can be customized according to link parameters.

3. GENERAL SYSTEM AND TEST SET-UP DESCRIPTION

To demonstrate the feasibility of the channel probing method in field deployments, we tested 17 different links in Tele2 Estonia's live networks. Twelve (12) links with lengths from 3 km to 1302 km were tested in a 10-Gbit/s optimized fixed-filter dispersion compensated ROADM based regional-haul network (routes A, B and C). The OSaaS service is configured with the 100-GHz nominal slot size in this network, making this a narrow-band OSaaS service, as the signals were added and dropped by arrayed waveguide grating (AWG) filters. Route A uses dispersion compensating fibres (DCFs) for optical dispersion compensation, whereas route B and C use a mix of DCFs and dispersion compensating gratings (DCGs). The central frequency of 193.2 THz was used on all of the links. Five links with lengths from 1016 km to 5738 km were tested in a pan-European coherent optimized flex-grid ROADM based long-haul dispersion compensation module (DCM) free network with colourless access architecture (route LH). The nominal slot size in this network is 50 GHz and a 400 GHz wide media channel with the central frequency 193.95 THz was configured for the channel probing tests, illustrating the wide-band OSaaS scenario. The OSaaS user spectrum was added and dropped at a free terminal ROADM port using 8:1 splitter/combiner module in test-site without applying additional optical filtering.

The underlying fibre infrastructure for all links and both networks conforms to the ITU-T 652.D standard for standard single mode fibres (SSMF). To extend the transmission distance and to allow single-ended measurements at test-site, the spectrum services were looped back in the far end ROADMs. Link specific data is given in Table 1.

The test set-up and spectral assignments of the links are illustrated in Fig. 3. Spans with black colour refer to DCM-free network infrastructure,

Table. 1: Link data

Loop-back	Network	DCM data	Looped link length	No of spans
A-4	Regional	DCM free	4km	2
A-144	Regional	DCF	144km	4
A-241	Regional	DCF	241km	6
A-382	Regional	DCF	382km	8
A-652	Regional	DCF	652km	12
B-70	Regional	DCF	70km	4
B-485	Regional	DCF+DCG	485km	8
B*-621	Regional	DCF+DCG	621km	10
B-822	Regional	DCF+DCG	822km	12
B-1182	Regional	DCF+DCG	1182km	16
B+2-1302	Regional	DCF+DCG	1302km	18
C-284	Regional	DCF+DCG	284km	4
LH-1016	Regional	DCM free	1016 km	14
LH-1792	Long-haul	DCM free	1792 km	24
LH-2943	Long-haul	DCM free	1792 km	36
LH-3751	Long-haul	DCM free	3751 km	48
LH-5738	Long-haul	DCM free	1792 km	74

while grey and orange mark the links compensated via dispersion compensation fibres (DCF) or dispersion compensation gratings (DCG) modules, respectively. Link acronyms are combined from route name and looped length of the link, for example A-144, B-485, C-284 or LH-1016. The only channel routed over two different routes on the link is B+A-1302 that was first routed over route B and then, starting from B-822, over route A.

The probing unit was implemented on reconfigurable TeraFlex transceiver from ADVA, providing 100 Gbit/s to 600 Gbit/s capacity per carrier by adjusting the modulation format and symbol rate. All tests were run with reduced power levels compared to the allowed maximum power levels per media channel, to avoid any impact on the live channels. Therefore the results do not allow to derive the end-of-life network capacity capabilities, which is business-critical information for the network operator.

The field networks with different sets of infrastructure components, like multiplexers, amplifiers, boosters, and ROADMs, set a good playground to demonstrate the capabilities of the channel probing toolkit in characterizing the spectral slot performance and optimizing the transceiver configuration, operation regime and transmission impairments regardless of the underlying network infrastructure and condition.

The probing exercises were carried out over a ten-month time-period between May 2020 and February 2021. For all estimated GSNR estimations in this work, a constant power spectral density was used.
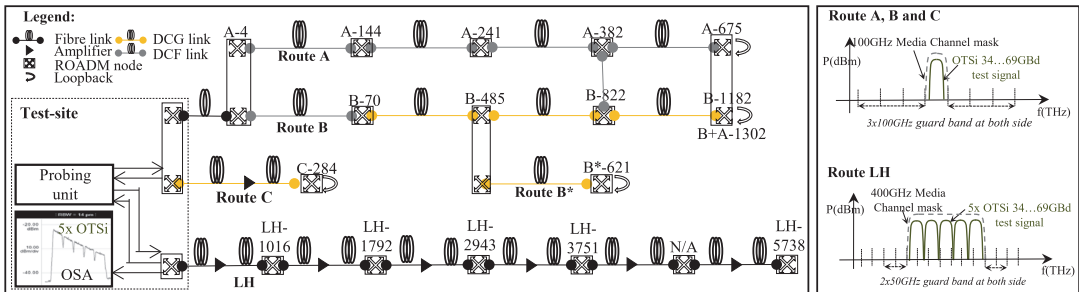

Fig. 3 General test set-up and spectral assignments on the routes

4. RESULTS

In this section we use channel probing method introduced in Section 2 to assess the missing parameters from Fig. 1 to fully characterize the spectrum slot performance and optimize the transceiver configuration to maximize the throughput. By adapting the symbol rate, frequency and power of the PLT configuration, we detect the possible filtering effects and estimate the GSNR of the spectrum slot, capture wavelength dependent performance differences within the OSaaS service and detect the operation regime.

A. Symbol rate variable channel probing

As the generic channel probing method introduced in section 2 can provide reliable spectrum performance estimations only for the exact bandwidth covered by the PLT configuration in the same probed power regime, a single measurement may introduce a bias in $GSNR_{est,link}$ estimations in case of bandwidth limited OSaaS. To address this, we use eleven pre-characterized PLT configurations in power spectral density-based probing regime, as suggested in [15] to estimate the $GSNR_{est,link}$.

As the maximum achievable linear OSNR of the link is fixed due to design-based power levels, the non-linear impairments from the transmission media set the maximum achievable GOSNR on the link. However, optical links can introduce bandwidth narrowing due to ROADMs, multiplexers or grating based dispersion compensation modules. While the mild penalty from bandwidth narrowing can be compensated in the transceivers, any significant bandwidth limitation could cause the degradation on achievable performance.

In networks without bandwidth limitations, probing operated with constant PSD should return constant GSNR estimations regardless of the required bandwidth of the PLT configuration. Fig. 4 (a) presents the original probing results from the long-haul dispersion compensation free network with a colourless access architecture. The X-axis present the link length in kilometres and the Y-axis the estimated GSNR, obtained by using different PLT configurations. As visible, all measurement results regardless of the PLT configuration are concentrated within ±0.4 dB around the probable GSNR of the link with no differentiation from the used symbol rate or the modulation format of the PLT unit.

This sets a straight-forward way for $GSNR_{est,link}$ calculations based on the average estimated value from all of the working PLT configurations. Achieved $GSNR_{est,link}$ can be then further used to derive $GSNR_{margin}$ as per equation (1). Fig. 4 (b) presents the achievable accuracy of the $GSNR_{margin}$ estimation based on the averaged $GSNR_{est,link}$ estimation from all working PLT configurations in long-haul network. Cross marks accompanying the near-zero margin estimation indicates the false estimation, where the verification signal condition as per measurement did not agree the estimated signal condition. Here, the X-axis presents the link length in kilometres and the Y-axis the estimated $GSNR_{margin}$ for different PLT configurations. Different marker styles refer to different symbol rates and line styles distinguish different modulation formats. The chart is zoomed in for the area near zero implementation margin, where the probability of false estimations is highest. Using symbol rate variable channel probing, 0.05 dB in $GSNR_{margin}$ accuracy in the long-haul network was achieved compared to previously reported 0.7 dB [34]. This can be attributed to multiple GSNR estimations for the same link provided by symbol rate variable probing, as it allows to average out the small time-dependent performance fluctuations in the network that cause different BER readings, and thus the variation in Q-value per each measurement.

Modern flex-grid networks with colourless access architectures are less prone to experience bandwidth limitations or these can be overcome by simple reconfigurations in the ROADMs. Bandwidth narrowing, however, is a problem in legacy fixed-filter systems. In case of significant bandwidth limitation, high symbol rate signals are subject

(a) Original probing results from symbol rate variable probing on long-haul network

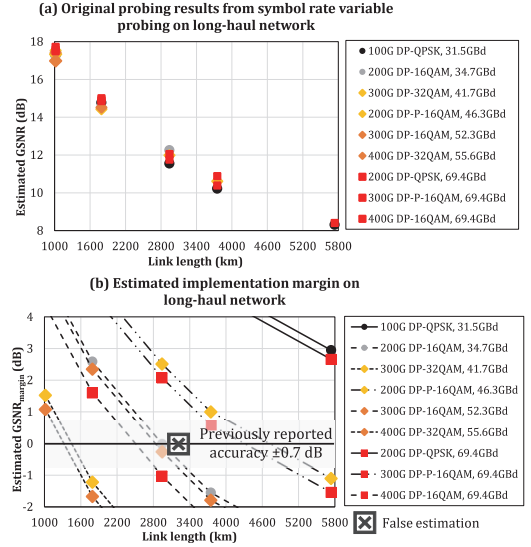(b) Estimated implementation margin on long-haul network

Fig. 4 (a) Results from symbol rate variable channel probing and (b) $GSNR_{margin}$ estimations for a long-haul network

to stronger narrow band filtering and using a wideband probing signal results in underestimating the link GSNR that would be achievable for lower symbol rate signals. Using narrow band probing configurations would create the illusion of a link with a high GSNR not achievable for higher symbol rate signals.

This effect can be assessed with GSNR penalty, which is a systematic decrease in estimated GSNR, caused by the variation in PLT symbol rate, modulation format, frequency or power setting. As theoretical, calculated GSNR values for the link are often not available for the OSaaS end user, GSNR penalty for the specific configuration under interest can be calculated as a GSNR estimation difference between the highest performing PLT configuration and the configuration under interest, measured on the same transmission link. To verify the symbol rate dependent changes in GSNR estimations caused by bandwidth limitation and eliminate the GSNR estimation differences due to non-linear behaviour, back-to-back measurements (with 0-km fibre length) to characterize the filtering penalty were carried out in the lab, emulating the first link on route A. This link includes two ROADM modules and three arrayed waveguide grating (AWG) based multiplexer modules and defines the minimum filtering penalty on all the links in the regional-haul network. Fig. 5 presents the results of the back-to-back (b-2-b) measurements for the symbol rate dependency of
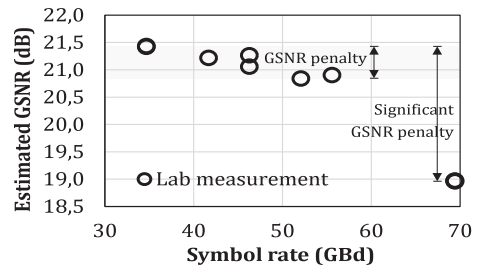

Fig. 5 Symbol rate variable probing results from b-2-b measurement

the estimated GSNR. The X-axis represent the symbol rate of the PLT configuration and the Y-axis present the estimated GSNR. While the estimated GSNR decreases up to 0.6 dB compared to the highest performing PLT configuration at 34.5 GBd for the symbol rates up to 55.5 GBd, PLT configurations with 69.4 GBd experience significantly higher GSNR penalty, reaching almost up to 2.5 dB. This behaviour can be explained with a bandwidth limitation penalty from the AWG based channel filter modules (3-dB bandwidth of 80 GHz) and ROADMs.

The probing results from the symbol rate variable channel probing in regional-haul network are presented in Fig. 6 (a). The X-axis presents the link length in kilometres and the Y-axis the estimated GSNR in dB. As expected, the link GSNR estimations by different PLT configurations are highly scattered for the legacy regional-haul links due to symbol rate dependent GSNR penalty caused by bandwidth narrowing. This leaves the average estimated GSNR value just as a statistical number for the bandwidth limited regional-haul network and further analyses on the original probing results are required to estimate the $GSNR_{est,link}$.

According to our results on Fig. 6 (a), PLT configurations with equal symbol rate experience similar penalties from the system and estimate the link GSNR with ±0.35 dB accuracy, regardless of the modulation type for up to 55.5 GBd signals, whereas a change to 69.4 GBd symbol rate in the PLT configuration resulted in a great variance in the estimated GSNR on live links. While the maximum variance between the estimated GSNR on links shorter than 500 km is below 0.7 dB for the probe settings between 31.5 and 46.3 GBd and below 1.1 dB for the probes up to

55.6 GBd, it quickly grows up to 7.1 dB for the probes including 69.4 GBd. For the links up to 1000 km, these figures are 0.7 dB, 1.3 dB and 7.5 dB, respectively. In addition to the bandwidth limitation penalty from the channel filter modules and ROADMs for the DCF based links, additional penalty from DCG modules (3-dB bandwidth of 60 GHz) is captured on the links including grating based dispersion compensation modules. For the two longest links in regional-haul network, only two PLT configurations between were working, having a GSNR penalty of 1.3 dB between the 31.5 and 46.3 GBd configurations. Fig. 6 (b) presents GSNR penalty for the PLT configurations that do not experience severe GSNR penalty from filtering. As visible from the figure, cascaded filtering from multiplexers, ROADMs and DCG modules decreases the effective bandwidth of the OSaaS on longer links, increasing the GSNR penalty even for the same PLT configurations.

In order to estimate the best possible transceiver configuration for the OSaaS offering at hand, it becomes essential to identify the highest usable symbol rate on the link – a symbol rate cap. To identify the symbol rate cap for the link, two criteria must be met: a) it must be acquired through working PLT configuration with the highest symbol rate and b) it does not experience significantly higher GSNR penalty compared to the other working PLT configurations on the link. According to our tested OSaaS services on Fig. 6 (b), four of the shortest links have a symbol rate cap 55.6 GBd. That is decreased to 52.3 GBd for links up to 1000 km and only 46.3 GBd for the longest two links. As visible from the Fig. 6 (b), the absolute values of the GSNR penalty itself are not consistent along the links nor important as long the two criteria for the symbol rate cap identification are met. All configurations exceeding the symbol rate cap should be removed from the pool of possible transceiver configurations before the $GSNR_{margin}$ calculation. In Fig. 6 (a), this means leaving out all high symbol rate configurations marked with red.

Then, the average estimated $GSNR_{est,link}$ can be calculated also for the bandwidth limited network, using the GSNR estimation results from PLT configurations with smaller and equal symbol rate than the symbol rate cap. The best transceiver configuration can be selected as per highest line rate from all possible configurations returning positive implementation margin as per equation (1).

Fig. 6 (c) presents the achievable accuracy of the $GSNR_{margin}$ estimation in legacy network together with the verification signal condition. The X-axis presents the link lengths in kilometres, and the Y-axis estimated $GSNR_{margin}$ in dB-s for the different PLT configurations. Different marker styles refer to different symbol rate regimes and line styles distinguish different modulation formats. The chart is zoomed in for the area near zero implementation margin and cross marks placed near the $GSNR_{margin}$ marker indicate the correctness of the estimation.

Following the identification of the symbol rate cap and applying this to original data from symbol rate variable channel probing, we achieved the selection of the best possible transceiver configuration with the estimation accuracy better than 0.10 dB for the links up to 822 km and 0.32 dB on the links up to 1302 km on the regional-haul network. The primary errors contributing to the false positive $GSNR_{margin}$ estimations were on the link B-1182 km, where the small number of working PLT configurations may have not contributed enough for the required averaging effect, to achieve more accurate $GSNR_{est,link}$ estimation. However, considering the margin values generally implemented for network robustness against aging and slow performance changes, the achieved result is an accurate measure of the network performance at a current moment.

B. Channel probing with frequency sweep

To capture the possible performance differences over the wider spectral slots, generic channel probing procedure introduced in section 2 must be repeated with sweeping the central frequency over the
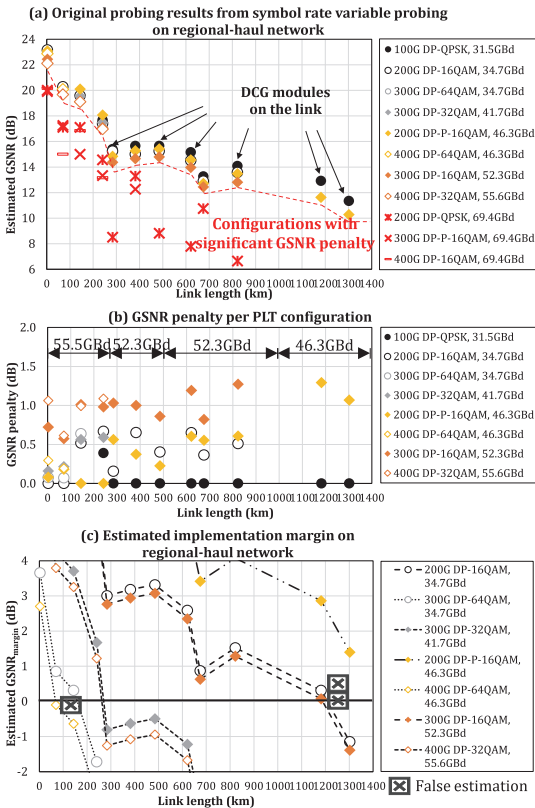

Fig, 6 (a) Results from symbol rate variable channel probing, (b) GSNR penalty and symbol rate cap and (c) $GSNR_{margin}$ estimations for a regional-haul network

available spectral slot with a suitably selected frequency step increments. For this, the frequency sweep exercise, similar to proposed in [35] was modified to OSaaS use-case, to detect the possible bandwidth limitations, frequency misalignments and spectral ripple/tilt on links A-241, C-284 and LH-1792.

A 100-GHz narrow-band spectrum service was investigated on routes A and C, whereas a 400-GHz wide-band service was used on route LH. Spectrum assignment for the tested routes are brought in Fig. 3. The channel performance on all routes was tested with reduced number of probes, utilizing only 200-Gbit/s 69-GBd DP-QPSK, 200-Gbit/s 46-GBd DP-P-16QAM, and 200-Gbit/s 34-GBd DP-16QAM probing signals with root raised cosine (RRC) spectral shape (roll-off factor r = 0.19). The DP-P-16QAM modulation format stands for a proprietary DP-8QAM, which is implemented using only partial constellation points from the standard constellation of the DP-16QAM modulation format. To obtain comparable results, constant power spectral density is maintained for all PLT configurations. This is possible when the DWDM line systems and their amplifiers operate in constant gain mode. The spectrum performance is evaluated by a GSNR, captured by sweeping in 6.25 GHz frequency steps over the allocated spectrum.

Fig. 7 shows the results of the channel probing on the routes A and C. While the nominal media channel width on route A and C is 100 GHz, the large predicted GSNR difference between the three modulation formats reveals that the usable effective optical bandwidth must be much smaller. Given that a 6.25-GHz mismatch of a 34-GBd signal already causes a noticeable penalty, we can conclude that the effective optical channel bandwidth is lower than 50 GHz. In Fig. 7 (a), up to 2 dB degradation in the estimated GSNR is observed for a 200-Gbit/s 34-GBd DP-16QAM signal configuration in case of 18.75 GHz offset. With the same offset, 200-Gbit/s 46-GBd DP-P-16QAM and 200-Gbit/s 69-GBd DP-QPSK signals are already experiencing outage as the attainable GSNR is insufficient.

The results in Fig. 7 (b) also indicate a misalignment of the nominal centre frequency on route C in addition to severe filtering penalty for the 200 Gbit/s 69-GBd DP-QPSK signal format. Without sweeping, this misalignment could have been left undiscovered and already a small fluctuation in the transceiver wavelength could cause a severe degradation of the service quality, especially with 46-GBd DP-P-16QAM modulation that generally requires higher margin, than a 200 Gbit/s 69-GBd DP-QPSK signal. To increase the robustness, the transceiver frequency should be fine-tuned to minimize frequency misalignment and to obtain the best spectrum performance.

Fig. 8 presents the GSNR variation over the LH-1792 link in a single 400 GHz media channel and a 5x75 GHz adjacent media channel configurations, the latter effectively providing a 375 GHz wide spectrum slot along with the approximation of the 69.4 GBd signal spectral shape. We call the representation of estimated GSNR over the OSaaS spectrum a GSNR profile. GSNR profile helps the wide-band OSaaS end users to evaluate the impact of the wavelength dependent performance
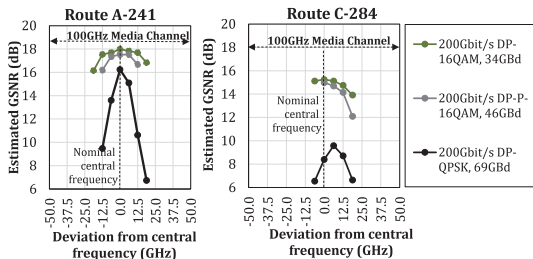
variations on achievable throughput in the OSaaS spectrum. It demonstrates the severity of filtering at the media channel edges and any ripple/tilt in the OSaaS performance over the spectrum. In general, GSNR profiles captured with the smallest bandwidth and frequency increment provided by the PLT unit have the highest granularity for intra-spectrum performance estimations. This is due to the fact that wide-band PLT configurations may not distinguish any dips in the spectrum caused by adjacent concatenated media channels. Generally wider frequency step may not capture the smaller performance changes in the spectrum. This is illustrated with the coarse sample set of the DP-P-16QAM modulation format data set on Fig. 8. GSNR profile captured with smaller frequency increments, than any modern coherent signal bandwidth enables OSaaS customers to decide the best possible transceiver configurations for any part of the spectrum, to maximize the OSaaS throughput.

According to our measurements, all three modulation formats predict a similar GSNR performance with a maximum deviation of 0.25 dB in $GSNR_{est,link}$ for the 400 GHz spectrum configuration, and up to 0.53 dB $GSNR_{est,link}$ difference between the captured $GSNR_{est,link}$ datapoints for the coarse sample set of the 5x75 GHz configured OSaaS. Higher deviation in results in this case can be attributed to a time dependent variation in the network performance, as the samples in this case were collected on different days. Based on the GSNR profiles, 400 GHz single MC and 5x75 GHz adjacent MC OSaaS configurations have a different wavelength dependent performance that is caused by the different intra-OSaaS equalization schemes.

The most evident is a 2.5-dB GSNR tilt over the 400 GHz wide MC configuration that leads the DP-16QAM probe configuration, requiring generally higher GSNR to lack sufficient margin to work at the lower part of the spectrum slot. Although this difference can be reduced to 0.3 dB GSNR tilt when operating 5x75 GHz network media channel configuration, it reveals that the signal degradation caused by underlying infrastructure cannot fully be diminished with equalization. This can be accounted for the Raman-enabled amplification scheme of the LH route, creating a spectral ripple in the amplified C-band region with peak performances following the Raman pump locations and valleys in the between areas. Although the equalization at the ROADM nodes helps to balance out this difference, the underlying effects from the longest hops on the infrastructure are still detectable in estimated $GSNR_{est,link}$. Based on the longest span examples, the signals travelling in the valley part of the spectrum are more prone to linear OSNR depletion in the end of the links due to reduced effectiveness of the Raman amplification in the valley areas of the spectrum, resulting in overall reduced power levels and OSNR. The signals travelling at the peak parts of the spectrum are more prone to nonlinear effects, as their power levels in the beginning of each new network span after the equalizing ROADM are generally higher than average. While the ripple effect may

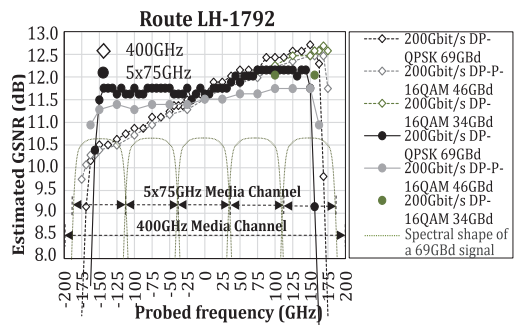Fig. 7 Channel probing sweep results on a) route A and b) route C

Fig. 8 Sweep results on LH-1792 with 400 GHz MC and 5x75 GHz MC

not be relevant for medium-haul distances, it does create a performance difference between different spectral locations on the longer spans.

Based on the estimated GSNR and GSNR implementation margins at different parts of the spectrum on our example route, 300-Gbit/s 69-GBd DP-P-16QAM modulation could be used at the lower end of the spectrum, while 300-Gbit/s 52-GBd DP-16QAM signals are possible at the higher end. For the 5x75 GHz media channel configuration, regardless of the 0.3 dB Q-value difference over the spectrum service, the achieved GSNR allows only 300-Gbit/s 60-GBd DP-16QAM/DP-P-16QAM hybrid configuration to be used over the whole 5x75GHz spectrum. In addition, 200-Gbit/s 34-GBd DP-16QAM PLT configuration in 5x75 GHz media channel configuration only works for a few central frequencies over the tested spectral slot, experiencing post-FEC errors on the rest of the tested frequencies.

Although for the current link both configurations resulted in the same usable capacity carried within the tested wide-band OSaaS service, longer links may introduce a difference in total achievable bandwidth between two configurations. At any case, the GSNR performance information obtained by this measurement could be used for a power pre-emphasis at the transmitter to equalize the signal performance across the spectral slot and increase the service margins.

C. Channel probing with power adjustments

According to [36], the maximum channel performance is reached at an optimal power, where the amplified spontaneous emission noise power is twice the nonlinear noise power. In many production networks, per channel to-the-line launch powers are optimized per amplifier output, by dividing the maximum amplifier output power with the number of end-of-life channels. This is mostly a fixed figure used to commission all the links and is rarely adjusted according to the specific span length between two amplifier stations or even less likely, according to the total link length. And although the available simulation or planner tools enable to estimate the non-linear penalty per link, the opportunity is mostly used in the commissioning stage of the new network and forgotten in operation state. While the new, high-performing transceivers enable to overcome the small degradations or changes implemented after the initial commissioning, it may introduce changes in the optimal operation regime and reduce service margins.

One straight-forward way to detect the per channel optimum operation is to increase the individual channel powers to see when the top of the SNR vs. power (or "bell") curve is achieved. Unfortunately, within power limited networks, this could lead to amplifier saturation or performance degradation on neighbouring channels due to spectral hole burning effect. Therefore, a method that accounts for the maximum total power allowed by the spectrum slot is required.

This can be achieved by comparing the results received from symbol rate variable channel probing with constant PSD to the constant signal power measurements. Measurements with constant signal power use only the highest allowed total signal power for all tested symbol rates (effectively, increasing the PSD for the narrower signal formats). In both cases, the total power per probing activity stays equal or below the maximum allowed power per spectral slot and reference power used for the network equalization.

A selection of links on the route A in the regional-haul network were analysed by comparing the design-based PSD mode GSNR estimations to design based signal power mode GSNR estimations. The operation regime detection results are presented on Fig. 9. The solid lines are the probing results with single, constant signal power for all PLT configurations and dotted lines are the same PLT configurations tested with PSD adjusted power levels. Different shades/colours refer to different link lengths. The visible symbol rate dependent tilt on the GSNR estimations on the lines measured with constant PSD refer to
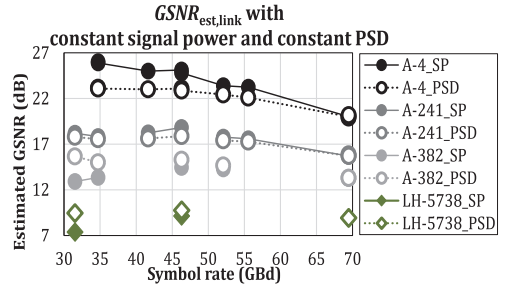

Fig. 9 Detection of the operation regime on different links

filtering penalty from the route. As a reference, also one link from the long-haul network is included on the Fig. 9, presented with diamond marker shape. For each of the links, the reference PSD and reference total allowed signal power per carrier is at 69 GBd, where the measurement lines for the constant PSD and constant signal power meet.

The operation regime of the specific configuration can be detected by comparing the estimated GSNR values for the constant PSD and constant signal power line. For the shorter links (black and dark gray lines), probing with constant signal powers provides better GSNR performance than probing with constant PSD. This means, the signals still do benefit from increased launch power, hence working in the linear regime. For the longest link in regional-haul network (light gray) and long-haul network (green), the constant signal power probing provides worse GSNR estimations, than the constant PSD probing. This indicates that, with constant signal power, the increased PSD of individual narrowband signals is too high, and the signal power is above the optimum between ASE noise and nonlinear distortions. This means, a reduction of the signal power at the specific OTSi should be considered.

It is worth mentioning that while the simple operation regime detection is sufficient in narrow band OSaaS configurations, wide-band OSaaS offerings may experience operation regime differences in different spectral parts of the OSaaS service. This has an increased probability in cases where high tilt is captured through the spectral sweep exercise. It is therefore recommended to carry out operation regime detection over the spectral range of the OSaaS service to characterize the spectral slot for highest usable power levels.

By detecting the operation regime, operators can adjust the to-the-line power levels per channel and per link to increase the service tolerance against random fluctuations in network performance that can lead to outages, when channels are operated at the BER threshold. Based on our example, it can be seen that while the $GSNR_{margin}$ can be improved up to +/- 2.5 dB for 31.5-GBd and 34.7-GBd signals depending on the link, the improvement on 46.3-GBd and 52.0-GBd signals is less, than 0.8 dB. However, this can be a great improvement when operated in low-margin regime.

The detected operation regime and possibility to increase to-the-line launch power levels only applies to narrow-band signals and does not impact the overall maximum allowed signal power per spectrum slot. Therefore, the power levels of the higher symbol rate signals can be only adjusted to lower levels, to avoid violations against contractually agreed highest total power per spectral slot. With verified filtering penalty, the power cut away by the filtering elements on higher symbol rate signals can be compensated by increasing the equalization threshold in the ROADM for the specific channel. However, verification of this opportunity is out of the scope of this paper, as it would require changes in the OLS parameters that spectrum end user cannot control.

5. FURTHER SYSTEM OPTIMIZATION POTENTIAL

In this section, we propose network optimization use-cases that focus on the throughput optimization potential based on the data acquired through the spectrum probing process.

A. OLS optimization potential

Based on the results from spectrum QoT characterization with symbol rate variable channel probing in narrow-band OSaaS scenario, it is possible to evaluate the impact of the filtering penalty on the total achievable capacity on the network link. To illustrate this, we use the probing results for the regional-haul network from section 3-A. First, we plot the achievable throughput per channel and link based on $GSNR_{est,link}$ and $GSNR_{margin}$. These are illustrated with black bars on Fig. 10. Then, the potential throughput increase is estimated based on the PLT configuration that did not experience bandwidth limitation: 200-Gbit/s 34-GBd DP-16QAM or 100-Gbit/s 31-GBd DP-QPSK. These throughput calculations, indicating the achievable throughput gain from a system without any filtering penalty, are shown with green bars on Fig. 10. While only a small increase can be achieved due to moderate filtering effects on short distances, up to 100% increase can be achieved on links with additional filtering penalty from the DCG modules. For some links, getting rid of filtering elements would only bring performance improvement in service margin, but not a change in the maximum achievable line rate (link length 675 km). However, considering the average increase per channel, the total throughput increase would aggregate to 4-Tbit capacity gain, when implemented over the full C-band in a 40-channel system.
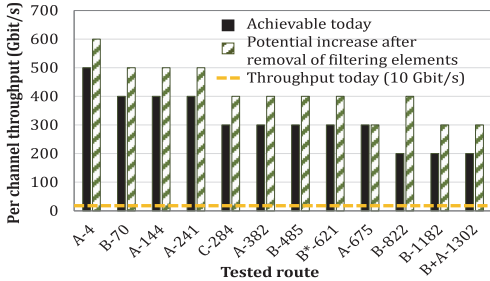

Fig. 10 Achievable and potential throughput estimations

This data can be used to make network upgrade decisions like adding colourless access structures. Caution must be taken when swapping DCG based dispersion modules to DCF based modules, as this could increase the nonlinear penalty on the link that might deplete the expected benefits from swapping the modules on the longer links (675-km link example). If possible, in the long run, going uncompensated and fully coherent also on the old legacy infrastructure links should be considered as an option instead.

B Time-dependent optimization potential

While the primary usage scenario for the channel probing toolkit is to characterize the spectrum slot QoT performance in disaggregated networking scenarios, the initial spectrum characterization only covers the QoT performance at the time of the characterization. To overcome that, continuous channel probing utilizing already commissioned transceivers could be used to monitor the changes in OSaaS service performance. These changes could be caused by daily and yearly variations in the network, added crosstalk penalty from changed channel load in the neighbouring spectrum or other. Continuous channel probing enables spectrum end users to learn about the daily

and yearly changes in the network performance and use the gained knowledge in running higher capacities during the network peak performance times. This can be useful in data-centre connectivity. According to our observations over the 10-month test-period, daily changes on a LH-3752 link during the summertime, impacted the estimated link GSNR on average 1.5 dB per 24 h period, while the performance fluctuations during the colder months reached at most 0.4 dB in amplitude per 24 hours. Since a better performance was observed during the colder night-time, users can optimize their higher-capacity demanding database back-ups to be run at night-time. On the observed link, 1.5 dB of GSNR difference would allow to switch from the default 200-Gbit/s 69-GBd DP-QPSK signal configuration to 200-Gbit/s 58-GBd DP-QPSK/DP-P-16QAM hybrid modulation and therefore reduce the required bandwidth from 75 GHz to 62.5 GHz per carrier, resulting in 2.56 Tbit/s capacity gain over C-band.

The benefits of continuous channel probing can also be used by the OLS operator. Probes operated inside the guard-band channels can be treated as a network monitoring point to perform OSaaS service policing in addition to general network performance monitoring and fault detection. Single characterized transceiver can be used to monitor multiple links. For this, an optical switch could be used to send the probing signal into different channel locations in multi-domain disaggregated network environments, providing ms-range switching time on already pre-provisioned lightpaths compared to reconfigurations in the ROADMs. These usage scenarios require additional research to provide solutions that reduce the investments costs per monitoring point.

6. CONCLUSIONS

In this paper, we have presented a practical toolkit based on the channel probing concept to characterize the QoT performance of the Optical Spectrum as a Service (OSaaS) in narrow-band and wide-band configurations. We have shown that the proposed methods and processes work over different network scenarios, utilizing both dispersion compensation free flex-grid systems and dispersion compensated fixed-grid filter-based systems. Symbol rate variable extended channel probing has been demonstrated to achieve a GNSR estimation accuracy of 0.05 dB for a wide-band OSaaS service compared to previously reported 0.7 dB and 0.32 dB for a narrow-band OSaaS service experiencing strong narrow band filtering. We have further presented the usefulness of spectral sweeping to capture the GSNR profile that could be used in OSaaS service contracts to demonstrate the service bandwidth and give insights to the OSaaS service performance and configuration. We have also demonstrated the usefulness of the operation regime detection in order to detect wavelength dependent performance differences within OSaaS, which allows to maximize service margins. Based on the performance data acquired from the proposed channel probing toolkit, spectrum users and OLS system operators can take fully informed decisions on how to leverage their spectral resources in the most efficient way without prior knowledge on the link set-up, channel transfer function or other impacting aspects, like operation regime, filtering penalty, neighbouring channel crosstalk, or other, directly contributing to GSNR of the service.

In our future research, we will investigate the impact of the different OSaaS configurations to GSNR profiles and compare it to other available metrics, capturing wavelength dependant performance relevant for OSaaS services.

References

1. K. Grobe, C. Fürst, A. Autenrieth, and T. Szyrkowiec, "Flexible spectrum-as-a-service," In TERENA Networking Conference (TNC), (2014).
2. ADVA, (2020), "ADVA Unlocks Network Potential With Spectrum As A Service, " press release, 12/03/2020
3. ITU-T Rec. G.807, online https://www.itu.int/rec/T-REC-G.807/en
4. Y. Pointurier, "Design of low-margin optical networks", Journal of Optical Communications and Networking, 9(1), pp.A9-A17 (2017)
5. E. Rivera-Hartling, P. Pecci, and M. Priyanth, "Subsea Open Cables: A Practical Perspective on the Guidelines and Gotchas," in Proc. Suboptic, Plenary (2019)
6. V. Curri, "Software-defined WDM optical transport in disaggregated open optical networks," In Proc. of 22nd International Conference on Transparent Optical Networks (ICTON), pp. 1-4 (2020)
7. A. Ferrari, M. Filer, K. Balasubramanian,Y. Yin, E. Le Rouzic, J. Kundrát, G. Grammel, G. Galimberti, and V. Curri, "GNPy: an open source application for physical layer aware open optical networks," Journal of Optical Communications and Networking, 12(6), pp.C31-C40 (2020)
8. A. Ferrari, J. Kundrát, E. Le Rouzic, M. Filer, A. Campanella, A. D'Amico, K. Balasubramanian, Y. Yin, O. Havliš, M. Hažlinský, and J. Vojtěch, "The GNPy Open Source Library of Applications for Software Abstraction of WDM Data Transport in Open Optical Networks," In Proc. of 6th IEEE Conference on Network Softwarization (NetSoft), pp. 386-394 (2020)
9. J. Slovak, M. Herrmann, W. Schairer, E. Torrengo, K. Pulverer, A. Napoli, and U. Häbel, "Aware optical networks: Leaving the lab," Journal of Optical Communications and Networking, 11(2), pp.A134-A143 (2019)
10. Y.R. Zhou, K. Smith, J. Weatherhead, P. Weir, A. Lord, J. Chen, W. Pan, D. Tanasoiu, and S. Wu, "Demonstration of a Novel Technique for Non-Intrusive In-Band OSNR Derivation Using Flexible Rate Optical Transponders Over a Live 727 km Flexible Grid Optical Link," Journal of Lightwave Technology, 35(20), pp.4399-4405 (2017).
11. C. Delezoide, K. Christodoulopoulos, A. Kretsis, N. Argyris, G. Kanakis, A. Sgambelluri, N. Sambo, P. Giardina, G. Bernini, D. Roccato, and A. Percelsi, "Marginless operation of optical networks," Journal of Lightwave Technology, 37(7), pp.1698-1705 (2019)
12. B. Spinnler, A.X. Lindgren, U. Andersen, S. Melin, J. Slovak, W. Schairer, K. Pulverer, J. Mårtensson, E. De Man, G. Khanna, and R.H. Derksen, "Autonomous intelligent transponder enabling adaptive network optimization in a live network field trial," Journal of Optical Communications and Networking, 11(9), pp.C1-C9 (2019)
13. S. Oda, M. Miyabe, S. Yoshida, T. Katagiri, Y. Aoki, T. Hoshida, J.C. Rasmussen, M. Birk, and K. Tse, "A learning living network with open ROADMs," Journal of Lightwave Technology, 35(8), pp.1350-1356 (2017)
14. K. Christodoulopoulos, C. Delezoide, N. Sambo, A. Kretsis, I. Sartzetakis, A. Sgambelluri, N. Argyris, G. Kanakis, P. Giardina, G. Bernini, and D. Roccato, "Toward efficient, reliable, and autonomous optical networks: the ORCHESTRA solution," IEEE/OSA Journal of Optical Communications and Networking, 11(9), pp.C10-C24 (2019)
15. K. Kaeval, H. Griesser, K. Grobe, J.P. Elbers, M. Tikas, and G. Jervan, "Channel Performance Estimations with Extended Channel Probing," In Proc. of Photonic Networks; 21th ITG-Symposium (pp. 1-5). VDE. (2020)
16. K. Kaeval, J.P. Elbers, K. Grobe, M. Tikas, T. Fehenberger, H. Griesser, and G. Jervan, "Black-box Assessment of Optical Spectrum Services," accepted for Optical Fiber Communications Conference and Exhibition (OFC) 2021
17. D. C. Kilper, R. Bach, D.J. Blumenthal, D. Einstein, T. Landolsi, L. Ostar, M. Preiss, and A.E. Willner, "Optical performance monitoring," in Journal of Lightwave Technology, vol. 22, no. 1, pp. 294-304 (2004)
18. C. Mas, I. Tomkos and O. K. Tonguz, "Failure location algorithm for transparent optical networks," in IEEE Journal on Selected Areas in Communications, vol. 23, no. 8, pp. 1508-1519 (2005)
19. V. Y. Wen, V. W. S. Chan and L. Zheng, "Efficient fault-diagnosis algorithms for all-optical WDM networks with probabilistic link failures," in Journal of Lightwave Technology, vol. 23, no. 10, pp. 3358-3371 (2005)
20. E. Torrengo, R. Cigliutti, G. Bosco, A. Carena, V. Curri, P. Poggiolini, A. Nespola, D. Zeolla, and F. Forghieri, "Experimental validation of an analytical model for nonlinear propagation in uncompensated optical links," Optics express, 19(26), pp.B790-B798 (2011)
21. P. Poggiolini, A. Carena, V. Curri, G. Bosco, and F. Forghieri, "Analytical modeling of nonlinear propagation in uncompensated optical transmission links," IEEE Photonics technology letters, 23(11), pp.742-744 (2011)
22. P. Poggiolini, "The GN model of non-linear propagation in uncompensated coherent optical systems," Journal of Lightwave Technology, 30(24), pp.3857-3879 (2012)
23. R. Borkowski, A.Caballero, V.Arlunno, D. Zibar, and I.T. Monroy, "Robust cognitive-GN BER estimator for dynamic WDM networks," In Proc. of The European Conference on Optical Communication (ECOC), pp. 1-3 (2014)
24. O.V. Sinkin, C.R. Davidson, H. Wang, L. Richardson, J.X. Cai, D. Kovsh, D.G. Foursa, B. Bakhshi, G. Mohs, and A.N. Pilipetskii, "Effective signal to noise ratio performance metric for dispersion-uncompensated links," In Proc. of 2015 European Conference on Optical Communication (ECOC), pp. 1-3 (2015)
25. M. Enright, "Open cables and integration with terrestrial networks,".in Proc. of SubOptic 2016, WE2A-4 (2016)
26. R. Hadaway, E.R. Hartling, P. Mehta, M. Hubbard, D. Evans, L. Berg, and M. Hinds, "Submarine cable upgrades," In Undersea Fiber Communication Systems, pp. 577-603 (2016)
27. P. Pecci, S. Dupont, S. Dubost, S. Ruggeri, O. Courtois, and V. Letellier, "Experimental characterization of submarine "open cable" using Gaussian-noise model and OSNRwet parameter," In Optical Fiber Communications Conference and Exhibition (OFC), pp. 1-3 (2017)
28. J. Slovak, W. Schairer, M. Herrmann, K. Pulverer, and E. Torrengo, "Benefits of performance awareness in coherent dynamic optical networks," In Optical Fiber Communication Conference, paper W4A-1 (2018)
29. C. Delezoide, K. Christodoulopoulos, A. Kretsis, N. Argyris, G. Kanakist, A. Sgambelluri, N. Sambo, P. Giardina, G. Bernini, D. Roccato, and A. Percelsi, "Field trial of marginless operations of an optical network facing ageing and performance fluctuations," In European Conference on Optical Communication (ECOC), pp. 1-3 (2018)
30. M. Filer, M. Cantono, A. Ferrari, G. Grammel, G. Galimberti, and V. Curri, "Multi-vendor experimental validation of an open source QoT estimator for optical networks," Journal of Lightwave Technology, 36(15), pp.3073-3082 (2018)
31. M. Cantono, J.L. Auge, and V. Curri, "Modelling the impact of SRS on NLI generation in commercial equipment: An experimental investigation," In Optical Fiber Communication Conference, paper M1D-2, (2018)
32. D. Gariépy, S. Searcy, G. He, S. Tibuleac, M. Leclerc, and P. Gosselin-Badaroudine, "Novel OSNR measurement techniques based on optical spectrum analysis and their application to coherent-detection systems," Journal of Lightwave Technology, 37(2), pp.562-570 (2018)
33. E.R. Hartling, A. Pilipetskii, D. Evans, E. Mateo, M. Salsi, P. Pecci, and P. Mehta, "Design, Acceptance and Capacity of Subsea Open Cables," Journal of Lightwave Technology, 39(3), pp.742-756 (2021)
34. K. Kaeval, D. Rafique, K. Blawat, K. Grobe, H. Grießer, J.P. Elbers, P. Rydlichowski, A. Binczewski, and M. Tikas, "Exploring Channel Probing to Determine Coherent Optical Transponder Configurations in a Long-Haul Network," In Optical Fiber Communications Conference and Exhibition (OFC), pp. 1-3 (2020)
35. A.C. Meseguer, P. Plantady, A. Calsat, S. Dubost, J.C Antona, and V. Letellier, "Automated Full C-Band Technique for Fast Characterization of Subsea Open Cable G-SNR," In Asia Communications and Photonics Conference, paper S4B-5 (2019)
36. E. Grellier, and A. Bononi, "Quality parameter for coherent transmissions with Gaussian-distributed nonlinear noise," Optics Express, 19(13), pp.12781-12788 (2011)

Publication VI

Kaeval, K., Myyry, J., Grobe, K., Grießer, H. and Jervan, G., 2021, October. "Concatenated GSNR Profiles for End-to-End Performance Estimations in Disaggregated Networks", *Optical Fibre Communication Conference 2022*, pp. 1–3.

Concatenated GSNR Profiles for End-to-End Performance Estimations in Disaggregated Networks

Kaida Kaeval[1,3], Jani Myyry[2], Klaus Grobe[1], Helmut Grieβer[1], Gert Jervan[3]

[1] ADVA Optical Networking SE, Martinsried, Germany
[2] CSC - IT Center for Science Ltd., Espoo, Finland
[3] Tallinn University of Technology, Tallinn, Estonia
kkaeval@adva.com

Abstract: The performance of a wide-band optical spectrum service is computed using individual segment characterizations and compared to measured end-to-end performance. An accuracy of ±1.4 dB is achieved for live network routes up to 3116 km. © 2021 The Author(s).

1. Introduction

Over the past years, Optical Spectrum as a Service (OSaaS) has gained traction among other high-capacity connectivity offerings and has been widely deployed in production networks [1,2]. Relying on open line systems (OLS), network operators can provide optical spectrum to customers who run traffic over it using their own DWDM terminals. Furthermore, this kind of transparent end-to-end connectivity is often realized by using spectrum infrastructure from multiple providers, creating a fully disaggregated networking scenario. This, however, requires a common service characterization method to be agreed between the providers and end users, in order to evaluate the end-to-end performance of the links before final purchase decisions and service handovers. In our recent work we proposed the GSNR profile as a reliable measure to estimate the individual link performance over the provided spectrum by using a channel probing method [3].

In this work, we investigate the channel probing method's ability to reliably estimate the performance of concatenated links when the GSNR profiles of the individual network segments are available. For this, two long-haul and one regional-haul link from the Funet production network are individually characterized and the estimation for the concatenated link performance is computed. Then, the links are transparently interconnected and the actual end-to-end performance of the merged link is captured by channel probing. Finally, the estimation accuracy is calculated.

2. Measurement set-up

Following the definitions in ITU-T Recommendation G.807 [4], we define an optical spectrum service as an optical media channel (MC) representing a transparent lightpath through an optical network on a predetermined frequency slot capable of carrying zero or more optical tributary signals (OTSi).

For this work, a 300-GHz media channel was provisioned in three non-overlapping network segments in Funet's long-haul Raman-enabled DWDM network. Two of the links featured a constant power adjustment algorithm on the OLS, equalizing the total power within the MC along the route, complicating the power spectral density based channel probing. The test set-up with spectral assignments is illustrated in Fig. 1. The optical user spectrum was added and dropped at a free terminal ROADM port using an 8:8 splitter/combiner module at the test site. To extend the transmission distance and to allow single-ended measurements from the test site, the spectral services were looped back in the far end ROADMs. To compensate for the insertion losses from the colorless access structures, signal
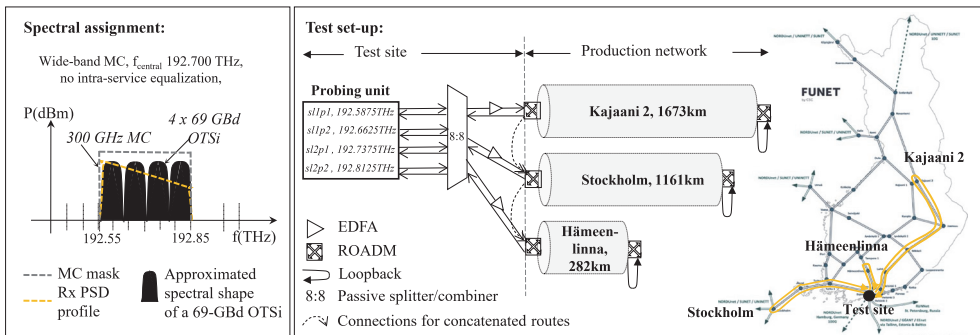

Fig. 1. Spectral assignment of the 300-GHz media channel and general test set-up

amplification after the 8:8 module was performed. Then the individual OTSi transmit powers to-the-line were equalized manually by adjusting the output powers of the probing unit. For concatenated route measurements, the add/drop structures were skipped and the signals were interconnected transparently to the next segment through physical patch-cords at the terminal ROADM C-ports. The received power spectral density (PSD) profile shows the tilt within the media channel, caused by the Raman gain spectrum.

Commercially available ADVA TeraFlex transceivers were used as probing units and two tests were performed per link: simultaneous probing with multiple probes and a single probe sweep with 12.5 GHz steps over the media channel bandwidth. For the multiple-probe scenario only 69-GBd DP-QPSK wide-band probing signals with 200-Gbit/s and a root raised cosine (RRC) spectral shape were used. For the case of a single-probe sweep, also 100-Gbit/s 31-GBd DP-QPSK or 200-Gbit/s 34-GBd DP-16QAM as a narrow-band probe configuration was used. To obtain comparable results from channel probing, a constant transmit power spectral density was maintained by adjusting the signal power at each symbol rate accordingly when switching between the configurations.

3. Results and interpretation

First, all routes were characterized by their GSNR profile. Fig. 2 shows the individual GSNR profiles along with receive power spectral densities for the multiple-probe and single-probe sweep results from three different network segments. The first route, Kajaani 2 with 1673 km, is the longest route characterized. The link features a power adjustment algorithm, that interferes with equal transmit power spectral density along the route, rising the power levels for narrow-band probes. This results in up to 3 dB higher power spectral density for narrow-band signals that causes them to operate slightly in non-linear regime at the peak side of the spectrum slot (192.55 THz). Unlike the Kajaani 2 link, the GSNR profiles of the 1161-km long Stockholm link follow the 1.8dB tilt of the received PSD and both probe configurations work in the linear regime over the full media channel bandwidth. Both of the longer links have a maximum deviation between the wide-band and narrow-band probe estimations below 0.6 dB for the estimated GSNR. The last link, Hämeenlinna with 282 km, has a high OSNR, not preferred for channel probing due to larger probing error due to saturation regimes of the probes [5]. The GSNR profiles recorded by the two probes used have a maximum of 2.0 dB deviation. The channel probing accuracy is further degraded by the enabled power adjustments on the link that is causing the up to 0.9 dB difference in received power spectral density.
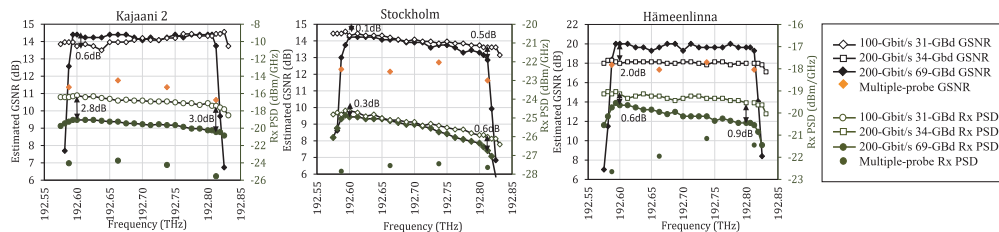

Fig. 2. Individual GSNR and Rx power spectral density profiles for the routes

The GSNR estimations for the concatenated routes are calculated according to

$$\frac{1}{GSNR_{TOT}} = \frac{1}{GSNR_1} + \frac{1}{GSNR_2} + \cdots \qquad (1).$$

First, two longer routes were concatenated, reproducing a service scenario with two independent core segment providers. The GSNR profile estimations and channel probing results for the concatenated segments are visualized in Fig.3 upper left. Then, the 260-km Hämeenlinna segment was added to the chain, illustrating the scenario with three service providers. The GSNR profile estimations and channel probing results with absolute values for the 3-provider scenario are presented in Fig.3 upper right. The bottom part of Fig. 3 presents the estimation error for both probes and multiple simultaneous probes for the two concatenated scenarios.

Within the effective service bandwidth, the GSNR values retrieved through direct channel probing on the concatenated link deviate from the individual segments` estimations by up to 1.4 dB. For most of the probing scenarios, the performance estimated by individual GSNR is underestimated by 0.4 to 1.4 dB compared to the real performance of the concatenated link. The only exception is the 100-Gbit/s 31-GBd DP-QPSK probe for the concatenated Kajaani 2 and Stockholm link, which was likely to overestimate the value due to the higher accumulated to-the-line launch power, contributing to higher nonlinear impact and hence, degrading the overall performance. Similar impact should be visible also on the 3-provider concatenated link, but here, all probe settings during the concatenated probing outperform the profile based estimations. The most probable cause for this is the biased GSNR profile estimated by

the narrow-band probe setting for the shortest link, showing almost 2.0 dB degradation compared to wide-band probe setting and effectively lowering the estimated GSNR for the whole concatenated media channel.

Regardless of the generally lower values of the coarse GSNR profile provided by the multiple simultaneous probes, the estimation error is also less than ±1.4 dB between the estimations and measurements. Due to higher robustness against the power adjustments on the link, the estimations results are in better alignment with the valleys and peaks within the spectral slot. Probes working in the valley part of the spectrum report slightly higher estimation accuracy compared to probes working at the peak of the spectrum slot. This can be explained with higher accumulated to-the-line transmit powers that contribute to higher nonlinear penalty, which cannot be estimated with channel probing.
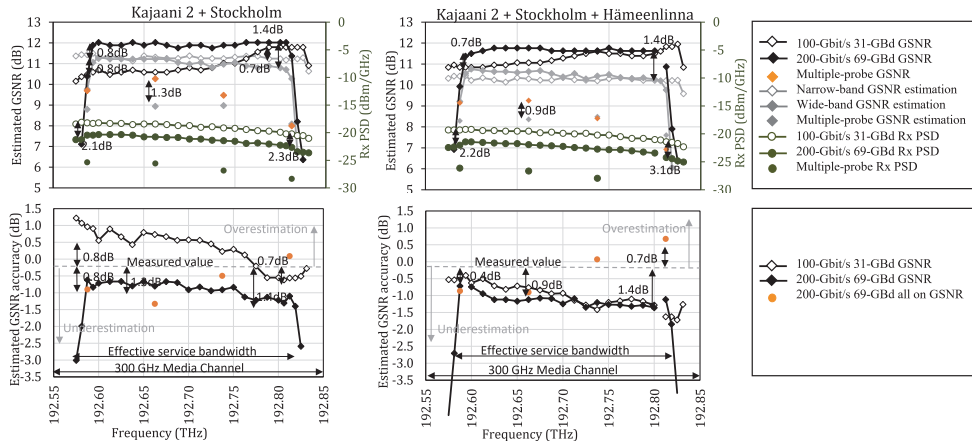

Fig. 3 Top: Comparisons of the estimations and channel probing results, Bottom: Estimation accuracy for different probes

In general, the accuracy of channel probing is very vulnerable to power adjustments at any point in the OLS, including the daily performance fluctuations on the link. In addition, the method is reliable only in linear operation within the effective bandwidth of the media channel. The primary method related error source is the poor alignment of the used probes with the available characterization curves. As the probing light transceiver characterization is often time- and resource-consuming task, readily available uncharacterized transceivers are often used as probes, which may lead to bias in the estimated GSNR profile. To avoid that, one single characterized probe, the golden transceiver, should be always used for the GSNR profile capture.

4. Conclusions

Optical Spectrum as a Service (OSaaS) has become an attractive service model for customers demanding high capacity, future proof network resources. For low-margin networking [6], reliable estimation for disaggregated networks is required. In black-box scenarios, where software-based QoT estimation tools [7] lack OLS-related input data, GSNR profiles can be used to calculate the expected end-to-end performance in multi-domain environments.

In this work, we have compared the GSNR estimations to end-to-end measurements for two- and three-provider scenarios with a maximum estimation error of ±1.4 dB. In service procurement scenarios where the OLS is treated as a black-box, this error magnitude can be justified as a rough estimation for long-haul links of 3000 km and more. Further accuracy improvements can be achieved by using characterized golden transceivers for the individual link characterizations and disabling any link power adjustments during the initial service characterization time.

6. References

[1] Colt, (2018), "Colt Spectrum brings cost effective Dark Fibre alternative to ultra-high bandwidth customers", press release, 08/05/2018
[2] GEANT, (2021), "Moldovan and Ukrainian R&E communities benefit from new 'spectrum' link with GÉANT", press release, 04/10/2021
[3] K. Kaeval et al., "QoT Assessment of the Optical Spectrum as a Service in Disaggregated Network Scenarios," in JOCN, 13(10), pp.E1-E12.
[4] ITU-T Rec. G.807, online https://www.itu.int/rec/T-REC-G.807/en
[5] E. Rivera-Hartling et al., "Design, Acceptance and Capacity of Subsea Open Cables," in JLT, vol. 39, no. 3, Feb. 2021
[6] Y. Pointurier, "Design of low-margin optical networks," JOCN, vol. 9, no. 1, pp. A9-A17, Jan. 2017
[7] A. Ferrari et al., "GNPy: an open source application for physical layer aware open optical networks," JOCN, vol. 12, no. 6, 2020

Publication VII

Kaeval, K., Slyne, F., Troia, S., Kenny, E., Pedreño-Manresa, J., Patri, S., Grobe, K., Kilper, D.C., Ruffini, M., Jervan, G., "Exploring Service Margins for Optical Spectrum Services", *European Conference on Optical Communication* 2022.

Publication VIII

Kaeval, K., Patri, S.K., Pedreno-Manresa, J., Grobe, K., Elbers, J.P., Grieβer, H., Tikas, M., Jervan, G., "Service Margins for Wide-Band Optical Spectrum Services Implemented in Long-Haul Raman-Enabled Networks", *Optical Fibre Communication Conference 2023,* pp. W3H-6.

The paper is included in the proceedings of the Optical Fiber Communication Conference 2023, held in San Diego California, United States, 5–9 March 2023*.*

Publication IX

Kaeval, K., Slyne, F., Troia, S., Kenny, E., Grobe, K., Griesβer, H., Kilper, D.C., Ruffini, M., Pedreño-Manresa, J., Patri, S.K., and Jervan, G., "Employing Channel Probing to Derive End-of-Life Service Margins for Optical Spectrum Services", *Journal of Optical Communications and Networking*, 15, C63-C73 (2023).

Appendix 2

OSaaS Survey questionnaire in SurveyMonkey environment:
https://www.surveymonkey.de/r/HNZ86CK

Q1 Please enter your details

Email:

Country:

Q2 What's the size of your company?

Up to 100 employees

Up to 1000 employees

More than 1000 employees

Q3 Is your company operational only in one country or in multiple countries?

One country only

Up to 10 countries

More than 10 countries

Q4 What's your primary field of operation?

Mission Critical / Hight Availability / Utility (power, gas, water, transportation, etc)

Business-critical / High Availability (banking, media distribution, data center operation, etc)

Governmental

Research and education (NRENs)

Wholesale carrier business

Mobile operator

Q5 What kind of a DWDM system do you operate today?

A standard fixed grid 10-Gbit/s optimized dispersion compensated DWDM system

A standard fixed grid 100-Gbit/s coherent transmission optimized DWDM system (80+ channels)

A standard flex-grid ROADM based 100-Gbit/s coherent transmission optimized DWDM system

A standard flex-grid ROADM, colorless access based 100-Gbit/s coherent transmission optimized DWDM system

No own DWDM system, we mostly buy the leased capacity from providers

Q6 How old is your current DWDM line system, that you would consider for providing OSaaS on average?

  We're in a RFP process/preparing an RFP to upgrade our existing/buy a new DWDM system

  Our system is fairly new (up to 3 years from commissioning)

  Our system is more than 3, but less than 8 years old

  Our system is more than 8 years old

  No own DWDM system, we mostly buy in the leased capacity from providers

Q7 How much free space do you have in your DWDM spectrum based on the already occupied native channels? Please tick all that apply, if you have multiple DWDM systems.

  Our spectrum has a lot of free room to add new channels and services (less than 20% occupied)

  There's plenty of free room in our C-band spectrum (20 to 40% occupied)

  Our spectrum is about half-way filled with the channels (about 40 to 60% occupied)

  We still have some room in our spectrum, but bigger part is already occupied ((about 60 to 80%)

  Our spectrum is basically full (more than 80% occupied)

Q8 In which part of the spectrum are your native channels operated?

  Equally distributed over the C-band

  Beginning of the C-band spectrum (1530 nm / 196.1 THz region)

  End of the C-band spectrum (1565 nm / 191.6 THz region)

  Not applicable due to leased capacity service

Q9 What is/would be your one main driver for considering providing Optical Spectrum as a Service (OSaaS)?

  Free/available spectrum in our DWDM system

  Customers are requesting services

  Interest to avoid 3R at domain borders (core-to-core or core-to-access)

  Upgrade network throughput without investing into the new transponders

  Other (please specify)

Q10 To whom would you consider providing the service?

  I only plan to use OSaaS myself, as I plan to implement vendor neutrality (at transponder or any further component level)

  As a partnership project only

  To other carriers and operators, who own a DWDM system themselves (they know, how to operate it)

  To everyone

Q11 How do you plan to charge for the service?

       Swap wavelength to wavelength with other carriers

       A percentage from the leased capacity cost. If so, which percentage?

       A percentage from fibre rental cost. If so, which percentage?

Q12 Would you consider to sell your free spectrum to a wholesale buyer?

       Yes

       No

       I don't know

Q13 Who should be responsible in keeping OSaaS performance within agreed thresholds (Service Level Agreement)?

       Service provider (me)

       Probably both, service provider (me) and service customer

       End customer

       At current state, I don't know

Q14 What is your one biggest concern, that restricts you providing OSaaS?

       Fluctuations in the total power of the incoming customer spectrum that can impact native channels or other customers (power transients, amplifier saturation, etc)

       Power distribution within the service can impact native channels or other customers

       Transmission outside of the service boundaries

       OOK signals in a coherent transmission optimized DWDM system

       My current DWDM system will probably not enable to provide this service

       Other

Q15 If providing OSaaS and gaining control over the primary technical concerns would be possible with a simple upgrade, would you consider to provide the service?

       Yes

       No

       I haven't decided

       Other

Q16 Thank you for your answers and your participation in the survey. Your feedback and opinion are very valuable for us. If you are ready to assist us in this research topic in the future please allow us to contact you.

       Yes

       No

Curriculum Vitae

Personal data

Name: Kaida Kaeval

Date of birth: 18th of November 1981

Place of birth: Kohtla-Järve, Estonia

Citizenship: Estonian

Contact data

E-mail: kaida.kaeval@taltech.ee;

Education

2019–2023   PhD, Information and Communication Technology, 2023
Supervisor(s) Gert Jervan; Helmut Grießer; Klaus Grobe,
Optical Spectrum Services in Open Disaggregated Transport Networks,
Technical University of Tallinn, School of Information Technology,
Institute of Computer Systems

2005–2007   Master's degree, Telecommunication, 2007,
Supervisor Aimur Raja,
Cum Laude for "Utilization of the IP based data transmission networks
in IEC-60870-5-101 based SCADA system",
Technical University of Tallinn, School of Information Technology,
Institute of Radio and Communication technology

2000–2005   BSC, Telecommunication, 2005
Technical University of Tallinn

1989–2000   Secondary education
Tallinn Secondary Science School

Language competence

Estonian   fluent (native)

English   fluent

Russian   beginner

Professional employment

2023– …   Tallinn University of Technology (Taltech), Visiting researcher

2019–2022   ADVA Optical Networking SE, Senior Engineer Advanced Technology

2017–2019   Tele2 Estonia AS, Optical infrastructure manager

2012–2017   Televõrgu AS, Head of Transmission Networks

2008–2012   Televõrgu AS, Principal Specialist, Transmission Networks

2006–2008   Televõrgu AS, Transmission networks specialist

2005–2006   AS EMT, Technical helpdesk consultant

Elulookirjeldus

Isikuandmed

Nimi: Kaida Kaeval

Sünniaeg: 18. November 1981

Sünnikoht: Kohtla-Järve, Eesti

Kodakondsus: Eesti

Kontaktandmed

E-post: kaida.kaeval@taltech.ee;

Hariduskäik

2019–2023   Tallinna Tehnikaülikool – PhD, Informatsiooni ja kommunikatsiooni tehnoloogia, 2023,

Juhendajad Gert Jervan; Helmut Grießer; Klaus Grobe, Optilise spektri teenused avatud lainepikkustihendus võrkudes,

Tallinna Tehnikaülikool, Infotehnoloogia teaduskond, Arvutisüsteemide instituut

2005–2007   Tallinna Tehnikaülikool – Magistrikraad, Telekommunikatsioon, 2007,

Juhendaja Aimur Raja,

IP põhiste andmesidevõrkude kasutamine IEC-60870-5-101 protokolli põhistes SCADA süsteemides, *Cum Laude*

Tallinna Tehnikaülikool; Raadio- ja Sidetehnika Instituut

2000–2005   Tallinna Tehnikaülikool – BSC, Telekommunikatsioon, 2005

1989–2000   Tallinna Reaalkool, Keskharidus

Keelteoskus

Eesti keel   kõrgtase (emakeel)

Inglise keel   kõrgtase

Vene keel   algtase

Teenistuskäik

2023– …   Tallinn University of Technology (Taltech), Külalisteadur

2019–2022   ADVA Optical Networking SE, Vaneminsener, Advanced Technology

2017–2019   Tele2 Eesti AS, Optilise infrastruktuuri valdkonnajuht

2012–2017   Televõrgu AS, Transmissioonivõrkude peaspetsiaslit

2008–2012   Televõrgu AS, Magistraalvõrkude peaspetsialist

2006–2008   Televõrgu AS, Magistraalvõrkude spetsialist

2005–2006   AS EMT, Tehnilise klienditoe spetsialist